



PHD

**Selective Catalytic C-H Functionalisation for Drug Discovery
(Alternative format thesis).**

Paterson, Andrew

Award date:
2017

Awarding institution:
University of Bath

[Link to publication](#)

Alternative formats

If you require this document in an alternative format, please contact:
openaccess@bath.ac.uk

Copyright of this thesis rests with the author. Access is subject to the above licence, if given. If no licence is specified above, original content in this thesis is licensed under the terms of the Creative Commons Attribution-NonCommercial 4.0 International (CC BY-NC-ND 4.0) Licence (<https://creativecommons.org/licenses/by-nc-nd/4.0/>). Any third-party copyright material present remains the property of its respective owner(s) and is licensed under its existing terms.

Take down policy

If you consider content within Bath's Research Portal to be in breach of UK law, please contact: openaccess@bath.ac.uk with the details. Your claim will be investigated and, where appropriate, the item will be removed from public view as soon as possible.

Selective Catalytic C-H Functionalisation for Drug Discovery

Andrew James Paterson

Under the supervision of Christopher G. Frost

A thesis submitted for the degree of Doctor of Philosophy University of Bath

Department of Chemistry

25 April 2017

COPYRIGHT Attention is drawn to the fact that copyright of this thesis/portfolio rests with the author and copyright of any previously published materials included may rest with third parties. A copy of this thesis/portfolio has been supplied on condition that anyone who consults it understands that they must not copy it or use material from it except as permitted by law or with the consent of the author or other copyright owners, as applicable. If you wish to include copyright material belonging to others in your thesis/portfolio, you are advised to check with the copyright owner (often the publisher) that they will give consent to the inclusion and public availability online of any of their material in the thesis/portfolio.

This thesis/portfolio may be made available for consultation within the University Library and may be photocopied or lent to other libraries for the purposes of consultation with effect from.....(date) Signed on behalf of the Faculty/School of.....

Contents

Contents.....	ii
Acknowledgements	iv
Abstract	v
Abbreviations.....	vi
1.0 Introduction.....	1
1.1 Overview of C-H Functionalisation	1
1.1.1 What? Why? and challenges	1
1.1.2 How? innate reactivity	1
1.1.3 How? chelate assisted.....	2
1.2 <i>Ortho</i> functionalisation	3
1.2.1 Mechanisms for catalysis.....	3
1.2.2 Summary of <i>ortho</i> selective transformations	4
1.3 Overcoming <i>ortho</i> selectivity: <i>meta</i> selective C-H functionalisation	7
1.3.1 Intrinsic control: Steric and electronic	7
1.3.2 Directing group assisted: Extended template approach	9
1.3.3 Removable and “traceless” directing group approach	12
1.3.4 Traceless directing groups: norbornene mediated	14
1.3.5 Utilising non-covalent interactions	18
1.4 Ruthenium catalysed σ -activation	20
1.4.1 Sulfonation	20
1.5 Aims and Objectives	24
1.6 References	25
2.0 Catalytic <i>meta</i> selective C-H functionalisation to construct quaternary carbon centres	29
2.1 Introduction and commentary.....	29
2.2 Authorship and permissions	33
2.3 Manuscript for: Catalytic <i>meta</i> -selective C-H functionalization to construct quaternary carbon centres	34

2.4 Post-commentary	45
2.5 References.....	46
3.0 Mechanistic insight into ruthenium catalysed <i>meta</i> sulfonation of 2-phenylpyridine....	47
3.1 Introduction and commentary	47
3.2 References.....	52
3.3 Authorship and permissions	53
3.4 Manuscript for: Mechanistic insight into ruthenium catalysed <i>meta</i> -sulfonation of 2-phenylpyridine	54
4.0 α -halo carbonyls enable <i>meta</i> primary, secondary and tertiary C-H alkylations.....	73
4.1 Introduction	73
4.2 Optimisation of primary α -halo carbonyl coupling partner	73
4.3 Scope of primary α -halo carbonyl coupling partner.....	76
4.4 Scope of secondary and tertiary α -halo carbonyl coupling partners.....	80
4.5 Mechanistic considerations: Computational.....	82
4.6 Mechanistic considerations: Role of Pd(PPh ₃) ₄	83
4.7 Mechanistic considerations: Addition to cyclometalated complex	86
4.8 Conclusions and overall mechanism	88
4.9 References.....	90
5.0 Overall conclusions and future work	91
6.0 Data and supporting information	94
6.1 Supporting information and data for: Catalytic <i>meta</i> -selective C-H functionalisation to construct quaternary carbon centres.	94
6.2 Supporting information and data for: Mechanistic insight into ruthenium catalysed <i>meta</i> -sulfonation of 2-phenylpyridine.....	125
6.3 Supporting information and data for: α -halo carbonyls enable <i>meta</i> primary, secondary and tertiary C-H alkylations	144

Acknowledgements

First and foremost, I would like to thank my main supervisor Professor Christopher Frost for his continued support throughout my time at Bath. His advice and patience were vital for the success of my PhD and personal development and I hope we continue this great relationship throughout our careers.

I would also like to thank the rest of the Frost group past and present for their support and friendship over the past four years. In particular Sean, Baz, Patricia, Bobo, Will, Sahra, Sinéad, Jamie and Callum have made the past four years especially memorable. We have all had our ups and downs, but it has been a real pleasure to work with everyone and we have shared some hilarious times together which will be missed. I would also like to extend this to the countless other people I have met while studying at the University of Bath who have made it such a pleasant place to work.

I would also like to thank those who have given me other technical support and supervision throughout my time at Bath. These include Darrell Patterson for his supervision in chemical engineering, John Lowe for his advice and assistance with NMR, Mary Mahon for X-Ray crystal analysis, Claire McMullin for her computational work and a special thanks to Neil Press for organising my placement in Basel which was one of the main highlights of my PhD.

Finally, I would like to give my sincerest gratitude to my parents, Tom and Marie, who have supported me fully throughout my life.

Abstract

This thesis details the current methods for *meta*-selective C-H functionalisation and contains three chapters relating to the area of ruthenium catalysed *meta* selective functionalisation by σ -activation.

The first of which contains a published manuscript entitled “Catalytic *meta*-selective C-H functionalization to construct quaternary carbon centres” and describes a *meta* selective tertiary alkylation procedure on 2-phenylpyridine substrates. Key findings from this work provide good evidence for a radical based mechanism and proposes a catalytic cycle involving two distinct roles for the ruthenium catalyst; both in the activation of the substrate molecule and in the formation of a tertiary radical coupling partner.

The second chapter contains another published manuscript entitled “Mechanistic insight into ruthenium catalysed *meta*-sulfonation of 2-phenylpyridine” and provides mechanistic analysis for the *meta* selective sulfonation of 2-phenylpyridine. Key findings from this work show through stoichiometric experiments that sulfonation occurs at the position para to the C-Ru bond formed following cyclometalation with a radical addition being implied. The work also shows that the catalytic species involved do not require an arene ligand and deuterium labelling studies identified a likely rate limiting radical sulfonation step.

The final chapter contains additional work relating to the use of α -halo carbonyl coupling reagents to enable *meta* selective primary, secondary and tertiary alkylations. The use of a triphenylphosphine ligand source was necessary for the coupling of primary α -halo carbonyl coupling partners at the *meta* position. Crucially, this transformation was not possible with simple, straight-chain alkyl halides, highlighting the privileged reactivity of α -halo carbonyl coupling reagents. This work also contains experimental and computational mechanistic analysis which reveals additional support for a dual activation pathway.

Abbreviations

ABCN	1,1'-azobis(cyclohexanecarbonitrile)
Ac	acetyl
Ad	adamantyl
Ar	aryl
aq.	aqueous
BHT	butylated hydroxytoluene
Boc	di-tert-butyl dicarbonate
Bpy	2,2'-bipyridine
Bu	butyl
CMD	concerted metallation deprotonation
COD	1,5-cyclooctadiene
Dbu	dibenzylideneacetone
DCE	1,2-dichloroethene
DG	directing group
DMA	dimethylacetamide
DMPU	1,3-dimethyl-3,4,5,6-tetrahydro-2(1H)-pyrimidinone
Dtbpy	4,4'-di-tert-butyl-2,2'-bipyridine
ESI	electrospray ionisation
Et	ethyl
eq	equivalent(s)
Hex	hexyl
HFIP	hexafluoro-2-propanol
HPLC	high performance liquid chromatography
Me	methyl
Mes	mesityl
NBO	natural bond orbital
MS	mass spectrometry
NBS	<i>N</i> -bromo succinimide
NMP	<i>N</i> -Methyl-2-pyrrolidone
Ns	nosyl
Nu	nucleophile
PEPPSI-IPr	[1,3-bis(2,6-diisopropylphenyl)imidazol-2-ylidene](3-chloropyridyl)palladium(II) dichloride
Ph	phenyl
Phen	1,10-phenanthroline

Pin	pinacol
Piv	pivalate
PMETA	pentamethyldiethylenetriamine
Pr	propyl
Py	pyridine
S _E Ar	electrophilic aromatic substitution
SET	single electron transfer
TEMPO	(2,2,6,6-tetramethylpiperidin-1-yl)oxyl
Tf	triflyl
TFA	trifluoroacetic acid
THF	tetrahydrofuran
TLC	thin layer chromatography
Ts	tosyl
Val	valine

1.0 Introduction

1.1 Overview of C-H Functionalisation

1.1.1 What? Why? and challenges

The direct selective activation and functionalisation of C-H bonds within an organic molecule has challenged synthetic chemists for decades. Whereas traditional synthetic methodologies for the construction of complex organic molecules rely predominantly on employing two complimentary reactive functional groups to generate new C-C or C-X bonds, direct C-H functionalisation instead utilises one (or more) C-H bonds as functional groups. There are a number of benefits of such an approach to synthetic chemistry. From a green chemistry perspective, step and atom economy can be significantly improved by negating the need to prepare two functionalised reagents or perform functional group interconversions. This can lead to particularly efficient processes as step economy is usually the dominant measure of synthetic efficiency.¹ In the context of target orientated synthesis and drug discovery, selective C-H bond functionalisation can also create new synthetic disconnections, leading to new strategies for preparing complex molecules and developing libraries of structurally analogous compounds.

While the benefits are apparent, there are intrinsic challenges associated with the selective functionalisation of C-H bonds. These challenges stem predominantly from the fact that C-H bonds are both ubiquitous within an organic molecule, and generally unreactive when compared to other functional groups. As such, functionalising one C-H bond selectively in the presence of many C-H bonds and functional groups in a molecule has been at the forefront of research into the area over the last decade.²⁻⁷ Overcoming these challenges is not straightforward. Nevertheless, there exist many examples in both traditional and modern synthetic methodology whereby a C-H bond can be directly functionalised. These strategies can be broadly categorised by utilising either “innate” or “chelate assisted” reactivity.

1.1.2 How? innate reactivity

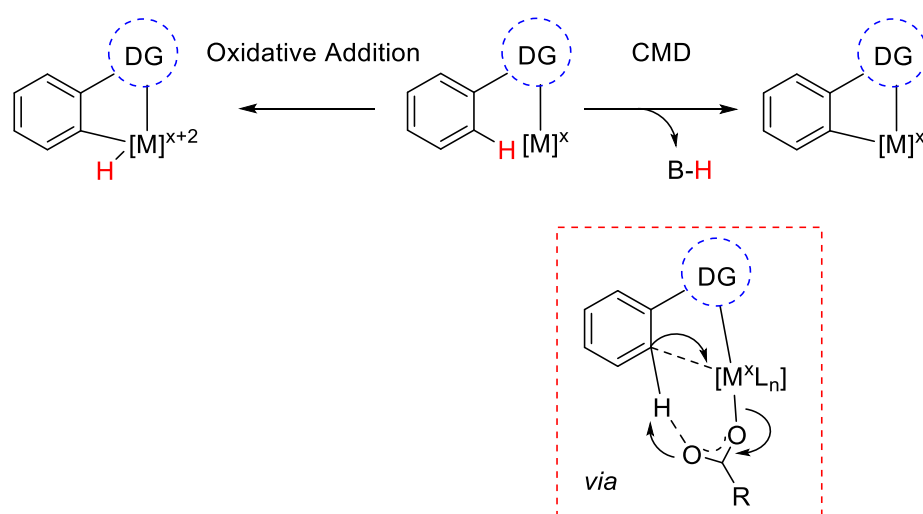
The innate reactivity of a C-H bond depends on both its electronic environment as well as any steric influences within the molecule. Early examples of selective C-H functionalisation via its innate reactivity include electrophilic aromatic substitution on both simple aromatics and heteroaromatics, free radical additions and deprotonations of acidic C-H bonds. Functionalised products can therefore be achieved through direct reaction with common reagents with predictable selectivity.

A number of modern transformations have also been achieved that exploit the innate reactivity of C-H bonds by homogeneous insertion of a transition metal. Again, these strategies rely on the most reactive C-H bond being either the one that is the most sterically available, the most electron rich, electron poor, or the most acidic. This approach to C-H functionalisation has been covered in a number of recent reviews and has been shown to be an effective strategy for the synthesis of complex organic molecules and natural products.^{2,8,9}

1.1.3 How? chelate assisted

The chelation assisted approach to C-H functionalisation overcomes the molecules innate reactivity by utilising pre-existing functional groups (directing groups) within a molecule to coordinate to a transition metal complex and position it for selective C-H bond cleavage. This type of reactivity overcomes the issues with reactivity and selectivity associated with multiple C-H bonds in a molecule by increasing the effective concentration of the transition metal complex in the vicinity of a particular C-H bond. This approach typically results in the formation of a conformationally stable 5 or 6 membered cyclometalated species that can be subsequently functionalised as part of a catalytic cycle to form new C-C and C-X bonds. The key mechanistic step of these reactions involves initial coordination of the directing group to a transition metal complex followed by a metal mediated C-H bond cleavage.

There are a number of pathways by which a transition metal complex can cleave a C-H bond. These include oxidative addition, concerted metalation-deprotonation (CMD), σ bond metathesis, electrophilic addition to a π system or abstraction of a hydrogen atom.¹⁰ Of these, oxidative additions and CMD mechanisms have become the most widely applicable for further functionalisation (**Scheme 1-1**).



Scheme 1-1: Cyclometalation *via* an oxidative addition or CMD pathway.

An oxidative addition is a process that increases both the oxidation state and coordination number of a metal centre and is typical for electron rich, low valent complexes of late transition metals. In C-H activation reactions this proceeds in a concerted manner with the oxidation state and coordination number of the metal increasing by 2. The active catalyst for this type of mechanism must be coordinatively unsaturated and is usually unstable. Therefore, they are often formed in situ from a stable precatalyst. In a concerted metalation-deprotonation pathway, both the metal and a base are implicated in the abstraction of the C-H proton. This occurs *via* a simultaneous metalation / intramolecular deprotonation with no net oxidation state change of the metal. The base implicit in the deprotonation can be a pre-existing ligand of the catalyst or can become coordinated under the reaction conditions and are typically carboxylates or carbonates.

These mechanisms result in conformationally stable metallacycles and have been proven to activate sp^2 aryl and vinyl C-H bonds as well as sp^3 alkyl C-H bonds. The following review will focus on the activation and functionalisation of aryl C-H bonds.

1.2 Ortho functionalisation

The utilisation of a directing group in a molecule to direct reactions to an *ortho* C-H bond has now been demonstrated with a wide range of transformations. These types of reactions have been covered extensively in a number of recent reviews^{7,6,5,4,3,2} so the following sections will show selected examples of some typical mechanisms associated with *ortho* selective C-H functionalisation reactions as well as a summary of many of the transformations performed to date.

1.2.1 Mechanisms for catalysis

Although transition metal mediated C-H bond cleavage and cyclometalation is a fundamental step in directed C-H functionalisation, a number of other conditions must be met for it to be developed into a synthetically useful catalytic methodology. A balance must be struck between a cyclometalated intermediate that is both stable enough to form in the first instance; which is usually governed by geometry; and yet must also be reactive enough to react further with a coupling partner.

Despite these requirements, a great number of catalytic transformations have been reported in recent years. These reactions often draw upon contemporary knowledge of organometallic mechanisms to generate closed catalytic cycles where the substrate is functionalised. In most cases a cyclometalated intermediate formed by one of the

mechanisms summarised in **section 1.1.2** forms an integral part of the mechanism. These processes may also require the use of stoichiometric oxidants in order for them to be catalytic and depends on the nature of the cyclometalation step and the manner in which the coupling partner interacts with the metal centre. Some common catalytic mechanisms are summarized in **Figure 1-1** however new transformations are continuing to challenge traditional logic in this ever growing field.

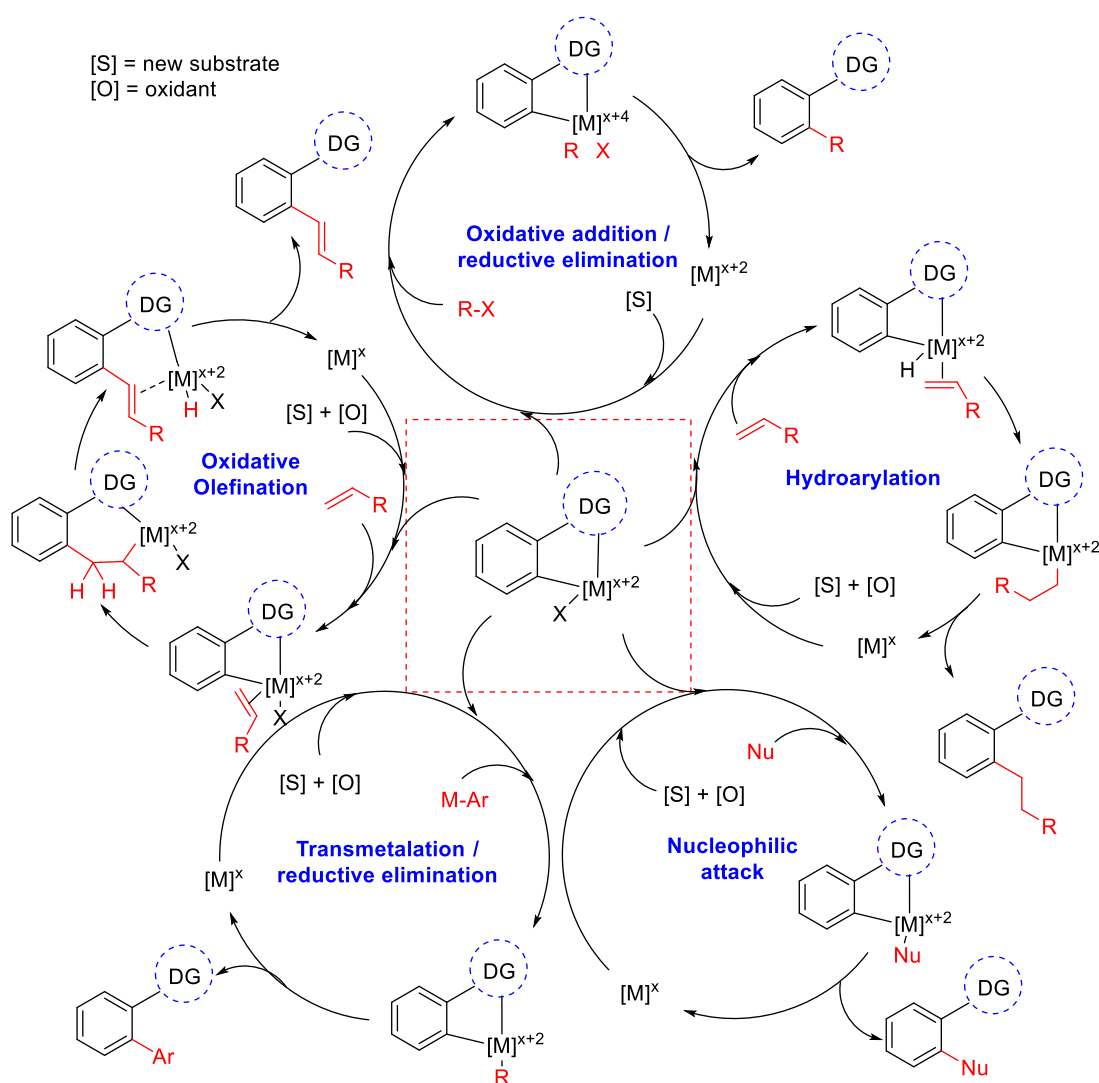


Figure 1-1: Some common catalytic mechanisms for *ortho* C-H bond functionalisation.

1.2.2 Summary of *ortho* selective transformations

The resurgence of interest into the area of C-H functionalisation in recent years has led to a vast number of new chemical transformations. Many of these utilise a directing group strategy, the majority of which leading to *ortho* and di-*ortho* substituted products. These transformations have been achieved using a range of metals whereby the most extensively

studied metals have been precious metals such as palladium,^{11,12} rhodium¹³ and ruthenium,^{14,15,16} however an ever growing number of transformations are beginning to be made using earth abundant metals such as cobalt,¹⁷ nickel¹⁸ and copper.¹⁹ The transformations achieved to date include a number of C-C bond forming reactions including acylations, arylations, alkylations, alkenylations, annulations and cyanations as well as a number of C-Heteroatom transformations including aminations, silylations, nitrations, sulfonations, halogenations and oxygenations (**Figure 1-2**).

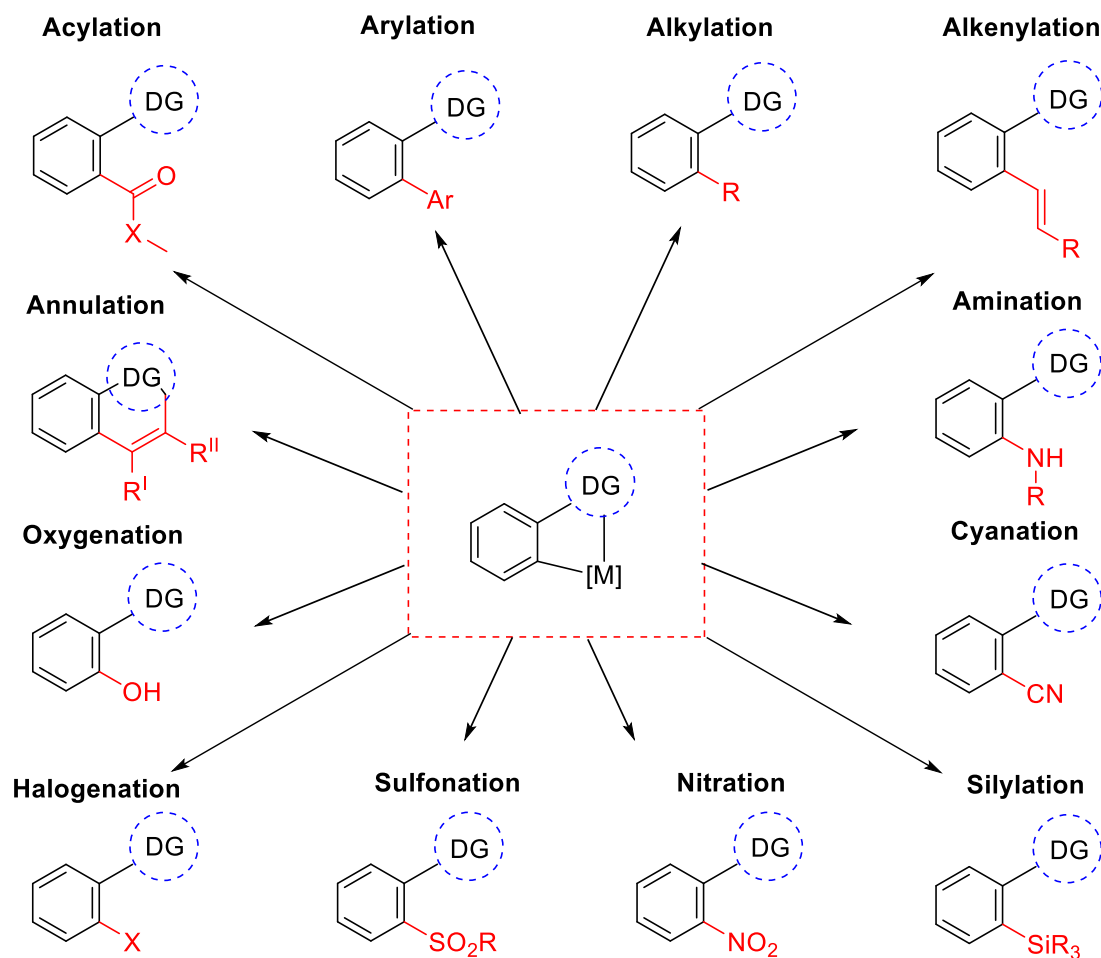


Figure 1-2: Summary of *ortho* C-H functionalisations.

A range of directing groups have also been widely demonstrated. Traditionally, these have been achieved using strongly Lewis basic functional groups which facilitate the cyclometalation step common to many directed C-H functionalisation reactions. Many examples of these include strongly coordinating heterocycles, however it is the stability of these complexes that can make them synthetically restrictive. Coordination *via* weaker,

more common directing groups such as carboxylic acids, alcohols or amines has therefore gained recent interest and has been demonstrated extensively (**Figure 1-3**).^{12,16}

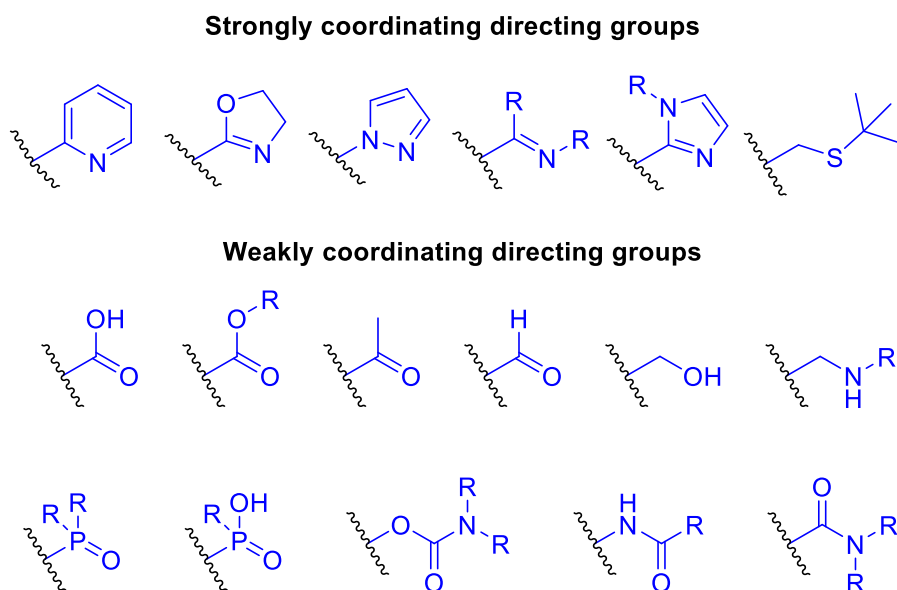


Figure 1-3: Examples of commonly used strong and weak directing groups.

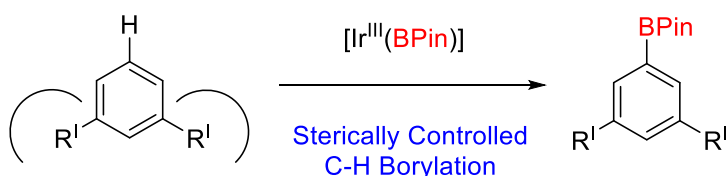
Much contemporary research into developing new broadly useful C-H functionalisations has been associated with the design of new directing groups that are readily removed or converted into useful functionality. This has led to strategies that incorporate directing group auxiliaries which can be readily installed and removed, or traceless directing groups that achieve the same result under the reaction conditions with no additional synthetic steps. These strategies will be explained in the context of *meta* selective reactions in the following section.

1.3 Overcoming *ortho* selectivity: *meta* selective C-H functionalisation

The application of the directing group strategy for C-H functionalisation has led to enormous success in the *ortho* functionalisation of arenes. Key to this success is the facile formation of 5 or 6 membered metallacycles for subsequent transformations as these intermediates are energetically and conformationally stable. However, when devising strategies to activate more remote C-H bonds, for example the position *meta* to a directing group, this approach becomes increasingly challenging as ring size increases and conformational stability decreases. As a result, existing approaches have adapted and new strategies have emerged to enable new reactions with complementary *meta* selectivity.

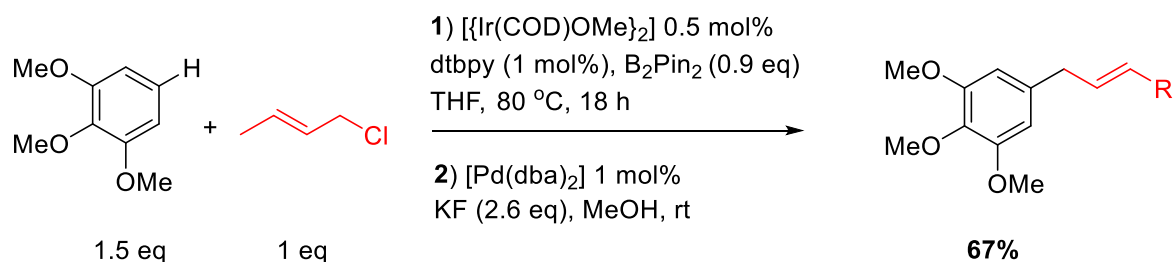
1.3.1 Intrinsic control: Steric and electronic

Among the first examples of *meta* selective C-H functionalisation were cases where the regioselectivity was governed by intrinsic properties of the substrate. Direct *meta* substitution by steric control was first reported by Hartwig *et al.*^{20,21} and Smith *et al.*²² who demonstrated a one pot Ir catalysed *meta* C-H borylation / functionalisation procedure for 1,3-disubstituted arenes. This approach demonstrated the selective borylation of sterically unhindered C-H bonds within substituted aromatics by iridium(III) catalysis with the capacity for further synthetic elaborations (**Scheme 1-2**).



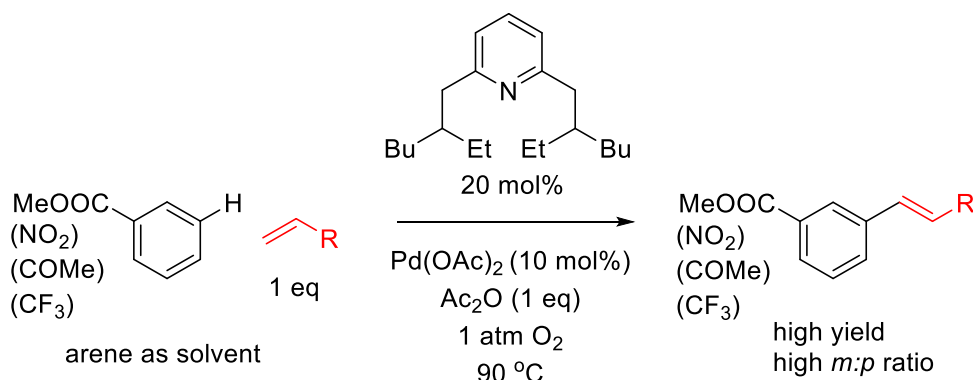
Scheme 1-2: Concept for sterically controlled C-H functionalisation.

Since this seminal work, a number of other transformations have been reported that utilise this sterically controlled iridium catalysed borylation / palladium catalysed coupling procedure to achieve one pot arylations,²² alkylations²³ (**Scheme 1-3**) and iodinations.²⁴ In addition to this, direct sterically controlled functionalisations have also been achieved using palladium²⁵ and rhodium²⁶ catalysis. Selectivity for the *meta* position in these reactions is governed by the steric bulk of the prefunctionalised substrate and therefore usually limits the substrate scope to disubstituted arenes.



Scheme 1-3: Sterically controlled C-H borylation / alkylation.

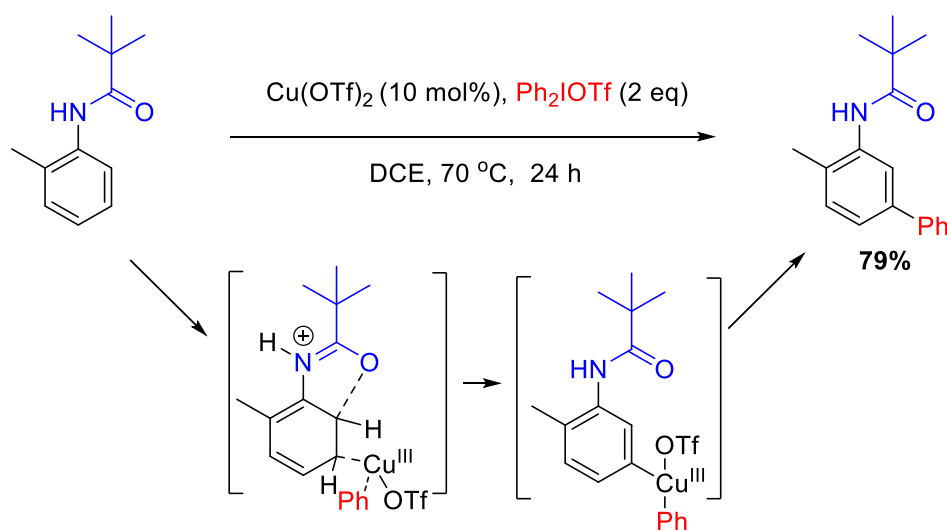
Exploiting the intrinsic electronic effects of a substrate has also led to a number of direct functionalisations with high *meta* selectivity. An early example of this was reported by Yu *et al.* who demonstrated a directing group free olefination of electron deficient arenes²⁷ (**Scheme 1-4**). Key to this reactivity was the use of branched 2,6 disubstituted pyridine ligands which the authors proposed could promote reoxidation of palladium(0) by O_2 whilst still being easily displaced following the reaction, although the exact mechanism is not fully understood.



Scheme 1-4: Electronic controlled C-H olefination.

Since this work, a number of electronically governed palladium catalysed transformations have been achieved, including acetoxylations,²⁸ olefinations²⁹ and imidations.³⁰ Furthermore, gold³¹ and rhodium³² catalysis has enabled *meta* selective arylations by similar electronic biases. An interesting example has also been achieved using copper catalysis by Gaunt *et al.* who reported on the first *meta* selective copper catalysed C-H arylation.³³ This was initially proposed to go *via* a mechanism as per **Scheme 1-5**. However, a more recent mechanistic study has cast doubt on this hypothesis, as this reaction works in the absence of copper albeit at higher temperatures.³⁴ This suggests that this is more

likely an intrinsic electronic property of the substrates used and the authors now propose that the copper salts facilitate the reaction through interaction with the diaryliodonium salt.



Scheme 1-5: Initial proposed mechanism for Cu catalysed *meta* selective direct C-H arylation.

Exploiting intrinsic properties of a molecule has enabled a range of transformations to be achieved on a number of different structural motifs. Because of their intrinsic bias, selectivity can be high, although this approach is fundamentally limited in substrate scope. The search for a more general methodology to access *meta* C-H bonds has therefore attracted significant interest.

1.3.2 Directing group assisted: Extended template approach

One of the major issues in developing directed C-H functionalisation reactions beyond the *ortho* position to a directing group is that the corresponding cyclometalated intermediates, which are paramount to their reactivity, are considerably less likely to form and be sufficiently stable to react. Among the first solutions to this issue came from Yu *et al.* who were the first to develop removable “templates” that could be installed to common functional groups and that would result in a conformationally stable cyclometalated complex akin to those demonstrated in *ortho* selective reactions. These templates were rationally designed with end-on nitrile containing coordinating groups (**Figure 1-4**). Weak coordination could therefore alleviate the ring strain of the resulting cyclophane-like pre-transition state and can hence form conformationally stable metallacycles. This pioneering work enabled access to *meta* alkenylated toluene and hydrocinammic acid derivatives following removal and recovery of the template (**Scheme 1-6**).³⁵

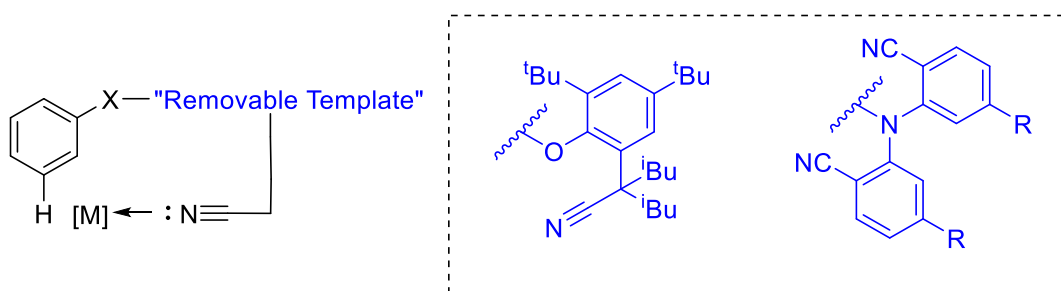
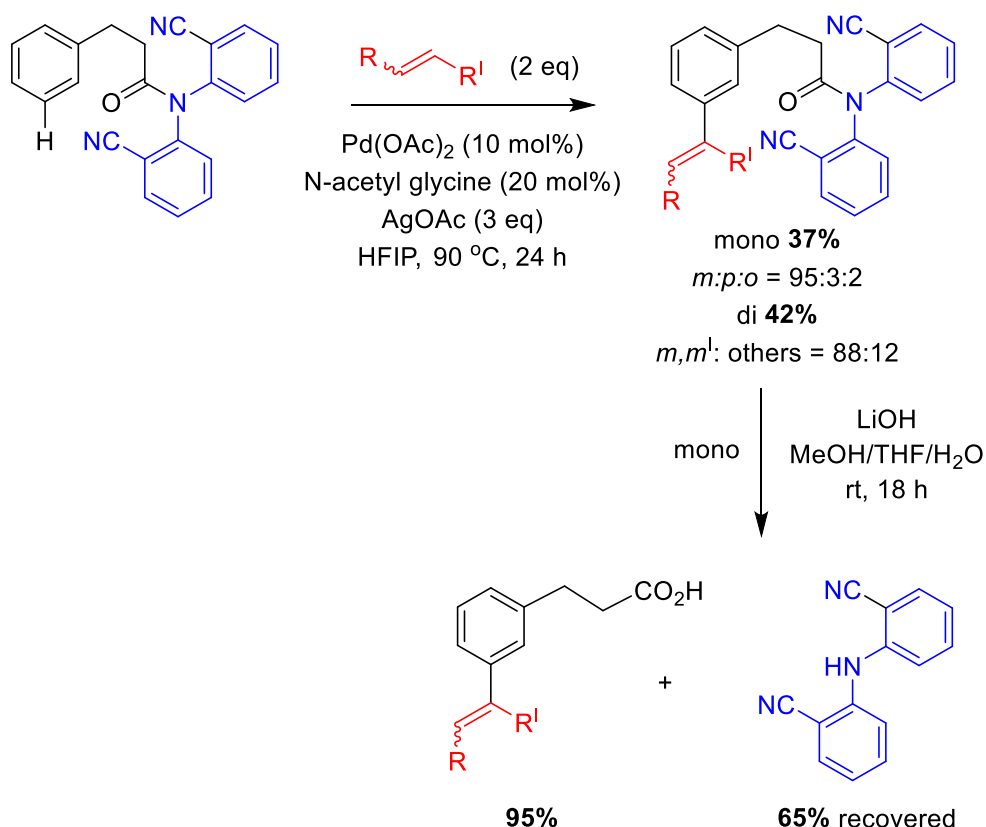


Figure 1-4: Concept for template approach and two early examples³⁵



Scheme 1-6: Template assisted *meta* olefination and subsequent recovery.³⁵

Since this initial report, a number of research groups including those headed by Yu, Tan, Li and Maiti have further utilised nitrile containing templates for the synthesis of *meta* substituted aromatic alcohol,^{36,37,38} amine,^{39,40,41} tolyl,^{35,38} phosphonate,⁴² aldehyde,³⁸ sulfonic acid,^{43,44} and carboxylic acid^{35,45,46,47,48} derivatives by a range of cleavable linkages to enable direct *meta* selective olefinations,^{35,36,37,46,39,40,43,47,41,42,48} arylations,^{45,40} acetoxylation^{39,40,48} and hydroxylations^{42,44} with the potential for further synthetic elaborations. A summary of the transformations by this approach achieved to date is given in **Figure 1-5**.

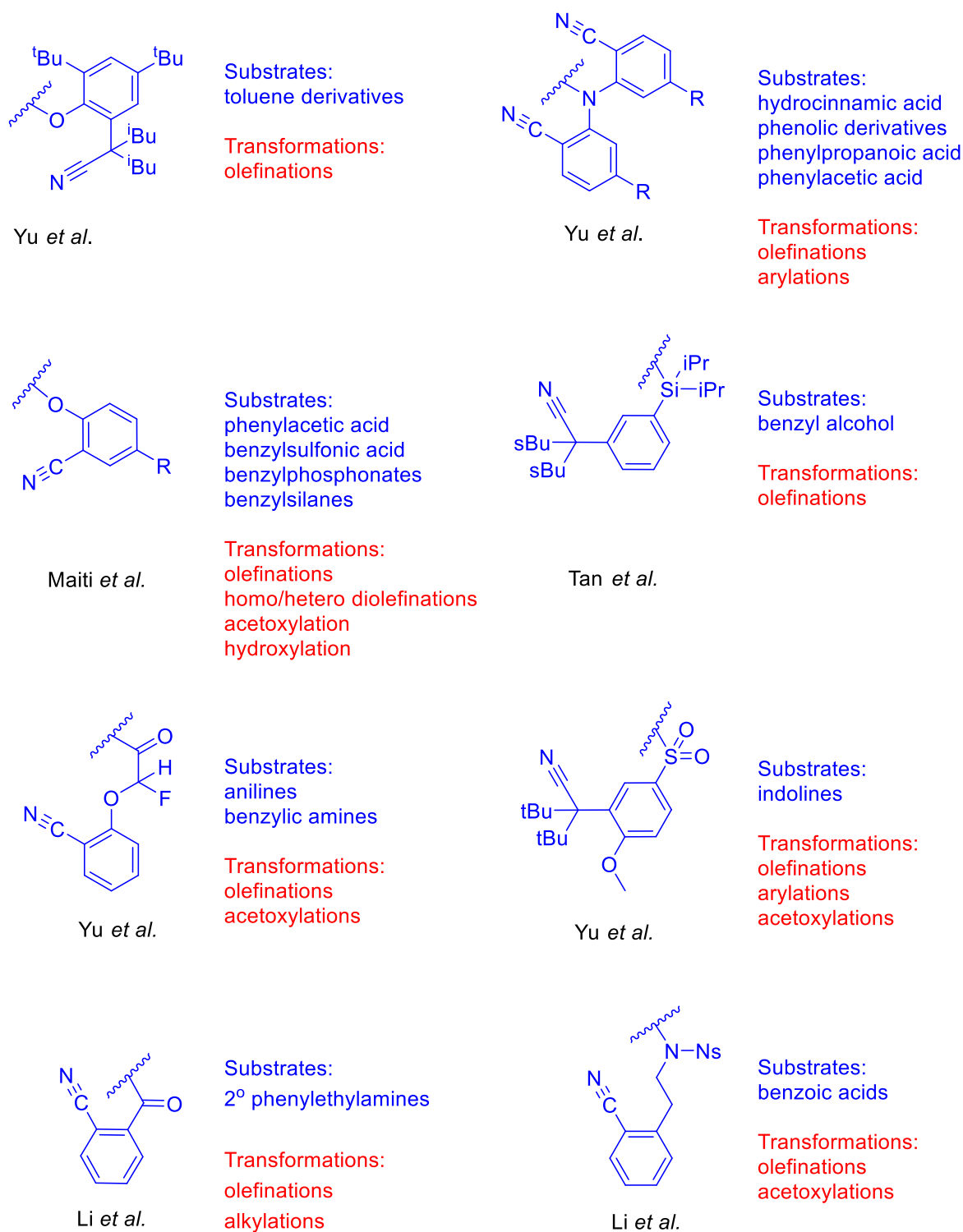


Figure 1-5: Removable “templates” developed for *meta* functionalisation.

Nitrile containing templates have therefore enabled an ever growing number of *meta* selective transformations. However, the use of such a weakly coordinating directing group does have some intrinsic limitations. These include competing coordination from other functional groups or solvents as well as the variable binding modes of nitrile groups,

affording potentially undesired switches in selectivity.⁴¹ In response to this, Yu *et al.*⁴⁹ have developed templates that incorporate more strongly coordinating pyridine groups. These templates overcome some of the limitations of nitrile groups and have successfully enabled alkenylations and iodinations on benzyl alcohol and phenylethyl alcohol derivatives *via* a template with an easily installed and cleavable ester linkage.

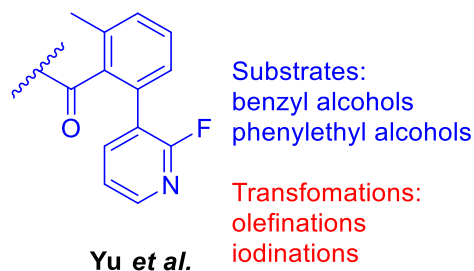


Figure 1-6: Template using coordinating pyridine group.

The “covalent template” approach to direct *meta* functionalisation offers an elegant solution for accessing distal C-H bonds, an approach which has also been demonstrated on the functionalisation of *para* C-H bonds.⁵⁰ However, despite the growing success in the area, this approach suffers from intrinsic drawbacks, particularly when step and atom economy are considered. Many of the templates reported to date have relatively elaborate structures and may require a multistep synthesis. When coupled with the synthetic steps necessary for the installation and removal of the template, the overall atom and step economy, that makes C-H functionalisation an attractive methodology in the first instance, is considerably diminished. Furthermore, this approach also suffers from drawbacks common to *ortho* functionalisation whereby potentially undesired di-*meta* substituted products can be formed. Nevertheless, this approach serves as a useful tool for accessing previously unknown disconnections by utilising common functional groups.

1.3.3 Removable and “traceless” directing group approach

An alternative approach to accessing *meta* substituted arenes is by using directing groups that can be readily removed following a transformation. Initially, this was demonstrated on substituted arenes in two step processes such that *meta* substituted products resulted following the removal of the directing group.

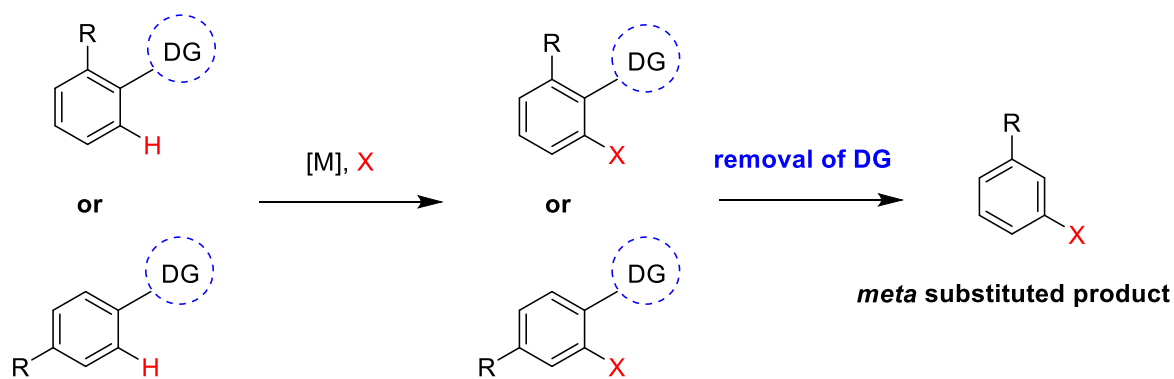
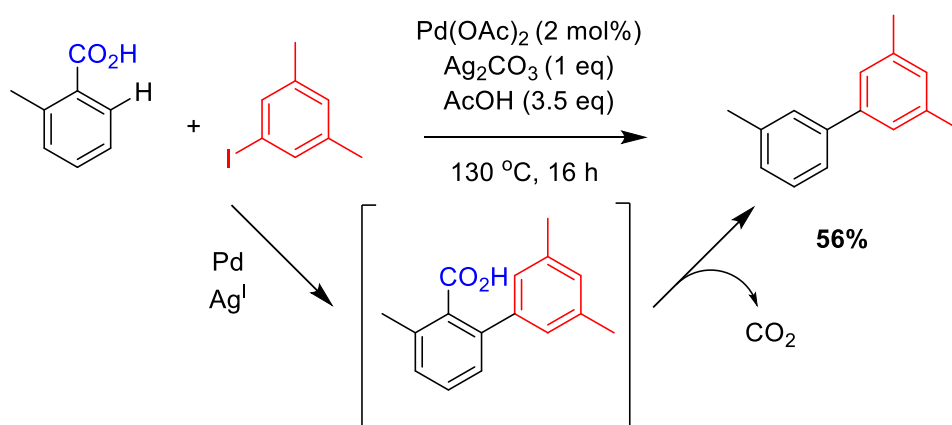


Figure 1-7: Concept for removable directing group approach.

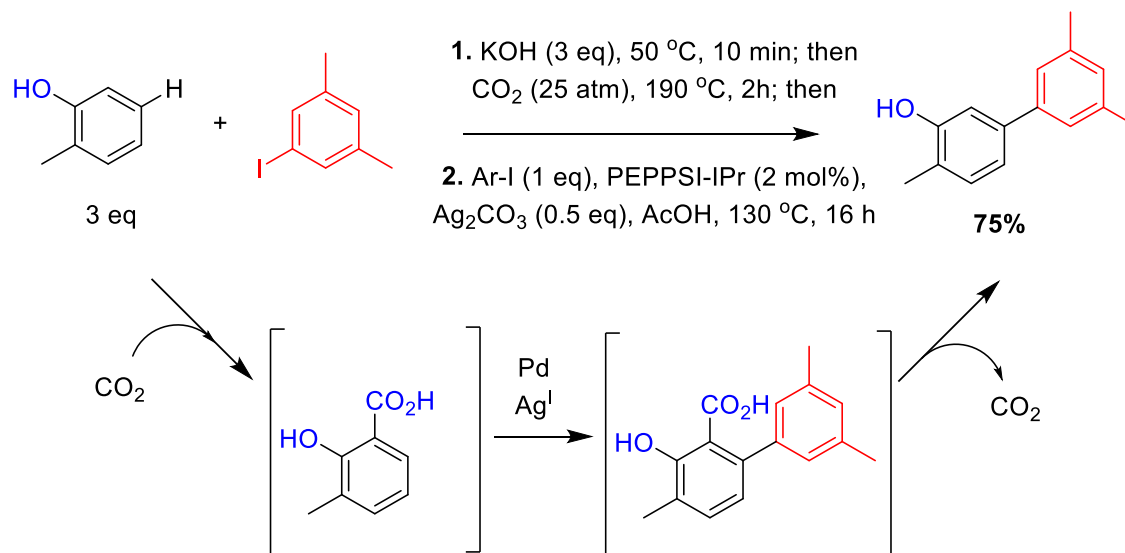
This strategy has been demonstrated on sulfoxide directed lithiation processes where the directing group can be removed under fairly forcing conditions using raney nickel,⁵¹ but more recently carboxylic acids have also been demonstrated. Carboxylic acid directing groups have advantages of being well established in transition metal catalysed *ortho* C-H functionalizations as well as benefiting from recent advances in transition metal protodecarboxylation processes. This can allow the transformation to be achieved in a one pot manner⁵² and hence, a number of examples utilising removable carboxylic acid directing groups on prefunctionalised substrates to access *meta* substituted products have been recently reported. These include olefinations,^{53,54} arylations,⁵⁵ heteroarylations,⁵⁶ acylations,⁵⁷ amidations⁵⁸ and aminations.⁵⁹ A representative decarboxylative arylation process reported by Larrosa *et al.* is shown in **Scheme 1-7**.⁵⁵



Scheme 1-7: Decarboxylative arylation of substituted benzoic acids.⁵⁵

This concept was further expanded by the Larrosa group to also include the installation of the carboxylate group in a “traceless” directing group strategy. This was achieved using a

modified Kolbe-Schmitt reaction to install the carboxylate *ortho* to a phenol directing group, which could then be coupled with a decarboxylative arylation process to yield *meta* arylated phenols in one pot (**Scheme 1-8**).⁶⁰



Scheme 1-8: *Meta* arylation of phenols by traceless carboxylic acid directing group.⁶⁰

The concept of using a removable directing group is a potentially synthetically versatile method for C-H functionalisation and the formation of *meta* substituted products. This method has been particularly successful for easily removable directing groups such as carboxylic acids. Furthermore, the elegant “traceless” directing group strategy employed by Larrosa introduced a conceptually new strategy for achieving *meta* functionalisation. However, the selective installation and complete removal of a directing group from an aromatic substrate is not typically straightforward so this early example suffers from a lack of generality.

1.3.4 Traceless directing groups: norbornene mediated

The “traceless” directing group approach to *meta* functionalisation has become an increasingly attractive strategy, and recent advances in this area have drawn inspiration from the Catellani reaction whereby aryl iodides can be used to perform bi or tri functionalisation utilising palladium catalysis and norbornene as a mediator (**Figure 1-8**). The key reaction mechanisms for this transformation are initial oxidative addition of an aryl halide, carbopalladation of the norbornene mediator, palladacycle formation, oxidative addition of the coupling partner to the palladacycle, reductive elimination from the palladacycle, norbornene extrusion and finally termination by a number of means including cross coupling reactions or crucially, protonation.

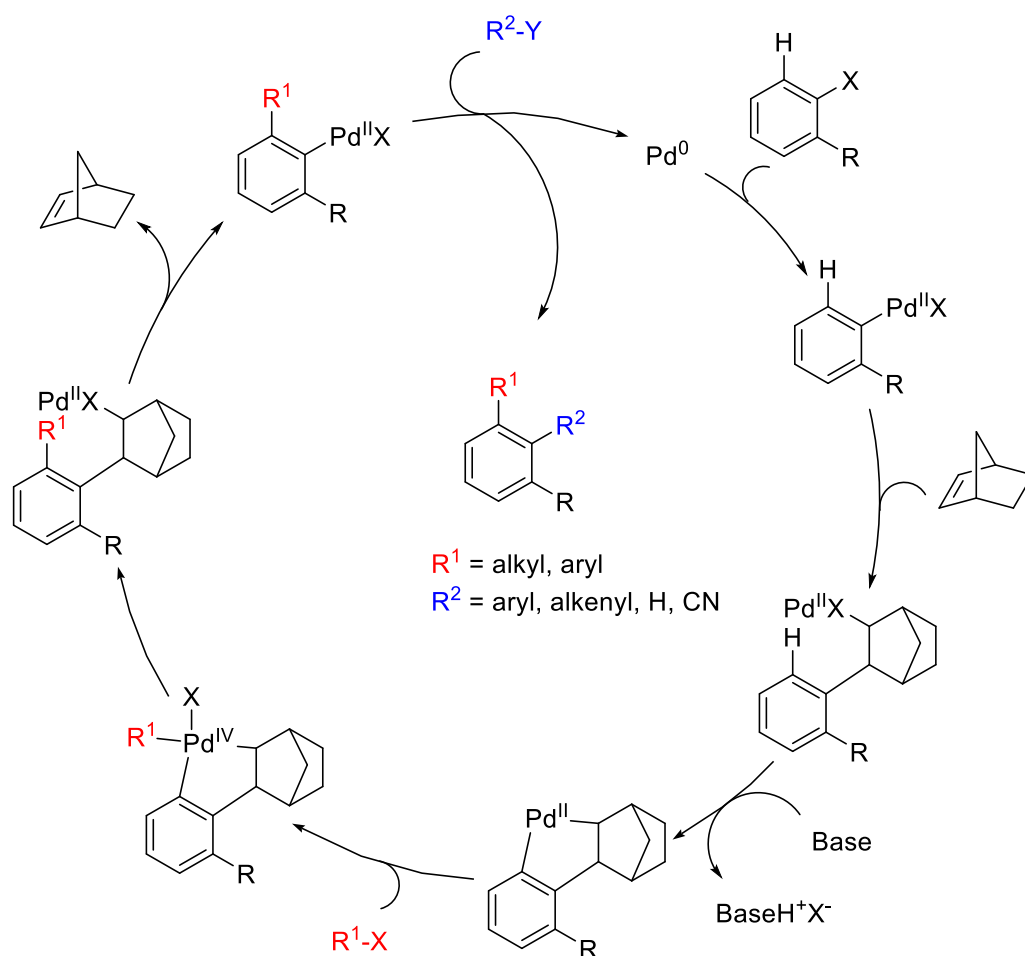
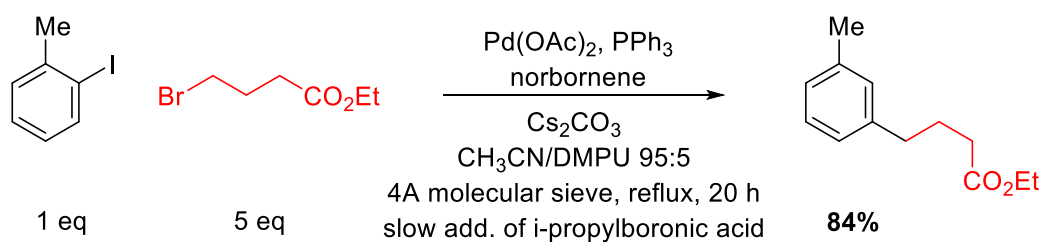


Figure 1-8: Catalytic cycle for Catellani reaction.

This was initially adapted in removable directing group fashion by Lautens *et al.*⁶¹ who utilised aryl iodides in an adapted Catellani reaction to form *meta* substituted products (**Scheme 1-9**). In this case, proto-termination could occur following transmetalation with isopropyl boronic acid, β -hydride elimination and subsequent reductive elimination of the hydride to afford mono *meta* substituted products.



Scheme 1-9: Palladium catalysed alkylation / hydride reduction sequence.⁶¹

Later this was adapted in a “traceless” fashion by Yu *et al.* incorporating the initial installation of the palladium through an *ortho* metalation strategy followed by application of the Catellani reaction and proto-demetalation.⁶² The authors recognised the potential for unwanted site reactions, however these could be minimised with the use of specialised pyridine ligands (**Figure 1-9**). This early example enabled direct *meta* alkylation and arylation on a range of substituted aromatics bearing an amide directing group (**Scheme 1-10**).⁶²

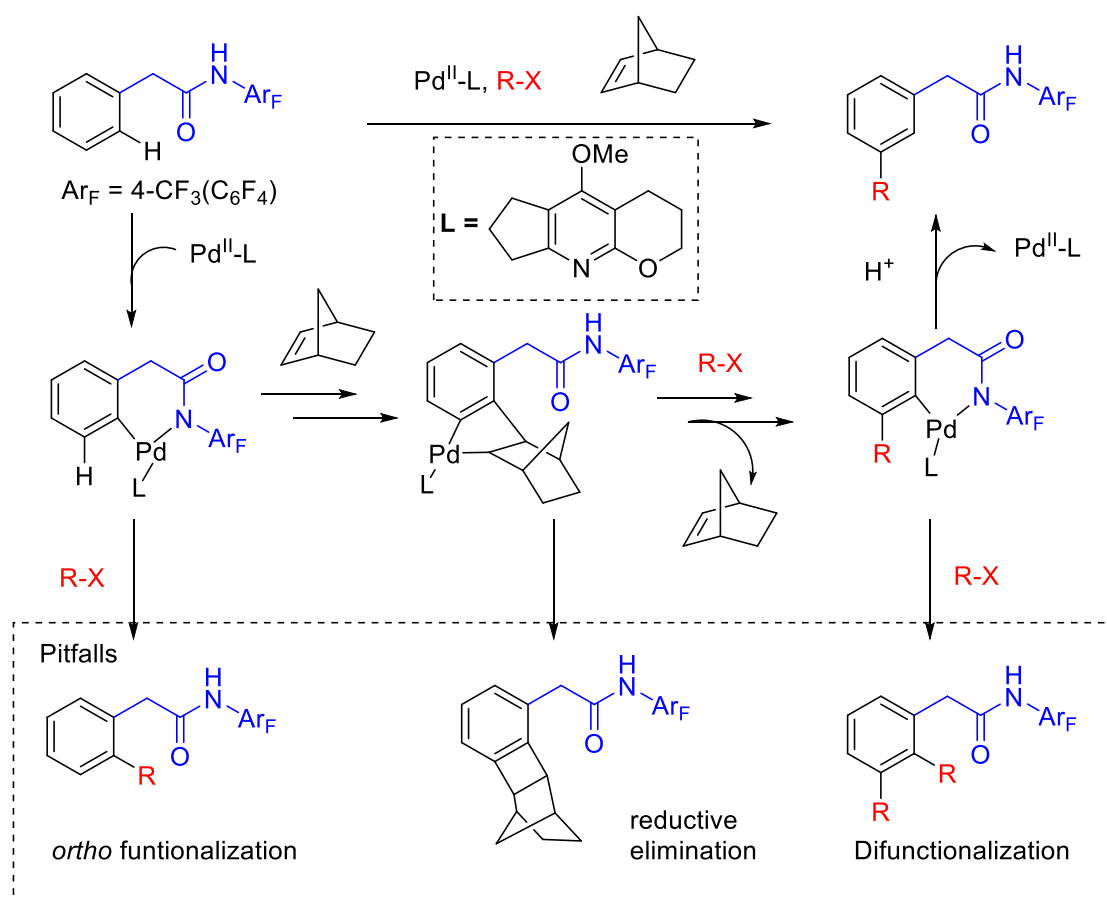
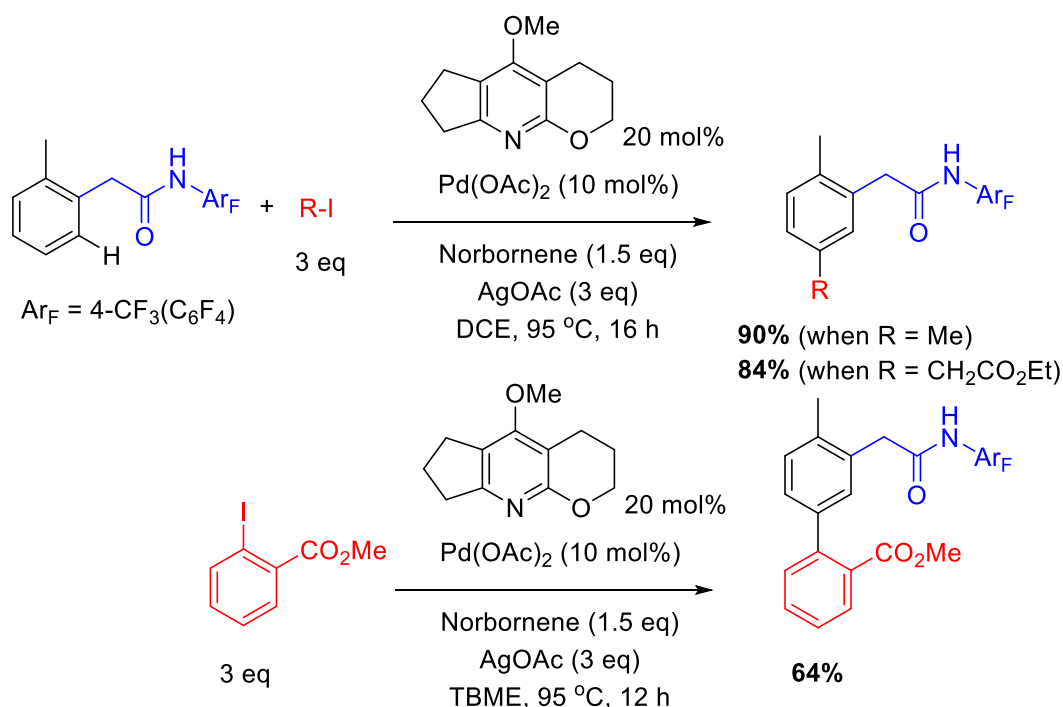
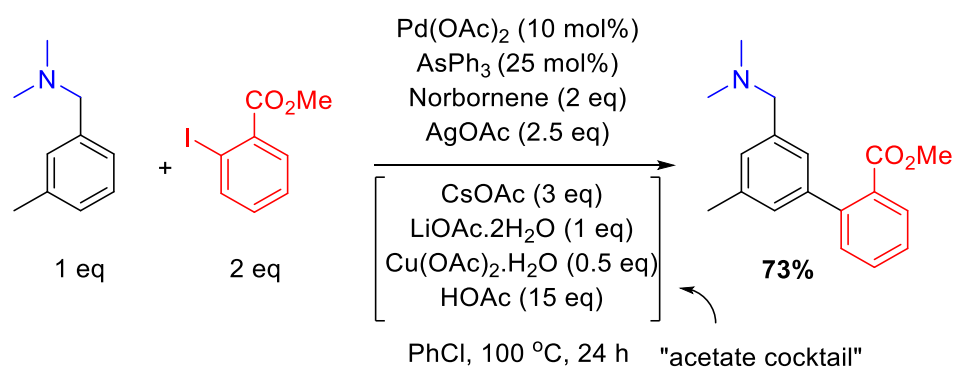


Figure 1-9: Concept for norbornene mediated *meta* functionalisation.



Scheme 1-10: Norbornene mediated *meta* alkylation and arylation.⁶²

Soon after, a similar example was reported by Dong *et al.*⁶³ to include *meta* arylations on aromatic substrates bearing simple benzyl amine directing groups. AsPh₃ as a ligand and an “acetate cocktail” were vital for reactivity (**Scheme 1-11**).



Scheme 1-11: Norbornene mediated *meta* arylation using acetate cocktail.⁶³

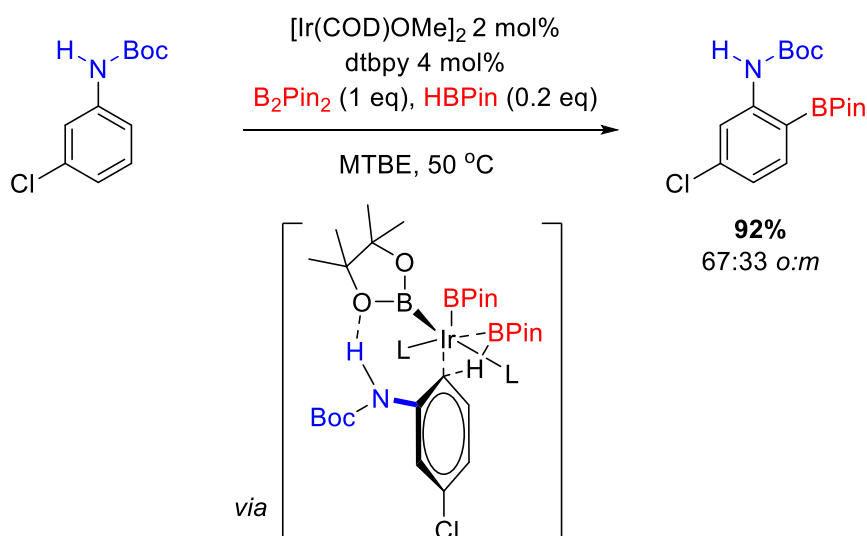
These seminal contributions did however suffer from a limited coupling partner scope. For example, alkylation procedures were only possible on alkyl halides with no β-hydrogen, and arylations were only possible using aryl iodides bearing an *ortho* electron withdrawing group. These drawbacks were addressed by Yu *et al.*⁶⁴ who expanded the coupling partner scope significantly on phenyl acetamide substrates to include a significantly wider range of

alkyl and aryl halide coupling partners. Key to this success was a modified norbornene coupling partner and quinolone type ligand. Zhao *et al.*⁶⁵ also achieved significantly improved aryl iodide scope with the assistance of a bidentate directing group.

Yu *et al.* have also utilised this norbornene assisted arylation procedure on aniline, phenol and heterocycle substrates⁶⁶ and the same group has also recently expanded the coupling partner scope to include *meta* selective amination,⁶⁷ alkynylation⁶⁷ and chlorination.⁶⁸ In all cases, specialised pyridine ligands are essential for this reactivity.

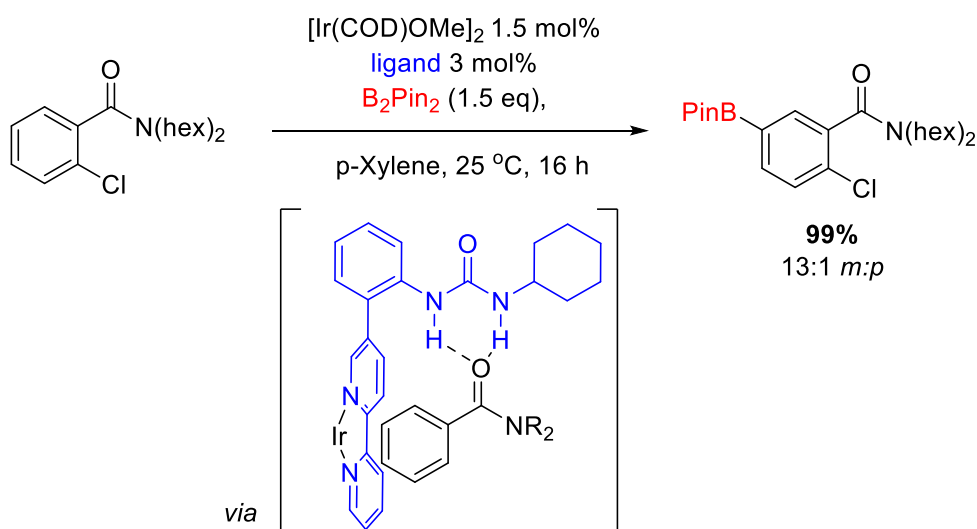
1.3.5 Utilising non-covalent interactions

Whereas most *meta* selective borylations are governed by steric factors in the absence of directing groups, the groups of Singleton, Malekzka and Smith⁶⁹ observed that borylation on 3 substituted N-Boc anilines gave mixtures of *ortho* and *meta* regioisomers, despite the *meta* position being sterically more accessible. Here, selectivity could be attributed to a hydrogen bonding interaction between the substrate N-H and a hydrogen bond acceptor on one of the pinacol ligands (**Scheme 1-12**).



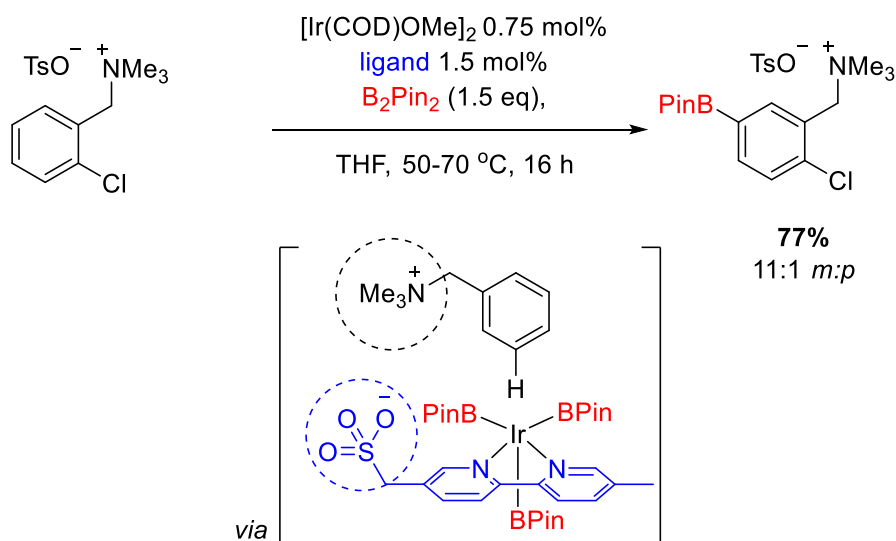
Scheme 1-12: *Ortho* borylation of N-Boc anilines governed by non-covalent interaction.⁶⁹

In a complementary approach, Kanai *et al.*⁷⁰ reported on a *meta* selective C-H borylation directed by non-covalent interactions between the ligand and the substrate on monosubstituted and 1,2 disubstituted arenes bearing amide or phosphonate groups. This strategy incorporates hydrogen bond donor groups onto a bipyridine ligand backbone so that hydrogen bond acceptor groups on the substrate molecule can interact with the ligand and guide the catalyst to the *meta* position (**Scheme 1-13**).



Scheme 1-13: *Meta* borylation governed by hydrogen bonding interaction with the ligand.⁷⁰

A similar strategy was later demonstrated by Phipps *et al.* who reported an ion pairing interaction between ligand and substrate to achieve *meta* selective borylations on arenes bearing quaternary ammonium salts.⁷¹ In this case, bipyridine ligands with an ionic sulfonate group could interact with quaternary ammonium salts derived from aniline and benzylamine derivatives (**Scheme 1-14**).



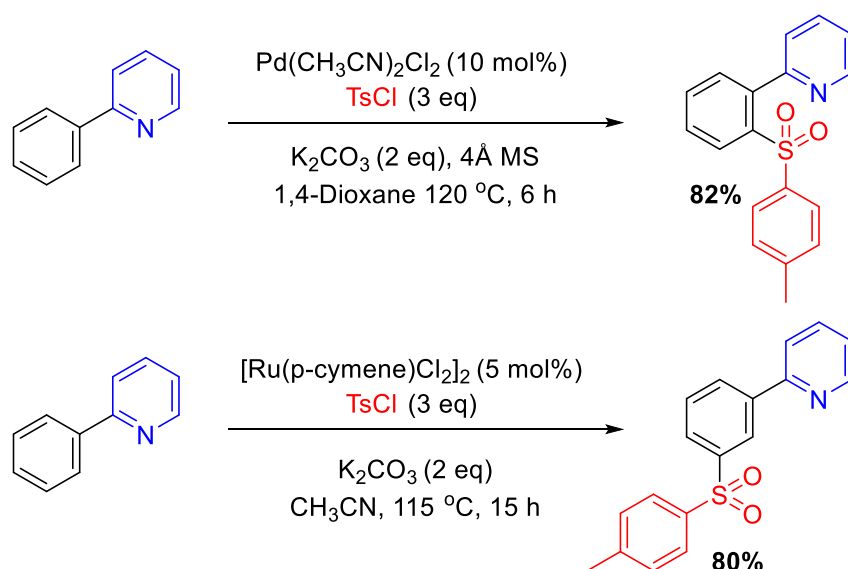
Scheme 1-14: *Meta* borylation governed by ion pair interaction with ligand.⁷¹

Utilising non-covalent interactions has led to a unique and elegant strategy for direct *meta* selective C-H borylations of arenes. This methodology has however only been demonstrated on borylation reactions, transformations which are compatible with mild conditions, effectiveness in non-polar solvents and lack of requirement for acidic additives. These requirements may limit this methodology as non-covalent interactions may be easily disrupted by more aggressive reaction conditions.

1.4 Ruthenium catalysed σ -activation

1.4.1 Sulfonation

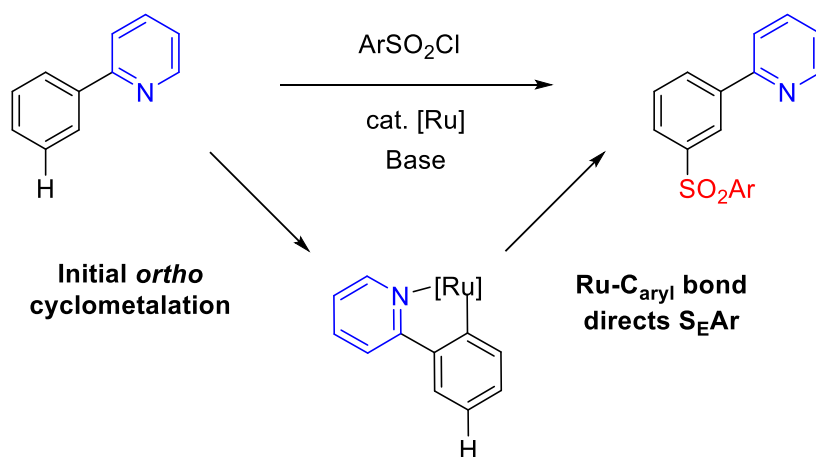
An interesting new approach to achieve *meta* C-H functionalisation by ruthenium catalysis is through remote C-H bond activation through catalytic σ -activation processes. This was first demonstrated by Frost *et al.* in the ruthenium catalysed *meta* sulfonation of 2-phenylpyridines.⁷² This finding was in contrast to an *ortho* selective sulfonation reaction previously reported by Dong *et al.* utilising palladium(II) catalysis⁷³ (**Scheme 15**).



Scheme 1-15: Palladium(II) catalysed *ortho* sulfonation⁷³ and ruthenium(II) catalysed *meta* C-H sulfonation.⁷²

In this reaction, the authors proposed that initial formation of a $\sigma\text{-Ru-C}_{\text{aryl}}$ bond activates the C-H bond *para* to the ruthenium metal centre by inductive and mesomeric effects. Subsequent reaction with aromatic sulfonyl chlorides results in electrophilic aromatic substitution ($\text{S}_{\text{E}}\text{Ar}$) at this activated position to yield net *meta* substituted products (**Scheme 1-16**). This was in contrast to mechanistic studies on the corresponding *ortho* selective

sulfonation where strong evidence for an oxidative addition / reductive elimination to a cyclopalladated complex has been reported.⁷⁴



Scheme 1-16: Proposed mechanism for ruthenium catalysed *meta* sulfonation of 2-phenylpyridines.⁷²

As justification for this mechanism, the authors cited previous stoichiometric transformations on ruthenium complexes bearing cyclometalated phenylpyridine ligands.⁷⁵ The metal atom of these complexes exert mesomeric and inductive effects such that they display increased electron density on the σ -bonded aryl ligand. This enabled organic transformations including nitrations and halogenations onto these complexes (**Figure 1-10**). The cyclometalated ruthenium(II) species shown in **Figure 1-11**, formed by the reaction of $[\text{Ru}(p\text{-cymene})\text{Cl}_2]_2$ with 2-phenylpyridine was also shown to be an effective catalyst, indicating the likely involvement of $\sigma\text{-Ru-C}_{\text{Aryl}}$ complexes in the catalytic cycle.

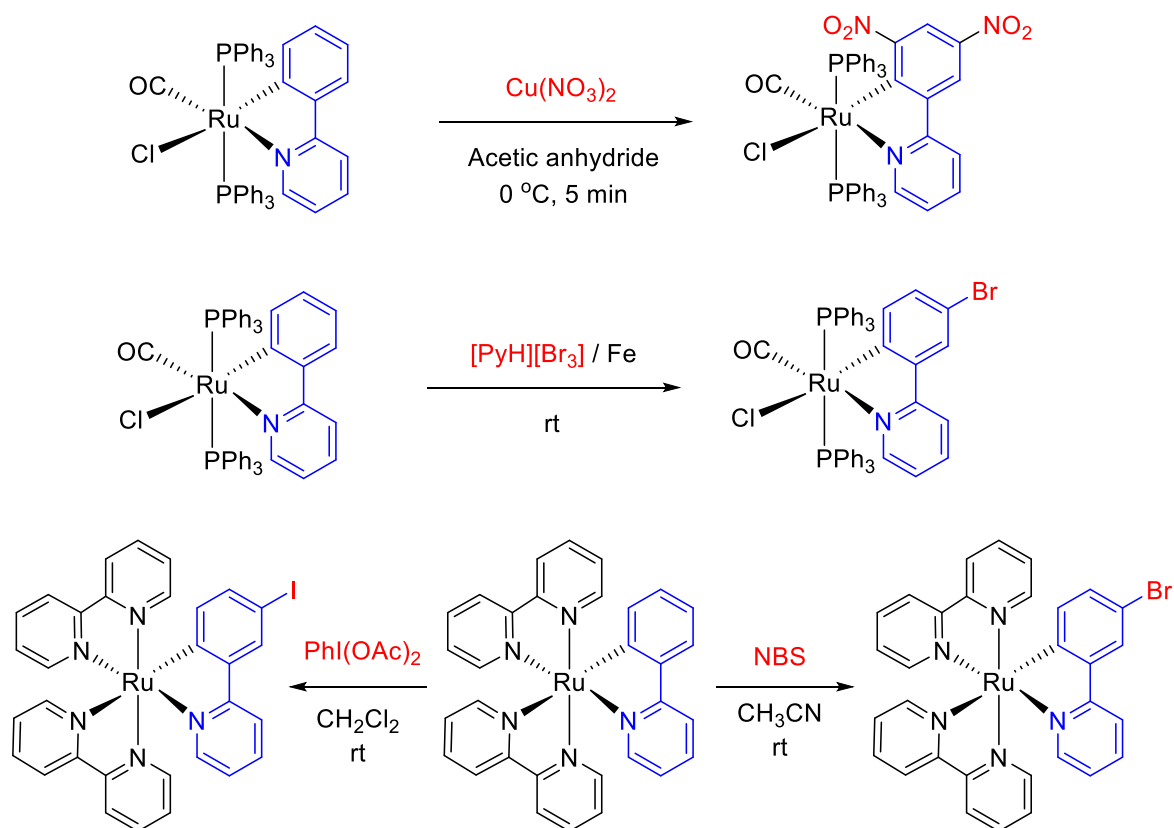


Figure 1-10: Stoichiometric nitrations, bromination and iodination onto ruthenium complexes.⁷⁵

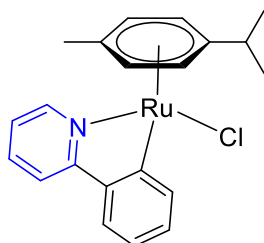
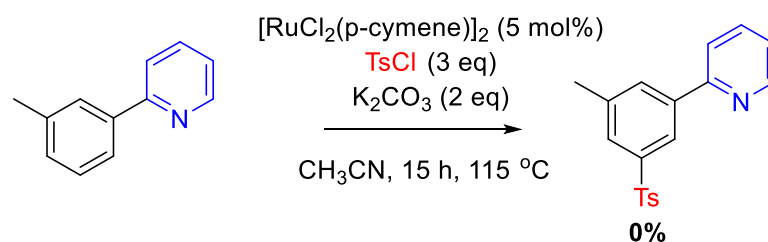


Figure 1-11: Cyclometalated ruthenium(II) species and active catalyst for *meta* sulfonation reaction.

Substrate scope for this reaction is limited to 2-phenylpyridine derivatives and only aromatic sulfonyl chloride derivatives were reported. The notion of substrate activation *para* to the C-Ru bond was also substantiated by the fact that blocking off one *meta* (C3) position resulted in no sulfone product being generated (**Scheme 1-17**). This was rationalised due to cyclometalation occurring at the least hindered *ortho* C-H bond resulting in a complex where the methyl substituent is *para* to the Ru-C_{aryl} bond. With this position blocked, no reaction can take place.



Scheme 1-17: *Meta* sulfonation reaction with C3 methylated substrate.⁷²

The *meta* selective sulfonation reaction of 2-phenylpyridines was the first example reported that utilised a ruthenium catalysed σ -activation strategy. Since this seminal work, a number of other examples have been reported and will be discussed in the following sections.

1.5 Aims and Objectives

At the outset of this investigation, just one example of a *meta* selective C-H functionalisation had been reported by a ruthenium catalysed σ -activation strategy: the *meta* sulfonation of 2-phenylpyridines. Given its benefits of being very operationally simple and highly selective, an overall goal was established to develop it into a broadly useful methodology for *meta* selective C-H functionalisation.

In order to achieve these eventual goals, our group approached the task with a number of complementary strategies. One of these strategies was mechanistically focused. This would include full mechanistic elucidation of the *meta* sulfonation reaction in order to identify the catalytic species and the rate limiting step of the catalytic cycle. With this additional insight, improved catalyst design could achieve the reaction with improved efficiency and could enable new reactions of this type.

Another strategy was to expand the substrate and coupling partner scope through the development of new catalytic reactions. This would have the impact of both making this methodology more synthetically useful as well as providing valuable mechanistic insight and exposing its limitations.

The work described herein details the use of these strategies to achieve new *meta* selective transformations and gain greater mechanistic understanding of *meta* selective ruthenium catalysed σ -activation methodologies.

1.6 References

1. P. A. Wender, V. A. Verma, T. J. Paxton, and T. H. Pillow, *Acc. Chem. Res.*, 2008, **41**, 40–49.
2. W. R. Gutekunst and P. S. Baran, *Chem. Soc. Rev.*, 2011, **40**, 1976–1991.
3. L. McMurray, F. O'Hara, and M. J. Gaunt, *Chem. Soc. Rev.*, 2011, **40**, 1885–1898.
4. J. Yamaguchi, A. D. Yamaguchi, and K. Itami, *Angew. Chem. Int. Ed.*, 2012, **51**, 8960–9009.
5. J. Yang, *Org. Biomol. Chem.*, 2015, **13**, 1930–1941.
6. J. F. Hartwig, *J. Am. Chem. Soc.*, 2016, **138**, 2–24.
7. H. M. L. Davies and D. Morton, *J. Org. Chem.*, 2016, **81**, 343–350.
8. T. Brückl, R. D. Baxter, Y. Ishihara, and P. S. Baran, *Acc. Chem. Res.*, 2012, **45**, 826–839.
9. N. Kuhl, M. N. Hopkinson, J. Wencel-Delord, and F. Glorius, *Angew. Chem. Int. Ed.*, 2012, **51**, 10236–10254.
10. J. Labinger and J. Bercaw, *Nature*, 2002, **417**, 507–514.
11. X. Chen, K. M. Engle, D.-H. Wang, and J.-Q. Yu, *Angew. Chem. Int. Ed.*, 2009, **48**, 5094–5115.
12. K. M. Engle, T. Mei, M. Wasa, and J. Yu, *Acc. Chem. Res.*, 2012, **45**, 788–802.
13. D. A. Colby, A. S. Tsai, R. G. Bergman, and J. A. Ellman, *Acc. Chem. Res.*, 2012, **45**, 814–825.
14. P. B. Arockiam, C. Bruneau, and P. H. Dixneuf, *Chem. Rev.*, 2012, **112**, 5879–5918.
15. S. Ruiz, P. Villuendas, and E. P. Urriolabeitia, *Tetrahedron Lett.*, 2016, **57**, 3413–3432.
16. S. De Sarkar, W. Liu, S. I. Kozhushkov, and L. Ackermann, *Adv. Synth. Catal.*, 2014, **356**, 1461–1479.
17. M. Moselage, J. Li, and L. Ackermann, *ACS Catal.*, 2016, **6**, 498–525.
18. S. Z. Tasker, E. A. Standley, and T. F. Jamison, *Nature*, 2014, **509**, 299–309.
19. X.-X. Guo, D.-W. Gu, Z. Wu, and W. Zhang, *Chem. Rev.*, 2015, **115**, 1622.
20. T. Ishiyama, J. Takagi, K. Ishida, N. Miyaura, N. R. Anastasi, and J. F. Hartwig, *J. Am. Chem. Soc.*, 2002, **124**, 390–391.
21. T. Ishiyama, J. Takagi, J. F. Hartwig, and N. Miyaura, *Angew. Chem. Int. Ed.*, 2002, **41**, 3056–3058.
22. J.-Y. Cho, M. K. Tse, D. Holmes, R. E. Maleczka, and M. R. Smith, *Science*, 2002, **295**, 305–8.
23. D. W. Robbins and J. F. Hartwig, *Angew. Chem. Int. Ed.*, 2013, **52**, 933–937.
24. B. M. Partridge and J. F. Hartwig, *Org. Lett.*, 2013, **15**, 140–143.

25. R. Shrestha, P. Mukherjee, Y. Tan, Z. C. Litman, and J. F. Hartwig, *J. Am. Chem. Soc.*, 2013, **135**, 8480–8483.
26. C. Cheng and J. F. Hartwig, *Science*, 2014, **343**, 853–858.
27. Y. Zhang, B. Shi, and J. Yu, *J. Am. Chem. Soc.*, 2009, **131**, 5072–5074.
28. M. H. Emmert, A. K. Cook, Y. J. Xie, and M. S. Sanford, *Angew. Chem. Int. Ed.*, 2011, **50**, 9409–9412.
29. X. Cong, H. Tang, C. Wu, and X. Zeng, *Organometallics*, 2013, **32**, 6565–6575.
30. G. B. Boursalian, M. Y. Ngai, K. N. Hojczyk, and T. Ritter, *J. Am. Chem. Soc.*, 2013, **135**, 13278–13281.
31. L. T. Ball, G. C. Lloyd-Jones, and C. A. Russell, *Science*, 2012, **337**, 1644–1648.
32. J. Wencel-Delord, C. Nimphius, H. Wang, and F. Glorius, *Angew. Chem. Int. Ed.*, 2012, **51**, 13001–13005.
33. R. J. Phipps and M. J. Gaunt, *Science*, 2009, **323**, 1593–7.
34. H. A. Duong, R. E. Gilligan, M. L. Cooke, R. J. Phipps, and M. J. Gaunt, *Angew. Chem. Int. Ed.*, 2011, **50**, 463–436.
35. D. Leow, G. Li, T.-S. Mei, and J.-Q. Yu, *Nature*, 2012, **486**, 518–522.
36. H. Dai, G. Li, X. Zhang, A. F. Stepan, and J. Yu, *J. Am. Chem. Soc.*, 2013, **135**, 7567–7571.
37. S. Lee, H. Lee, and K. L. Tan, *J. Am. Chem. Soc.*, 2013, **135**, 18778–18781.
38. T. Patra, R. Watile, S. Agasti, T. Naveen, and D. Maiti, *Chem. Commun.*, 2016, **52**, 2027–2030.
39. R.-Y. Tang, G. Li, and J.-Q. Yu, *Nature*, 2014, **507**, 215–220.
40. G. Yang, P. Lindovska, D. Zhu, J. Kim, P. Wang, R. Tang, M. Movassaghi, and J. Yu, *J. Am. Chem. Soc.*, 2014, 10807–10813.
41. S. Li, H. Ji, L. Cai, and G. Li, *Chem. Sci.*, 2015, **6**, 5595–5600.
42. M. Bera, S. K. Sahoo, and D. Maiti, *ACS Catal.*, 2016, **6**, 3575–3579.
43. M. Bera, A. Maji, S. K. Sahoo, and D. Maiti, *Angew. Chem. Int. Ed.*, 2015, **54**, 8515–8519.
44. A. Maji, B. Bhaskararao, S. Singha, R. B. Sunoj, and D. Maiti, *Chem. Sci.*, 2016, **7**, 3147–3153.
45. L. Wan, N. Dastbaravardeh, G. Li, and J. Q. Yu, *J. Am. Chem. Soc.*, 2013, **135**, 18056–18059.
46. M. Bera, A. Modak, T. Patra, A. Maji, and D. Maiti, *Org. Lett.*, 2014, **16**, 5760–5763.
47. Y. Deng and J.-Q. Yu, *Angew. Chem. Int. Ed.*, 2015, **54**, 888–891.
48. S. Li, L. Cai, H. Ji, L. Yang, and G. Li, *Nat. Commun.*, 2016, **7**, 10443.
49. L. Chu, M. Shang, K. Tanaka, Q. Chen, N. Pissarnitski, E. Streckfuss, and J.-Q. Yu, *ACS Cent. Sci.*, 2015, **1**, 394–399.

50. S. Bag, T. Patra, A. Modak, A. Deb, S. Maity, U. Dutta, A. Dey, R. Kancharla, A. Maji, A. Hazra, M. Bera, and D. Maiti, *J. Am. Chem. Soc.*, 2015, **137**, 11888–11891.
51. J. P. Flemming, M. B. Berry, and J. M. Brown, *Org. Biomol. Chem.*, 2008, **6**, 1215–1221.
52. N. Rodríguez and L. J. Goossen, *Chem. Soc. Rev.*, 2011, **40**, 5030–5048.
53. S. Mochida, K. Hirano, T. Satoh, and M. Miura, *Org. Lett.*, 2010, **12**, 5776–5779.
54. S. Mochida, K. Hirano, T. Satoh, and M. Miura, *J. Org. Chem.*, 2011, **76**, 3024–3033.
55. J. Cornella, M. Righi, and I. Larrosa, *Angew. Chem. Int. Ed.*, 2011, **50**, 9429–9432.
56. X. Qin, D. Sun, Q. You, Y. Cheng, J. Lan, and J. You, *Org. Lett.*, 2015, **17**, 1762–1765.
57. P. Mamone, G. Danoun, and L. J. Gooßen, *Angew. Chem. Int. Ed.*, 2013, **52**, 6704–6708.
58. X. Y. Shi, K. Y. Liu, J. Fan, X. F. Dong, J. F. Wei, and C. J. Li, *Chem. - A Eur. J.*, 2015, **21**, 1900–1903.
59. D. Lee and S. Chang, *Chemistry*, 2015, **21**, 5364–5368.
60. J. Luo, S. Preciado, and I. Larrosa, *J. Am. Chem. Soc.*, 2014, **136**, 4109–12.
61. T. Wilhelm and M. Lautens, *Org. Lett.*, 2005, **7**, 4053–4056.
62. X.-C. Wang, W. Gong, L.-Z. Fang, R.-Y. Zhu, S. Li, K. M. Engle, and J.-Q. Yu, *Nature*, 2015, **519**, 334–338.
63. Z. Dong, J. Wang, and G. Dong, *J. Am. Chem. Soc.*, 2015, **137**, 5887–5890.
64. P.-X. Shen, X.-C. Wang, P. Wang, R.-Y. Zhu, and J.-Q. Yu, *J. Am. Chem. Soc.*, 2015, **137**, 11574–11577.
65. J. Han, L. Zhang, Y. Zhu, Y. Zheng, X. Chen, and Z. Huang, *Chem. Commun.*, 2016, **52**, 6903–6906.
66. P. Wang, M. E. Farmer, X. Huo, P. Jain, P. X. Shen, M. Ishoey, J. E. Bradner, S. R. Wisniewski, M. D. Eastgate, and J. Q. Yu, *J. Am. Chem. Soc.*, 2016, **138**, 9269–9276.
67. P. Wang, G.-C. Li, P. Jain, M. E. Farmer, J. He, P.-X. Shen, and J.-Q. Yu, *J. Am. Chem. Soc.*, 2016, **138**, 14092–14099.
68. H. Shi, P. Wang, S. Suzuki, M. E. Farmer, and J.-Q. Yu, *J. Am. Chem. Soc.*, 2016, **138**, 14876–14879.
69. P. C. Roosen, V. A. Kallepalli, B. Chattopadhyay, D. A. Singleton, R. E. Maleczka, and M. R. Smith, *J. Am. Chem. Soc.*, 2012, **134**, 11350–11353.
70. Y. Kuninobu, H. Ida, M. Nishi, and M. Kanai, *Nat. Chem.*, 2015, **7**, 712–717.
71. H. J. Davis, M. T. Mihai, and R. J. Phipps, *J. Am. Chem. Soc.*, 2016, **138**, 12759–12762.
72. O. Saidi, J. Marafie, A. E. W. Ledger, P. M. Liu, M. F. Mahon, G. Kociok-Köhn, M. K.

- Whittlesey, and C. G. Frost, *J. Am. Chem. Soc.*, 2011, **133**, 19298–19301.
73. X. Zhao, E. Dimitrijević, and V. M. Dong, *J. Am. Chem. Soc.*, 2009, **131**, 3466–3467.
74. X. Zhao and V. M. Dong, *Angew. Chemie - Int. Ed.*, 2011, **50**, 932–934.
75. M. Gagliardo, D. J. M. Snelders, P. A Chase, R. J. M. Klein Gebbink, G. P. M. van Klink, and G. van Koten, *Angew. Chem. Int. Ed.*, 2007, **46**, 8558–8573.

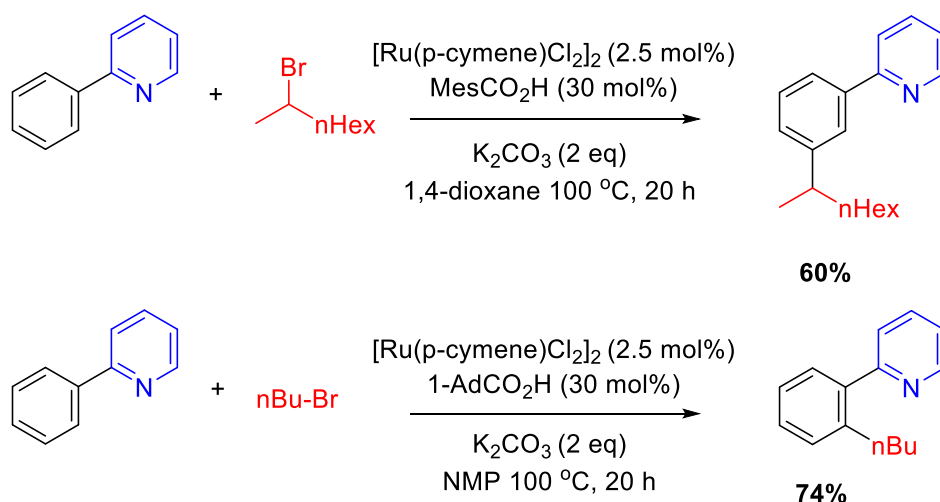
2.0 Catalytic *meta* selective C-H functionalisation to construct quaternary carbon centres

2.1 Introduction and commentary

At the outset of our investigation, there was only one example of ruthenium catalysed *meta* C-H functionalisation; the *meta* sulfonation reaction first reported within the Frost group (**Scheme 1-15**). At this time our research was focused into two interconnected areas: mechanistic studies of the sulfonation reaction (which is discussed in detail in **Chapter 3**) and the development of new *meta* selective reactions.

In order to develop new *meta* selective reactions, many previous attempts within the group had focused on the screening of new electrophilic coupling partners. This was because the working theory was that cyclometalation with ruthenium activated the position *para* to the newly formed C-Ru bond towards S_EAr type reactivity. Within the group this led to limited success in finding new *meta* selective reactions.

In 2013, a second example of *meta* selective functionalisation promoted by ruthenium catalysed σ -activation was reported by Ackermann *et al.*, who achieved a direct *meta* C-H alkylation process using secondary alkyl halides.¹ This was in contrast to other work conducted within the same group which reported *ortho* selective alkylation with primary alkyl halides under similar reaction conditions (**Scheme 2-1**).^{2,3}



Scheme 2-1: *Meta* alkylation with secondary alkyl halides¹ and *ortho* alkylation with primary alkyl halides.²

This process was achieved on substrates directed by pyridine, pyrazole, pyrimidine, imidazole and benzimidazole derivatives. The use of catalytic carboxylic acid additives was also necessary for optimum yields, with 1-AdCO₂H and MesCOOH proving to be especially effective. It was determined that the ruthenium species shown in **Figure 2-1** was generated *in situ* and this complex was subsequently isolated and shown to be catalytically active. It was also noted that the complex given in **Figure 1-11** was not catalytically active in the absence of MesCOOH additive, highlighting the importance of carboxylate assistance.

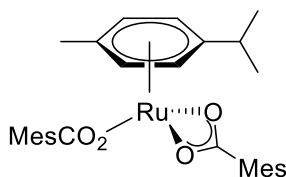
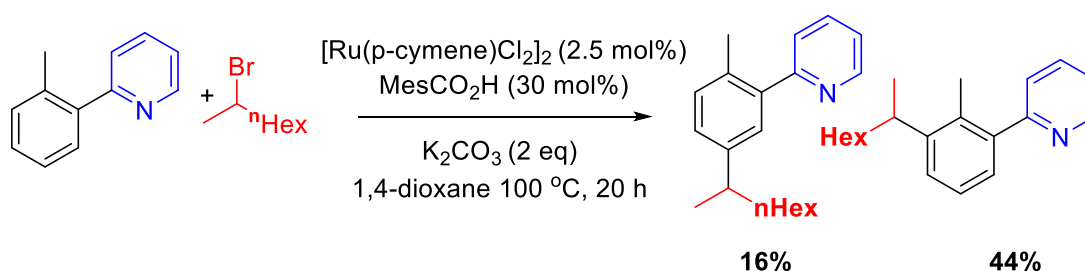


Figure 2-1: Active catalytic species generated *in situ* under the conditions in **Scheme 2-1**.

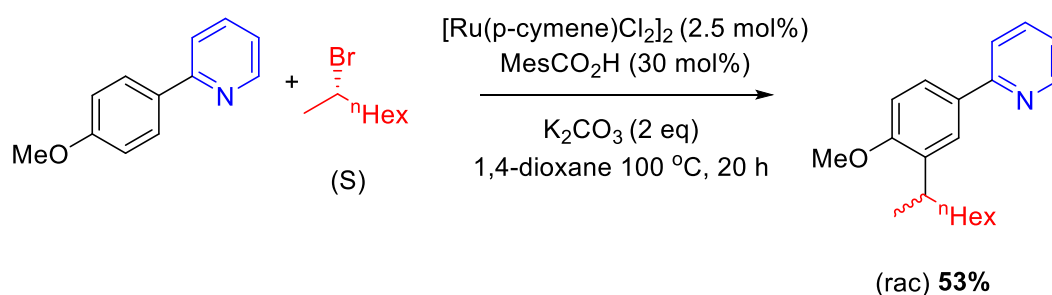
As per the *meta* sulfonation reaction, this reaction was proposed to occur due to initial σ -Ru-C_{aryl} bond formation activating the position *para* to the ruthenium centre for S_EAr. However, unlike the *meta* sulfonation, C2-substituted substrates yielded a mixture of the two possible *meta* regioisomers resulting from electrophilic attack at the *ortho* and *para* positions with respect to the ruthenium centre. A clear preference for the least hindered *para* position was nevertheless observed (**Scheme 2-2**).



Scheme 2-2: *meta* alkylation reaction using C2-substituted substrates.¹

Some additional mechanistic studies were also carried out on this reaction. KIE experiments were conducted and were indicative of a reversible *ortho* C-H activation and a non-kinetically relevant *meta* C-H bond cleavage step. Reaction with an enantiomerically pure alkyl halide showed that racemisation occurred under the reaction conditions (**Scheme 2-3**) and it was also noted that in the presence of stoichiometric amounts of

TEMPO, no alkylation of the substrate was observed. Nevertheless, the authors proposed an overall mechanism with an electrophilic alkylation step (**Figure 2-2**).



Scheme 2-3: *meta* alkylation reaction using enantiomerically pure alkyl halide.

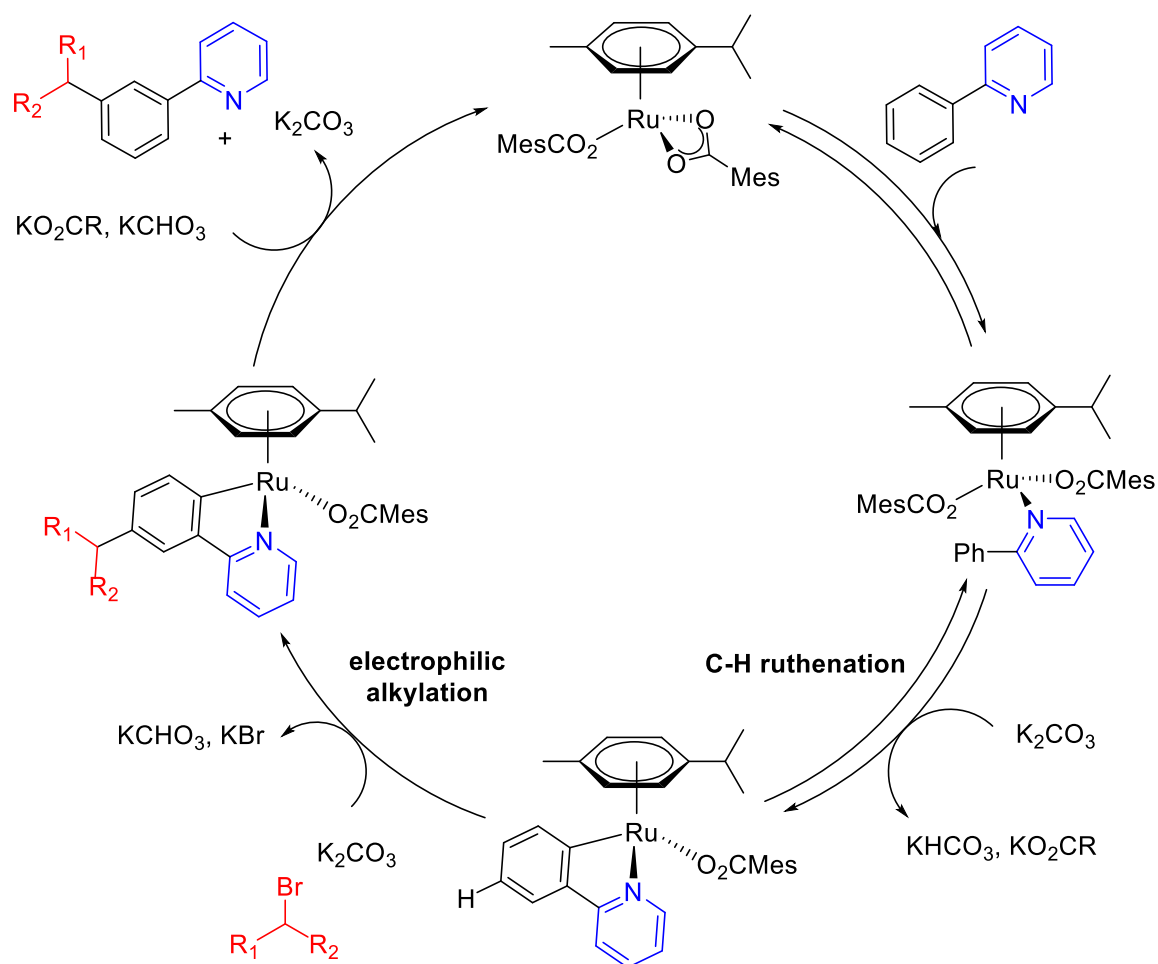


Figure 2-2: Proposed mechanism for *meta* alkylation with secondary alkyl halides.

While this second example of ruthenium catalysed σ -activation provided valuable new insight into this class of reaction, it was not immediately apparent why sulfonyl chlorides

and secondary alkyl halides would react with overall *meta* selectivity while many more examples in the literature reacted with *ortho* selectivity under analogous conditions. However, the crucial result shown in **Scheme 2-3** began to narrow our search of effective coupling partners. Reaction with an enantiomerically enriched secondary alkyl halide resulted in a racemic product, showing that this reaction could not be reacting via an S_N2 type mechanism. Instead a planar intermediate consistent with either an S_N1 or a radical mechanism must have been operative. As a result of this, our focus changed to testing coupling partners that could readily react *via* one of these two mechanisms and it was soon found that tert-butyl bromide was a successful coupling partner. This was the first result in the paper entitled: "Catalytic *meta* selective C-H functionalisation to construct quaternary carbon centres." which was accepted as a communication by the RSC journal Chemical Communications.

2.2 Authorship and permissions

Statement of Authorship Form

This declaration concerns the article entitled:									
Catalytic <i>meta</i> -selective C-H functionalization to construct quaternary carbon centres.									
Publication status (tick one)									
Draft manuscript	<input type="checkbox"/>	Submitted	<input type="checkbox"/>	In review	<input type="checkbox"/>	Accepted	<input type="checkbox"/>	Published	<input checked="" type="checkbox"/>
Publication details	<p>Chem. Commun., 2015,51, 12807-12810</p> <p>DOI: 10.1039/C5CC03951G</p> <p>Received 12 May 2015, Accepted 06 Jul 2015</p> <p>First published online 06 Jul 2015</p>								
Candidates contribution to the paper	<p>The candidate contributed to/ considerably contributed to/predominantly executed the...</p> <p>Formulation of ideas (33%):</p> <p>Andrew J. Paterson, Sahra St John-Campbell and Christopher G. Frost contributed equally.</p> <p>Design of methodology (70%):</p> <p>First reaction hit achieved by Sahra St John-Campbell. Subsequent optimization conducted by Andrew J. Paterson.</p> <p>Experimental work (50%):</p> <p>Andrew J. Paterson: Synthesis of Starting materials. Reaction Optimization. Reactions with t-Bu-Br. Mechanistic studies. Sahra St John-Campbell: Reactions with different tertiary alkyl halides. Mary F. Mahon: X-Ray Crystallography.</p> <p>Presentation of data in journal format (80%):</p> <p>Andrew J. Paterson: Main author of manuscript and supporting information. Sahra St John-Campbell: Structure assignment of some novel compounds. Christopher G. Frost: Predominant author of manuscript introduction and accompanying Scheme.</p>								
Statement from Candidate	This paper reports on original research I conducted during the period of my Higher Degree by Research candidature.								
Signed						Date			

2.3 Manuscript for: Catalytic *meta*-selective C-H functionalization to construct quaternary carbon centres

Catalytic *meta*-selective C-H functionalization to construct quaternary carbon centres

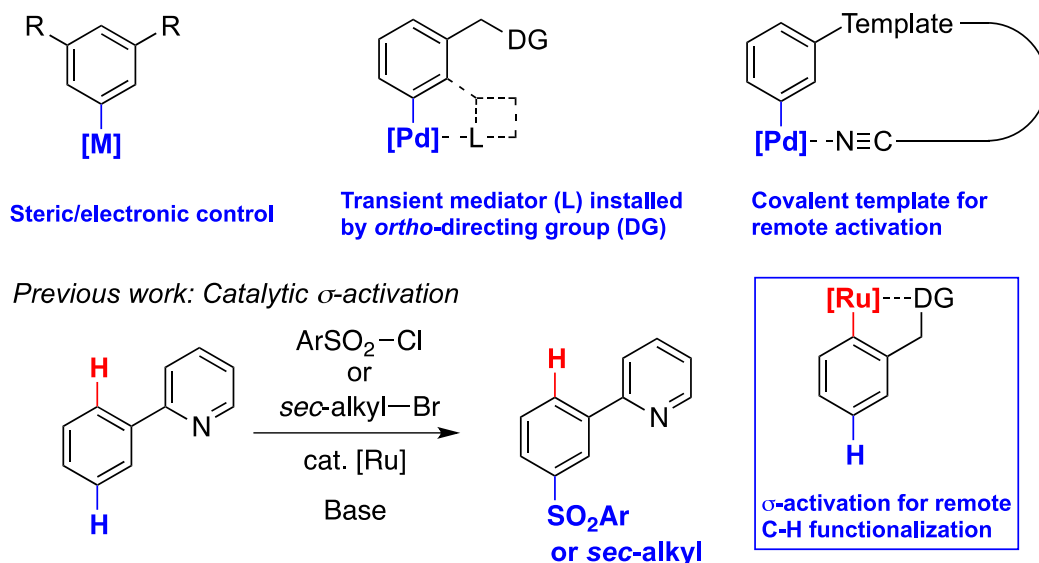
Andrew J. Paterson, Sahra St John-Campbell, Mary F. Mahon, Neil J. Press and Christopher G. Frost

A catalytic *meta*-selective C-H functionalization of 2-phenylpyridines using a range of tertiary halides is described. The protocol is simple to perform and uses commercially available reagents to construct challenging quaternary carbon centres in a regioselective manner. Preliminary studies suggest the C-H functionalization proceeds through a radical process directed via a remote σ -activation.

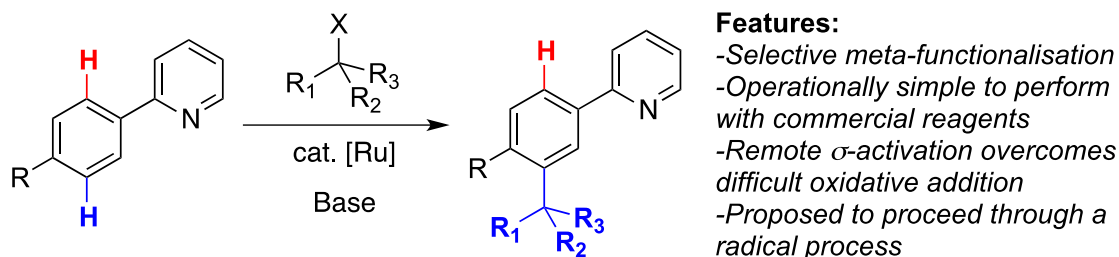
The transition-metal catalyzed cleavage and functionalization of inert C-H bonds is evolving into a fundamental methodology for the design of atom economical approaches to useful organic molecules.¹ While the direct functionalization at the *ortho* position of aromatic compounds by chelation assisted C-H bond cleavage has become well established in recent years, developing reactions with complementary regioselectivity continues to challenge contemporary catalytic methodology.² In this context, examples of *meta* selective catalytic C-H functionalization have been reported offering diversity in molecular design through alternative reaction strategies (Scheme 1a). These include substrate controlled systems,³ transient mediators such as a carboxylic acid⁴ or norbornene⁵ and covalent template strategies for remote activation.⁶ We first reported a novel catalytic σ -activation protocol for C-H functionalization that allows the *meta* sulfonation of 2-phenylpyridines *via* cyclometalated ruthenium intermediates.⁷ Interestingly, the catalytic σ -activation strategy proved effective for *meta*-alkylations with secondary alkyl halides⁸ whilst acyl halides and primary alkyl halides afford only the *ortho*-functionalized products consistent with a mechanism involving oxidative addition of the organohalide.⁹

Here we report a new catalytic *meta*-selective C-H functionalization of 2-phenylpyridines to construct quaternary carbon centres (Scheme 1b). The transition-metal catalyzed coupling of tertiary alkyl halides and aromatic C-H bonds is an especially challenging reaction due to the difficult oxidative addition of a metal complex into a bulky C–X bond.¹⁰ We hypothesized that a catalytic σ -activation strategy would therefore be amenable to establishing quaternary carbon centres by avoiding a general oxidative addition pathway.

(a) Key catalytic strategies for meta-directed C-H functionalization



(b) This work: Catalytic meta-directed construction of quaternary carbon centres



Scheme 1 Catalytic *meta*-directed C-H functionalization

In preliminary experiments, 2-phenylpyridine **1a** was treated under conditions analogous to those developed in our *meta*-sulfonation reaction: $[\text{RuCl}_2(p\text{-cymene})]_2$ (5 mol%) K_2CO_3 (2 equiv), *t*-BuBr **2a** (3 equiv) using MeCN as the solvent.⁷ Unfortunately no coupled products were formed under these conditions however the desired *meta*-substituted product was observed in 12% conversion when the reaction solvent was changed to 1,4-Dioxane (Table 1: Entries 1-2). By simply changing the base from K_2CO_3 to various acetate salts, a significant increase in conversion was observed with KOAc proving the most effective (Entry 6). In the absence of ruthenium complex, no product was observed (Entry 11). This catalytic system was found to perform well in a range of solvents as well as under solvent free conditions and was completed in as little as 4 hours (Entry 14). When *t*-BuCl **2b** was used as the coupling reagent, a significant drop in conversion was observed, however by using a combination of K_2CO_3 and KOAc, the reaction performed competitively (Entry 17). For full optimisation see Supporting Information.

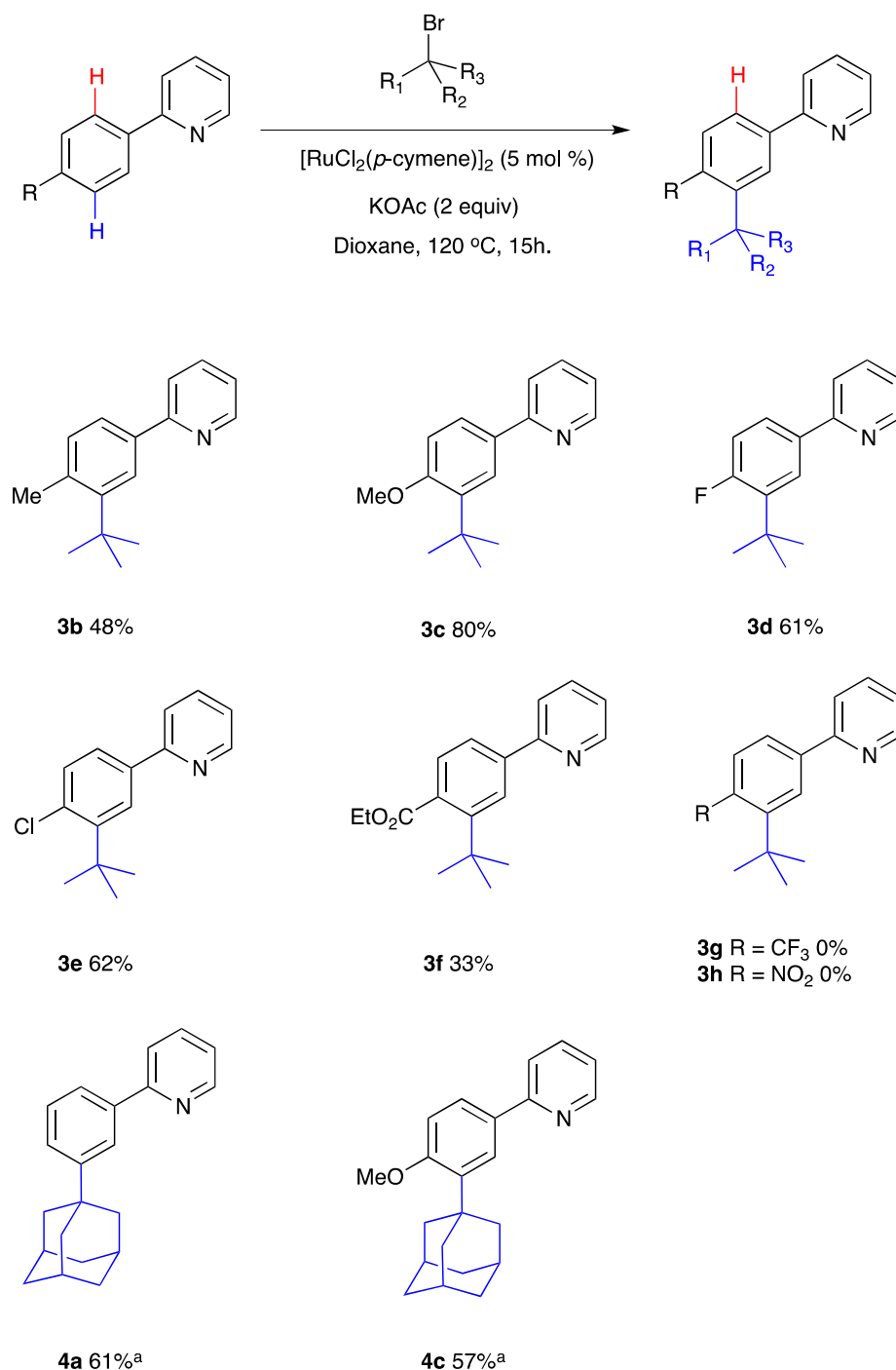
Table 1 Optimization of catalytic *meta* tertiary alkylation

Entry	<i>t</i> -Bu-X	Base	Solvent	Conversion (%) ^a
1	2a	K ₂ CO ₃	MeCN	0
2	2a	K ₂ CO ₃	1,4-Dioxane	12
3	2a	KOAc	neat	69
4	2a	KOAc	2-Me-THF	68
5	2a	KOAc	2-Butanone	61
6	2a	KOAc	1,4-Dioxane	74
7 ^b	2a	K ₂ CO ₃	1,4-Dioxane	60
8	2a	NaOAc	1,4-Dioxane	31
9	2a	CsOAc	1,4-Dioxane	64
10	2a	Bu ₄ NOAc	1,4-Dioxane	13
11 ^c	2a	KOAc	1,4-Dioxane	0
12 ^d	2a	KOAc	1,4-Dioxane	25
13 ^e	2a	KOAc	1,4-Dioxane	50
14 ^f	2a	KOAc	1,4-Dioxane	72
15	2b	KOAc	1,4-Dioxane	20
16	2b	K ₂ CO ₃	1,4-Dioxane	27
17	2b	KOAc (0.5 equiv) K ₂ CO ₃ (1.5 equiv)	1,4-Dioxane	63
18 ^b	2b	K ₂ CO ₃	1,4-Dioxane	62

^a Conversion of **1a** to **3a** by ¹H NMR. ^b With 30 mol% MesCOOH ^c Without [RuCl₂(*p*-cymene)]₂. ^d Reaction in air. ^e [RuCl₂(*p*-cymene)]₂ (1 mol%). ^f Reaction time 4 h.

With optimized catalytic systems in hand, we then investigated how reaction conversions were affected when substituents at the 4-position of the aryl ring were varied (Scheme 2). It was found that electron donating substituents favoured the reaction whereas strongly electron withdrawing groups shut the reaction down entirely. The reaction was tolerant of halogen and ester substituents which is useful for further synthetic transformations. The reactions led to the sole formation of the mono substituted *meta* products with no

decomposition or by-products observed although quantitative separation by conventional methods was not always possible (see supporting information for full analysis). Intriguingly, 1-bromoadamantane was found to be an effective coupling partner and product **4c** was characterised by X-ray analysis confirming the regioselective *meta* substitution (Figure 1).¹¹



Scheme 2 Catalytic *meta* functionalization using tertiary alkyl bromides. Numbers quoted are direct conversions to product by ¹H NMR. ^a Using KOAc (0.5 equiv) and K₂CO₃ (1.5 equiv).

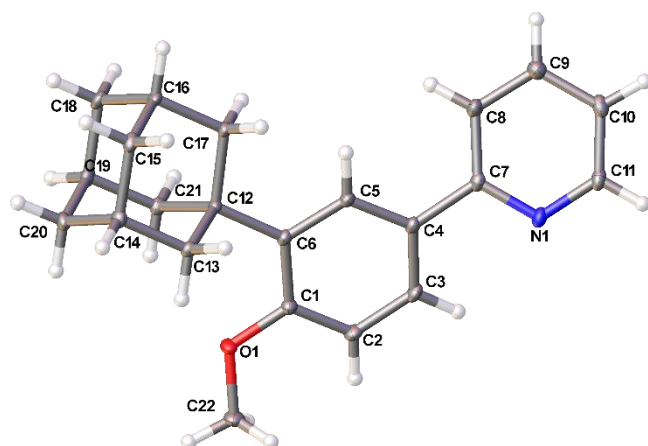
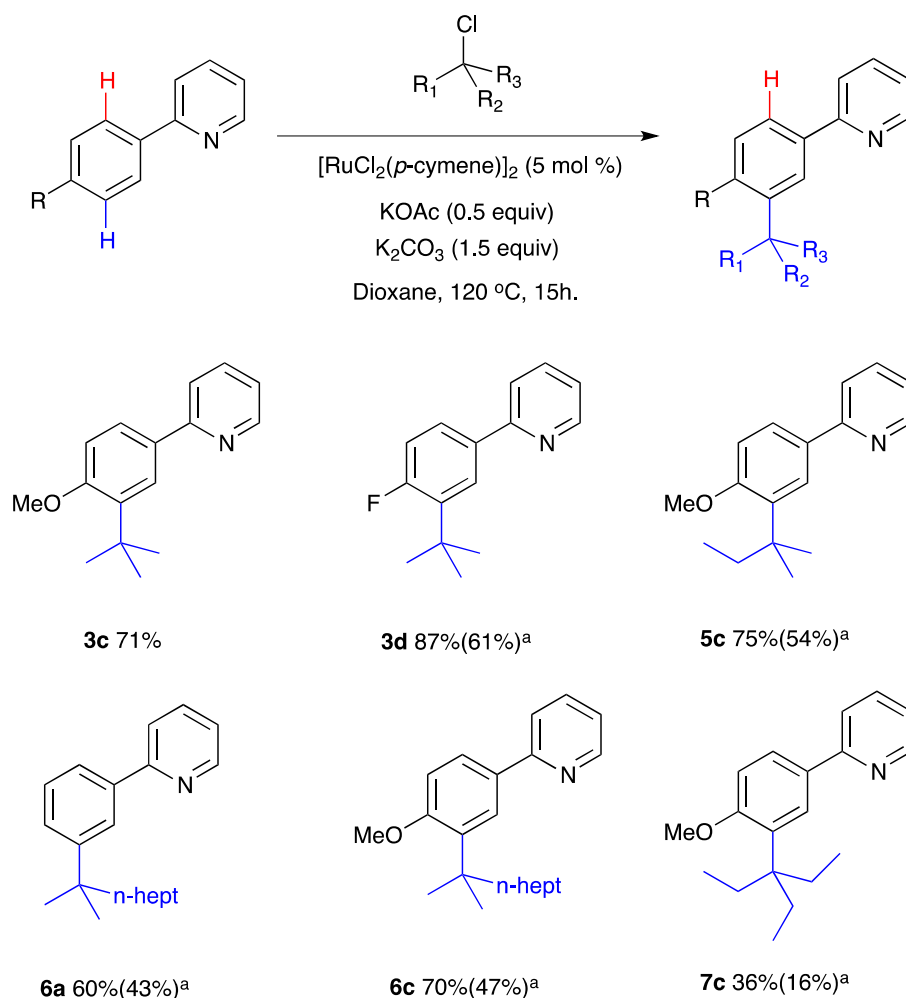


Figure 1 The asymmetric unit in the crystal structure of **4c**. Ellipsoids are illustrated at 30% probability.

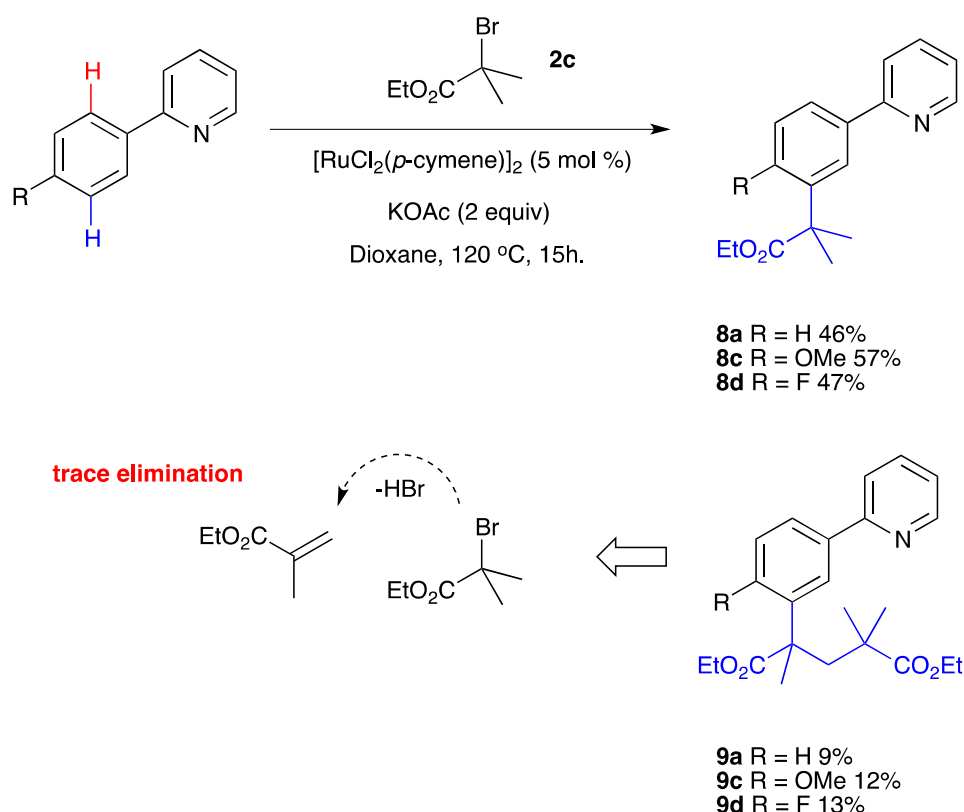
Our procedure also effectively coupled a range of tertiary alkyl chlorides, reagents which are readily available and generally considered to be less reactive (Scheme 3). In these examples, it was found that the incorporation of longer alkyl chain lengths maintained high conversions and enabled better separation of the products by normal phase flash chromatography.



Scheme 3 Catalytic *meta* functionalization using alkyl chloride reagents. Numbers quoted are direct conversions to product by ^1H NMR. ^a Numbers in brackets indicate isolated yields.

In addition to the alkyl halide reagents outlined in Schemes 2 and 3, tertiary α -bromo ester **2c** was effectively coupled, generating *meta*-substituted products **8a**, **8c** and **8d**, compounds with a useful functional handle, in reasonable isolated yields (Scheme 4). This result provided key insight into the reaction mechanism and strongly suggested a radical type pathway, rather an $\text{S}_{\text{E}}\text{Ar}$ type mechanism previously proposed in our *meta*-sulfonation reaction.⁷ Heterolytic cleavage of the C-X bond of **2c** in an $\text{S}_{\text{N}}1$ -type manner would result in a strongly disfavoured carbocation residing alpha to an electron withdrawing ester. It is therefore unlikely that reaction with the aromatic substrate would occur in this fashion. The possibility of $\text{S}_{\text{N}}2$ type reactivity can also be effectively ruled out given the steric effects of the tertiary alkyl halides used. The generation of tertiary alkyl radicals has however been widely reported with a range of transition metal catalysts and shown to be effective in the substitution of aromatics, heteroaromatics and olefins.¹² In contrast to the reactions with simple alkyl-halides outlined in Schemes 2 and 3 which led to the sole formation of one

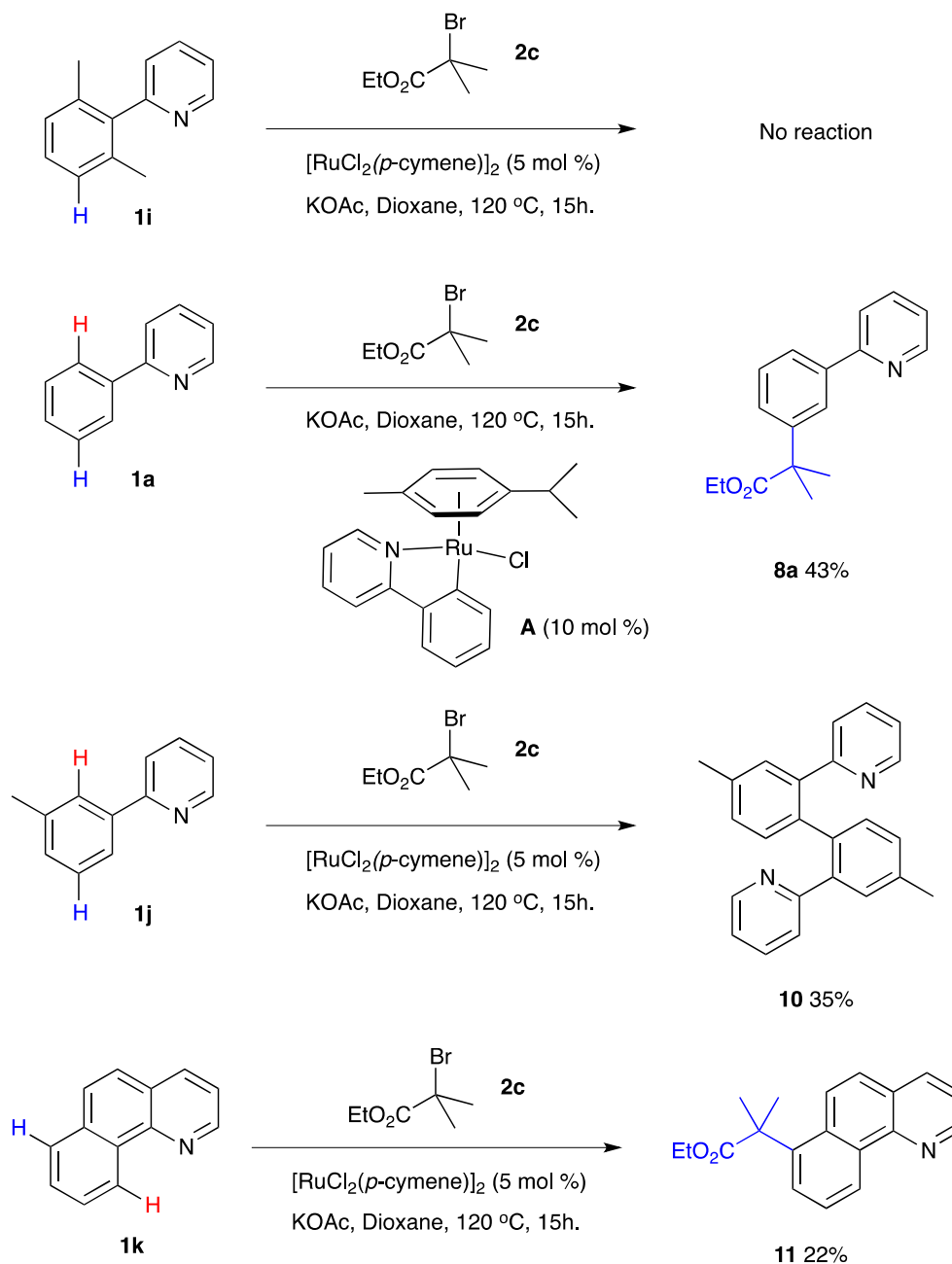
product, reaction with **2c** generated additional by-products. Compounds **9a**, **9c** and **9d** were isolated along with spectroscopic evidence of trace higher oligomers and are consistent with a radical conjugate polymerisation pathway. We hypothesise that a tertiary carbon-centered radical species can add onto elimination products formed under the reaction conditions, which can in turn propagate onto a cyclometalated (σ -activated) substrate molecule to afford the observed by-products. Furthermore, the addition of radical scavenger TEMPO proved detrimental to the reaction with no desired product observed when stoichiometric quantities were used (See Supporting Information).



Scheme 4 Catalytic *meta* functionalization with α -bromo ester **2c**. Numbers quoted are isolated yields.

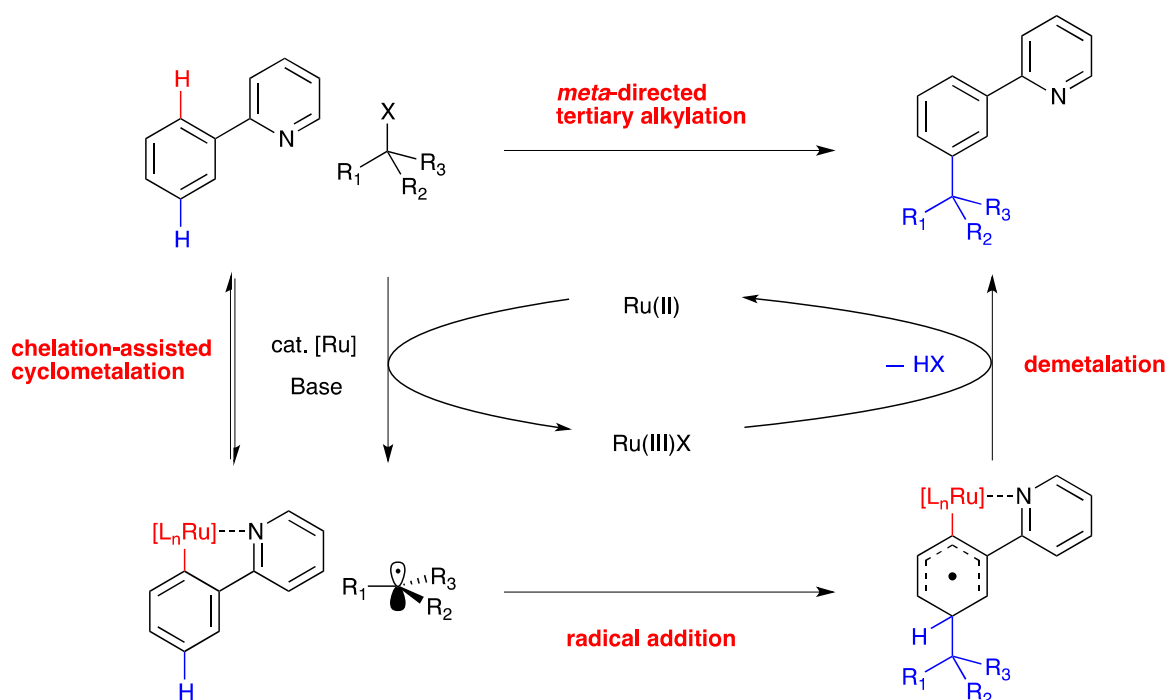
Further mechanistic work was conducted to provide additional insight into the interesting *meta* selectivity displayed by this reaction (Scheme 5). It has previously been proposed that initial ruthenium insertion into an *ortho* C-H bond to generate a cyclometalated complex is key to this type of reactivity.^{7,8} In support of this, reaction of the *ortho*, *ortho* dimethyl substrate **1i** resulted in no conversion to the desired *meta* substituted product. The importance of ruthenium σ -activation is also highlighted with the successful *meta*-selective reaction using pre-formed complex **A**. No *meta*-substituted product was observed when substrate **1j** bearing a methyl group at the 3-position of the aromatic ring was used. Instead,

the only product isolated was dimer **10** suggesting a competing reductive elimination of two coordinated substrate molecules when the site *para* to the C-Ru bond is blocked.¹³ Conformationally locked benzoquinoline **1k** was however effectively alkylated generating **11** as the only isolated product. Together these results suggest that substitution occurs preferentially at a position *para* to the C-Ru bond formed following cyclometalation. Interestingly, analogous reactivity has also recently been reported in a stoichiometric process on iridium complexes.¹⁴



Scheme 5 Mechanistic Investigation. Numbers quoted are isolated yields.

In light of this work we now propose the following mechanism (Scheme 6). Initial *ortho* C-H insertion generates a cyclometalated complex, a process shown to be reversible and aided by carboxylate ligands.¹⁵ Substitution at the position *para* to the newly installed C-Ru bond then most likely occurs *via* a radical process whereby single-electron transfer (SET) from a ruthenium(II) species can generate a tertiary alkyl radical and the corresponding ruthenium(III)X species. The carbon-centered radical then adds to the aromatic ring to generate a cyclohexadienyl radical intermediate. Rearomatisation could occur *via* single-electron oxidation and deprotonation to regenerate a ruthenium(II) complex and furnish the *meta* alkylated product after proto-demetalation.



Scheme 6 Proposed Catalytic Cycle.

In summary, we have developed a novel *meta* selective catalytic C-H functionalisation of 2-phenylpyridine substrates for the installation of quaternary carbon centres. The procedure is operationally simple and was found to couple a useful range of tertiary alkyl bromides and more challenging tertiary alkyl chlorides. Mechanistic studies indicate that site selective radical addition occurs at the position *para* to the C-Ru bond formed following cyclometalation to afford products with net *meta* substitution. More detailed mechanistic studies are underway to determine the precise nature of the organometallic species and redox processes involved.

Notes and references

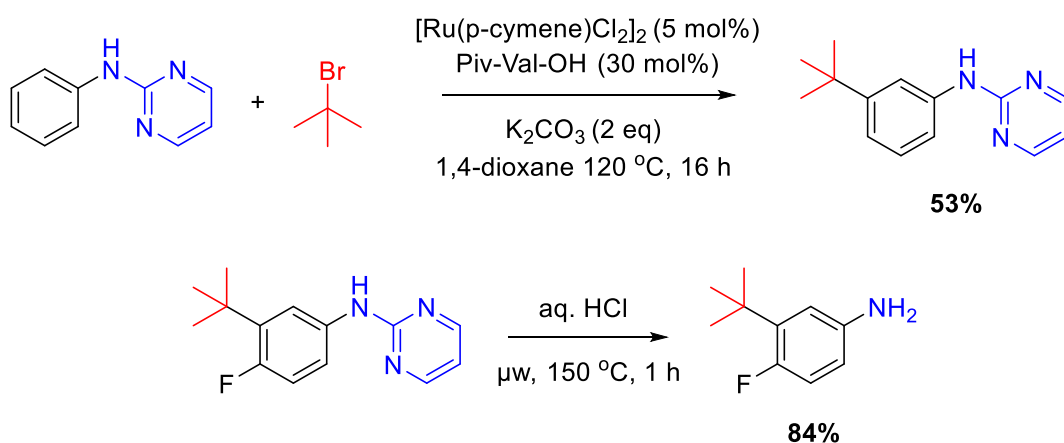
- 1 For selected reviews, see: (a) J. Yamaguchi, A. D. Yamaguchi and K. Itami, *Angew. Chem., Int. Ed.*, 2012, **51**, 8960; (b) L. McMurray, F. O'Hara and M. J. Gaunt, *Chem. Soc. Rev.*, 2011, **40**, 1885; (c) C.-L. Sun, B.-J. Li and Z.-J. Shi, *Chem. Rev.*, 2011, **111**, 1293; (d) J. Wencel-Delord, T. Droge, F. Liu and F. Glorius, *Chem. Soc. Rev.*, 2011, **40**, 4740; (e) C. S. Yeung and V. M. Dong, *Chem. Rev.*, 2011, **111**, 1215; (f) *Topics in Current Chemistry: C–H Activation*, ed. J. -Q. Yu and Z. Shi, 1st edn, 2010, Springer, Berlin Heidelberg.
- 2 (a) F. Julia-Hernandez, M. Simonetti and I. Larrosa, *Angew. Chem., Int. Ed.*, 2013, **52**, 11458; (b) J. Yang, *Org. Biomol. Chem.*, 2015, **13**, 1930.
- 3 (a) H. A. Duong, R. E. Gilligan, M. L. Cooke, R. J. Phipps and M. J. Gaunt, *Angew. Chem., Int. Ed.*, 2011, **50**, 463; (b) R. J. Phipps and M. J. Gaunt, *Science*, 2009, **323**, 1593. For an excellent review of non-chelate-assisted C-H activation, see: (c) N. Kuhl, M. N. Hopkinson, J. Wencel-Delord and F. Glorius, *Angew. Chem., Int. Ed.*, 2012, **51**, 10236.
- 4 (a) J. Luo, S. Preciado and I. Larrosa, *J. Am. Chem. Soc.*, 2014, **136**, 4109; (b) S. Mochida, K. Hirano, T. Satoh and M. Miura, *Org. Lett.*, 2010, **12**, 5776; (c) J. Cornella, M. Righi and I. Larrosa, *Angew. Chem., Int. Ed.*, 2011, **50**, 9429.
- 5 (a) X. -C. Wang, W. Gong, L. -Z. Fang, R. -Y. Zhu, S. Li, K. M. Engle and J.-Q. Yu, *Nature*, 2015, **519**, 334; (b) Z. Dong, J. Wang and G. Dong, *J. Am. Chem. Soc.*, 2015, **137**, DOI: 10.1021/jacs.5b02809.
- 6 For selected examples, see: (a) D. Leow, G. Li, T.-S. Mei and J.-Q. Yu, *Nature*, 2012, **486**, 518; (b) H.-X. Dai, G. Li, X.-G. Zhang, A. F. Stepan and J.-Q. Yu, *J. Am. Chem. Soc.*, 2013, **135**, 7567; (c) L. Wan, N. Dastbaravardeh, G. Li and J.-Q. Yu, *J. Am. Chem. Soc.*, 2013, **135**, 18056; (d) G. Yang, P. Lindovska, D. Zhu, J. Kim, P. Wang, R.-Y. Tang, M. Movassaghi and J.-Q. Yu, *J. Am. Chem. Soc.*, 2014, **136**, 10807; (e) R.-Y. Tang, G. Li and J.-Q. Yu, *Nature*, 2014, **507**, 215.
- 7 (a) O. Saidi, J. Marafie, A. E. W. Ledger, P. M. Liu, M. F. Mahon, G. Kociok-Köhn, M. K. Whittlesey and C. G. Frost, *J. Am. Chem. Soc.*, 2011, **133**, 19298; (b) W. R. Reynolds, P. M. Liu, G. Kociok-Köhn and C. G. Frost, *Synlett*, 2013, **24**, 2687.
- 8 N. Hofmann and L. Ackermann, *J. Am. Chem. Soc.*, 2013, **135**, 5877.
- 9 (a) P. M. Liu and C. G. Frost, *Org. Lett.*, 2013, **15**, 5862; (b) L. Ackermann, N. Hofmann and R. Vicente, *Org. Lett.* 2011, **13**, 1875.
- 10 For selected reviews, see: (a) J. Christoffers and A. Mann, *Angew. Chem. Int. Ed.*, 2001, **40**, 4591; (b) P. G. Cozzi, R. Hilgraf and N. Zimmermann, *Eur. J. Org. Chem.* 2007, 5969; (c) O. Riant and J. Hannedouche, *Org. Biomol. Chem.* 2007, **5**, 873; (d)

- Y. Tu and B. Wang, *Acc. Chem. Res.* 2011, **44**, 1207; (e) A. Y. Hong and B. M. Stoltz, *Eur. J. Org. Chem.*, 2013, 2745; (f) T. Nishikata and S. Ishikawa, *Synlett*, 2015, **26**, 716.
- 11 Crystallographic data have been deposited with Cambridge Crystallographic Data Centre; CCDC-1064109. Copies of these data can be obtained free of charge via <http://www.ccdc.cam.ac.uk/conts/retrieving.html> (or from the Cambridge Crystallographic Data Centre, 12, Union Road, Cambridge, CB2 1EZ, UK; Fax: +44 1223 336033; email: deposit@ccdc.cam.ac.uk).
- 12 For selected examples, see: (a) C. Liu, D. Liu, W. Zhang, L. Zhou, and A. Lei, *Org. Lett.*, 2013, **15**, 6166; (b) X. Wu, J. W. T. See, K. Xu, H. Hirao, J. Roger, J.-C. Hierso, and J. S. Zhou, *Angew. Chemie Int. Ed.*, 2014, **53**, 13573; (c) T. Nishikata, Y. Noda, R. Fujimoto, and T. Sakashita, *J. Am. Chem. Soc.*, 2013, **135**, 16372.
- 13 This pathway is also favoured on steric grounds when substrate bearing a methyl group at the 2-position of the aromatic ring was used (see supporting information).
- 14 J. J. Devery III, J. J. Douglas, J. D. Nguyen, K. P. Cole, R. a. Flowers II, and C. R. J. Stephenson, *Chem. Sci.*, 2015, **6**, 537.
- 15 (a) E. Ferrer Flegeau, C. Bruneau, P. H. Dixneuf, and A. Jutand, *J. Am. Chem. Soc.*, 2011, **133**, 10161. (b) L. Ackermann, *Chem. Rev.*, 2011, **111**, 1315.

2.4 Post-commentary

Since being published, this paper has received a number of citations and was selected among the top 25 most downloaded by Chemical Communications July-September 2015. Crucially this work gave significant evidence for a radical type mechanism, particularly from the results obtained using the α -halo carbonyl reagents and the associated polymer type products. Furthermore, this work was the first to propose a potential dual role of the ruthenium catalyst, both as an activator for the substrate and the coupling partner.

In the months following, an analogous tertiary alkylation from the Ackermann group, was reported which supported many of the propositions made by the title manuscript and also provided additional scope and insight.⁴ In addition to enabling *meta* tertiary alkylations with alkyl bromides on phenylpyridine, pyrimidine and pyrazole containing substrates, a removable pyrimidine based auxiliary was also demonstrated, enabling a range of *meta* functionalised aniline derivatives (**Scheme 2-4**). The authors also reported on the importance of N-protected amino acid ligands with Piv-Val-OH providing the best results.



Scheme 2-4: Tertiary alkylation on aniline derivatives with removable auxiliary.⁴

Additional mechanistic work was also conducted on phenylpyridine derivatives. This revealed the importance of the alkyl bromide in the demetallation step and deuterium labelling studies identified the *meta* C-H bond cleavage as being kinetically relevant. The authors also proposed a radical addition of the alkyl halide onto the substrate. This was substantiated by epimerisation of bromo-4-phenylcyclohexanes as well as radical clock experiments. Furthermore the authors also proposed a dual role of the ruthenium, for activation of the substrate molecule and for the generation of an alkyl radical, and led to an overall mechanism, consistent with the one previously proposed by our group.⁵

2.5 References

1. N. Hofmann and L. Ackermann, *J. Am. Chem. Soc.*, 2013, **135**, 5877–5884.
2. L. Ackermann, P. Novák, R. Vicente, and N. Hofmann, *Angew. Chem. Int. Ed.*, 2009, **48**, 6045–6048.
3. L. Ackermann, N. Hofmann, and R. Vicente, *Org. Lett.*, 2011, **13**, 1875–1877.
4. J. Li, S. Warratz, D. Zell, S. De Sarkar, E. E. Ishikawa, and L. Ackermann, *J. Am. Chem. Soc.*, 2015, **137**, 13894–13901.
5. A. Paterson, S. St John-Campbell, M. F. Mahon, N. Press, and C. G. Frost, *Chem. Commun.*, 2015, **51**, 12807–12810.

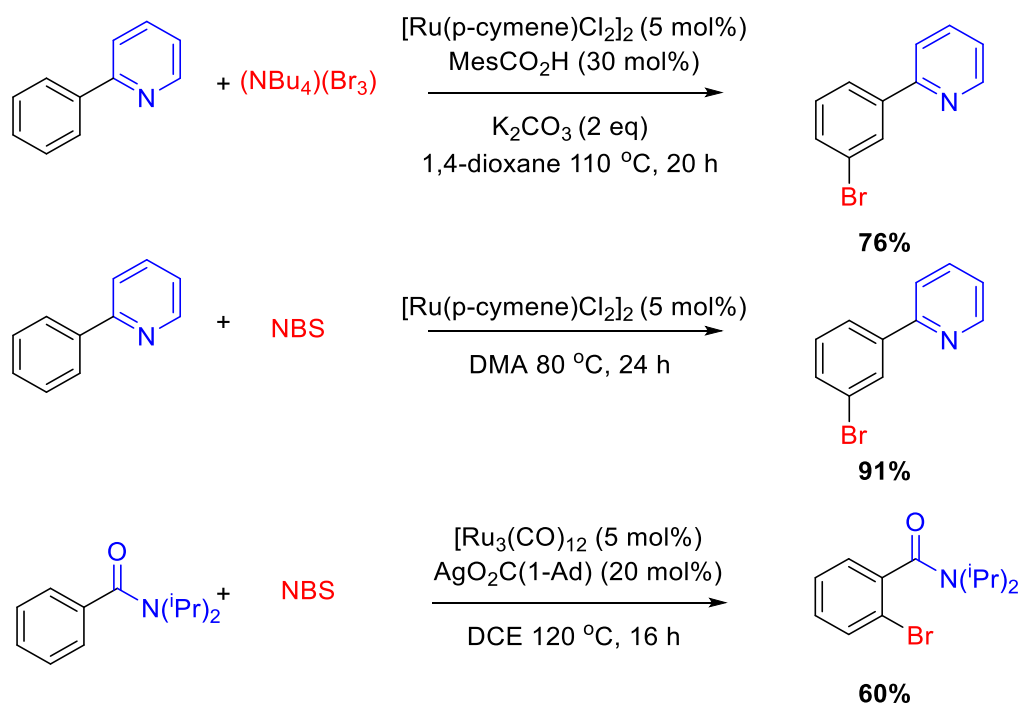
3.0 Mechanistic insight into ruthenium catalysed *meta* sulfonation of 2-phenylpyridine

3.1 Introduction and commentary

Following publication of the *meta* sulfonation of 2-phenylpyridines,¹ work was conducted within our group to accurately elucidate the mechanism in order to better understand the reaction and to develop more reactions of this type. There were several reasons to undertake this approach and several goals were sought. One was to identify the catalytic species and the rate limiting step of the reaction in order to aid in future catalyst design. It was hoped that the eventual development of a second generation catalyst or set of conditions that minimised the rate limiting step could achieve the reaction with increased efficiency and could enable future reactions. A greater understanding of the privileged reactivity of sulfonyl chlorides was also sought.

At the outset of this investigation, the working theory was that cyclometalation of a substrate molecule with a ruthenium complex activated the position *para* to the newly formed carbon-ruthenium bond for electrophilic aromatic substitution (S_EAr). However, during the preparation of this manuscript, a number of other contributions in the field challenged this theory. As well as contributions to *meta* selective alkylations detailed in **Chapter 2**, a number of other *meta* selective C-Heteroatom transformations were successfully achieved.

The groups of Greaney *et al.* reported on the ruthenium(II) catalysed *meta* selective bromination of 2-phenylpyridine derivatives using $(NBu_4)(Br_3)$ as the halogenating reagent.² Soon after Huang *et al.* reported a similar system utilising NBS as the brominating reagent while extending the substrate scope to also include phenylpyrimidine and phenylpyrazole derivatives.³ Both works also demonstrated subsequent synthetic elaborations by palladium cross coupling chemistry. These *meta* selective bromination reactions were complementary to an *ortho* selective halogenation reported by Ackermann *et al.* using ruthenium(0) catalysis⁴, as well as numerous other examples of *ortho* halogenations using copper,^{5–7} palladium,⁸ rhodium^{9–12} and cobalt¹³ catalysis.



Scheme 3-1: Ruthenium(II) catalysed *meta* bromination with $(\text{NBu}_4)(\text{Br}_3)$,² ruthenium(II) catalysed *meta* bromination with NBS,³ ruthenium(0) catalysed *ortho* bromination with NBS.⁴

Both authors suggested the likely involvement of cycloruthenation for the *meta* selectivity observed and additional mechanistic analysis conducted by Huang *et al.* suggested a kinetically relevant radical based bromination step based on KIE studies and the shutdown of the reaction by a radical scavenger. Furthermore, the authors noted the likelihood of coordination by multiple substrates based on deuterium labelling experiments. These observations led to an overall mechanistic proposal (**Figure 3-1**).

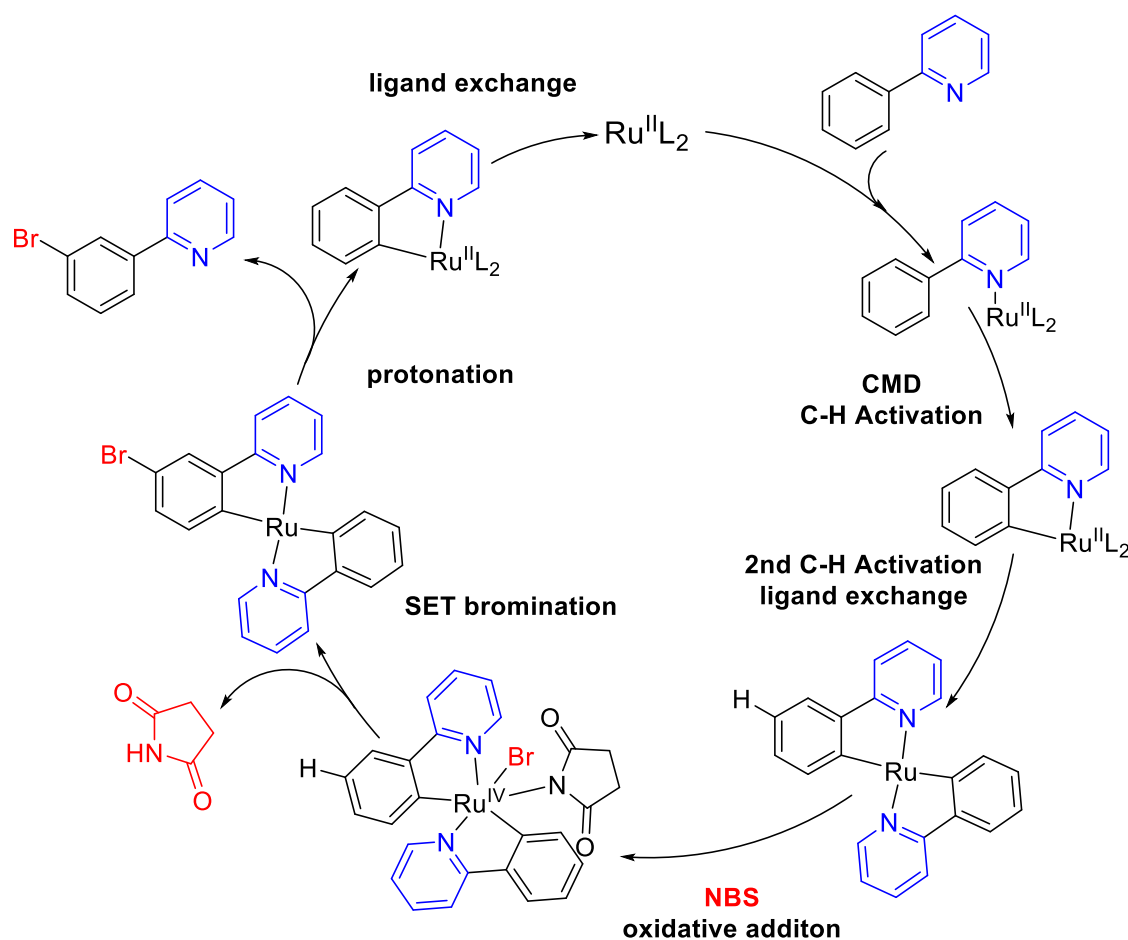
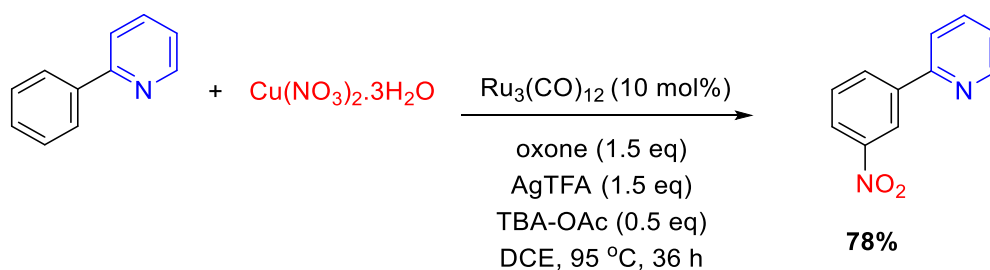


Figure 3-1: Proposed mechanism for *meta* bromination with NBS.³

Soon after, Zhang *et al.* demonstrated a *meta* nitration directed by a range of pyridine, pyrimidine, pyrazole, isoquinoline, quinoxaline, pyridazinone, oxime and benzimidazole containing substrates.¹⁴ Key to the success of this transformation was the use of $\text{Cu}(\text{NO}_3)_2$ as the nitrate source as well as the addition of co-catalytic silver salts in combination with an oxidant, which the authors proposed promoted radical formation. The use of the phase transfer catalyst tetrabutylammonium acetate also led to significantly higher yields (**Scheme 3-2**).



Scheme 3-2: Ruthenium catalysed *meta* nitration.¹⁴

The authors also demonstrated that the nitro group could be further elaborated into a wide range of other functional groups including amines, aniline derivatives, sulfonamides, indoles, thiazoles, and the nitro group itself could be used as a directing group for a subsequent *ortho* arylation procedure.

Additional mechanistic studies were also conducted. These revealed the importance of *ortho* ruthenation and deuterium labelling studies showed that this was a reversible process. In contrast, the *meta* C-H cleavage was found to be irreversible and was also found to be a kinetically relevant step. Radical scavengers TEMPO and BHT were found to shut down the reaction, prompting the authors to suggest that a radical nitration step was likely involved. On the basis of these observations and the isolation of a potential catalytic intermediate, the authors proposed the following mechanism (**Figure 3-2**).

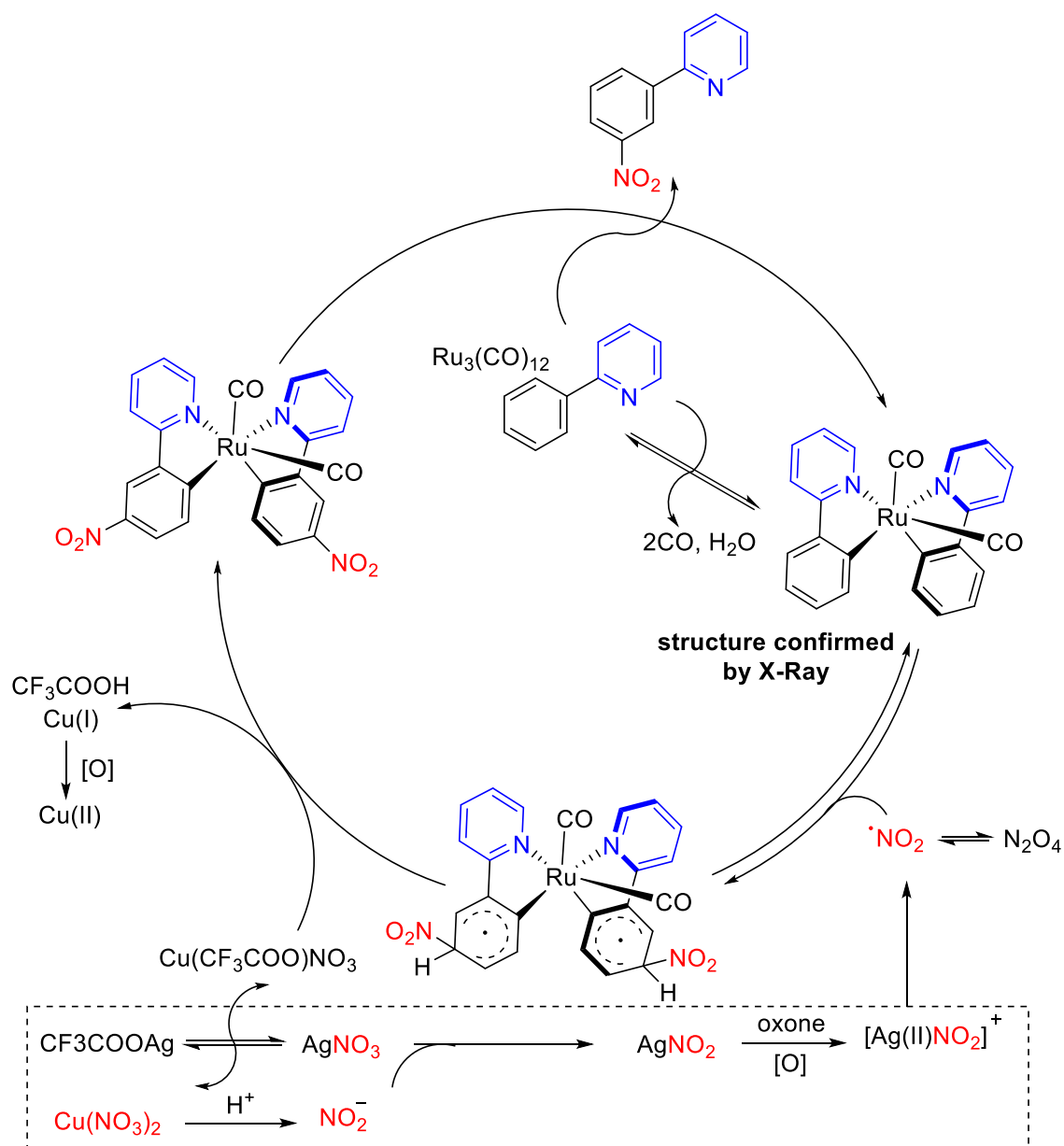


Figure 3-2 : proposed mechanism for ruthenium catalysed *meta* nitration.¹⁴

These contributions to the field were very valuable to our ongoing work into the mechanism of the *meta* sulfonation reaction and supported many of our own observations. Suggestions that radical mechanisms were likely to be involved were consistent with our previously reported alkylation procedure.¹⁵ In addition to this, suggestions that the catalytic species involved did not require an arene ligand and the likely coordination of multiple substrate molecules supported many of our own observations. The following manuscript outlines our approach to gain greater mechanistic understanding of the *meta* sulfonation reaction and was achieved through reaction monitoring, stoichiometric experiments and deuterium

labelling studies. This manuscript was accepted by the RSC journal Catalysis Science and Technology.

3.2 References

1. O. Saidi, J. Marafie, A. E. W. Ledger, P. M. Liu, M. F. Mahon, G. Kociok-Köhn, M. K. Whittlesey, and C. G. Frost, *J. Am. Chem. Soc.*, 2011, **133**, 19298–19301.
2. C. J. Teskey, A. Y. W. Lui, and M. F. Greaney, *Angew. Chem. Int. Ed.*, 2015, **54**, 11677–11680.
3. Q. Yu, L. Hu, Y. Wang, S. Zheng, and J. Huang, *Angew. Chem. Int. Ed.*, 2015, **54**, 15284–15288.
4. L. Wang and L. Ackermann, *Chem. Commun.*, 2014, **50**, 1083–1085.
5. W. Wang, C. Pan, F. Chen, and J. Cheng, *Chem. Commun.*, 2011, **47**, 3978.
6. X. Chen, X. Hao, C. E. Goodhue, and J. Yu, *J. Am. Ceram. Soc.*, 2006, **128**, 6790–6791.
7. B. Li, B. Liu, and B.-F. Shi, *Chem. Commun.*, 2015, **51**, 5093–5096.
8. D. Kalyani, A. R. Dick, W. Q. Anani, and M. S. Sanford, *Tetrahedron*, 2006, **62**, 11483–11498.
9. G. Qian, X. Hong, B. Liu, H. Mao, and B. Xu, *Org. Lett.*, 2014, **16**, 5294–5297.
10. N. Schröder, J. Wencel-Delord, and F. Glorius, *J. Am. Chem. Soc.*, 2012, **134**, 8298–8301.
11. N. Schröder, F. Lied, and F. Glorius, *J. Am. Chem. Soc.*, 2015, **137**, 1448–1451.
12. H. Hwang, J. Kim, J. Jeong, and S. Chang, *J. Am. Chem. Soc.*, 2014, **136**, 10770–10776.
13. D. G. Yu, T. Gensch, F. De Azambuja, S. Vásquez-Céspedes, and F. Glorius, *J. Am. Chem. Soc.*, 2014, **136**, 17722–17725.
14. Z. Fan, J. Ni, and A. Zhang, *J. Am. Chem. Soc.*, 2016, **138**, 8470–8475.
15. A. Paterson, S. St John-Campbell, M. F. Mahon, N. Press, and C. G. Frost, *Chem. Commun.*, 2015, **51**, 12807–12810.

3.3 Authorship and permissions

This declaration concerns the article entitled									
Mechanistic insight into ruthenium catalysed <i>meta</i> -sulfonation of 2-phenylpyridine									
Publication status (tick one)									
Draft manuscript		Submitted		In review		Accepted		Published	✓
Publication details	<p>Catal. Sci. Technol., 2016, 6, 7068-7076</p> <p>DOI: 10.1039/C6CY01254J</p> <p>Received 08 Jun 2016, Accepted 28 Jun 2016</p> <p>First published online 29 Jun 2016</p>								
Candidates contribution to the paper (detailed and also given as a percentage)	<p>The candidate contributed to/ considerably contributed to/predominantly executed the...</p> <p>Formulation of ideas (33%): Patricia Marcé, Andrew J. Paterson, and Christopher G. Frost</p> <p>Design of methodology (50%): Patricia Marcé and Andrew J. Paterson contributed equally.</p> <p>Experimental work (45%): Patricia Marcé: Reaction monitoring, stoichiometric experiments, leaving group studies. Andrew J. Paterson: Deuterium labelling experiments, single turnover experiment. Mary F. Mahon: X-ray crystallography.</p> <p>Presentation of data in journal format (10%): Patricia Marcé: Main author of manuscript and supporting information. Andrew J. Paterson: section in manuscript and supporting information regarding deuterium labelling studies and single turnover experiment.</p>								
Statement from Candidate	This paper reports on original research I conducted during the period of my Higher Degree by Research candidature.								
Signed						Date			

3.4 Manuscript for: Mechanistic insight into ruthenium catalysed *meta*-sulfonation of 2-phenylpyridine

Mechanistic Insight into Ruthenium Catalysed *Meta*-Sulfonation of 2-Phenylpyridine

Patricia Marcé, Andrew J. Paterson, Mary F. Mahon and Christopher G. Frost.

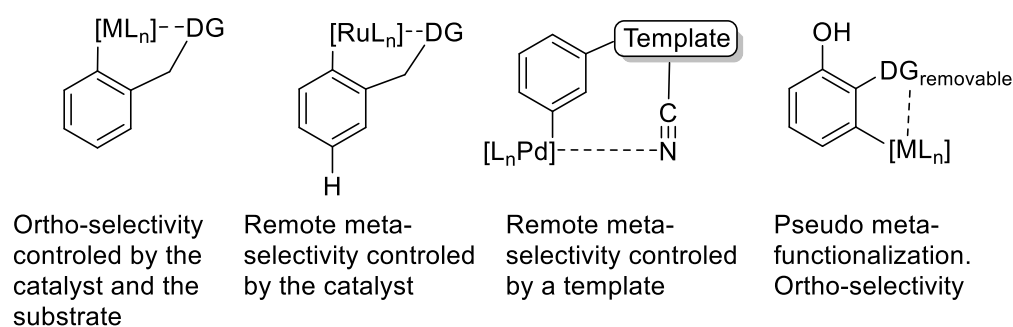
The catalytic *meta*-functionalization of arenes has emerged as important synthetic methodology in the last decade. We report herein structural and mechanistic studies of the *meta*-sulfonation of phenylpyridine using ruthenium complexes. Furthermore, we disclose that the catalytically active species does not require the presence of a η^6 -arene ligand. Furthermore, the novel cycloruthenated phenylpyridine complex tosylated at the *para* position to the metal has been isolated and fully characterised. Protodemetalation studies suggest that a concerted C-H activation-demetalation process may be involved. Overall, this study provides fundamental insight into the *meta*-sulfonation phenylpyridine reaction pathway and uncovers new reaction intermediates that will guide the design of new catalytic systems for remote *meta*-functionalization.

Introduction

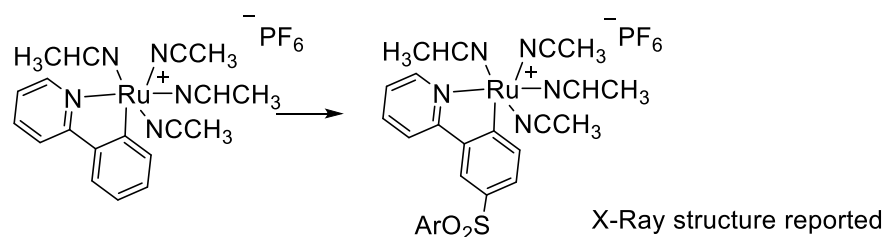
The functionalization of arenes catalysed by a metal complex *via* C-H activation has attracted great attention in the last decade.^{1,2} This transformation requires the presence of a directing group (DG) that coordinates to the metal centre to facilitate the C-H activation at the *ortho* position to form a metallacycle. Once the metallacycle is formed the introduction of a functional group can be achieved at the *ortho*^{1,2} and *meta* positions.³ The *ortho*-functionalization of arenes has been widely studied and there are many transformations reported in the literature such as arylations,⁴ alkylations,⁵ olefinations⁶ and amidations^{7,2a} among others.^{1,2} Despite the great achievements in this area, the direct introduction of a functional group at the *meta* position remains a challenge. We reported the first example of catalytic *meta*-functionalization by remote electronic activation using ruthenium catalysis.^{8,9} This important switch of regioselectivity in the sulfonation of phenylpyridines from the *ortho*¹⁰ to the *meta* position was realised by changing the catalyst from Pd(II) to Ru(II). The innovative template assisted direct *meta*-C–H bond activation first reported by Yu *et al.* involves the use of a removable tethered directing group capable of coordinating to the catalyst and directing it to the *meta* position.¹¹ Other strategies involve transient mediators such as a carboxylic acid¹² or norbornene¹³ that direct *ortho* but reveal *meta*-arylated products after their removal (Scheme 1a).

Recently, new examples of *meta* selective catalytic C-H functionalization controlled by the catalyst have been achieved using secondary¹⁴ or tertiary^{15,16} alkyl halides and bromination reagents.¹⁷ To account for the switch in regioselectivity in the *meta*-sulfonation, we hypothesized that the chelating group facilitates the formation of a stable Ru-C_{aryl} σ -bond that induces a strong *para* directing effect.⁸ Although the σ -activation of aromatics has been studied for a range of stoichiometric processes such as electrophilic halogenation,¹⁸ acylation,¹⁹ and nitration,^{18b,18c,20} a catalytic σ -activation process invokes a novel mechanistic pathway for C-H functionalization processes.¹⁵ Recent studies have revealed that the *meta*-functionalization of arenes *via* cycloruthenated complexes may follow a radical pathway.^{14,15,16}

a) Strategies for the C-H functionalization of arenes



b) This work: catalytically active species in the meta-sulfonation of phenylpyridine



Scheme 1 Strategies for meta-selective C-H functionalization.

Herein, we present mechanistic studies to establish important steps and intermediates in the *meta*-sulfonation of phenylpyridines. We also demonstrate that the presence of a *p*-cymene ligand is not essential for catalytic turnover. Moreover, this is the first time that the cycloruthenated tosylpyridine complex has been isolated and fully characterised confirming the σ -activation pathway in the catalytic *meta*-sulfonation process (Scheme 1b). This study provides fundamental insight into the reaction pathway and contributes to the broader understanding needed to design future catalytic processes for *meta*-selective C-H functionalization.

Results and discussion

The catalytic species. The C-H activation step of heteroarenes is crucial for further functionalization at the *ortho* position²¹ and has been thoroughly investigated.²² Recent studies carried out by Dixneuf and Jutand have revealed that C-H activation is an autocatalytic process which goes through a S_E3 mechanism when [Ru(O₂CR)(*p*-cymene)] complexes are employed.^{23,24} In contrast, DFT calculations carried out by Dixneuf and Maseras postulated that the C-H activation with Ru(II)-NHC complexes goes through a concerted metalation-deprotonation (CMD) mechanism.²⁵

Intrigued by the nature of the active species involved in the catalytic cycle for *meta*-functionalization, a number of ruthenium complexes were synthesised. Based on previous studies in which ruthenium cyclometallated complexes were shown to be key intermediates, complexes **3**, **4** and **5** were initially investigated (Table 1).^{23,24,26} As we have previously reported, complex **3** selectively delivered the sulfonated phenylpyridine in good yield.⁸ Preformed cationic complex **4** was also found to perform competitively. Remarkably, Ru(II) complex **5** with no *p*-cymene coordinated was also catalytically competent. This is in contrast to the work of Jutand *et al.* who showed that this ligand was essential for catalytic turnover in *ortho* arylation reactions catalysed by Ru(II).²⁴ It is worth noting that *ortho* arylations employing Ru(III) and Ru(IV) complexes did not require the presence of a *p*-cymene ligand to achieve high reaction conversions.²⁷

In order to observe the evolution of the ruthenium intermediates during the catalytic process, a series of reactions were followed by *in situ* ¹H-NMR. [RuCl₂(*p*-cymene)]₂ as well as complexes **3** and **4** were employed as the precatalysts. When [RuCl₂(*p*-cymene)]₂ was used, it was converted into cyclometallated complex **4** within 40 min at 393 K (Figure 1). The presence of a new doublet at 9.22 ppm (*J* = 5.82 Hz, H12) along with two doublets at 0.95 ppm and 0.92 ppm (*J* = 6.92 Hz, H17, H18) confirmed the formation of complex **4**. A new doublet at 1.23 ppm (*J* = 6.93 Hz, H17, H18) was also observed and assigned to free *p*-cymene (**6**). After 2 h, signals from complex **4** and free *p*-cymene (**6**) were also identified along with characteristic signals from the tosylated phenylpyridine (**2**). After 4 h, only traces of ruthenium complex **4** remained with a significant increase in the signals corresponding to free *p*-cymene. The fact that complex **4** was detected along with the formation of the final product indicates that the Ru(II) species **4** is not involved in the catalytic cycle. Additionally, the increase of the signals of the free *p*-cymene together with the formation of the final product suggests that the active catalytic species does not contain *p*-cymene as ligand. Similar behaviour was observed when complex **3** was employed. In this case, in the initial

stages of the reaction the characteristic signals of **3** appeared at 9.32 ppm (d, $J = 5.79$ Hz, H12), 0.92 ppm and 0.82 ppm (d, $J = 6.92$, H17, H18).

Table 1 Catalytic sulfonation using Ru(II) complexes potentially involved in the reaction

Entry	Catalyst loading (mol%)	Ru Catalyst	Yield (%) ^a
1	5	[RuCl ₂ (<i>p</i> -cymene)]	50
2	10	 3	52
3	10	 4	53
4	10	 5	50

a) Isolated yields.

After 40 min at 393 K these signals disappeared to give new peaks which were assigned to complex **4** and free *p*-cymene (Figure S2, see ESI[†]). When the reaction was performed with complex **4**, no changes in the ruthenium complex were observed after 1 h at 393 K (Figure S3, see ESI[†]). These results were consistent with previous observations.

In order to know whether the chloride anion was involved in a coordination-discoordination equilibrium, complex **4** was treated with 15 equivalents of KCl in CD₃CN and heated at 363 K overnight. Changes in the ¹H-NMR splitting pattern showed the formation of **5** along with

the dissociation of the *p*-cymene, but no evidence for the formation of **3** was detected. This experiment supported the fact that when the chloride dissociates from the metal centre it is very unlikely to re-coordinate under these reaction conditions (Figure S4, see ESI[†]). In recent work published by Dixneuf and Jutand,²² the attempt to isolate [Ru(OAc)(PhPy)(*p*-cymene)] by flash chromatography using a chloroform as eluent failed and gave **3** instead, showing that chloride is a better ligand for the Ru(II) centre than acetate. Although under Dixneuf conditions the re-coordination of the chloride was evident, the ruthenium species detected by ¹H-NMR in our experiment confirms that the ruthenium precatalyst does not contain chloride as ligand.

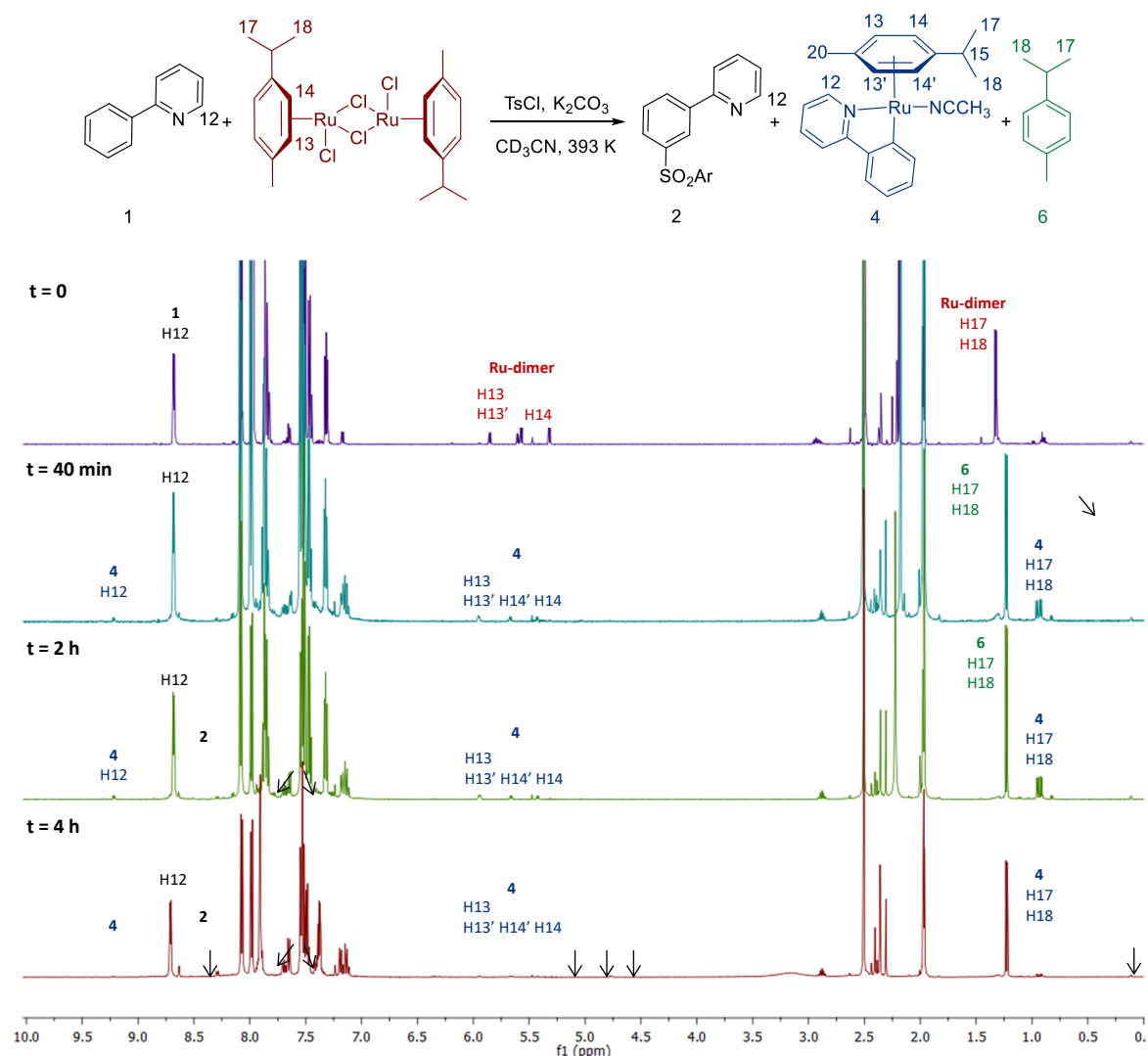
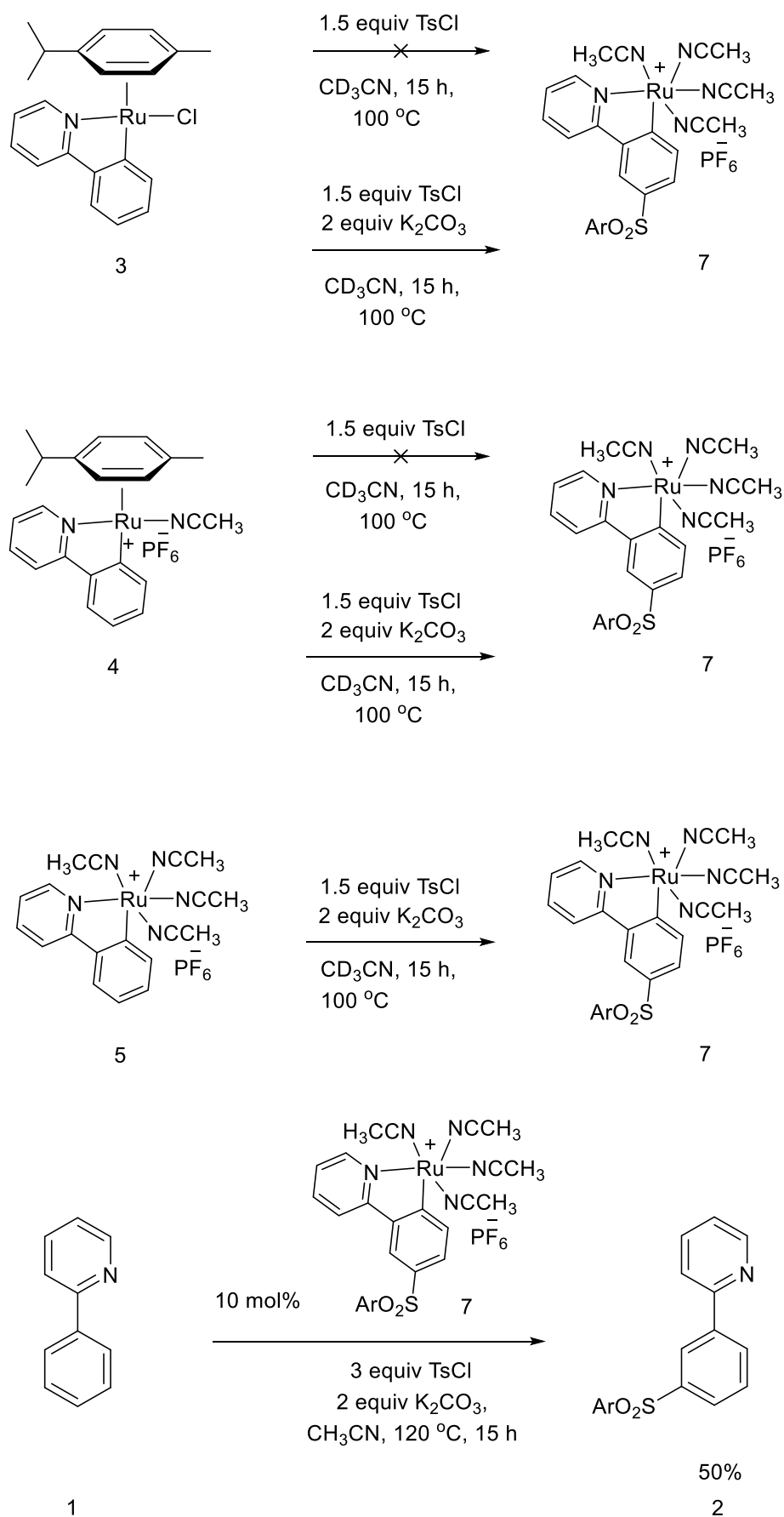


Figure 1 ¹H NMR *meta*-sulfonation of phenylpyridine using [RuCl₂(*p*-cymene)]₂

Tosylation step. The tosylation step was also subjected to investigation. The cycloruthenated complex **3** was placed in a NMR tube and treated with 1.5 equivalents of *p*-toluenesulfonyl chloride (TsCl) in CD₃CN at 373 K (Scheme 2). Interestingly, after heating

the reaction overnight only the formation of **5** was observed. Taking into account that during the tosylation step a proton has to be abstracted, the presence of a base would favour the substitution. Thus, complex **3** was treated with TsCl and 2 equivalents of K_2CO_3 . When the NMR tube was heated at 373 K the dissociation of the *p*-cymene ligand started taking place and, after 2 h the formation of a new complex was observed.

The appearance of a new doublet at 8.92 ppm with a coupling constant of 5.5 Hz and a new doublet at 8.14 ppm with a small coupling constant of 1.8 Hz prompted us to think that the formation of the cycloruthenated tosylpyridine complex **7** was occurring. An analogous stoichiometric experiment was also performed on complex **4** and similar reactivity to **3** was observed (Scheme 2). The treatment of **4** with TsCl afforded complex **5** with concomitant dissociation of the *p*-cymene. Subsequent addition of K_2CO_3 was also necessary to detect the formation of the new ruthenium complex observed previously.



Scheme 2 Tosylation step studies

To prove that this new ruthenium complex was indeed **7**, the tosylation on **5** was carried out under the same reaction conditions. After purification of the reaction mixture and full spectroscopic and X-ray analysis of the product, compound **7** was unequivocally assigned to the tosylated phenylpyridine complex with the tosyl group located at the *para* position to the Ru(II) (Figure 2). In light of these results, it could be confirmed that the *meta*-tosylation reaction proceeds by the activation of the *para* position to the Ru(II). This evidence corroborates the role of Ru(II) acting as a *para* directing group.²⁸ Finally, complex **7** was also used as precatalyst in the sulfonation reaction. Gratifyingly, it was found to be catalytically active, indicating the likelihood of sulfonated complexes involved in the catalytic cycle (Scheme 2). Interestingly, it has recently been demonstrated that similar ruthenium complexes such as [Ru(^tBuCN)₆][BF₄]₂ can catalyse the C-H arylation of fluoroarenes and arenes with directing groups.³⁰

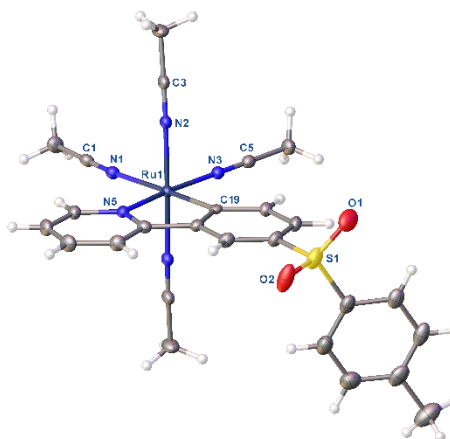


Figure 2 Single crystal X-ray structure of the cation in complex **7**.²⁹ Ellipsoids are represented at 30% of probability.

Dissociation of *p*-cymene. In all previous experiments it was impossible to detect the tosylated Ru(II) complex with the *p*-cymene coordinated. This indicated that the dissociation of the *p*-cymene is faster than the tosylation reaction under stoichiometric conditions.

At this point, we decided to investigate the nature of the *p*-cymene dissociation. In order to study the stability of the cyclometallated Ru complex **3**, a NMR tube was charged with **3** in CD₃CN. The sample was heated at 343 K for one hour, showing no modification of the splitting pattern. Then, 1.5 equivalents of tosyl chloride were added and the sample was kept at 343 K. After 24 min the dissociation of *p*-cymene was observed showing that TsCl promotes the dissociation of the *p*-cymene ligand. The mechanism of this process is still

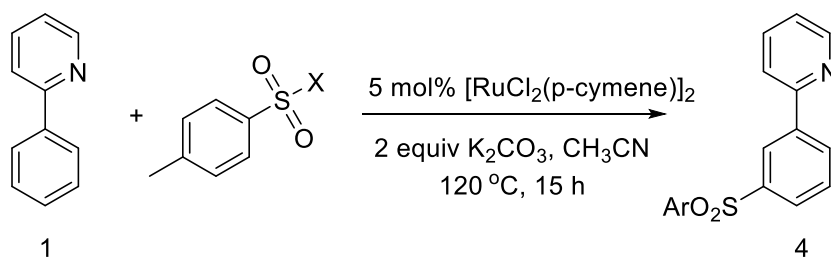
uncertain. However, it is worth noting that the dissociation of *p*-cymene can be accomplished by a thermal process but longer reaction times are required.³¹

Nature of the *meta*-functionalization. Having confirmed that sulfonation occurs at the *para* position to the newly installed C-Ru bond, we became intrigued by the nature of this process. We had previously proposed that cyclometallation increases the electron density of the aromatic ring, activating it for S_EAr type reactivity. However, recent studies have shown the likelihood of a radical mechanism in *meta*-selective alkylation reactions.^{14,15,16}

In order to investigate a possible S_EAr pathway, the effect of various sulfonating reagents were subjected to study (Table 2). Sulfonating reagents more susceptible to react with nucleophiles such as tosylimidazole, TsOBt and *p*-toluenesulfonic anhydride were employed in this transformation. Analysis of the crude reaction mixture did not show any evidence for the formation of **2** indicating that a simple S_EAr pathway was doubtful.

We also noted that the use of the radical scavenger TEMPO caused a detrimental effect on the reaction conversions (see ESI[†]). Other mechanistic studies carried out on *meta*-functionalization catalysed by ruthenium have also shown inhibition when TEMPO was employed as radical scavenger.^{14,15} In this context, we have previously proposed a mechanism involving a distinct Ru(II)/Ru(III)Cl redox cycle whereby a Ru(II) species can cause homolytic cleavage of a C-X bond to generate reactive radical species. Upon site selective addition to the aromatic substrate, the newly formed Ru(III)Cl species can reoxidise the resulting cyclohexadienyl radical intermediate.

This proposal was independently supported by Ackermann in analogous *meta*-selective alkylation reactions.¹⁶ It is therefore possible that the *meta*-selective sulfonation reaction follows analogous reactivity. This is supported by the precedence for the generation of sulfonyl radicals throughout the literature, including those promoted by ruthenium complexes.³²

Table 2 Effect of various sulfonating reagents on the *meta*-sulfonation^a

Entry	X	Yield (%) ^b
1	Cl	50
2		0
3		0
4		0

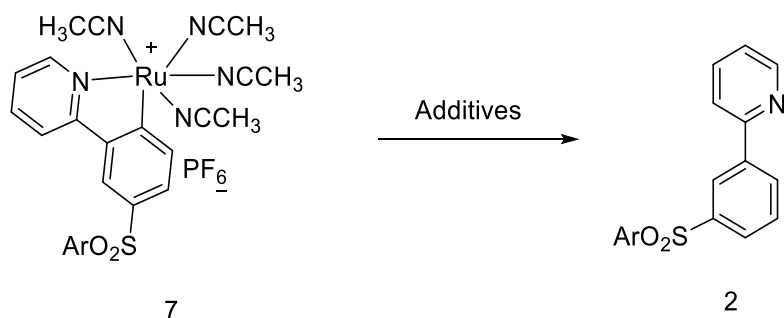
a) Reaction conditions: 2-phenylpyridine (1.0 mmol), sulfonating reagent (3.0 mmol), [RuCl₂(p-cymene)]₂ (5 mol%), CH₃CN (3 mL), 120 °C, 15 h. b) Isolated yield.

Protodemetalation. The protodemetalation of the cyclometallated ruthenium tosylphenylpyridine is the process responsible of the release of the product with the concomitant regeneration of the catalyst. Precedent in the literature has hypothesized that the proton coming from the C-H activation is involved in the demetallation step.²² The demetallation of product **2** from complex **7** was subjected to study (Table 3). Since KHCO₃ is generated during the reaction we thought that this was a plausible proton source. Thus, complex **7** was treated with 10 equivalents of KHCO₃ in CD₃CN. However after heating the mixture at 393 K overnight the release of **2** was not detected (Table 3, entry 1). A number of other acid sources were tested in the same manner yet none resulted in the release of product **2** (Table 3, entries 2-4), nor did the addition of 1 equivalent of phenylpyridine (Table 3, entry 5).

Treatment of **7** with *p*-toluenesulfonic acid (*p*-TSA) afforded a new product. The spectroscopic analysis revealed that the carbon (Ru-C) was no longer coordinated to the Ru(II), but the nitrogen from the pyridyl unit was still coordinated (Figure S7, see ESI[†]). In order to study the influence of TsCl and phenylpyridine on the reaction turnover, complex **7** was treated with 4.5 equivalents of TsCl. After heating the reaction mixture at 363 K overnight, 23% of the demetallated tosyl phenylpyridine was observed (Table 3, entry 7). A

parallel experiment was carried out using 10 equivalents of phenylpyridine and 26% of the final product was detected (Table 3, entry 8). These results demonstrated that both TsCl and phenylpyridine¹⁶ are important in facilitating the demetallation process and that KHCO₃ does not play a significant role. A concerted C-H activation-demetallation step cannot be ruled out which would also explain the formation of dimers as by-products during the reaction.^{33,34}

Table 3 Study of the protodemetallation of the TsPhPy from the metal centre.

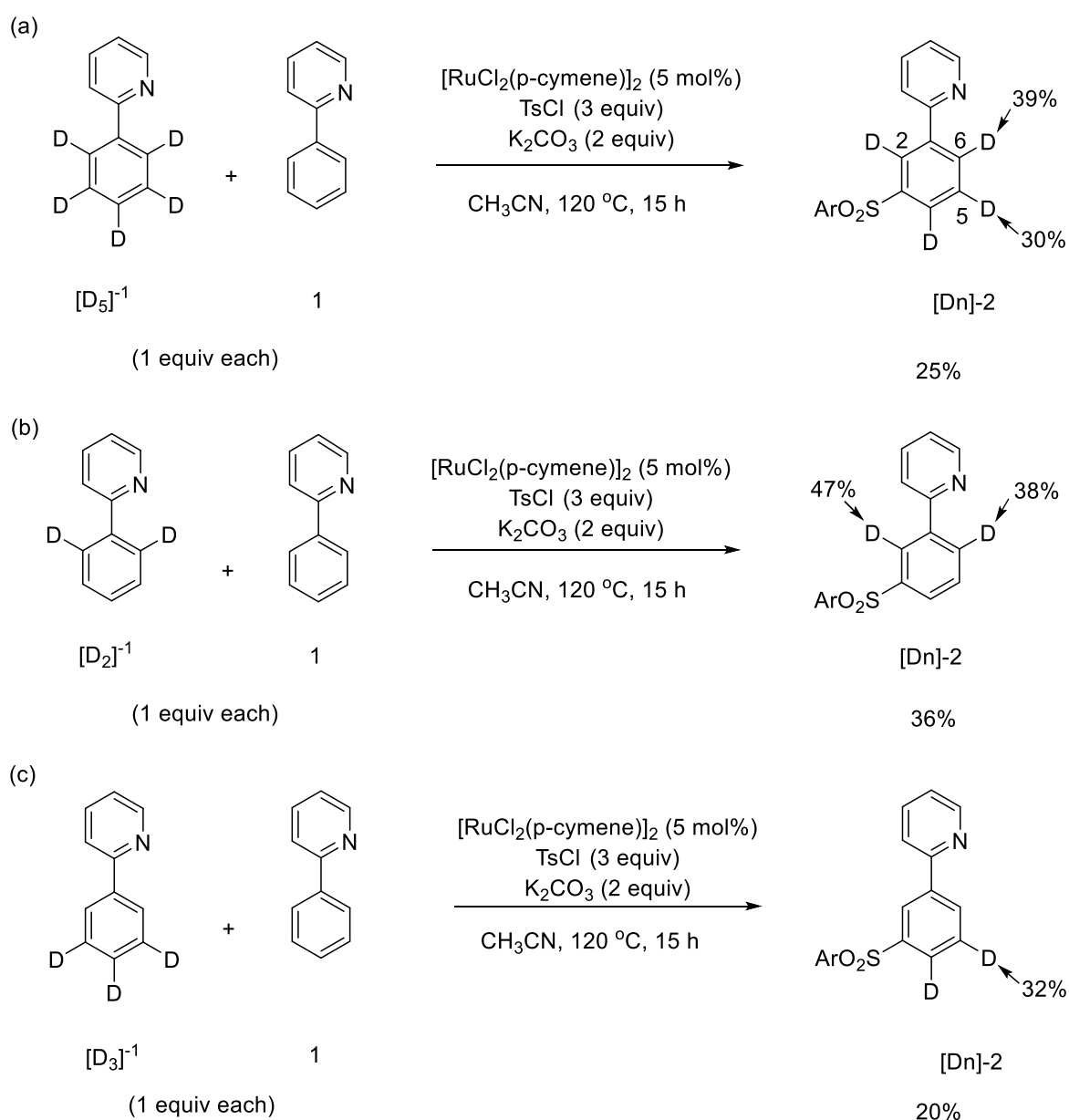


Entry	Additives	2 (%)
1	10 equiv KHCO ₃	--
2	1 equiv MesCO ₂ H 2 equiv K ₂ CO ₃	--
3	1.5 equiv MesCO ₂ H	--
4	10 equiv MesCO ₂ H	--
5	1 equiv PhPy 2 equiv K ₂ CO ₃	--
6	1.5 equiv <i>p</i> -TSA	-- ^a
7	4.5 equiv TsCl 2 equiv K ₂ CO ₃	23
8	10 equiv PhPy 2 equiv K ₂ CO ₃	26

a) Demetallation of the sulfone was observed but the pyridyl moiety was still coordinated to the Ru. b) 1.5 equivalents of tosyl chloride were added for the formation of the sulfone. The reaction was performed at 363 K in an NMR tube.

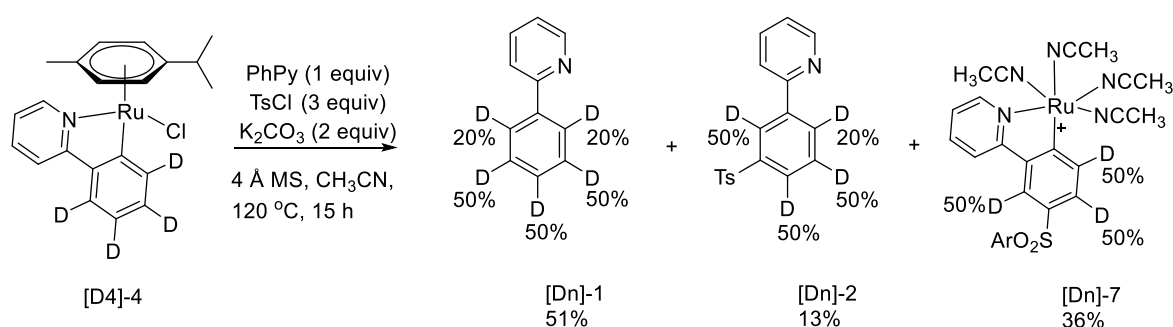
Deuterium labelled experiments. In order to determine the C-H bonds involved in kinetically relevant steps, deuterium labelled experiments were performed. Competitive reaction of [D₅]-1 and [D₀]-1 showed a kinetic preference to react with unlabelled [D₀]-1

(Scheme 3a) similar to that demonstrated in previous studies.^{8,14} In order to ascertain whether it was the *ortho* or *meta* C-H protons causing this effect, **[D₂]-1** and **[D₃]-1** were studied. A competitive reaction between **[D₂]-1** and **1** was carried out and the mixed product fraction was analysed. This revealed a product ratio of almost 1:1 of the deuterated and non-deuterated **2** when the H2 protons were considered. This is consistent with no kinetically relevant *ortho* C-H bond cleavage. Comparison of H2 and H6 in **[D_n]-2** showed a different ratio of deuterium incorporation. This may reflect the involvement of **2** in a reversible C-H activation reaction³⁵ which could cause this proton enrichment at the less hindered position. In contrast, the competitive reaction between **[D₃]-1** and **1** showed a higher percentage of the non-labelled product indicating a clear isotopic effect (Scheme 3c).



Scheme 3 Studies with isotopically labelled compounds.

Single Turnover Experiment. To provide further insight into the mechanism of catalyst turnover, a stoichiometric experiment was performed using an isotopically labelled ruthenium complex **[D₄]-4** and unlabelled 2-phenylpyridine. The deuterium incorporation of the resulting organic and inorganic components was then analysed by ¹H-NMR (Scheme 4). In recovered fractions **[D_n]-1**, **[D_n]-2** and **[D_n]-7**, 50% deuteration was observed at the *meta* and *para* positions to the pyridine ring. These results indicate that **1** and the labelled phenylpyridine ligand exchange multiple times before a slower tosylation step. Analysis of the *ortho* positions in **[D_n]-1** and **[D_n]-2** also revealed proton enrichment at the less hindered positions. This evidence supports the fact that tosylphenylpyridine is also involved in a reversible C-H activation.



Scheme 4 Single turnover experiment with isotopically labelled ruthenium complex **[D₄]-4**.

We propose that the catalytic cycle starts by the breaking of the dimer followed by C-H activation of phenylpyridine with concomitant dissociation of the chloride to give complex **4**. Once complex **4** is formed, the presence of CH₃CN favours the dissociation of the *p*-cymene ligand generating **5** which is the active Ru(II) species involved in the catalytic cycle. This cycloruthenated species **5** activates the phenyl ring from the phenylpyridine towards a radical addition of tosyl chloride at the *para* position. The tosylation step has been determined as a kinetically relevant step. The demetallation step has been proved to be promoted by the presence of TsCl and phenylpyridine. The latter is believed to proceed through a concerted C-H activation-demetallation process (Scheme 5).

Conclusions

The mechanism of the *meta*-sulfonation catalysed by Ru(II) complexes has been subjected to study. This is the first time in which the *meta*-sulfonylated Ru(II) complex **7** has been isolated and fully characterized. This proves that this new catalytic C-H functionalization goes unequivocally *via* the activation of the *para* position to the Ru(II) complex. It has also been demonstrated that complexes **5** and **7** are the active catalytic species which has been shown to be inactive in other catalytic processes. This study reveals that the presence of a *p*-cymene ligand is not crucial for the *meta*-sulfonation of phenylpyridines and it is postulated that the *meta*-sulfonation follows a radical mechanism.

References

- 1 (a) L. Ackermann, *Modern Arylation Methods*; Wiley-VCH: Weinheim, 2009; (b) G. Dyker, *Handbook of C-H Transformations*; Wiley-VCH: Weinheim, 2005; for selected representative general reviews on C-H bond functionalizations see: (c) T. W. Lyons and M. S. Sanford, *Chem. Rev.*, 2010, **110**, 1147-1169; (d) A. Gunay and K. H. Theopold, *Chem. Rev.*, 2010, **110**, 1060-1081; (e) I. A. I. Mkhalid, J. H. Barnard, T. B. Marder, J. M. Murphy and J. F. Hartwig, *Chem. Rev.*, 2010, **110**, 890-931; (f) P. Sehnal, R. J. K. Taylor and I. J. S. Fairlamb, *Chem. Rev.*, 2010, **110**, 824-889; (g) M. C. Willis, *Chem. Rev.*, 2010, **110**, 725-748; (h) G. E. Dobereiner and R. H. Crabtree, *Chem. Rev.*, 2010, **110**, 681-703; (i) F. Kakiuchi and T. Kochi, *Synthesis*, 2008, 3013-3039; (j) R. G. Bergman, *Nature*, 2007, **446**, 391-393; (k) K. Godula and D. Sames, *Science*, 2006, **312**, 67-72 and references cited therein; (l) For a review on enzymatic functionalization of C-H bonds, see: J. C. Lewis, P. S. Coelho and F. H. Arnold, *Chem. Soc. Rev.*, 2011, **40**, 2003-2021 and references cited therein.
- 2 For representative examples of C-X bond formation see: (a) V. S. Thirunavukkarasu, S. I. Kozhushkov and L. Ackermann, *Chem. Commun.*, 2014, **50**, 29-39; (b) V. S. Thirunavukkarasu, J. Hubrich and L. Ackermann, *Org. Lett.*, 2012, **14**, 4210-4213; (c) K. Padala and M. Jeganmohan, *Chem. Commun.*, 2013, **49**, 9651-9653; (d) R. K. Chinnagolla, S. Pimparkar and M. Jeganmohan, *Chem. Commun.*, 2013, **49**, 3146-3148; (e) L. Wang and L. Ackermann, *Chem. Commun.*, 2014, **50**, 1083-1085.
- 3 (a) R. J. Philipps and M. J. Gaunt, *Science*, 2009, **323**, 1593-1597; (b) Y. Zhou, J. Zhao and L. Liu, *Angew. Chem., Int. Ed.*, 2009, **48**, 7126-7128; (c) F. Juliá-Hernández, M. Simonetti and I. Larrosa, *Angew. Chem., Int. Ed.*, 2013, **52**, 11458-11460.

- 4 P. B. Arockiam, C. Bruneau and P. H. Dixneuf, *Chem. Rev.*, 2012, **112**, 5879-5918.
- 5 (a) L. Ackermann, P. Novak, R. Vicente and N. Hofmann, *Angew. Chem., Int. Ed.*, 2009, **48**, 6045-6048; (b) S. Murai, F. Kakiuchi, S. Sekine, Y. Tanaka, A. Kamatani, M. Sonoda and N. Chatani, *Nature*, 1993, **366**, 529-531.
- 6 (a) C. S. Yi and D. W. Lee, *Organometallics*, 2009, **28**, 4266-4268; (b) C. S. Yi and D. W. Lee, *Organometallics*, 2010, **29**, 1883-1885.
- 7 (a) W. G. Shou, J. A. Li, T. X. Guo, Z. Y. Lin and G. C. Jia, *Organometallics*, 2009, **28**, 6847-6854; (b) M. Shang, S.-H. Zeng, S.-Z. Sun, H.-X. Dai and J.-Q. Yu, *Org. Lett.*, 2013, **15**, 5286-5289; (c) M. R. Yadav, R. K. Rit and A. K. Sahoo, *Org. Lett.*, 2013, **15**, 1638-1641; (d) M. Bhanuchandra, M. R. Yadav, R. K. Rit, M. R. Kuram and A. K. Sahoo, *Chem. Commun.*, 2013, **49**, 5225-5227.
- 8 O. Saidi, J. Marafie, A. E. W. Ledger, P. M. Liu, M. F. Mahon, G. Kociok-Köhn, M. K. Whittlesey and C. G. Frost, *J. Am. Chem. Soc.*, 2011, **133**, 19298-19301.
- 9 It is worth noting that the formation of traces of *meta*-alkylated phenylpyridine was first observed as a byproduct in the *ortho*-alkylation of phenylpyridines. L. Ackermann, N. Hofmann and R. Vicente, *Org. Lett.*, 2011, **13**, 1875-1877.
- 10 X. Zhao, E. Dimitrijević and V. M. Dong, *J. Am. Chem. Soc.*, 2009, **131**, 3466-3467.
- 11 (a) D. Leow, G. Li, T.-S. Mei and J.-Q. Yu, *Nature*, 2012, **486**, 518-522; (b) L. Wang, N. Dastbaravardeh, G. Li and J.-Q. Yu, *J. Am. Chem. Soc.*, 2013, **135**, 18056-18059; (c) H.-X. Dai, G. Li, X.-G. Zhang, A. F. Stepa and J.-Q. Yu, *J. Am. Chem. Soc.*, 2013, **135**, 7567-7571; (d) R.-Y. Tang, G. Li and J.-Q. Yu, *Nature*, 2014, **507**, 215-220; (e) S. Lee, H. Lee and K. L. Tan, *J. Am. Chem. Soc.*, 2013, **135**, 18778-18781; (f) M. Bera, A. Modak, T. Patra, A. Maji and D. Maiti, *Org. Lett.*, 2014, **16**, 5760-5763; (g) M. Bera, A. Maji, S. K. Sahoo and D. Maiti, *Angew. Chem., Int. Ed.*, 2015, **54**, 8515-8519; (h) S. Li, H. Ji, L. Cai and G. Li, *Chem. Sci.*, 2015, **6**, 5595-5600; (i) A. Maji, B. Bhaskararao, S. Singha, R. B. Sunoj and D. Maiti, *Chem. Sci.*, 2016, **7**, 3147-3153.
- 12 (a) J. Cornella, M. Righi and I. Larrosa, *Angew. Chem., Int. Ed.*, 2011, **50**, 9429-9432; (b) J. Luo, S. Preciado and I. Larrosa, *J. Am. Chem. Soc.*, 2014, **136**, 4109-4112; (c) J. Luo, S. Preciado and I. Larrosa, *Chem. Commun.*, 2015, **51**, 3127-3130; (d) J. Luo, S. Preciado, S. O. Araromi and I. Larrosa, *Chem.-Asian J.*, 2015, **6**, 5595-5600; (e) N. Y. P. Kumar, A. Bechtoldt, K. Raghuvanshi and L. Ackermann, *Angew. Chem., Int. Ed.*, 2016, **55**, 6929-6932.

- 13 (a) X. -C. Wang, W. Gong, L. -Z. Fang, R. -Y. Zhu, S. Li, K. M. Engle and J.-Q. Yu, *Nature*, 2015, **519**, 334-338; (b) Z. Dong, J. Wang and G. Dong, *J. Am. Chem. Soc.*, 2015, **137**, 5887-5890.
- 14 N. Hofmann and L. Ackermann, *J. Am. Chem. Soc.*, 2013, **135**, 5877-5884.
- 15 A. J. Paterson, S. St John-Campbell, M. F. Mahon, N. J. Press and C. G. Frost, *Chem. Commun.*, 2015, **51**, 12807-12810.
- 16 J. Li, S. Warratz, D. Zell, S. De Sarkar, E. E. Ishikawa and L. Ackermann, *J. Am. Chem. Soc.*, 2015, **137**, 13894-13901.
- 17 (a) C. J. Teskey, A. Y. W. Lui and M. C. Greaney, *Angew. Chem.*, 2015, **127**, 11843-11846; (b) Q. Yu, L. Hu, Y. Wang, S. Zheng and J. Huang, *Angew. Chem., Int. Ed.*, 2015, **54**, 15284-15288.
- 18 (a) A. M. Clark, C. E. F. Rickard, W. R. Roper and L. J. Wright, *Organometallics*, 1998, **17**, 4535-4537; (b) A. M. Clark, C. E. F. Rickard, W. R. Roper and L. J. Wright, *Organometallics*, 1999, **18**, 2813-2820; (c) A. M. Clark, C. E. F. Rickard, W. R. Roper and L. J. Wright, *J. Organomet. Chem.*, 2000, **598**, 262-275; (d) C. Coudret, S. Frayssse and J. P. Launay, *Chem. Commun.*, 1998, 663-664; (e) K. M. Cheung, Q. F. Zhang, K. W. Chan, M. H. W. Lam, I. D. Williams and W. H. Leung, *J. Organomet. Chem.*, 2005, **690**, 2913-2921.
- 19 M. K. Lau, Q. F. Zhang, J. L. C. Chim, W. T. Wong and W. H. Leung, *Chem. Commun.*, 2001, 1478-1479.
- 20 G. R. Clark, C. E. L. Headford, W. R. Roper, L. J. Wright and V. P. D. Yap, *Inorg. Chim. Acta*, 1994, **220**, 261-272.
- 21 (a) L. Ackermann, R. Vicente and A. R. Kapdi, *Angew. Chem. Int. Ed.*, 2009, **48**, 9792-9826; (b) L. Ackermann, *Chem. Rev.*, 2011, **111**, 1315-1345; (c) P. B. Arcockiam, C. Bruneau and P. H. Dixneuf, *Chem. Rev.*, 2012, **112**, 5879-5918; (d) B. Li. and P. H. Dixneuf, *Chem. Soc. Rev.*, 2013, **42**, 5744-5767.
- 22 (a) D. L. Davies, S. M. A. Donald, S. A. Macgregor, O. Al-Duaij and M. Polleth, *J. Am. Chem. Soc.*, 2006, **128**, 4210-4211; (b) D. L. Davis, S. M. A. Donald and S. A. Macgregor, *J. Am. Chem. Soc.*, 2005, **127**, 13754-13755; (c) D. L. Davis, S. M. A. Donald, O. Al-Duaij, J. Fawcett, C. Little and S. A. Macgregor, *Organometallics*, 2006, **25**, 5976-5978; (d) S. I. Gorelsky, D. Lapointe and K. Fagnou, *J. Am. Chem. Soc.*, 2008, **130**, 10848-10849; (e) J.-P. Djukic, J.-B. Sortais, L. Barloy and M. Pfeffer, *Eur. J. Inorg. Chem.*, 2009, 817-853.
- 23 E. F. Flegeau, C. Bruneau, P. H. Dixneuf and A. Jutand, *J. Am. Chem. Soc.*, 2011, **133**, 10161-10170.
- 24 I. Fabre, N. von Wolff, G. Le Duc, E. F. Flegeau, C. Bruneau, P. H. Dixneuf and A. Jutand, *Chem. Eur. J.*, 2013, **19**, 7595-7604.

- 25 I. Özdemir, S. Demor, B. Çetinkaya, C. Gourlaouen, F. Maseras, C. Bruneau and P. H. Dixneuf, *J. Am. Chem. Soc.*, 2008, **130**, 1156-1157.
- 26 (a) J.-P. Djukic, A. Berger, M. Duquenne, M. Pfeffer, A. de Cian and N. Kyritsakas-Gruber, *Organometallics*, 2004, **23**, 5757-5767; (b) Y. Boutadla, O. Al-Duaij, D. L. Davies, G. A. Griffith and K. Singh, *Organometallics*, 2009, **28**, 433-440.
- 27 (a) L. Ackermann, R. Born and P. Álvarez-Bercedo, *Angew. Chem., Int. Ed.*, 2007, **46**, 6364-6367; (b) L. Ackermann, A. Althammer and R. Born, *Synlett*, 2007, 2833-2836; (c) L. Ackermann, A. Althammer and R. Born, *Tetrahedron*, 2008, 6115-6124.
- 28 M. Gagliardo, D. J. M. Snelders, P. A. Chase, R. J. M. Klein Gebbink, G. P. M. van Klink and G. van Koten, *Angew. Chem., Int. Ed.*, 2007, **46**, 8558-8573.
- 29 **Crystal Data** for compound **7**: C₃₀H₃₆F₆N₅O₃PRuS, *M* = 792.74 g mol⁻¹, triclinic, space group *P*-1 (no. 2), *a* = 8.2870(1), *b* = 8.4860(1), *c* = 25.3050(5) Å, *α* = 95.062(1), *β* = 92.854(1), *γ* = 97.449(1)°, *U* = 1754.25(5) Å³, *Z* = 2, *T* = 150 K, *μ*(MoKα) = 0.622 mm⁻¹, *D*_c = 1.501 g cm⁻³, 29703 reflections measured (7.162° ≤ 2θ ≤ 55.304°), 7976 unique (*R*_{int} = 0.0668) which were used in all calculations. The final *R*1 was 0.0439 (*I* > 2σ(*I*)) and *wR*2 was 0.0883 (all data). CCDC 1479685 contain the supplementary crystallographic data for this paper. These data can be obtained free of charge from The Cambridge Crystallographic Data Centre via www.ccdc.cam.ac.uk/data_request/cif.
- 30 M. Simonetti, G. J. P. Perry, X. C. Cambeiro, F. Juliá-Hernández, J. N. Arokianathar and I. Larrosa, *J. Am. Chem. Soc.*, 2016, **138**, 3596–3606.
- 31 S. Fernandez, M. Pfeffer, V. Ritleng and C. Sirlin, *Organometallics*, 1999, **18**, 2390-2394.
- 32 (a) R. P. Nair, T. H. Kim and B. J. Frost, *Organometallics*, 2009, **28**, 4681–4688; (b) C. K. Prier, D. A. Rankic and D. W. C. MacMillan, *Chem. Rev.*, 2013, **113**, 5322–5363; (c) J. J. Devery III, J. J. Douglas, J. D. Nguyen, K. P. Cole, R. A. Flowers II and C. R. J. Stephenson, *Chem. Sci.*, 2015, **6**, 537-541.
- 33 The crude reaction mixture was fully analysed by LC-MS to determine all possible by-products formed in this transformation. In all cases, traces of heterodimer and homodimer were detected.
- 34 (a) M. E. Tauchert, C. D. Incarvito, A. L. Rheingold, R. G. Bergman and J. A. Ellman, *J. Am. Chem. Soc.*, 2012, **134**, 1482-1485; (b) W. R. Reynolds, P. Man Liu, G. Kociok-Köhn and C. G. Frost, *Synlett*, 2013, **24**, 2687-2690; (c) S. H. Park, J. Kwak, K. Shin, J. Ryu, Y. Park and S. Chang, *J. Am. Chem. Soc.*, 2014, **136**, 2492–2502.

- 35 L. Ackermann, R. Vicente, H. K. Potukuchi and V. Pirovano, *Org. Lett.*, 2010, **12**, 5032-5035.
- 36 (a) S. I. Kozhushkov, D. S. Yufit and L. Ackermann, *Org. Lett.*, 2008, **10**, 3409;
(b) V. Bonnet, F. Mongin, F. Trécourt, G. Quéguiner and P. Knochel, *Tetrahedron*, 2002, **58**, 4429.
- 37 L. A. Carpino, J. Xia, C. Zhang and A. El-Faham, *J. Org. Chem.*, 2004, **69**, 62.
- 38 D. R. Hicks and B. Fraser-Reid, *Synthesis*, 1974, 203.

4.0 α -halo carbonyls enable *meta* primary, secondary and tertiary C-H alkylations

4.1 Introduction

Shortly after publication of our groups Chemical Communications article entitled “Catalytic *meta* selective C-H functionalisation to construct quaternary carbon centres”¹, a similar piece of work was reported by Ackermann *et al.* to achieve similar tertiary alkylation² (**Chapter 2**). The work was largely in agreement with our own and included a number of extra experiments which helped draw light to the mechanism. It was of particular interest that the authors also supported our original proposition that there was a dual role of the ruthenium; for both the activation of the substrate molecule and for the generation of the tertiary alkyl radical. It was therefore apparent that the possibility of a dual catalytic system could enable new *meta* selective reactions, a concept which was exemplified in ruthenium catalysed *meta* selective nitrations.³

4.2 Optimisation of primary α -halo carbonyl coupling partner

During the development of our tertiary alkylation procedure, we had attempted to utilise primary α -halo carbonyls to achieve *meta* selective primary alkylations, transformations that had not been reported at the time. Using our previously developed system, this led to disappointing yields with mixtures of regioisomers. We rationalised that homolytic C-Br cleavage was less easily achieved on the primary substrates due to lack of captodative stabilisation of the resulting radical and that *ortho* substituted by-products were being formed by competing oxidative addition / reductive elimination pathways. We therefore envisaged that the addition of a co-catalyst to generate a radical would favour a *meta* selective radical addition over the *ortho* selective oxidative addition / reductive elimination pathway (**Table 4-1**).

We initially began our investigation using conditions known in the field, a ruthenium(II) precatalyst with carboxylate ligands.^{4,5} However, these resulted in low combined yields of inseparable regioisomers. Due to our theory that there was a dual role of ruthenium in tertiary alkylation reactions; activation of the substrate by cyclometalation, and a single electron redox catalyst to generate an alkyl radical, we tried a number of catalysts capable of acting as single electron redox catalysts. A number of copper systems were first employed given their natural abundance and precedence to form alkyl radicals in single electron processes⁶⁻⁹ however no products were observed. Similarly, photocatalytic

ruthenium complexes were also ineffective, providing no benefit over the monocatalytic system. However, the addition of $\text{Pd}(\text{PPh}_3)_4$ significantly improved reactions yields, with 10 mol% loading resulting in near complete selectivity to the *meta* substituted product. Other palladium(II) precatalysts were ineffective whereby $\text{Pd}_2(\text{dba})_3$ and $\text{Pd}(\text{OAc})_2$ yielded no additional benefit however $\text{PdCl}_2(\text{PPh}_3)_2$ was somewhat more effective. Gratifyingly, ethyl chloroacetate showed comparable reactivity with high selectivity, expanding the range of potential commercial coupling partners available. Crucially when no ruthenium complex was employed, no alkylated products were formed, highlighting a potential dual activation pathway.

Table 4-1. Optimisation of *meta* primary alkylation.

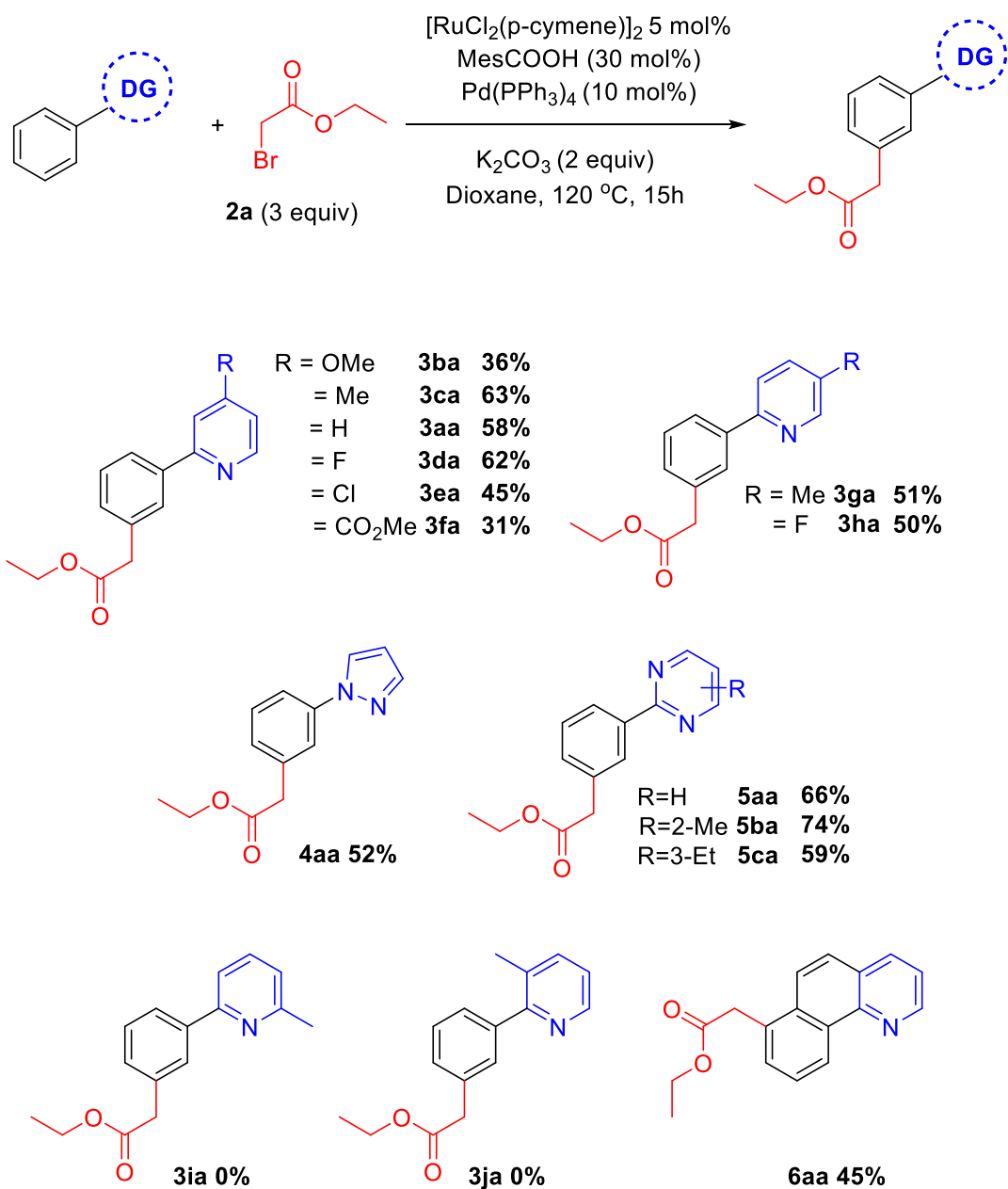
$[RuCl_2(p\text{-cymene})]_2$ 5 mol%
 Carboxylate Ligand (30 mol%)
 Co-Catalyst / Co-Ligand
 K_2CO_3 (2 equiv)
 Dioxane, 120 °C, 15h

Entry	Ligand	Co-Catalyst	Yield (%) ^a	<i>m</i> : <i>o</i> ^b
1	No ligand	-	21	2.5:1
2	KOAc	-	24	2:1
3	MesCOOH	-	26	2.3:1
4	AdCOOH	-	15	2:1
6	MesCOOH	CuCl (20%), 1,10-Phen (20%)	0	0
7	MesCOOH	CuCl (20 mol%) PMETA (1eq)	0	0
8	MesCOOH	Cu ₂ O (10 %) 1,10-Phen (12%)	0	0
9 ^c	MesCOOH	Ru(bpy) ₃ Cl ₂	21	1:1
10 ^c	MesCOOH	Ru(Phen) ₃ Cl ₂	19	0.6:1
11	MesCOOH	Pd(PPh ₃) ₄ (5%)	47	3.3:1
12	MesCOOH	Pd(PPh₃)₄ (10%)	58	20:1
13	MesCOOH	Pd ₂ (dba) ₃ (5%)	17	2.5:1
14	MesCOOH	Pd(OAc) ₂ (10%)	17	1.5:1
15	MesCOOH	PdCl ₂ (PPh ₃) ₂ (10%)	46	10:1
15	MesCOOH	Pd(PPh ₃) ₄ (12.5%)	54	20:1
16	MesCOOH	Pd(PPh ₃) ₄ (15%)	55	19:1
17	AcOH	Pd(PPh ₃) ₄ (10%)	55	15:1
18	AdCOOH	Pd(PPh ₃) ₄ (10%)	44	12:1
19	MesCOOH	Pd(PPh ₃) ₄ (No Ru)	0	0
20 ^d	MesCOOH	Pd(PPh ₃) ₄ (10%)	54	10:1
21 ^e	MesCOOH	Pd(PPh ₃) ₄ (10%)	46	2.9:1

^aCombined yield for both regioisomers. ^b*meta:ortho* ratio calculated by ¹H NMR. ^cIrradiated with blue LEDs. ^dUsing ethyl chloroacetate. ^eUsing ethyl iodoacetate.

4.3 Scope of primary α -halo carbonyl coupling partner

With optimised catalytic conditions in hand, we aimed to explore the substrate scope with respect to the directing group. In all cases, near complete selectivity (>20:1) to the *meta* substituted product was observed. Substitution on the pyridine ring was generally well tolerated although significantly increasing or decreasing electron density had a negative effect on reaction yields. Pyrazole and a range of substituted pyrimidines were also effective directing groups affording the *meta* alkylated products in good yields. Substitution at the 3 or the 6 position of the pyridine ring completely shut down reactivity, likely due to hindering the ability of the substrate to form a planar cyclometalated complex. Meanwhile conformationally locked benzoquinoline afforded exclusively alkylated product **6aa**. X-Ray analysis could unequivocally confirm this regioselectivity (**Figure 4-1**) and supports the proposition that substitution occurs at the position *para* to the C-Ru bond formed following cyclometalation.



Scheme 4-2. Directing group scope on unsubstituted arenes.

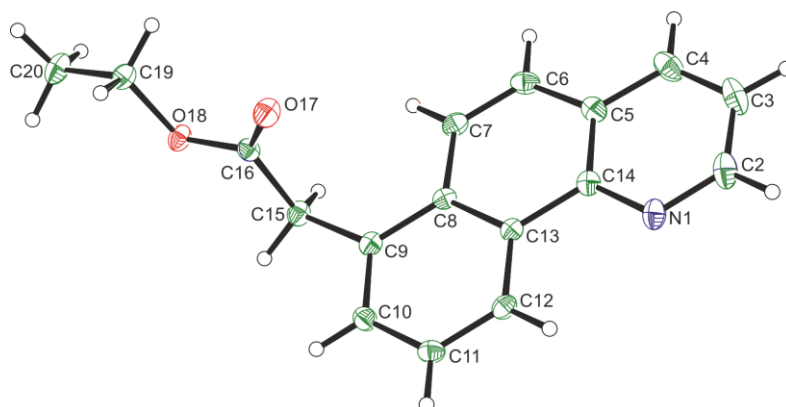
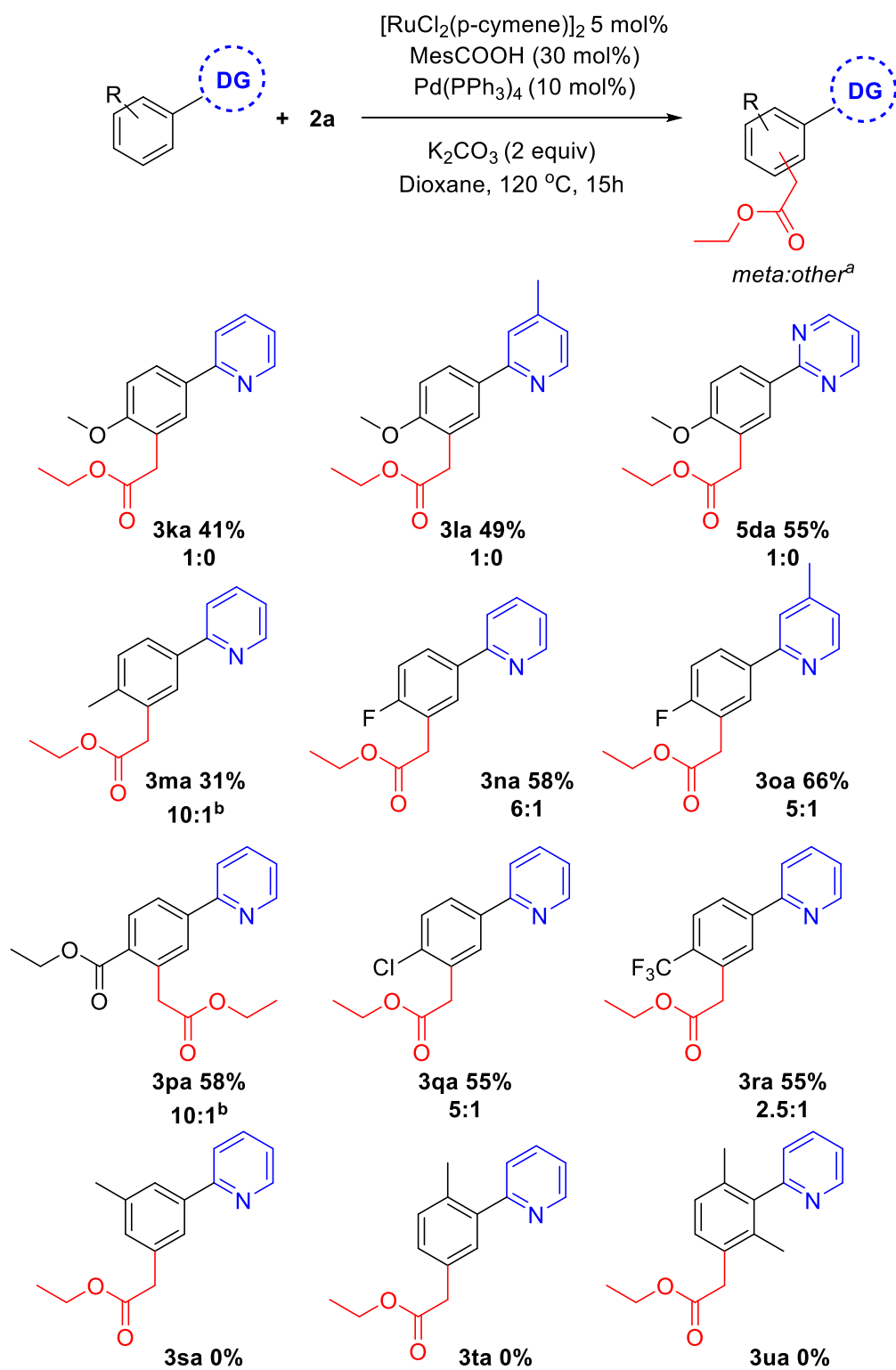


Figure 4-1. X-Ray crystal structure of compound **6aa**. Ellipsoids are depicted at 30% probability.¹⁰

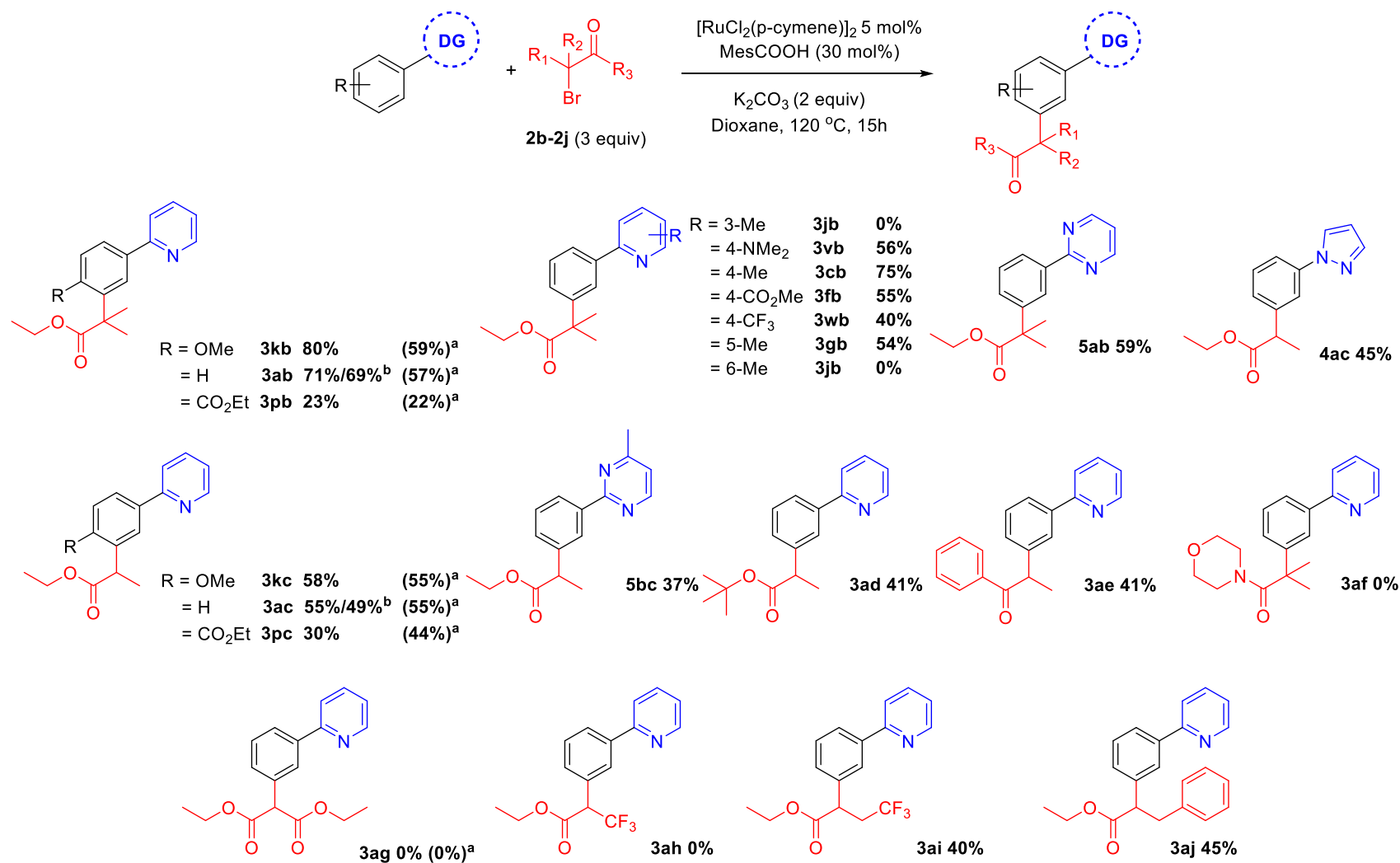
Next, substitution on the aryl component was considered (**Scheme 4-3**). Whereas unsubstituted substrates afforded nearly exclusively the *meta* substituted products, some regioisomeric products were formed when the electronic properties of the aromatic ring were altered. Generally, electron donating groups at the *para* position yielded either exclusively the *meta* product or high selectivity towards this product in modest yields. In contrast, electron withdrawing groups yielded a higher proportion of regioisomeric by-products but with improved combined yield. Dimethylated substrate **3u** afforded none of the *meta* alkylated product **3ua**, likely due to its inability to form a cyclometalated complex. Similarly, incorporating methyl substituents at the *ortho* or *meta* position also shut down reactivity, despite being effective substrates in other ruthenium catalysed *meta* alkylations.^{11,2}



Scheme 4-3. Scope of substituted arenes ^aYields quoted are combined yields of both regioisomers. ^bMinor isomer could be assigned as *ortho* substituted product.

4.4 Scope of secondary and tertiary α -halo carbonyl coupling partners

Next we saw the potential for other α -halo carbonyls to be used to install other useful functionality at the *meta* position (**Scheme 4-4**). When simple secondary and tertiary α -halo carbonyl reagents were used, the addition of palladium had a negligible effect on the yield of the corresponding *meta* substituted products. Thus, in agreement with previous work conducted in the field, a range of secondary and tertiary alkylated products could be achieved using solely a ruthenium complex.^{11,1,2} In agreement with the reactions carried out in **Scheme 4-2**, changing the electronics on pyridine ring generally had a detrimental effect on reaction yields with a 4-Me substituent again proving to be the most effective directing group. We have previously proposed that the key to this type of reactivity when tertiary α -halo carbonyl **2b** was employed was the facile generation of an alkyl radical.¹ Captodative stabilization by the electron donating geminal dimethyl substituent along with the electron withdrawing effect of the ester could allow facile homolytic cleavage of the C-Br bond. Thus, coupling partners with solely electron withdrawing groups bound to the α -carbon did not result in alkylated products (**3ag**, **3ah**) whereas the corresponding coupling partners with short alkyl chains introduced could furnish the *meta* substituted products (**3ai**). α -halo ketones could also be effectively coupled (**3ae**) however α -halo amides were ineffective (**3af**), again highlighting the importance of captodative stabilization in the coupling partner.



Scheme 4-4. Scope of α -bromo carbonyl coupling reagents. ^aReaction with co-catalytic $\text{Pd}(\text{PPh}_3)_4$ (10 mol%). ^bReaction with corresponding α -chloro carbonyl.

4.5 Mechanistic considerations: Computational

We previously proposed a dual metallic radical based mechanism for *meta* alkylation reactions involving initial cyclometalation, which activates the position *para* to the newly installed C-Ru bond for site selective addition.¹ Recently, we also showed that substitution happens at the *para* position of the newly formed C-Ru bond in stoichiometric reactions with cyclometalated complexes in analogous *meta* sulfonation reactions.¹⁴ In order to investigate this further, we applied computational methods to model the electronic properties of the cyclometalated intermediates based on the work of Ritter and co-workers.¹⁵ This approach accurately predicts reaction regioselectivity using relative nucleophilic Fukui indices calculated from carbon NBO values and was applied to four substituted phenylpyridines (**1a**, **1k**, **1n** and **1r**) and their equivalent cyclometalated complexes, **Aa**, **Ak**, **An** and **Ar**, [Ru(OMes) (*p*-cymene)] (**1x**). The relative Fukui indices in **Figure 4-2** show that if the organic substrate alone was the active species, then reaction with an electrophile would most likely occur at C4, *para* to the phenyl group, or in the case of **1a** (when X = H), at C10; *para* to the pyridine ring due to increased electron density at these positions. However, the regioselectivity of the substrate is altered after cyclometalation (**Ax**), with the most reactive (electron rich) carbon site for functionalisation now indicating addition at C11; the C-H position *para* to the new Ru-C bond. The analysis conducted on substituted arenes (**1n**, **1r**) that had previously displayed significant regioisomeric byproducts (**Scheme 3**), did not show significantly enhanced reactivity at the free *ortho* position (C8/C12). This suggests that these products are formed *via* an alternative mechanism, likely an oxidative addition / reductive elimination pathway as has previously been proposed in ruthenium catalysed *ortho* alkylations.¹²

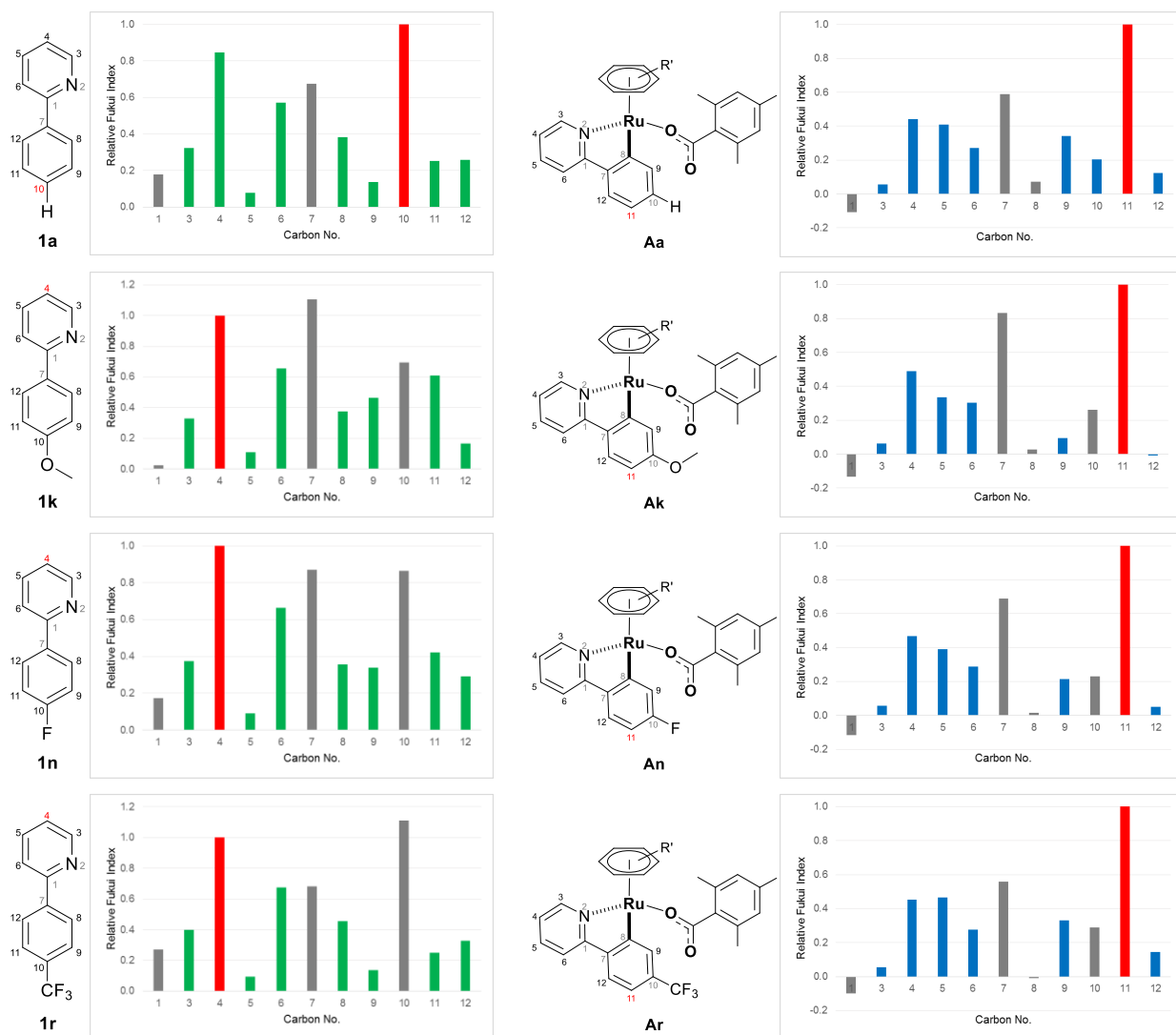


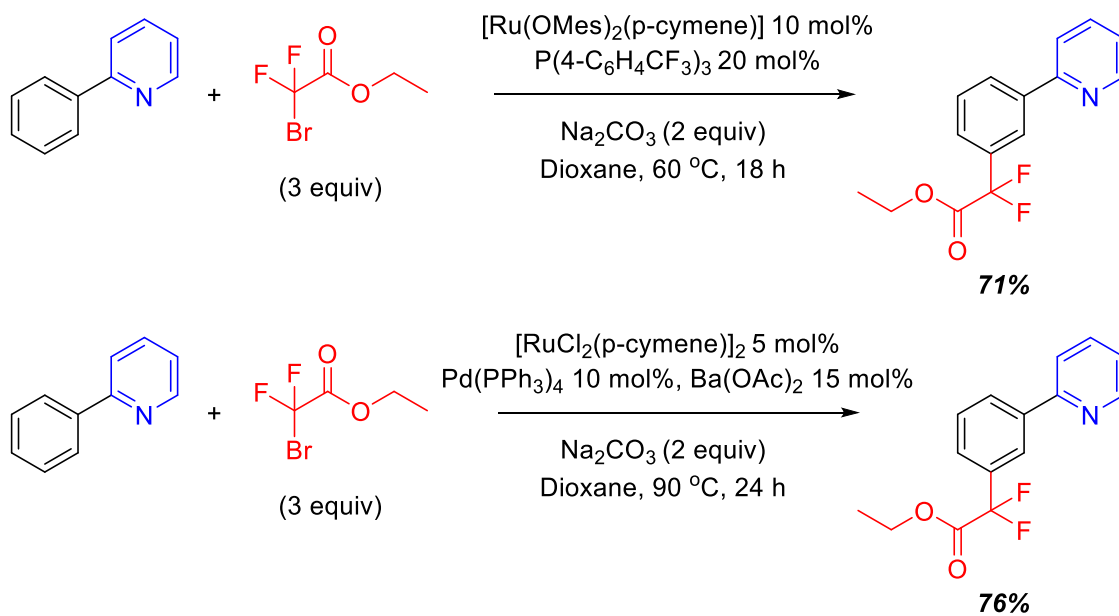
Figure 4-2. Relative nucleophilicity Fukui indices (f_A^-) calculated for computed substrates **1a**, **1k**, **1n**, **1r** and the corresponding cyclometalated complexes, **Ax**, [(*p*-cymene)Ru(OMe)(1x)]. Calculations were performed at the BP86/6-31G**&SDD(Ru) level of theory. Fukui indices were calculated with NBO total atomic charges from the optimised neutral structure. The most reactive C-H position is highlighted in red.

4.6 Mechanistic considerations: Role of Pd(PPh₃)₄

Given the effectiveness of palladium(0) assistance in the above procedure, we had initially believed that the role of this additive was to assist in the activation of the α -halo carbonyl reagent via an oxidative addition pathway. However, during the preparation of this work, the groups of Ackermann¹⁶ and Wang¹⁷ reported on a procedure for ruthenium catalysed *meta*

selective mono and difluoromethylation reactions using α -bromo ester reagents and cast significant doubt onto this hypothesis (**Scheme 4-6**).

Scheme 4-6. *Meta* difluoromethylation reported by Ackermann¹⁶ (top) and Wang¹⁷ (bottom).



In a similar manner to our previously developed procedure, the Wang group reported co-catalytic palladium as being necessary to achieve this transformation. However, the Ackermann group reported that only phosphine assistance was necessary with $\text{P}(4\text{-C}_6\text{H}_4\text{CF}_3)_3$ performing as the optimum ligand and simpler phosphines such as PPh_3 performing nearly as well. Other phosphine sources were significantly less effective, including a range of bisphosphines, trialkyl phosphines, phosphites and electron rich triaryl phosphines such as $\text{P}(p\text{Tol})_3$ and $\text{P}(\text{Mes})_3$. When applied to our procedure, the addition of PPh_3 instead of $\text{Pd}(\text{PPh}_3)_4$ led to comparable reaction yields and selectivity's (**Table 4-2**).

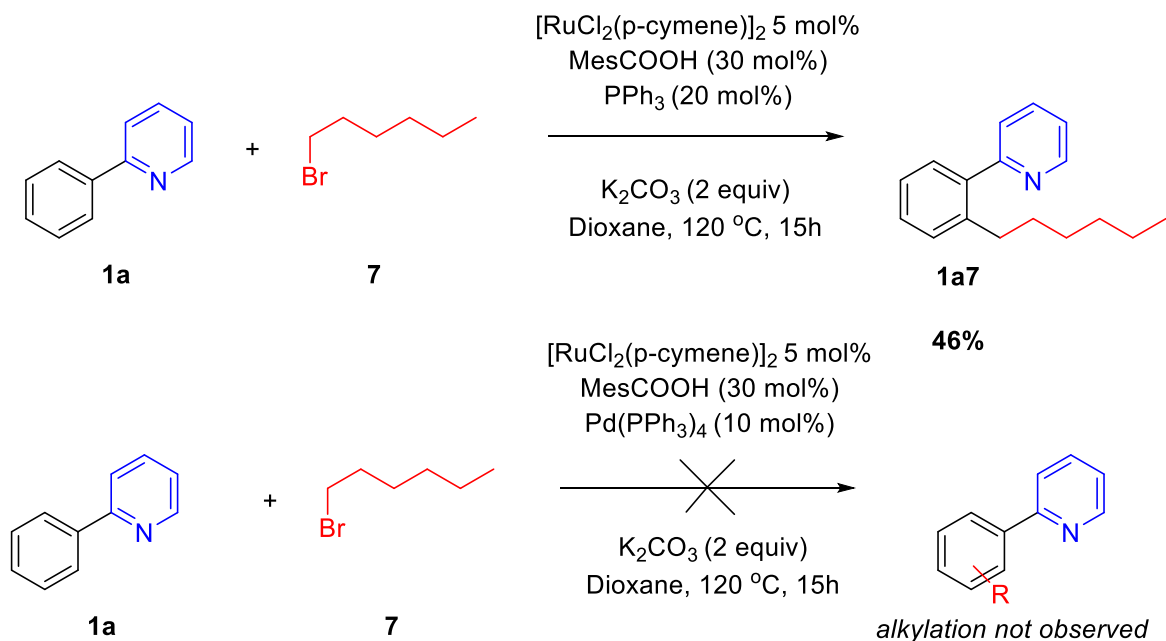
Table 4-2. Control experiments.

Entry	Additive	Yield (%)	<i>m</i> : <i>o</i>	
1	none	24	0.4:1	
2	Pd(PPh ₃) ₄ (10 mol%)	55	20:1	
3	PPh ₃ (20 mol%)	58	18:1	
4	PPh ₃ (40 mol%)	57	19:1	
5	Pd(PPh ₃) ₄ (10 mol%) and PPh ₃ (20 mol%)	56	18:1	
6 ^a	PPh ₃ ^a (20 mol%)	16	1:1	

^a Using Na₂CO₃, [Ru(OMes)₂(p-cymene)] at 60°C, 24 h¹⁶

These results strongly indicated that the addition of Pd(PPh₃)₄ serves only as a source of PPh₃. It therefore seems likely that PPh₃ becomes de-coordinated from the palladium center under the reaction conditions and serves as a ligand for the ruthenium. This could provide additional electron density at the position para to the C-Ru bond formed after cyclometalation. Furthermore, the additional steric bulk of the phosphine ligand could also serve to block the coordination sphere of the ruthenium metal and disfavor oxidative addition of the alkyl halide which could lead to *ortho* substitution. These properties can help to explain the increased reaction yields and selectivity when compared with reactions with no phosphine assistance.

The privileged reactivity of α-halo carbonyls was further highlighted when reaction with unactivated alkyl bromide **7** resulted in no *meta* alkylated products (**Scheme 4-5**) and led to *ortho* substituted products in agreement with other work in the field.^{12,13} No disubstituted products were isolated. The use of Pd(PPh₃)₄ led to no alkylated products and could be due to undesirable oxidative addition / β-hydride elimination pathways.

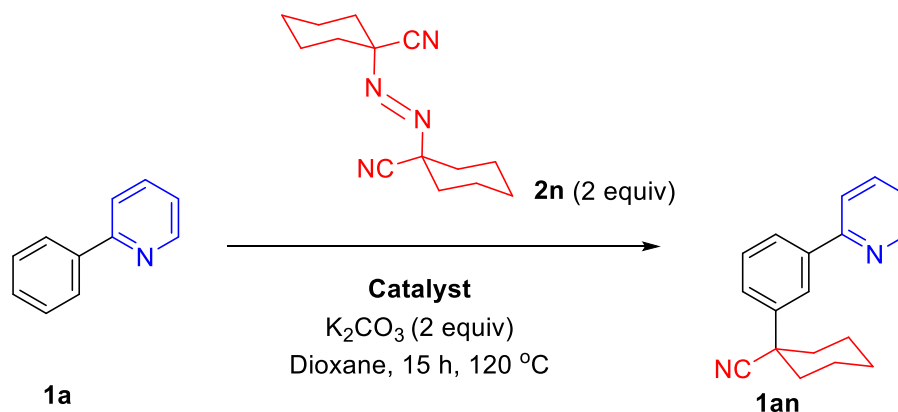


Scheme 4-5. Reaction with unactivated alkyl halide 7.

4.7 Mechanistic considerations: Addition to cyclometalated complex

We were then interested to discover the manner in which the alkyl halide coupling partners reacted with the activated arene. In our previous work with *meta* selective tertiary alkylation reactions, we proposed a second distinct single electron redox cycle that can generate the tertiary alkyl radical, which can add to the cyclometalated complex in a site selective manner.¹ To investigate this further, a series of experiments were conducted using radical coupling partner 1,1'-Azobis(cyclohexanecarbonitrile) (ABCN, **2n**) (Table 4-3).

Table 4-3. Reactions with ABCN

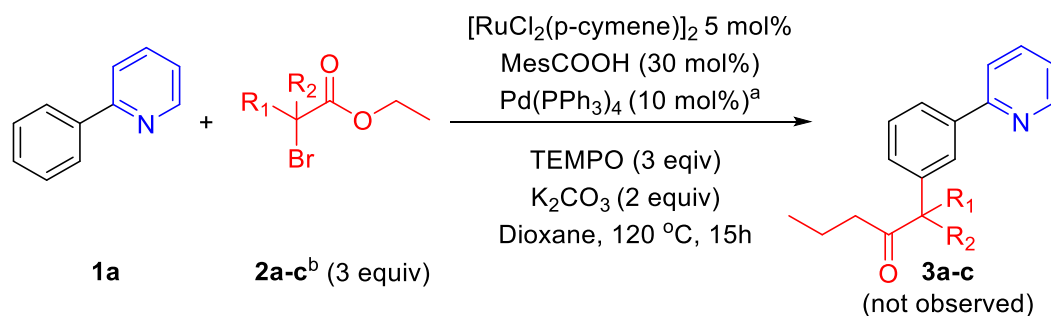


Entry	Catalyst	Yield
1	No catalyst	0%
2	$[Ru(OMes)_2(p\text{-cymene})]$ (10 mol%)	9%
3	$[Ru(OMes)_2(p\text{-cymene})]$ (50 mol%)	26%
4	PPh_3	0%
5	$[Ru(OMes)_2(p\text{-cymene})]$ (10 mol%) + PPh_3 (20 mol%)	8%

Thermal generation of a tertiary radical through loss of nitrogen resulted in no conversion to the *meta* product when no ruthenium complex was used however when 10 mol% preformed complex $[Ru(OMes)_2(p\text{-cymene})]$ was employed, *meta* alkylated product **1an** was formed in a 9% yield showing that ruthenium is essential for the activation of the substrate molecule. Increasing the catalyst loading increased the yield somewhat showing that this is a stoichiometric process. The sole use of PPh_3 led to no product formation and did not provide any additional benefit when used with a ruthenium complex. These results support the proposition that cyclometalation activates the position *para* to the C-Ru bond and external activation of the coupling partner and generation of a tertiary alkyl radical can then result in addition to this complex.

We were then interested to determine whether primary α -halo carbonyls reacted in the same manner as the corresponding secondary and tertiary coupling partners. Reactions with stoichiometric amounts of radical scavenger TEMPO led to no product formation (**Scheme 4-6**) however this does not necessarily imply a radical mechanism when primary coupling partner **2a** was used. Unlike the secondary or tertiary α -halo carbonyl coupling partners that were shown to be effective in **Scheme 4** or the thermally generated tertiary radical formed from

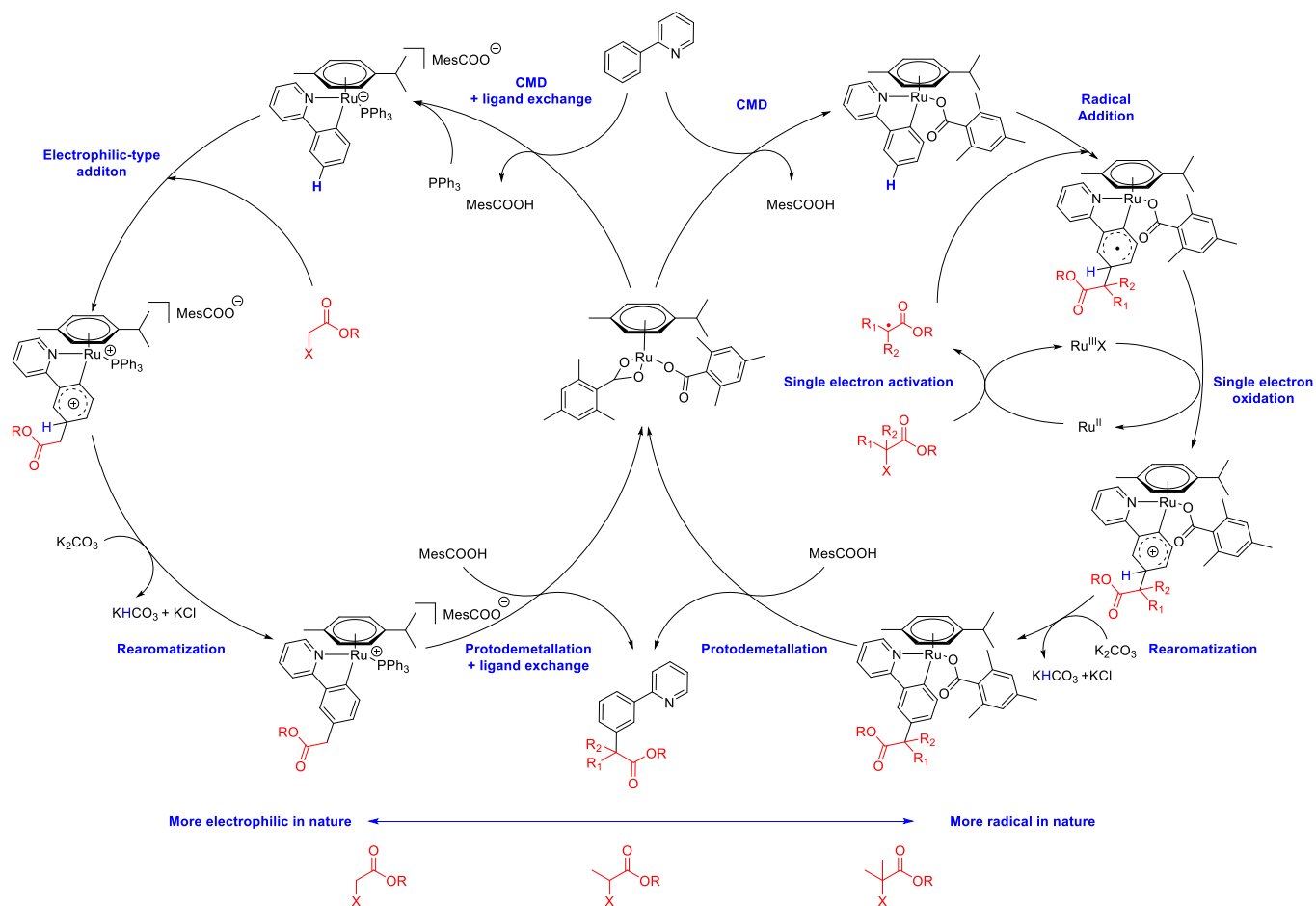
ABCN, the radical formed from homolytic cleavage of the C-Br bond in **2a** would not benefit from any captodative stabilization and attempts to trap this radical with TEMPO were unsuccessful. It is possible still that this coupling partner could react via an electrophilic mechanism and would be consistent with the previously calculated nucleophilic NBO calculations.



Scheme 4-7. Reactions with TEMPO ^aOnly added for reaction with **2a** ^b**2a** ($\text{R}_1 = \text{R}_2 = \text{H}$) **2b** ($\text{R}_1 = \text{H}$ $\text{R}_2 = \text{Me}$) **2c** ($\text{R}_1 = \text{R}_2 = \text{Me}$)

4.8 Conclusions and overall mechanism

Based on our most recent mechanistic observations and on previous work conducted by ourselves¹ and others^{11,2} in the field, we propose the following mechanism for *meta* selective alkylations with primary, secondary and tertiary α -halo carbonyls (**Scheme 4-8**). Reaction of a substrate molecule with ruthenium results in a cyclometalated complex activated with additional electron density at the position *para* to the C-Ru bond. Reaction of this complex with secondary or tertiary radicals externally generated by a single electron Ru(II)/Ru(III)X process then leads to the formation of a cyclometalated arene radical. Single electron oxidation, rearomatization and demetallation then leads to the *meta* substituted products. When primary α -halo carbonyl radicals are instead utilised, phosphine coordination to the ruthenium catalyst further promotes activation of the substrate molecule for *meta* selectivity. Addition then occurs at the position *para* to the C-Ru bond and could occur via either a single electron or electrophilic process.



Scheme 4-8. Plausible catalytic cycles.

4.9 References

1. A. Paterson, S. St John-Campbell, M. F. Mahon, N. Press, and C. G. Frost, *Chem. Commun.*, 2015, **51**, 12807–12810.
2. J. Li, S. Warratz, D. Zell, S. De Sarkar, E. E. Ishikawa, and L. Ackermann, *J. Am. Chem. Soc.*, 2015, **137**, 13894–13901.
3. Z. Fan, J. Ni, and A. Zhang, *J. Am. Chem. Soc.*, 2016, **138**, 8470–8475.
4. E. Ferrer Flegeau, C. Bruneau, P. H. Dixneuf, and A. Jutand, *J. Am. Chem. Soc.*, 2011, **133**, 10161–10170.
5. L. Ackermann, *Chem. Rev.*, 2011, **111**, 1315–1345.
6. T. Nishikata, Y. Noda, R. Fujimoto, and T. Sakashita, *J. Am. Chem. Soc.*, 2013, **135**, 16372–16375.
7. X. Zhang, H. Yi, Z. Liao, G. Zhang, C. Fan, C. Qin, J. Liu, and A. Lei, *Org. Biomol. Chem.*, 2014, **12**, 6790–6793.
8. G. Caillot, J. Dufour, M.-C. Belhomme, T. Poisson, L. Grimaud, X. Pannecoucke, and I. Gillaizeau, *Chem. Commun.*, 2014, **50**, 5887–5890.
9. R. Zhu and S. L. Buchwald, *J. Am. Chem. Soc.*, 2015, **137**, 8069–8077.
10. Crystal structure determination of **6aa**: C₁₇H₁₅NO₂ (M = 265.30 g/mol): monoclinic, space group *P*2₁/*c*, *a* = 17.0838(3), *b* = 5.23428(9), *c* = 14.8641(3) Å, β = 90.8577(17)°, *U* = 1329.01(4) Å³, *Z* = 4, *T* = 150.00(10) K, μ (CuK α) = 0.698 mm⁻¹, *D*_{calc} = 1.326 g cm⁻³, 12751 reflections measured (5.174° ≤ 2 θ ≤ 146.686°), 2679 unique (*R*_{int} = 0.0339) which were used in all calculations. The final *R*1 was 0.0369 (*I* > 2 σ (*I*)) and *wR*2 was 0.0998 (all data). CCDC 1526788 contains the supplementary crystallographic data for **6aa**
11. N. Hofmann and L. Ackermann, *J. Am. Chem. Soc.*, 2013, **135**, 5877–84.
12. L. Ackermann, N. Hofmann, and R. Vicente, *Org. Lett.*, 2011, **13**, 1875–7.
13. L. Ackermann, P. Novák, R. Vicente, and N. Hofmann, *Angew. Chemie - Int. Ed.*, 2009, **48**, 6045–8.
14. P. Marcé, A. J. Paterson, M. F. Mahon, and C. G. Frost, *Catal. Sci. Technol.*, 2016.
15. G. B. Boursalian, W. S. Ham, A. R. Mazzotti, and T. Ritter, *Nat. Chem.*, 2016, **8**, 1–6.
16. Z. Ruan, S.-K. Zhang, C. Zhu, P. N. Ruth, D. Stalke, and L. Ackermann, *Angew. Chemie Int. Ed.*, 2017, **3**, 2045–2049.
17. G.-W. Wang, Z.-Y. Li, L. Li, Q.-L. Li, K. Jing, and H. Xu, *Chem. - A Eur. J.*, 2017.

5.0 Overall conclusions and future work

The field of selective catalytic C-H functionalisation has grown substantially in recent years and is still a topic of great importance in synthetic research. The benefits of improved step and atom economy over traditional approaches, as well as generating new synthetic disconnections, means that developing broadly useful methodologies remains as attractive as ever.

The strategies devised to tackle the significant challenge of achieving selective functionalisation of a C-H bond within a molecule rely largely on either exploiting its innate reactivity or by utilising a directing group approach. In the best case scenario, these methodologies can result in the highly efficient coupling of two molecules in a catalytic cycle without the use of stoichiometric additives or the need for pre or post synthetic modifications. However, due to the complexity of molecular systems, it is difficult to develop a one-size-fits-all strategy for direct C-H functionalisation.

The field of *ortho* functionalisation has become sufficiently developed such that most common Lewis basic functional groups can now be recognised for their potential to direct a transition metal catalyst to a C-H bond in a predictable manner. Conceptually, the use of a directing group strategy has largely prevailed, and through appropriate choice of catalyst and reaction conditions a great number of transformations have been made possible. In contrast, the field of *meta* selective C-H functionalisation has been less developed whereby a simple directing group strategy cannot always be as readily applied.

Several approaches have nevertheless come into recent prominence, each with their own advantages and limitations. Early examples which relied solely on a molecule's innate reactivity through electronic or steric biases afford reactions with excellent selectivity however are inherently limited in scope. Directing group strategies such as those utilising extended templates or transient mediators effectively address issues of scope by converting common functional groups into *meta* selective directing groups however often come at the expense of overall step and atom economy. The work in this thesis has described the development of another strategy for *meta* selective C-H functionalisation by ruthenium catalysed σ -activation, which can be viewed as a hybrid method between innate and directed functionalisation. It benefits from being operationally simple and highly selective, however at present is somewhat limited in scope.

At the outset of this work, just one example had been reported: the *meta* sulfonation of 2-phenylpyridines with aryl sulfonyl chlorides. The mechanism and scope of this reaction was not immediately clear but recent work conducted in the field has led to significant advances in

understanding with the work described in this thesis making valuable contributions to this. The manuscript entitled “Catalytic *meta* selective C-H functionalization to construct quaternary carbon centres” was the second contribution to the field from our group and crucially this work gave significant insight into the reaction mechanism and potential scope. Specifically, this work gave good evidence for a radical based mechanism, especially because of the effective coupling of α -halo carbonyl reagents and the associated polymer type products which were consistent with a radical mechanism. Furthermore, this work was the first to propose a potential dual role of the ruthenium catalyst, activating both the substrate and the coupling partner, and this proposition was independently supported by similar work conducted in the field. Other work reported in this thesis using α -halo carbonyls expanded the scope of the *meta* alkylation procedure and enabled *meta* selective primary alkylations. This work also provided additional mechanistic insight into the substrate activation pathway, with experimental and computational support showing that cyclometalation activates the position *para* to the newly installed C-Ru bond for reaction with an externally activated coupling partner.

The manuscript entitled “Mechanistic insight into ruthenium catalysed *meta* sulfonation of 2-phenylpyridine” provided additional mechanistic analysis to the *meta* sulfonation reaction, with a focus on the catalytic species and mechanisms involved. A key result from this work was a stoichiometric experiment with a ruthenium complex, showing that sulfonation occurred *para* to the C-Ru bond, in agreement with previous mechanistic propositions. The work also showed that the catalytic species involved did not require an arene ligand and deuterium labelling studies identified a likely rate limiting radical tosylation step.

Now, ruthenium catalysed σ -activation has been extended to include *meta* selective alkylations, brominations and nitrations. In most cases, generation of radical coupling partners are implied and could be key to the development of new *meta* selective transformations. This methodology has also been demonstrated on a range of substrates with directing groups including pyridine, pyrimidine, pyrazole, isoquinoline, quinoxaline, pyridazinone, imine, oxime and benzimidazole. This strategy for *meta* functionalisation usually also benefits from being very operationally simple, utilising cheap and readily available materials.

However, despite the successes so far, we have not yet achieved our original ambitious goal of developing ruthenium catalysed σ -activation into a broadly useful methodology for *meta* selective C-H functionalisation. While the coupling partner scope is continually growing, a significant limitation is that to date, the methodology has only been demonstrated on substrates containing strongly coordinating nitrogen containing directing groups. While the use of removable auxiliaries has been demonstrated, this methodology likely requires a stable cyclometalated complex for

functionalisation and could hence be fundamentally limited in scope. This limitation in scope is however largely true of all of the current *meta* selective C-H functionalisation methodologies and represents a significant challenge to the field.

In order to tackle these challenges in the context of ruthenium catalysed σ -activation, we have begun to show that new computational methods can be applied to predict the reactivity of the resulting complexes. This could be an effective tool for rapid and rational catalyst design and the use of appropriate ligands could be the key to enabling more substrates to react in a highly site selective manner, an approach that has recently enabled mono and difluoromethylations and primary alkylations. This, along with devising new ways of activating coupling partners by alternative methods, could be instrumental in developing this methodology into one that can be broadly synthetically useful.

6.0 Data and supporting information

The following section contains the reformatted supporting information for each of the manuscripts in the previous sections. NMR Spectra for novel compounds have been omitted, however can be found online free of charge on the journal webpages.

6.1 Supporting information and data for: Catalytic *meta*-selective C-H functionalisation to construct quaternary carbon centres.

General Considerations:

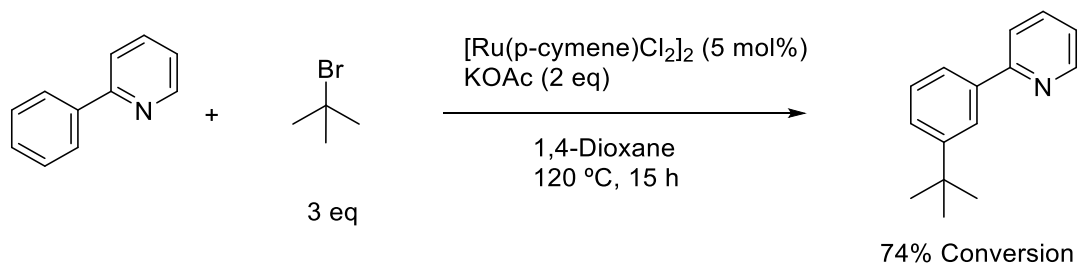
^1H , ^{13}C and ^{19}F nuclear magnetic resonance (NMR) spectra were recorded on an Agilent Technologies spectrometer (^1H NMR at 500 MHz, ^{13}C NMR at 126 MHz, and ^{19}F NMR at 470 MHz). Chemical shifts for protons are reported downfield from tetramethylsilane and are referenced to residual protium in the solvent (^1H NMR: CHCl_3 at 7.26 ppm). Chemical shifts for carbons are reported in parts per million downfield from tetramethylsilane and are referenced to the carbon resonances of the solvent peak (^{13}C NMR: CDCl_3 at 77.0 ppm). Chemical shifts for fluorine resonances are reported in parts per million referenced to CFCl_3 . NMR data are represented as follows: chemical shift (integration, multiplicity [s = singlet, bs = broad singlet, d = double, dd = doublet of doublet, t = triplet, q = quartet, hept = heptet, m = multiplet], coupling constants (Hz)). IR spectra were recorded on a Perkin-Elmer 1600 FT IR spectrophotometer, with absorbencies quoted as ν in cm^{-1} . High resolution mass spectrometry was performed on a Bruker Daltonik μTOF electrospray time-of-flight (ESI-TOF) mass spectrometer. HPLC analysis was conducted on an Agilent 1260 infinity quaternary LC instrument equipped with a Zorbax Eclipse XDB-C18 4.6 x 250 mm 5 μm analytical column. Analytical thin layer chromatography (TLC) were performed using aluminium-backed plates coated with Alugram[®] SIL G/UV₂₅₄ purchased from Macherey-Nagel and visualised by UV light (254 nm) and/or KMnO_4 staining. Silica gel column chromatography was carried out using 60 Å, 200-400 mesh particle size silica gel purchased from Sigma-Aldrich.

Materials:

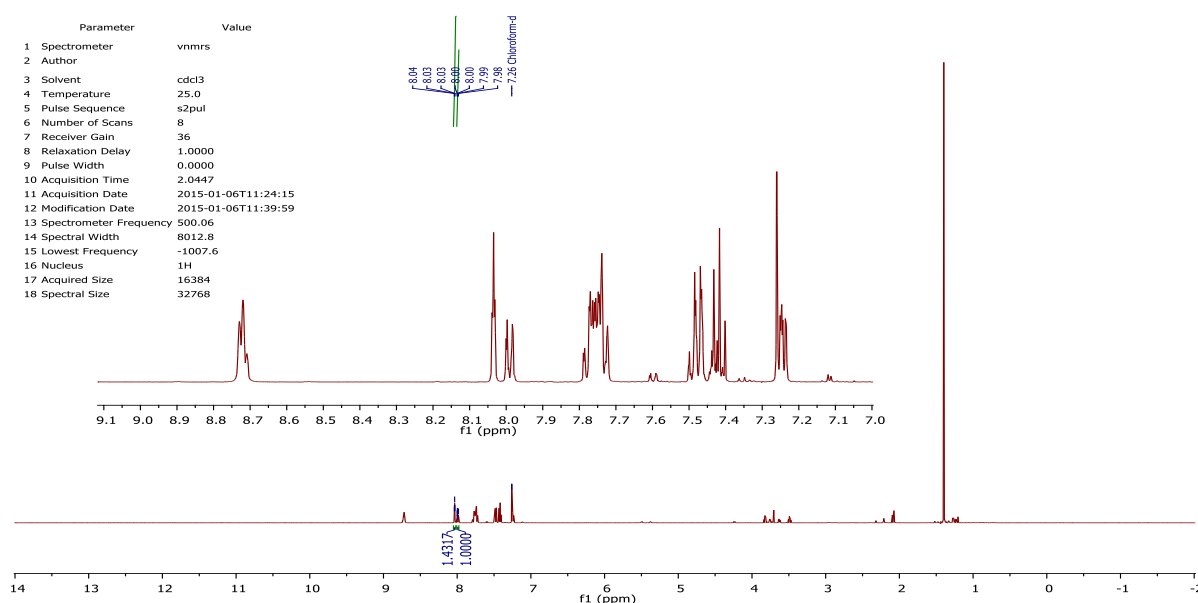
All reactions were carried out under an atmosphere of argon, in oven-dried glassware unless otherwise stated. Anhydrous solvents were used in all experiments and stored under an atmosphere of argon prior to use. $[\text{RuCl}_2(p\text{-cymene})]_2$ was purchased from Strem chemicals. Boronic acids were purchased from Fronteir Scientific. 2-chloro-2methylpropane, 2-bromo-2methylpropane, 2-bromo-2methylbutane, 1-bromo adamantane and 3-chloro-3-ethyl pentane were purchased from sigma Aldrich. All other chemicals were bought from Alfa Aesar. All commercially bought chemicals were used without further purification.

Reaction Conversions

Reaction conversions were calculated using ^1H NMR and confirmed using ^{19}F NMR where possible. With the exception of those carried out using ethyl 2-bromoisobutrate (**2c**) all reactions formed one product exclusively and thus conversions represent conversion of the starting material to the desired product. Suitably resolved signals in the crude reaction mixture were used for these calculations. Orthogonal analysis using TLC and HPLC-MS revealed negligible by-products. This is exemplified below.



Conversion by ^1H NMR of Crude Reaction Mixture: Signal at 8.05 ppm (dd, $J = 1.8$ Hz, 1H) from product **3a** and signal at 8.00 – 7.98 (m, $J = 5.3, 3.4$ Hz, 2H) from starting material **1a** used for conversion calculation.



HPLC analysis of the crude reaction mixture showing the major components: starting material **1a** (retention time 5.93 min) and product **3a** (retention time 11.28 min).

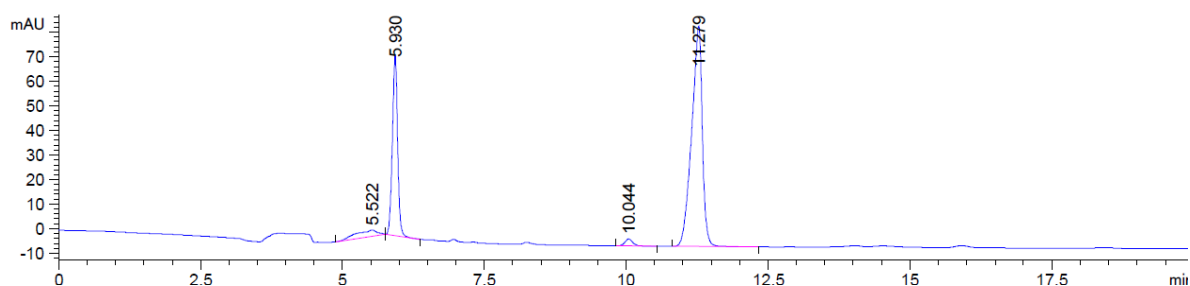
Sample prepared to approximate 10 μmol / mL in acetonitrile

Column: Zorbax Eclipse XDB-C18 4.6 x 250 mm 5 μm analytical column

Mobile Phase: Isocratic 70/30 acetonitrile/ H_2O with 0.1% formic acid

Flow Rate: 0.5 mL / min

UV detection: 254 nm

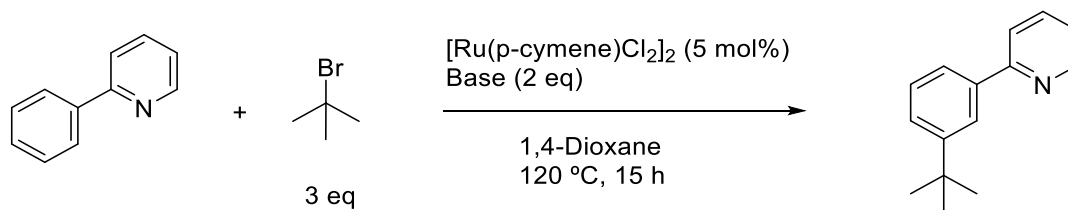


Reaction Optimisation

General Procedure

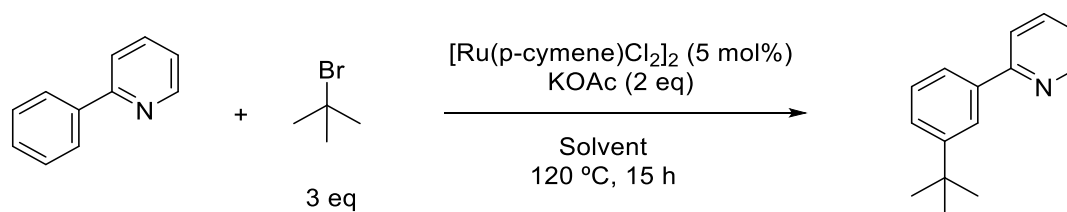
To an oven dried, argon purged ampule equipped with magnetic stirrer was added 2-phenylpyridine (1 mmol, 0.14 mL), a solvent (4 mL), 2-Bromo-2-methylpropane, $[\text{RuCl}_2(\text{p-cymene})]_2$ and a base in the amounts specified. The ampule was then sealed and refluxed on a carousel at 120 °C for the amount of time specified. After cooling to room temperature, aqueous NaHCO_3 (saturated) and EtOAc were added. A sample of the organic phase was taken, evaporated to dryness and then conversions analysed by ^1H NMR and HPLC-MS.

Base Screen



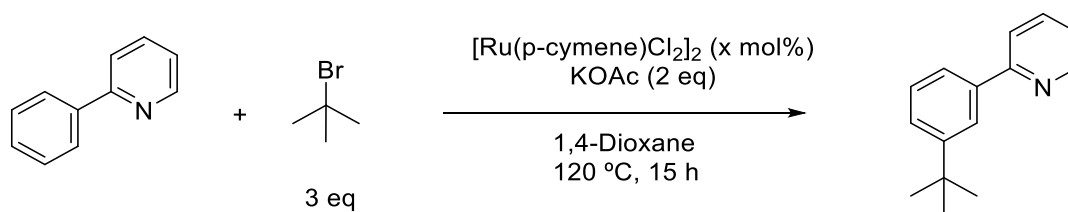
Base	Conversion (%)
No Base	0
K_2CO_3	12
NaOAc	31
KOAc	74
CsOAc	64
Bu_4NOAc	13
$\text{Cu}(\text{OAc})_2$	0
AgOAc	0

Solvent Screen



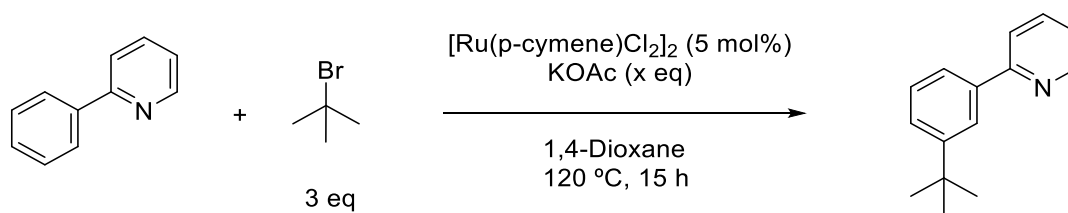
Solvent	Conversion (%)
No Solvent	69
2-Bromo-2-methylpropane	72
Acetonitrile	0
1,2-Dichloroethane	0
N-Methyl-2-pyrrolidone	0
2-methyl-2-butanol	61
H ₂ O	0
Toluene	66
Trifluoromethyl-benzene	70
Ethylene glycol	0
Dimethylformamide	0
Dimethoxyethane	56
Diglyme	43
Triglyme	44
THF	59
2-Methyltetrahydrofuran	68
Methyl tert-butyl ether	55
Cyclopentyl methyl ether	68
2-Butanone	61

Catalyst Loading



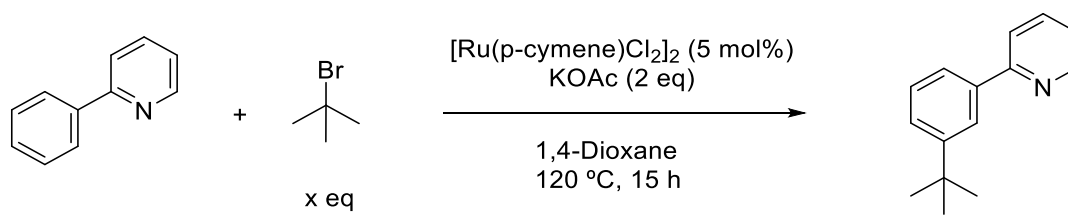
Catalyst Loading (mol %)	Conversion (%)
No Catalyst	0
0.5	7
1	50
2.5	58
5	74
7.5	68

KOAc Stoichiometry



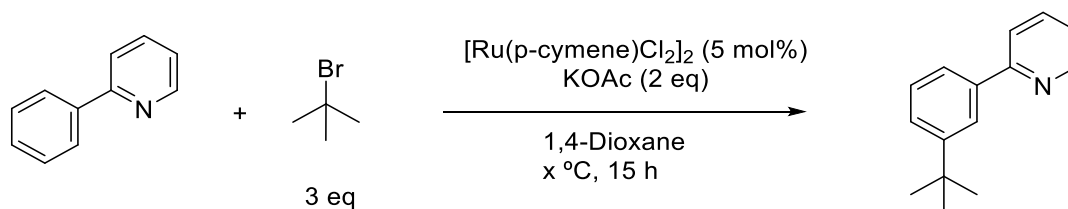
Base Equivalents	Conversion (%)
No Base	0
0.5	24
1.5	58
1.75	65
2	74
2.5	72
3	56
4	59

Alkyl Halide Stoichiometry



Alkyl Halide Equivalents	Conversion (%)
1	0
1.5	38
2	58
3	74
As solvent	72

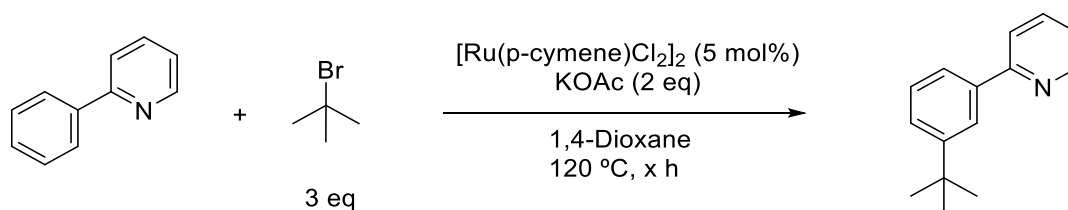
Temperature



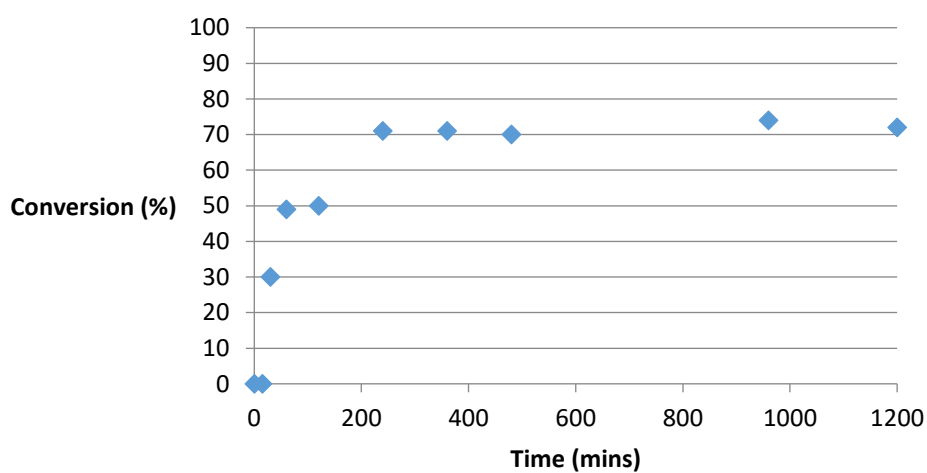
Temperature (°C)	Conversion (%)
25	0
80	18
100	50
120	74
135	65

Reaction Time

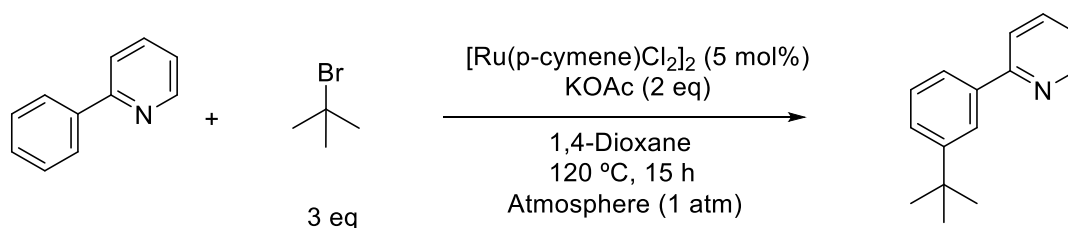
Multiple reactions were set up in series and after the designated reaction time were immediately cooled in an ice bath, worked up and analysed as per the general procedure.



Time (min)	Conversion (%)
0	0
15	0
30	30
60	49
120	50
240	71
360	71
480	70
960	74
1200	72



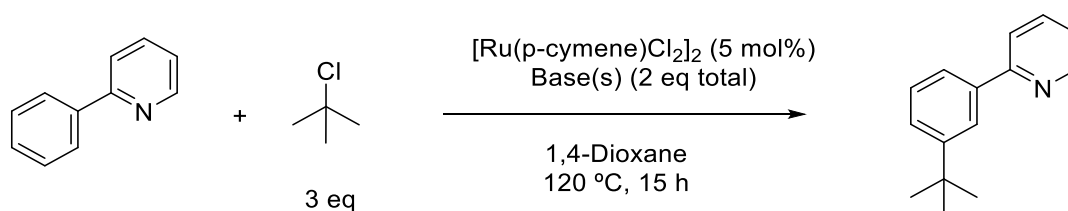
Reaction Atmosphere



Atmosphere (1 atm)	Conversion (%)
Argon	74
Air	25
Oxygen	0*

*No formation of **3a**, starting material **1a** completely destroyed.

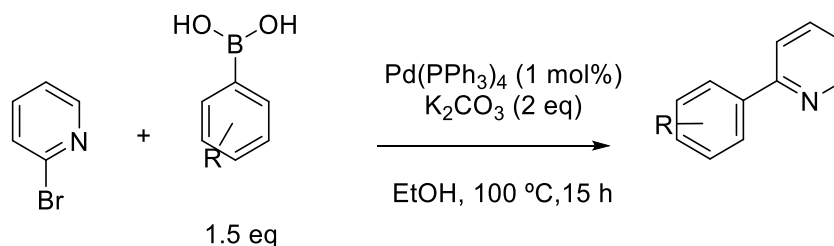
Optimisation for 2-Chloro-2-methylpropane



KOAc Equivalents	K ₂ CO ₃ Equivalents	Conversion (%)
0	2	27
0.5	1.5	63
1	1	38
1.5	0.5	0
2	0	0

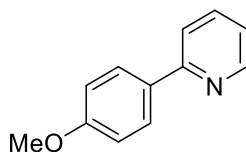
Synthesis of 2-Substituted Pyridine Derivatives

General Procedure



To an oven dried, argon purged flask equipped with magnetic stirrer and condenser was added Pd(PPh₃)₄ (1 mol%), K₂CO₃ (2 eq) and ethanol (1 M). A solution of the boronic acid (1.5 eq) in EtOH (1 M) was then added *via* a dropping funnel to the reaction vessel followed by the addition of 2-bromopyridine (1 eq). The reaction mixture was then heated to 100 °C and refluxed for 15 hours. After cooling to room temperature, aqueous NaOH (1 M) was added and extracted three times with EtOAc. The organic extracts were then combined, washed with brine, dried with MgSO₄ and then concentrated under reduced pressure. The crude product was then purified by silica gel column chromatography (Hexane / EtOAc).

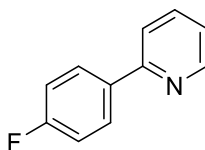
2-(4-methoxyphenyl)pyridine (1c)



2-bromopyridine (25 mmol, 2.4 mL), 4-methoxyphenyl boronic acid (33 mmol, 5.0 g), Pd(PPh₃)₄ (0.25 mmol, 289 mg), K₂CO₃ (50 mmol, 6.90 g) were reacted together in EtOH (25 mL) according to the general procedure to afford the title compound as a white solid (4.4 g, 95%). ¹H NMR (500 MHz, CDCl₃) δ 8.65 (ddd, *J* = 4.8, 1.7, 1.0 Hz, 1H), 7.96 (d, *J* = 8.9 Hz, 2H), 7.76 – 7.64 (m, 2H), 7.17 (ddd, *J* = 7.2, 4.8, 1.3 Hz, 1H), 7.00 (d, *J* = 8.9 Hz, 2H), 3.87 (s, 3H). ¹³C NMR (126 MHz, CDCl₃) δ 160.43, 157.08, 149.47, 136.67, 131.92, 128.15, 121.38, 119.79, 114.11, 55.34.

Data conforms to literature.¹

2-(4-fluorophenyl)pyridine (1d)

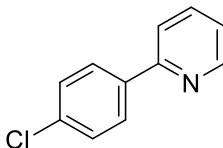


2-bromopyridine (20 mmol, 1.9 mL), 4-fluorophenyl boronic acid (30 mmol, 4.20 g), Pd(PPh₃)₄ (0.2 mmol, 231 mg), and K₂CO₃ (40 mmol, 5.52 g) were reacted together in EtOH (20 mL) according to the general procedure to afford the title compound as a yellow / white crystalline solid (3.20 g, 92%).

¹H NMR (500 MHz, CDCl₃) δ 8.68 (ddd, J = 4.8, 1.6, 0.9 Hz, 1H), 7.98 (dd, J = 8.9, 5.4 Hz, 2H), 7.77 – 7.72 (m, 1H), 7.68 (dt, J = 8.0, 1.0 Hz, 1H), 7.22 (ddd, J = 7.4, 4.8, 1.1 Hz, 1H), 7.16 (t, J = 8.7 Hz, 2H). **¹³C NMR** (126 MHz, CDCl₃) δ 163.51 (d, ¹J_{C-F} = 248.4 Hz), 135.51 (d, ⁴J_{C-F} = 3.1 Hz), 128.68 (d, ³J_{C-F} = 8.4 Hz), 115.63 (d, ²J_{C-F} = 21.6 Hz). **¹⁹F NMR** (470 MHz, CDCl₃) δ -113.14 – -113.24 (m).

Data conforms to literature.¹

2-(4-chlorophenyl)pyridine (1e)



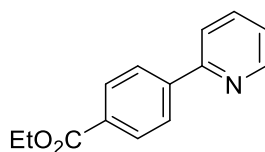
2-bromopyridine (13 mmol, 1.2 mL), 4-chlorophenyl boronic acid (20 mmol, 3.04 g), Pd(PPh₃)₄ (0.13 mmol, 150 mg), and K₂CO₃ (26 mmol, 3.58 g) were reacted together in EtOH (13 mL) according to the general procedure to afford the title compound as a pale yellow crystalline solid (1.20 g, 89%).

¹H NMR (500 MHz, CDCl₃) δ 8.69 (dd, J = 4.8, 0.8 Hz, 1H), 7.95 (d, J = 8.4 Hz, 2H), 7.81 – 7.74 (m, 1H), 7.71 (dd, J = 7.9, 0.9 Hz, 1H), 7.45 (d, J = 8.5 Hz, 2H), 7.29 – 7.24 (m, 1H).

¹³C NMR (126 MHz, CDCl₃) δ 155.97, 149.35, 137.31, 137.26, 135.30, 128.97, 128.23, 122.45, 120.49.

Data conforms to literature.¹

2-(4-(ethoxycarbonyl)phenyl)pyridine (1f)

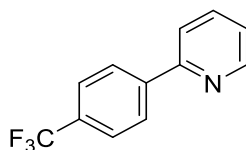


2-bromopyridine (13 mmol, 1.2 mL), 4-(methoxycarbonyl)phenyl boronic acid (20 mmol, 3.04 g), Pd(PPh₃)₄ (0.13 mmol, 150 mg), and K₂CO₃ (26 mmol, 3.58 g) were reacted together in EtOH (13 mL) according to the general procedure to afford the title compound as a white solid (2.42 g, 82%).

¹H NMR (500 MHz, CDCl₃) δ 8.73 (d, *J* = 4.6 Hz, 1H), 8.15 (d, *J* = 8.2 Hz, 2H), 8.07 (d, *J* = 8.3 Hz, 2H), 7.87 – 7.71 (m, 2H), 7.29 (dd, *J* = 8.3, 4.8 Hz, 1H), 4.41 (q, *J* = 7.1 Hz, 2H), 1.42 (t, *J* = 7.1 Hz, 3H). **¹³C NMR** (126 MHz, CDCl₃) δ 166.56, 156.38, 149.93, 143.42, 137.15, 130.90, 130.16, 126.95, 123.00, 121.19, 77.16, 61.22, 14.50.

Data conforms to literature.¹

2-(4-(trifluoromethyl)phenyl)pyridine (1g)

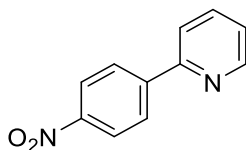


2-bromopyridine (10 mmol, 0.92 mL), 4-(trifluoromethyl)phenyl boronic acid (15 mmol, 2.85 g), Pd(PPh₃)₄ (0.10 mmol, 115 mg), and K₂CO₃ (20 mmol, 2.76 g) were reacted together in EtOH (10 mL) according to the general procedure to afford the title compound as an off white solid (1.38 g, 62%).

¹H NMR (500 MHz, CDCl₃) δ 8.73 (d, *J* = 4.7 Hz, 1H), 8.11 (d, *J* = 8.2 Hz, 2H), 7.84 – 7.69 (m, 4H), 7.33 – 7.27 (m, 1H). **¹³C NMR** (126 MHz, CDCl₃) δ 155.98 (s), 150.03 (s), 142.77 (s), 137.13 (s), 130.91 (q, ²*J*_{C-F} = 32.5 Hz), 127.31 (s), 125.81 (q, ³*J*_{C-F} = 3.8 Hz), 124.32 (q, ¹*J*_{C-F} = 272.0 Hz), 123.09 (s), 121.00 (s). **¹⁹F NMR** (470 MHz, CDCl₃) δ -62.61 (s).

Data conforms to literature.²

2-(4-(trifluoromethyl)phenyl)pyridine (1h)

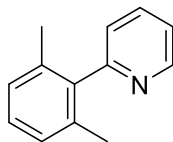


2-bromopyridine (4.5 mmol, 0.43 mL), 4-nitrophenyl boronic acid (6 mmol, 1.0 g), Pd(PPh₃)₄ (0.045 mmol, 52 mg), and K₂CO₃ (9 mmol, 1.24 g) were reacted together in EtOH (5 mL) according to the general procedure to afford the title compound as a yellow solid (609 mg, 68%).

¹H NMR (500 MHz, CDCl₃) δ 8.76 (d, *J* = 4.7 Hz, 1H), 8.34 (d, *J* = 8.6 Hz, 2H), 8.19 (d, *J* = 8.6 Hz, 2H), 7.89 – 7.74 (m, 2H), 7.35 (t, *J* = 5.6 Hz, 1H). **¹³C NMR** (126 MHz, CDCl₃) δ 155.03, 150.30, 148.22, 145.41, 137.26, 127.83, 124.16, 123.66, 121.36

Data conforms to literature.¹

2-(2,6-dimethylphenyl)pyridine (1i)

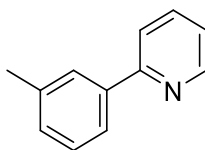


2-bromopyridine (13 mmol, 1.2 mL), 2,6-dimethylphenylboronic acid (20 mmol, 3.0 g), Pd(PPh₃)₄ (0.13 mmol, 150 mg), and K₂CO₃ (26 mmol, 3.59 g) were reacted together in EtOH (15 mL) according to the general procedure to afford the title compound as a red oil (1.96 g, 82%).

¹H NMR (500 MHz, CDCl₃) δ 8.74 (d, *J* = 4.5 Hz, 1H), 7.82 (dd, *J* = 7.6 Hz, 1H), 7.34 – 7.30 (m, 1H), 7.28 (d, *J* = 8.2 Hz, 1H), 7.21 (t, *J* = 7.6 Hz, 1H), 7.12 (d, *J* = 7.6 Hz, 2H). **¹³C NMR** (126 MHz, CDCl₃) δ 159.56, 149.17, 139.76, 137.09, 135.93, 128.25, 127.72, 124.93, 122.02, 77.16, 20.33.

Data conforms to literature.³

2-(3-dimethylphenyl)pyridine (1j)

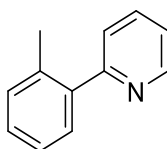


2-bromopyridine (5 mmol, 0.46 mL), 3-methylphenylboronic acid (7 mmol, 1.0 g), $\text{Pd}(\text{PPh}_3)_4$ (0.05 mmol, 58 mg), and K_2CO_3 (10 mmol, 1.38 g) were reacted together in EtOH (7.5 mL) according to the general procedure to afford the title compound as a yellow oil (772 mg, 91%).

^1H NMR (500 MHz, CDCl_3) δ 8.73 (d, J = 4.7 Hz, 1H), 7.87 (s, 1H), 7.84 – 7.73 (m, 3H), 7.39 (dd, J = 7.6 Hz, 1H), 7.29 – 7.24 (m, 2H), 2.46 (s, 3H). **^{13}C NMR** (126 MHz, CDCl_3) δ 157.40, 149.18, 138.81, 138.50, 137.16, 129.94, 128.69, 127.72, 124.09, 122.11, 120.86, 21.51.

Data conforms to literature. ⁴

2-(2-methylphenyl)pyridine (1l)



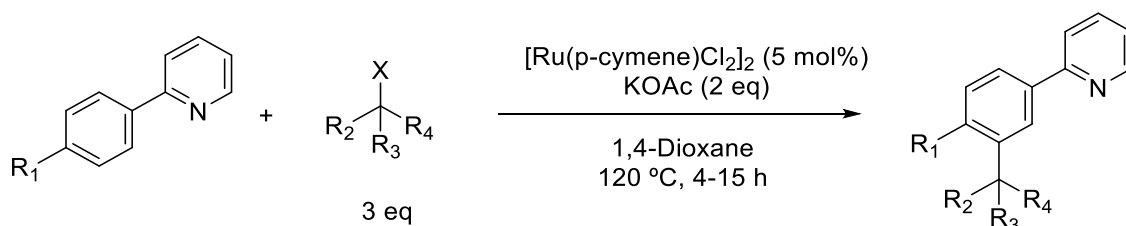
2-bromopyridine (20 mmol, 1.84 mL), 2-methylphenylboronic acid (30 mmol, 4.08 g), $\text{Pd}(\text{PPh}_3)_4$ (0.2 mmol, 231 mg), and K_2CO_3 (40 mmol, 5.52 g) were reacted together in EtOH (30 mL) according to the general procedure to afford the title compound as a yellow oil (2.96 g, 88%).

^1H NMR (500 MHz, CDCl_3) δ 8.71 (d, J = 3.9 Hz, 1H), 7.85 – 7.69 (m, 1H), 7.42 (dd, J = 13.6, 4.5 Hz, 2H), 7.33 – 7.25 (m, 4H), 2.29 (s, 3H). **^{13}C NMR** (126 MHz, CDCl_3) δ 159.67, 148.75, 139.86, 136.60, 135.77, 130.77, 129.64, 128.46, 125.91, 124.30, 121.76, 20.27.

Data conforms to literature. ³

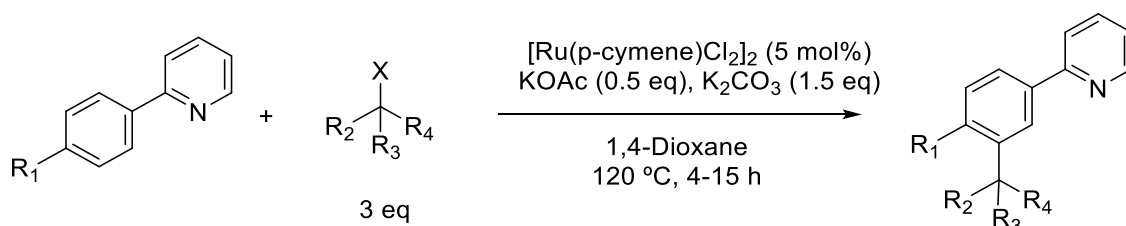
Synthesis of *meta*-Substituted 2-Phenylpyridine Derivatives.

General Procedure A



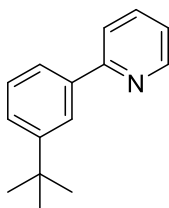
To an oven dried, argon purged ampule equipped with magnetic stirrer was added the 2-phenylpyridine derivative (1 mmol), the alkyl halide (3mmol), $[\text{RuCl}_2(\text{p-cymene})]_2$ (5 mol%, 30 mg), KOAc (2 mmol, 196 mg) and 1,4-Dioxane (4 mL). The ampule was then sealed and refluxed on a carousel at 120 °C for the amount of time specified. After cooling to room temperature, aqueous NaHCO_3 (saturated) was added and then was extracted three times with EtOAc. The organic extracts were then combined, washed with brine, dried with MgSO_4 and then concentrated under reduced pressure. The crude product was then purified by silica gel column chromatography (Hexane / EtOAc).

General Procedure B



To an oven dried, argon purged ampule equipped with magnetic stirrer was added the 2-phenylpyridine derivative (1 mmol), the alkyl halide (3mmol), $[\text{RuCl}_2(\text{p-cymene})]_2$ (5 mol%, 30 mg), KOAc (0.5 mmol, 49 mg), K_2CO_3 (1.5 mmol, 207 mg) and 1,4-Dioxane (4 mL). The ampule was then sealed and refluxed on a carousel at 120 °C for the amount of time specified. After cooling to room temperature, aqueous NaHCO_3 (saturated) was added and then was extracted three times with EtOAc. The organic extracts were then combined, washed with brine, dried with MgSO_4 and then concentrated under reduced pressure. The crude product was then purified by silica gel column chromatography (Hexane / EtOAc).

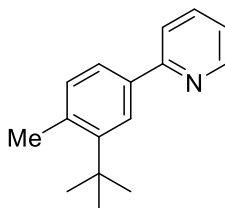
2-(3-tert-butylphenyl)pyridine (3a)



2-phenylpyridine (1 mmol, 0.14 mL), 2-bromo-2-methylpropane (3 mmol, 0.34 mL), [RuCl₂(p-cymene)]₂ (5 mol%, 30 mg), and KOAc (2 mmol, 196 mg) were reacted together in 1,4-Dioxane (4 mL) according to general procedure A to afford the title compound as a yellow oil (15 mg, 7%).

¹H NMR (500 MHz, CDCl₃) δ 8.71 (d, *J* = 4.8 Hz, 1H), 8.05 (dd, *J* = 1.8 Hz, 1H), 7.86 – 7.65 (m, 3H), 7.47 (d, *J* = 7.9 Hz, 1H), 7.42 (t, *J* = 7.7 Hz, 1H), 7.22 (ddd, *J* = 6.7, 4.9, 1.9 Hz, 1H), 1.40 (s, 9H). **¹³C NMR** (126 MHz, CDCl₃) δ 158.19, 151.74, 149.75, 139.32, 136.78, 128.57, 126.20, 124.30, 124.10, 122.04, 120.90, 77.16, 35.01, 31.54. **HR-MS** (ESI) *m/z*: calculated for C₁₅H₁₈N [M+H]⁺ 212.1439, found: 212.1395. **v_{max}** (neat) / cm⁻¹; 2960, 1584, 1564, 1461.

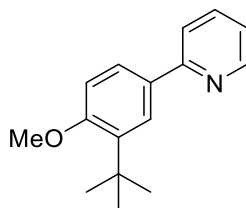
2-(3-tert-butyl-4-methylphenyl)pyridine (3b)



2-(4-methylphenyl)pyridine (1 mmol, 0.17 mL), 2-bromo-2-methylpropane (3 mmol, 0.34 mL), [RuCl₂(p-cymene)]₂ (5 mol%, 30 mg), and KOAc (2 mmol, 196 mg) were reacted together in 1,4-Dioxane (4 mL) according to general procedure A to afford the title compound as a colourless oil (12 mg, 5%).

¹H NMR (500 MHz, CDCl₃) δ 8.70 (d, *J* = 4.0 Hz, 1H), 8.05 (s, 1H), 7.77 (dd, *J* = 7.4 Hz, 1H), 7.74 – 7.68 (m, 2H), 7.24 (d, *J* = 7.6 Hz, 2H), 2.60 (s, 3H), 1.49 (s, 9H). **¹³C NMR** (126 MHz, CDCl₃) δ 157.83, 151.32, 149.12, 148.63, 137.41, 133.47, 125.07, 124.54, 122.86, 121.93, 120.90, 36.18, 30.98, 23.27. **HR-MS** (ESI) *m/z*: calculated for C₁₆H₁₉N [M+H]⁺ 226.1596, found: 226.1594. **v_{max}** (neat) / cm⁻¹; 2958, 1586, 1464, 1433.

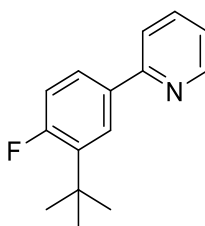
2-(3-tert-butyl-4-methoxyphenyl)pyridine (3c)



2-(4-methoxyphenyl)pyridine (1 mmol, 185 mg), 2-bromo-2-methylpropane (3 mmol, 0.34 mL), $[\text{RuCl}_2(\text{p-cymene})]_2$ (5 mol%, 30 mg), and KOAc (2 mmol, 196 mg) were reacted together in 1,4-Dioxane (4 mL) according to general procedure A to afford the title compound as a colourless oil (100 mg, 42%).

^1H NMR (500 MHz, CDCl_3) δ 8.67 (d, J = 4.7 Hz, 1H), 7.96 (d, J = 1.3 Hz, 1H), 7.83 (d, J = 8.4 Hz, 1H), 7.74 (t, J = 7.5 Hz, 1H), 7.68 (d, J = 7.9 Hz, 1H), 7.19 (br s, 1H), 6.98 (d, J = 8.5 Hz, 1H), 3.90 (s, 3H), 1.44 (s, 9H). **^{13}C NMR** (126 MHz, CDCl_3) δ 159.84, 157.66, 149.06, 138.70, 137.25, 126.05, 125.71, 121.40, 120.38, 111.84, 77.16, 55.29, 35.19, 29.84. **HR-MS** (ESI) m/z : calculated for $\text{C}_{16}\text{H}_{19}\text{NO}$ $[\text{M}+\text{H}]^+$ 242.1545, found: 242.1549. ν_{max} (neat) / cm^{-1} : 2954, 1586, 1462, 1430.

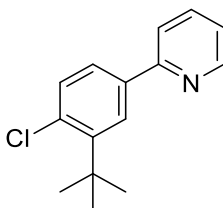
2-(3-tert-butyl-4-fluorophenyl)pyridine (3d)



2-(4-fluorophenyl)pyridine (1 mmol, 173 mg), 2-bromo-2-methylpropane (3 mmol, 0.34 mL), $[\text{RuCl}_2(\text{p-cymene})]_2$ (5 mol%, 30 mg), KOAc (0.5 mmol, 49 mg) and K_2CO_3 (1.5 mmol, 207 mg) were reacted together in 1,4-Dioxane (4 mL) according to general procedure B to afford the title compound as a colourless oil (140 mg, 61%).

^1H NMR (500 MHz, CDCl_3) δ 8.68 (d, J = 4.6 Hz, 1H), 8.00 (d, J = 8.1 Hz, 1H), 7.79 – 7.74 (m, 1H), 7.70 (dd, J = 7.1 Hz, 1H), 7.65 (d, J = 7.9 Hz, 1H), 7.22 – 7.16 (m, 1H), 7.08 (dd, J = 12.0, 8.6 Hz, 1H), 1.46 (s, 9H). **^{13}C NMR** (126 MHz, CDCl_3) δ 162.83 (d, $^1J_{\text{C-F}}$ = 250.7 Hz), 157.14 (s), 149.60 (s), 137.41 (d, $^2J_{\text{C-F}}$ = 12.1 Hz), 136.82 (s), 135.13 (d, $^4J_{\text{C-F}}$ = 3.0 Hz), 126.29 (d, $^3J_{\text{C-F}}$ = 6.4 Hz), 126.25 (d, $^3J_{\text{C-F}}$ = 9.3 Hz), 121.89 (s), 120.43 (s), 116.64 (d, $^2J_{\text{C-F}}$ = 25.0 Hz), 34.53 (d, $^3J_{\text{C-F}}$ = 2.7 Hz), 29.97 (d, $^4J_{\text{C-F}}$ = 3.4 Hz). **^{19}F NMR** (470 MHz, CDCl_3) δ -109.38 (s). **HR-MS** (ESI) m/z : calculated for $\text{C}_{15}\text{H}_{16}\text{NF}$ $[\text{M}+\text{H}]^+$ 230.1345, found: 230.1342. ν_{max} (neat) / cm^{-1} : 2959, 1589, 1461, 1433.

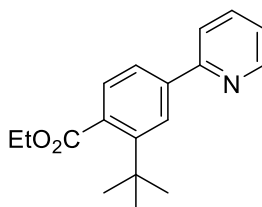
2-(3-tert-butyl-4-chlorophenyl)pyridine (3e)



2-(4-(chlorophenyl)pyridine (1 mmol, 190 mg), 2-bromo-2-methylpropane (3 mmol, 0.34 mL), $[\text{RuCl}_2(\text{p-cymene})]_2$ (5 mol%, 30 mg), and KOAc (2 mmol, 196 mg) were reacted together in 1,4-Dioxane (4 mL) according to general procedure A to afford the title compound as a colourless oil (70 mg, 25%).

^1H NMR (500 MHz, CDCl_3) δ 8.72 (d, $J = 4.1$ Hz, 1H), 8.10 (d, $J = 2.2$ Hz, 1H), 7.81 (td, $J = 7.8$, 1.8 Hz, 1H), 7.72 (d, $J = 8.2$ Hz, 1H), 7.72 (d, $J = 8.3$ Hz, 1H), 7.45 (d, $J = 8.2$ Hz, 1H), 7.29 (ddd, $J = 7.3$, 4.9, 0.8 Hz, 1H), 1.55 (s, 9H). **^{13}C NMR** (126 MHz, CDCl_3) δ 156.47, 148.97, 146.95, 137.60, 136.82, 135.08, 132.37, 126.67, 125.65, 122.36, 120.91, 36.31, 29.58. **HR-MS** (ESI) m/z calculated for $\text{C}_{15}\text{H}_{16}\text{NCl}$ $[\text{M}+\text{H}]^+$ 246.1050, found: 246.1030. ν_{max} (neat) / cm^{-1} : 2960, 1586, 1459, 1431.

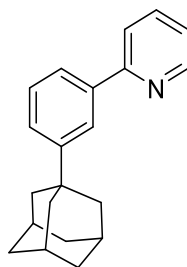
ethyl 2-tert-butyl-4-(pyridin-2-yl)benzoate (3f)



2-(4-(ethoxycarbonyl)phenyl)pyridine (1 mmol, 190 mg), 2-bromo-2-methylpropane (3 mmol, 0.34 mL), $[\text{RuCl}_2(\text{p-cymene})]_2$ (5 mol%, 30 mg), and KOAc (2 mmol, 196 mg) were reacted together in 1,4-Dioxane (4 mL) according to general procedure A to afford the title compound as a colourless oil (23 mg, 8%).

^1H NMR (500 MHz, CDCl_3) δ 8.74 (d, $J = 3.7$ Hz, 1H), 8.17 (s, 1H), 7.85 – 7.78 (m, $J = 13.6$, 7.5 Hz, 2H), 7.75 (d, $J = 7.8$ Hz, 1H), 7.42 (d, $J = 7.9$ Hz, 1H), 7.33 – 7.28 (m, 1H), 4.39 (q, $J = 7.1$ Hz, 2H), 1.48 (s, 9H), 1.40 (t, $J = 7.1$ Hz, 3H). **^{13}C NMR** (126 MHz, CDCl_3) δ 171.75, 156.49, 149.00, 148.31, 139.50, 137.64, 133.94, 129.34, 125.93, 124.05, 122.62, 121.26, 61.48, 36.20, 31.36, 14.08. **HR-MS** (ESI) m/z calculated for $\text{C}_{18}\text{H}_{21}\text{NO}_2$ $[\text{M}+\text{H}]^+$ 284.1651, found: 284.1645. ν_{max} (neat) / cm^{-1} : 2965, 1722, 1586, 1464, 1434.

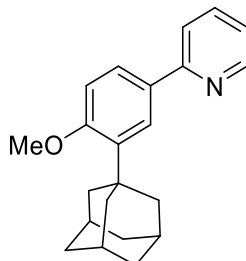
2-(3-(adamantan-1-yl)phenyl)pyridine (4a)



2-Phenylpyridine (1 mmol, 140 μ L), 1-adamantyl bromide (3.00 mmol, 645 mg), $[\text{RuCl}_2(\text{p-cymene})]_2$ (5 mol%, 30 mg), KOAc (0.5 mmol, 49 mg) and K_2CO_3 (1.5 mmol, 207 mg) were reacted together in 1,4-Dioxane (4 mL) according to general procedure B to afford the title compound as a white solid (15 mg, 5%).

^1H NMR: (500 MHz, CDCl_3) δ 8.75 (d, J = 4.6 Hz, 1H), 8.14 – 7.96 (m, 1H), 7.85 – 7.74 (m, 3H), 7.50 – 7.42 (m, 2H), 7.31 – 7.24 (m, 1H), 2.14 (s, 3H), 2.02 (s, 6H), 1.85 – 1.76 (m, 6H). **^{13}C NMR** (126 MHz, CDCl_3) δ 158.29, 152.00, 149.76, 139.35, 136.74, 128.60, 125.79, 124.36, 123.80, 122.00, 120.87, 43.34, 36.95, 36.54, 29.13. **HR-MS** (ESI) m/z : calculated for $\text{C}_{21}\text{H}_{23}\text{NO}$ $[\text{M}+\text{H}]^+$ 290.1909, found: 290.1883. **ν_{max} (neat)** / cm^{-1} : 3252, 2898, 2856, 1622, 1584, 1564, 1461.

2-(3-(adamantan-1-yl)-4-methoxyphenyl)pyridine (4c)



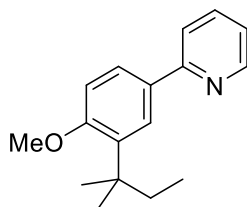
2-(4-Methoxyphenyl)pyridine (1 mmol, 185 mg), 1-adamantyl bromide (3.00 mmol, 645 mg), $[\text{RuCl}_2(\text{p-cymene})]_2$ (5 mol%, 30 mg), KOAc (0.5 mmol, 49 mg) and K_2CO_3 (1.5 mmol, 207 mg) were reacted together in 1,4-Dioxane (4 mL) according to general procedure B to afford the title compound as a white solid (114 mg, 36%). Crystals large enough for single crystal X-ray analysis were generated using CHCl_3 / Hexane.

^1H NMR (500 MHz, CDCl_3) δ 8.66 (ddd, J = 4.9, 1.7, 1.0 Hz, 1H), 7.92 (d, J = 2.3 Hz, 1H), 7.81 (dd, J = 8.5, 2.3 Hz, 1H), 7.74 – 7.69 (m, 1H), 7.68 (ddd, J = 8.0, 1.2 Hz, 1H), 7.17 (ddd, J = 7.0, 4.9, 1.4 Hz, 1H), 6.97 (d, J = 8.5 Hz, 1H), 3.89 (s, 3H), 2.20 – 2.15 (m, J = 2.9 Hz, 6H), 2.09 (s, 3H), 1.79 (s, 6H). **^{13}C NMR** (126 MHz, CDCl_3) δ 159.99, 157.81, 149.31, 138.83, 136.95, 131.29, 125.67, 125.64, 121.32, 120.22, 111.90, 55.24, 40.64, 37.29, 37.25, 29.22. **HR-MS** (ESI) m/z calculated for $\text{C}_{22}\text{H}_{25}\text{NO}$ $[\text{M}+\text{H}]^+$ 320.2014, found: 320.2008

Crystal Data 4c, C₂₂H₂₅NO (M = 319.43 g/mol): monoclinic, space group P21/c (no. 14), a = 12.82457(18), b = 6.61539(9), c = 20.0798(3) Å, β = 93.3829(13)°, U = 1700.59(4) Å³, Z = 4, T = 150(2) K, μ (CuK α) = 0.581 mm⁻¹, D_{calc} = 1.248 g/cm³, 17596 reflections measured (8.82° ≤ 2 θ ≤ 143.96°), 3328 unique (R_{int} = 0.0403, R_{sigma} = 0.0297) which were used in all calculations. The final R1 was 0.0384 ($I > 2\sigma(I)$) and wR2 was 0.0964 (all data).

Crystallographic data have been deposited with Cambridge Crystallographic Data Centre; CCDC-1064109. Copies of these data can be obtained free of charge via <http://www.ccdc.cam.ac.uk/conts/retrieving.html> (or from the Cambridge Crystallographic Data Centre, 12, Union Road, Cambridge, CB2 1EZ, UK; Fax: +44 1223 336033; email: deposit@ccdc.cam.ac.uk).

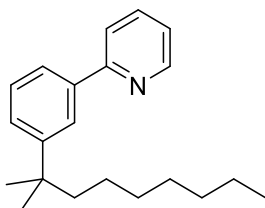
2-[4-methoxy-3-(2-methylbutan-2-yl)phenyl]pyridine (5c)



2-(4-Methoxyphenyl)pyridine (1 mmol, 185 mg), 2-chloro-2-methylbutane (367 μ L, 3 mmol), [RuCl₂(p-cymene)]₂ (5 mol%, 30 mg), KOAc (0.5 mmol, 49 mg) and K₂CO₃ (1.5 mmol, 207 mg) were reacted together in 1,4-Dioxane (4 mL) according to general procedure B to afford the title compound as a colourless oil (139 mg, 54%).

¹H NMR (500 MHz, CDCl₃) δ 8.67 (ddd, J = 4.9, 1.7, 1.0 Hz, 1H), 7.90 (d, J = 2.3 Hz, 1H), 7.83 (dd, J = 8.5, 2.3 Hz, 1H), 7.73 – 7.69 (m, 1H), 7.68 (ddd, J = 8.0, 1.2 Hz, 1H), 7.21 – 7.05 (m, 1H), 6.96 (d, J = 8.5 Hz, 1H), 3.87 (s, 3H), 1.89 (q, J = 7.5 Hz, 2H), 1.41 (s, 6H), 0.66 (t, J = 7.5 Hz, 3H). **¹³C NMR** (126 MHz, CDCl₃) δ 159.68, 157.79, 149.33, 136.91, 136.87, 131.11, 126.92, 125.89, 121.30, 120.20, 111.62, 55.28, 38.79, 33.22, 28.01, 9.78. **HR-MS** (ESI) *m/z*: calculated for C₁₇H₂₁NO [M+H]⁺ 256.1701, found: 256.1725. **ν_{\max}** (neat) / cm⁻¹: 2979, 1602, 1585, 1562, 1460.

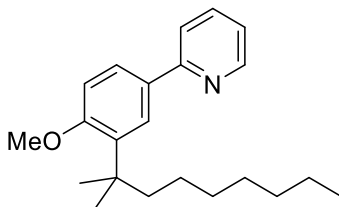
2-[3-(2-methylnonan-2-yl)phenyl]pyridine (6a)



2-Phenylpyridine (1 mmol, 140 μ L), 2-chloro-2-methylnonane (3 mmol, 530 mg), $[\text{RuCl}_2(\text{p-cymene})]_2$ (5 mol%, 30 mg), KOAc (0.5 mmol, 49 mg) and K_2CO_3 (1.5 mmol, 207 mg) were reacted together in 1,4-Dioxane (4 mL) according to general procedure B to afford the title compound as a colourless oil (146 mg, 43%).

^1H NMR: (500 MHz, CDCl_3) δ 8.72 (d, J = 4.7 Hz, 1H), 8.00 – 7.96 (m, 1H), 7.83 – 7.71 (m, 3H), 7.46 – 7.39 (m, 2H), 7.28 – 7.22 (m, 1H), 1.70 – 1.62 (m, 2H), 1.37 (s, 6H), 1.30 – 1.04 (m, 10H), 0.84 (t, J = 7.1 Hz, 3H). **^{13}C NMR:** (126 MHz, CDCl_3) δ 157.85, 150.47, 149.20, 138.55, 137.09, 128.43, 126.85, 124.58, 124.14, 121.98, 120.95, 44.63, 37.90, 31.87, 30.31, 29.23, 29.01, 24.76, 22.65, 14.09. **HR-MS** (ESI) m/z : calculated for $\text{C}_{21}\text{H}_{29}\text{NO}$ $[\text{M}+\text{H}]^+$ 296.2378, found: 296.2401. **ν_{max} (neat)** / cm^{-1} ; 2957, 2926, 2855, 1584, 1564, 1461

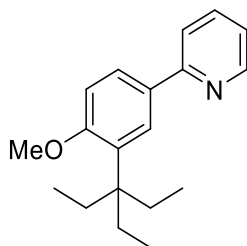
2-[4-methoxy-3-(2-methylnonan-2-yl)phenyl]pyridine (6c)



2-(4-methoxyphenyl)pyridine (1 mmol, 185 mg), 2-chloro-2-methylnonane (3 mmol, 530 mg), $[\text{RuCl}_2(\text{p-cymene})]_2$ (5 mol%, 30 mg), KOAc (0.5 mmol, 49 mg) and K_2CO_3 (1.5 mmol, 207 mg) were reacted together in 1,4-Dioxane (4 mL) according to general procedure B to afford the title compound as a colourless oil (139 mg, 54%).

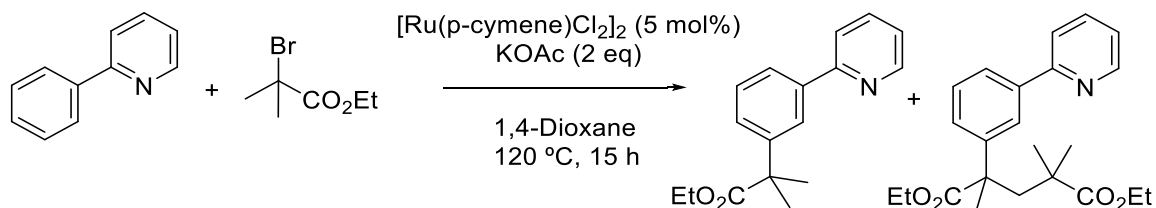
^1H NMR: (500 MHz, CDCl_3) δ 8.67 (d, J = 4.6 Hz, 1H), 7.91 (d, J = 1.9 Hz, 1H), 7.84 (dd, J = 8.5, 2.3 Hz, 1H), 7.74 – 7.65 (m, 2H), 7.20 – 7.12 (m, 1H), 6.95 (d, J = 8.5 Hz, 1H), 3.87 (s, 3H), 1.93 – 1.78 (m, 2H), 1.44 (d, J = 6.7 Hz, 6H), 1.31 – 1.15 (m, 8H), 1.06 – 0.97 (m, 2H), 0.85 (t, J = 7.1 Hz, 3H). **^{13}C NMR:** (126 MHz, CDCl_3) δ 159.59, 157.64, 149.17, 137.12, 136.84, 130.93, 126.64, 125.77, 121.20, 120.09, 111.51, 55.13, 40.80, 38.42, 31.89, 30.39, 29.21, 28.48, 25.26, 22.69, 14.12. **HR-MS** (ESI) m/z : calculated for $\text{C}_{22}\text{H}_{31}\text{NO}$ $[\text{M}+\text{H}]^+$ 326.2484, found: 326.2521. **ν_{max} (neat)** / cm^{-1} ; 2951, 2921, 2854, 1602, 1588, 1498, 1462

2-(3-(3-ethylpentan-3-yl)-4-methoxyphenyl)pyridine (7c)



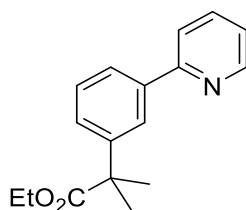
2-(4-methoxyphenyl)pyridine (1 mmol, 185 mg), 3-chloro-3-ethylpentane (1.70 mmol, 229 mg), $[\text{RuCl}_2(\text{p-cymene})]_2$ (5 mol%, 30 mg), KOAc (0.5 mmol, 49 mg) and K_2CO_3 (1.5 mmol, 207 mg) were reacted together in 1,4-Dioxane (4 mL) according to general procedure B to afford the title compound as a colourless oil (139 mg, 54%).

^1H NMR: (500 MHz, CDCl_3) δ 8.69 (s, 1H), 7.95 – 7.68 (m, 4H), 7.22 (s, 1H), 6.97 (d, J = 6.2 Hz, 1H), 3.86 (s, 3H), 1.88 (q, J = 7.2 Hz, 6H), 0.66 (t, J = 7.3 Hz, 9H). **^{13}C NMR** (126 MHz, CDCl_3) δ 160.11, 157.43, 148.85, 137.83, 135.10, 129.89, 128.57, 126.10, 121.57, 120.67, 111.80, 77.16, 55.44, 44.78, 26.21, 8.65. **HR-MS** (ESI) m/z : calculated for $\text{C}_{19}\text{H}_{25}\text{NO}$ $[\text{M}+\text{H}]^+$ 284.1936, found: 284.1949. ν_{max} (neat) / cm^{-1} : 2979, 2888, 1603, 1587, 1494, 1460



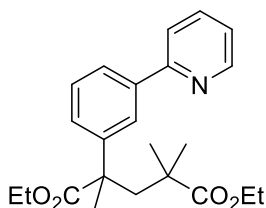
2-phenylpyridine (1 mmol, 0.14 mL), ethyl 2-bromoisobutyrate (3 mmol, 0.44 mL), $[\text{RuCl}_2(\text{p-cymene})]_2$ (5 mol%, 30 mg), and KOAc (2 mmol, 196 mg) were reacted together in 1,4-Dioxane (4 mL) according to general procedure A. The crude mixture was purified by flash column chromatography to yield products **8a** (125 mg, 46%) as a colourless oil and product **9a** (25 mg, 9%) as a colourless oil.

ethyl 2-methyl-2-[3-(pyridin-2-yl)phenyl]propanoate (8a)

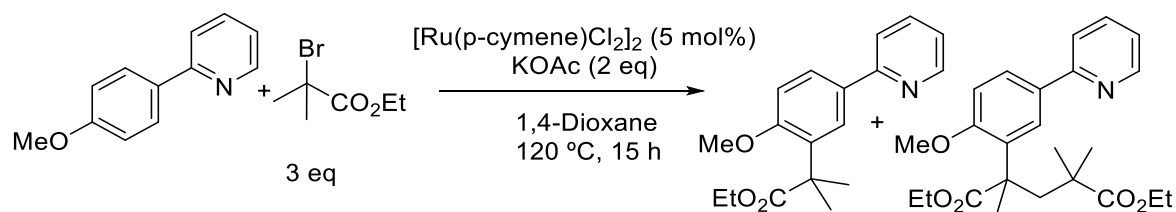


¹H NMR (500 MHz, CDCl₃) δ 8.69 (ddd, *J* = 4.9, 1.7, 1.0 Hz, 1H), 7.99 (dd, *J* = 1.9 Hz, 1H), 7.86 – 7.83 (m, 1H), 7.77 – 7.74 (m, 1H), 7.71 (ddd, *J* = 8.0, 1.1 Hz, 1H), 7.43 (dd, *J* = 7.7 Hz, 1H), 7.40 – 7.37 (m, 1H), 7.23 (ddd, *J* = 7.3, 4.9, 1.3 Hz, 1H), 4.13 (q, *J* = 7.1 Hz, 2H), 1.64 (s, 6H), 1.18 (t, *J* = 7.1 Hz, 3H). **¹³C NMR** (126 MHz, CDCl₃) δ 176.80, 157.50, 149.54, 145.50, 139.34, 137.05, 128.87, 126.72, 125.45, 124.36, 122.27, 120.92, 60.96, 46.73, 26.70, 14.18. **HR-MS** (ESI) *m/z*: calculated for C₁₇H₁₉NO₂ [M+H]⁺ 270.1494, found: 270.1533. **v_{max}** (neat) / cm⁻¹: 2978, 1722, 1584, 1461, 1433

diethyl 2,2,3-trimethyl-3-[3-(pyridin-2-yl)benzyl]butanedioate (9a)

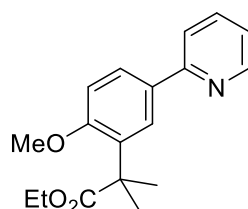


¹H NMR (500 MHz, CDCl₃) δ 8.70 (d, *J* = 4.8 Hz, 1H), 8.02 (s, 1H), 7.86 (d, *J* = 7.3 Hz, 1H), 7.77 (dd, *J* = 7.6 Hz, 1H), 7.72 (d, *J* = 7.9 Hz, 1H), 7.47 – 7.39 (m, 2H), 7.26 – 7.23 (m, 1H), 4.24 – 3.98 (m, 4H), 2.64 (d, *J* = 14.5 Hz, 1H), 2.56 (d, *J* = 14.5 Hz, 1H), 1.57 (s, 3H), 1.25 (t, *J* = 7.1 Hz, 3H), 1.20 (t, *J* = 7.1 Hz, 3H), 1.20 (s, 3H), 1.13 (s, 3H). **¹³C NMR** (126 MHz, CDCl₃) δ 178.44, 176.08, 157.25, 149.16, 145.42, 137.59, 136.00, 128.97, 127.11, 125.76, 124.90, 122.43, 121.20, 61.19, 60.69, 49.64, 48.05, 41.92, 29.35, 23.99, 21.04, 14.20, 14.09. **HR-MS** (ESI) *m/z*: calculated for C₂₃H₂₉NO₄Na [M+Na]⁺ 406.1994, found: 406.1971
v_{max} (neat) / cm⁻¹: 2979, 1721, 1584, 1461



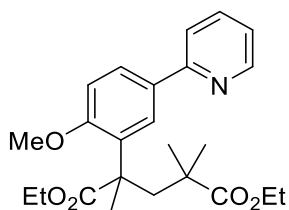
2-(4-methoxyphenyl)pyridine (1 mmol, 185 mg), ethyl 2-bromoisobutyrate (3 mmol, 0.44 mL), $[\text{RuCl}_2(\text{p-cymene})]_2$ (5 mol%, 30 mg), and KOAc (2 mmol, 196 mg) were reacted together in 1,4-Dioxane (4 mL) according to general procedure A. The crude mixture was purified by flash column chromatography to yield products **8c** (170 mg, 57%) as a white amorphous solid and product **9c** (45 mg, 12%) as a colourless oil.

ethyl 2-[2-methoxy-5-(pyridin-2-yl)phenyl]-2-methylpropanoate (**8c**)

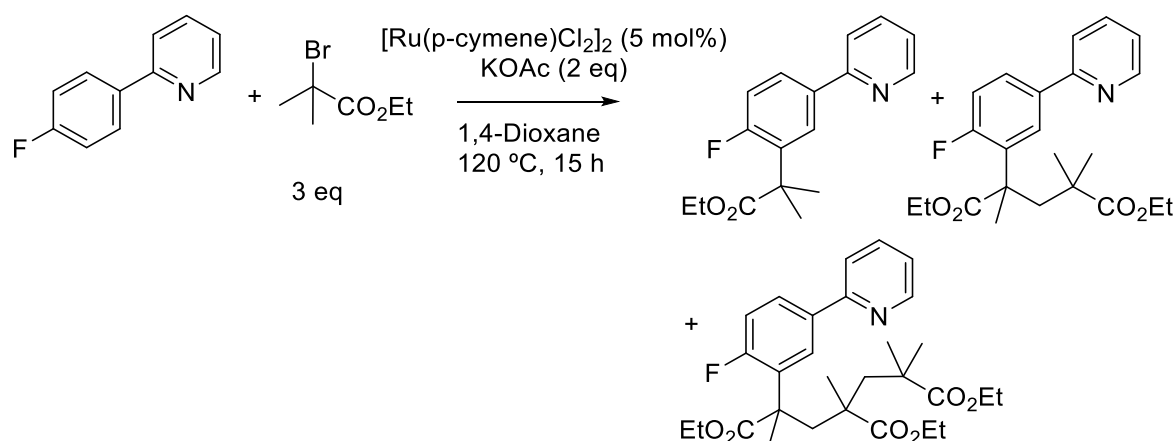


^1H NMR (500 MHz, CDCl_3) δ 8.66 (d, $J = 4.4$ Hz, 1H), 7.99 (d, $J = 2.1$ Hz, 1H), 7.86 (dd, $J = 8.4$, 1.9 Hz, 1H), 7.73 (dd, $J = 7.5$ Hz, 1H), 7.69 (d, $J = 7.9$ Hz, 1H), 7.21 – 7.14 (m, 1H), 6.94 (d, $J = 8.5$ Hz, 1H), 4.11 (q, $J = 7.1$ Hz, 2H), 3.82 (s, 3H), 1.59 (s, 6H), 1.15 (t, $J = 7.1$ Hz, 3H). **^{13}C NMR** (126 MHz, CDCl_3) δ 177.87, 157.87, 157.36, 149.31, 137.08, 134.68, 131.52, 126.70, 124.68, 121.55, 120.28, 110.96, 60.44, 55.37, 44.55, 25.74, 14.32. **HR-MS** (ESI) m/z calculated for $\text{C}_{18}\text{H}_{22}\text{NO}_3$ $[\text{M}+\text{H}]^+$ 300.1600, found: 300.1613. **ν_{max} (neat)** / cm^{-1} : 2979, 1727, 1587, 1465

diethyl 2-[2-methoxy-5-(pyridin-2-yl)phenyl]-2,3,3-trimethylbutanedioate (9c)

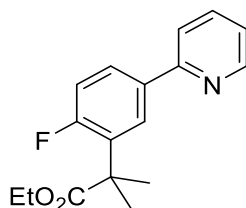


¹H NMR (500 MHz, CDCl₃) δ 8.66 (ddd, *J* = 4.8, 1.7, 1.0 Hz, 1H), 7.91 (d, *J* = 2.2 Hz, 1H), 7.89 (dd, *J* = 8.4, 2.2 Hz, 1H), 7.74 – 7.70 (m, 1H), 7.69 (ddd, *J* = 8.0, 1.3 Hz, 1H), 7.17 (ddd, *J* = 6.9, 4.8, 1.5 Hz, 1H), 6.90 (d, *J* = 8.4 Hz, 1H), 4.11 – 4.02 (m, 2H), 3.87 – 3.82 (m, *J* = 7.2, 1.5 Hz, 2H), 3.81 (s, 3H), 2.67 (d, *J* = 14.8 Hz, 1H), 2.50 (d, *J* = 14.8 Hz, 1H), 1.64 (s, 3H), 1.18 (s, 3H), 1.12 (t, *J* = 7.1 Hz, 3H), 1.11 (t, *J* = 7.1 Hz, 3H), 0.88 (s, 3H). **¹³C NMR** (126 MHz, CDCl₃) δ 177.98, 177.32, 159.13, 156.04, 135.99, 132.74, 130.08, 128.28, 128.06, 127.10, 122.09, 121.53, 111.27, 60.67, 60.43, 55.50, 48.06, 44.59, 41.47, 28.10, 27.38, 23.16, 14.21, 14.11. **HR-MS** (ESI) *m/z* calculated for C₂₄H₃₁NO₅Na [M+Na]⁺ 436.2100, found: 436.2096. **v_{max} (neat)** / cm⁻¹; 2979, 1727, 1587, 1465



2-(4-fluorophenyl)pyridine (1 mmol, 173 mg), ethyl 2-bromoisobutyrate (3 mmol, 0.44 mL), $[\text{RuCl}_2(\text{p-cymene})]_2$ (5 mol%, 30 mg), and KOAc (2 mmol, 196 mg) were reacted together in 1,4-Dioxane (4 mL) according to general procedure A. The crude mixture was purified by flash column chromatography to yield products **8c** (135 mg, 47%) as a colourless oil, product **9c** (50 mg, 13%) as a colourless oil and product **9d** (15 mg, 3%).

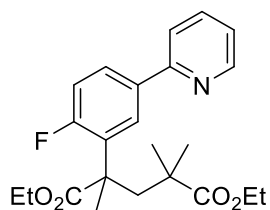
ethyl 2-[2-fluoro-5-(pyridin-2-yl)phenyl]-2-methylpropanoate (**8d**)



^1H NMR (500 MHz, CDCl_3) δ 8.68 (d, $J = 4.1$ Hz, 1H), 8.03 (dd, $J = 7.7, 2.2$ Hz, 1H), 7.82 (ddd, $J = 8.3, 4.8, 2.2$ Hz, 1H), 7.77 (dd, $J = 7.6$ Hz, 1H), 7.70 (d, $J = 7.9$ Hz, 1H), 4.15 (q, $J = 7.1$ Hz, 2H), 1.63 (s, 6H), 1.17 (t, $J = 7.1$ Hz, 3H). **^{13}C NMR** (126 MHz, CDCl_3) δ 176.65 (s), 161.64 (d, $^1J_{\text{C-F}} = 249.7$ Hz), 156.59 (s), 149.40 (s), 137.32 (s), 135.14 (s), 133.31 (d, $^2J_{\text{C-F}} = 14.0$ Hz), 127.19 (d, $^3J_{\text{C-F}} = 9.2$ Hz), 125.76 (d, $^3J_{\text{C-F}} = 5.2$ Hz), 122.24 (s), 120.70 (s), 116.00 (d, $^2J_{\text{C-F}} = 23.2$ Hz), 61.03 (s), 44.37 (s), 25.84 (d, $^4J_{\text{C-F}} = 0.7$ Hz), 14.14 (s).

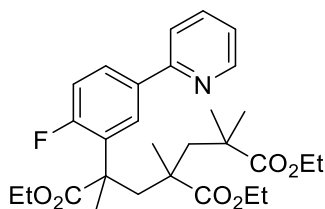
^{19}F NMR (470 MHz, CDCl_3) δ -112.82. **HR-MS** (ESI) m/z : calculated for $\text{C}_{17}\text{H}_{18}\text{FNO}_2\text{Na}$ $[\text{M}+\text{H}]^+$ 288.1400, found: 288.1402. ν_{max} (neat) / cm^{-1} : 2980, 1723, 1589, 1464

diethyl 2-[2-fluoro-5-(pyridin-2-yl)phenyl]-2,3,3-trimethylbutanedioate (9d)



¹H NMR (500 MHz, CDCl₃) δ 8.69 (d, *J* = 4.1 Hz, 1H), 7.96 (dd, *J* = 7.7, 2.2 Hz, 1H), 7.89 (ddd, *J* = 8.2, 4.7, 2.2 Hz, 1H), 7.79 (dd, *J* = 7.1 Hz, 1H), 7.71 (d, *J* = 7.9 Hz, 1H), 7.31 – 7.23 (m, 1H), 7.09 (dd, *J* = 11.3, 8.5 Hz, 1H), 4.19 – 4.07 (m, 2H), 3.98 – 3.80 (m, 2H), 2.61 (d, *J* = 14.9 Hz, 1H), 2.58 (d, *J* = 14.9 Hz, 1H), 1.65 (s, 3H), 1.20 (s, 3H), 1.18 (t, *J* = 7.2 Hz, 3H), 1.16 (t, *J* = 7.2 Hz, 3H), 0.96 (s, 3H). **¹³C NMR** (126 MHz, CDCl₃) δ 177.83 (s), 176.17 (s), 161.89 (d, ¹*J*_{C-F} = 249.9 Hz), 156.36 (s), 149.19 (s), 137.60 (s), 131.69 (d, ²*J*_{C-F} = 12.9 Hz), 127.63 (d, ³*J*_{C-F} = 9.4 Hz), 127.40 (d, ³*J*_{C-F} = 5.0 Hz), 122.32 (s), 120.85 (s), 116.12 (d, ²*J*_{C-F} = 23.9 Hz), 61.22 (s), 60.53 (s), 47.98 (s), 45.44 (d, ³*J*_{C-F} = 2.8 Hz), 41.49 (s), 27.63 (s), 27.13 (s), 22.48 (s), 14.04 (s), 14.03 (s). **¹⁹F NMR** (470 MHz, CDCl₃) δ -110.60. **HR-MS** (ESI) *m/z*: calculated for C₂₃H₂₈FNO₄Na [M+Na]⁺ 424.1900, found: 424.1905. **v_{max}** (neat) / cm⁻¹: 2980, 1723, 1589, 1463

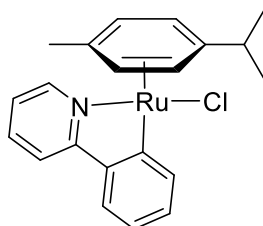
triethyl 2-[2-fluoro-5-(pyridin-2-yl)phenyl]-3,5-dimethylhexane-2,3,5-tricarboxylate (9e)



¹H NMR (500 MHz, CDCl₃) δ 8.72 (s, 1H), 8.03 – 7.89 (m, *J* = 21.0, 11.2, 4.3 Hz, 2H), 7.86 (s, 1H), 7.77 (s, 1H), 7.36 – 7.28 (m, *J* = 10.0, 5.7 Hz, 1H), 7.16 – 7.04 (m, 1H), 4.21 – 3.95 (m, 4H), 3.73 – 3.56 (m, *J* = 46.8, 10.8, 7.2 Hz, 2H), 2.83 – 2.65 (m, 1H), 2.42 – 2.29 (m, *J* = 25.8, 13.9 Hz, 1H), 2.21 – 2.09 (m, 1H), 2.09 – 1.95 (m, 1H), 1.71 – 1.59 (m, 3H), 1.31 – 1.05 (m, 15H), 1.03 – 0.95 (m, 3H). **¹⁹F NMR** (470 MHz, CDCl₃) δ -109.10. **HR-MS** (ESI) *m/z*: calculated for C₂₉H₃₈FNO₆Na [M+Na]⁺ 538.2580, found: 538.2611. **v_{max}** (neat) / cm⁻¹: 2980, 1723, 1589, 1464

Mechanistic Studies

Synthesis of Complex A

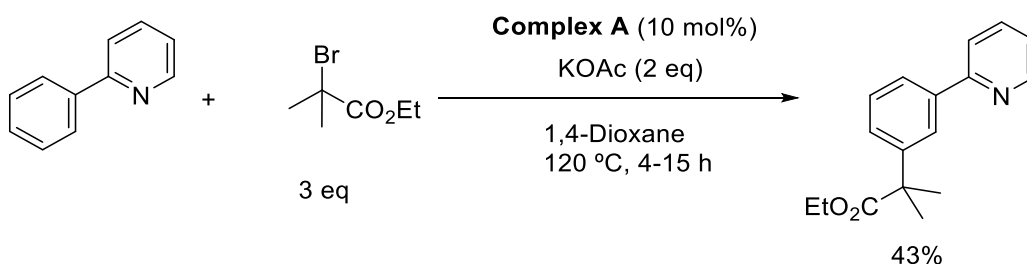


Complex A was synthesised according to literature procedure.⁵ To an oven dried, argon purged round bottom flask was added $[\text{RuCl}_2(\text{p-cymene})]_2$ (1.5 mmol, 918 mg), KOAc (6 mmol, 588 mg) followed by 2-phenylpyridine (3 mmol, 0.42 mL) and dry MeOH (30 mL). The reaction was stirred at room temperature for 48 h. The reaction was then concentrated to dryness, dissolved in a minimal amount of EtOAc and then purified through neutral alumina with EtOAc as the solvent to yield the title compound as a yellow solid (1.1 g, 86%).

^1H NMR (500 MHz, CDCl_3) δ 9.23 (d, J = 5.5 Hz, 1H), 8.15 (d, J = 7.5 Hz, 1H), 7.70 (d, J = 7.9 Hz, 1H), 7.65 (dd, J = 7.6 Hz, 1H), 7.60 (d, J = 7.6 Hz, 1H), 7.17 (dd, J = 7.3 Hz, 1H), 7.06 – 6.99 (m, 2H), 5.58 (d, J = 5.8 Hz, 1H), 5.55 (d, J = 5.9 Hz, 1H), 5.17 (d, J = 5.9 Hz, 1H), 4.98 (d, J = 5.8 Hz, 1H), 2.43 (hept, J = 6.8 Hz, 1H), 2.04 (s, 3H), 0.98 (d, J = 6.9 Hz, 3H), 0.88 (d, J = 6.9 Hz, 3H). **^{13}C NMR** (126 MHz, CDCl_3) δ 181.50, 165.44, 154.70, 143.41, 139.67, 136.70, 129.53, 123.96, 122.57, 121.48, 118.87, 100.73, 100.59, 90.83, 89.72, 84.24, 82.27, 30.89, 22.61, 21.81, 18.85.

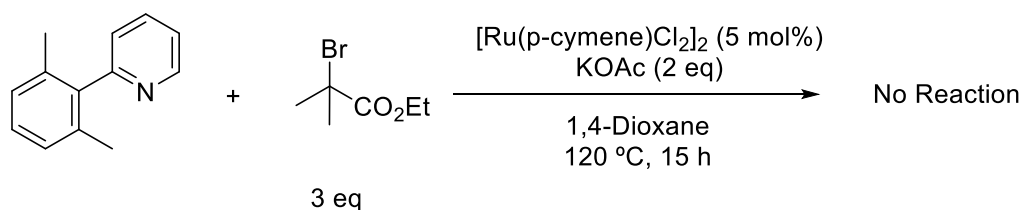
Data conforms to literature.⁵

Catalytic Reaction using Complex A

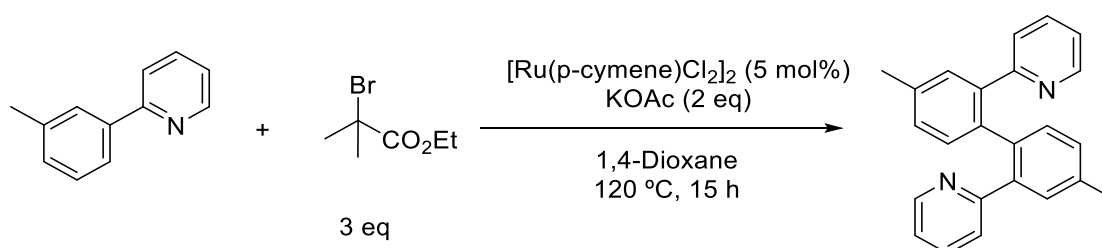


2-phenylpyridine (1 mmol, 0.14 mL), ethyl 2-bromoisobutyrate (3 mmol, 0.44 mL), Complex A (10 mol%, 41 mg), and KOAc (2 mmol, 196 mg) were reacted together in 1,4-Dioxane (4 mL) according to general procedure A. The crude mixture was purified by flash column chromatography to yield product **8a** as a colourless oil (115 mg, 43%). Data in accordance with previous synthesis.

Reactions with Substrates 1j-1l

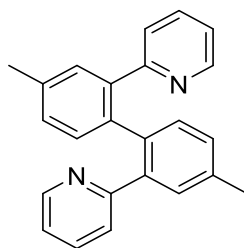


2-(2,6-dimethylphenyl)pyridine (1 mmol, 183 mg), ethyl 2-bromoisobutyrate (3 mmol, 0.44 mL), $[\text{RuCl}_2(\text{p-cymene})]_2$ (5 mol%, 30 mg), and KOAc (2 mmol, 196 mg) were reacted together in 1,4-Dioxane (4 mL) according to general procedure A. No conversion of the starting material was observed.



2-(3-methylphenyl)pyridine (1 mmol, 169 mg), ethyl 2-bromoisobutyrate (3 mmol, 0.44 mL), $[\text{RuCl}_2(\text{p-cymene})]_2$ (5 mol%, 30 mg), and KOAc (2 mmol, 196 mg) were reacted together in 1,4-Dioxane (4 mL) according to general procedure A to afford product **10** as a yellow solid (60 mg 35%).

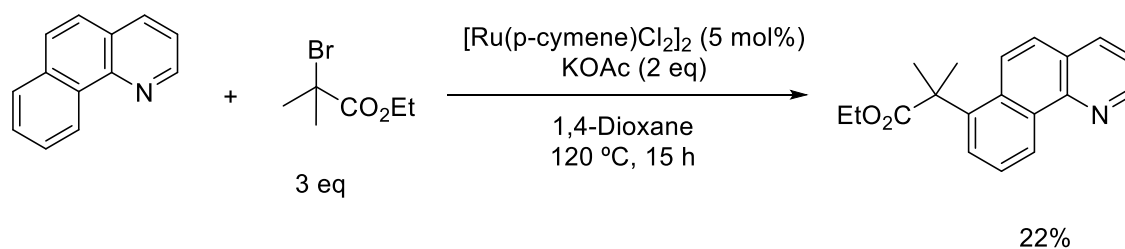
2,2'-(4,4'-dimethylbiphenyl-2,2'-diyl)dipyridine (**10**)



^1H NMR (500 MHz, CDCl_3) δ 8.34 (d, J = 2.7 Hz, 2H), 7.43 – 7.33 (m, 4H), 7.29 (d, J = 7.7 Hz, 2H), 7.25 (t, J = 6.7 Hz, 2H), 7.06 (bs, 1H), 6.80 (d, J = 7.7 Hz, 2H), 2.40 (s, 6H).

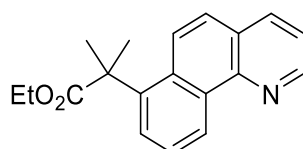
^{13}C NMR (126 MHz, CDCl_3) δ 157.80, 148.48, 138.98, 137.69, 136.81, 136.07, 131.42, 130.80, 129.78, 124.80, 121.52, 21.17. **HR-MS** (ESI) m/z : calculated for $\text{C}_{24}\text{H}_{20}\text{N}_2$ $[\text{M}+\text{Na}]^+$ 359.1524, found: 359.1533

Data conforms to literature.⁶

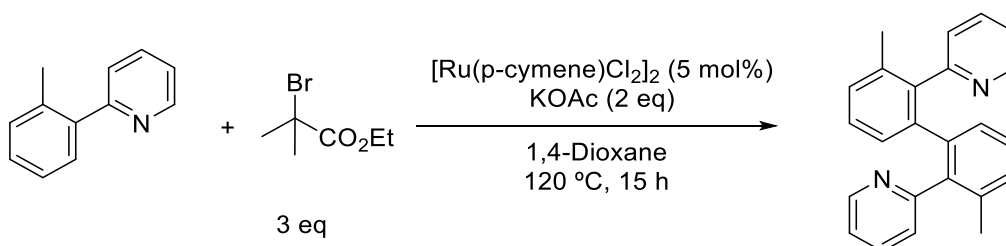


Benzoquinoline (1 mmol, 179 mg), ethyl 2-bromoisobutyrate (3 mmol, 0.44 mL), $[\text{RuCl}_2(\text{p-cymene})]_2$ (5 mol%, 30 mg), and KOAc (2 mmol, 196 mg) were reacted together in 1,4-Dioxane (4 mL) according to general procedure A. The crude mixture was purified by flash column chromatography to yield product **11** as a colourless oil (63 mg, 22%)

ethyl 2-(benzo[h]quinolin-7-yl)-2-methylpropanoate (11)

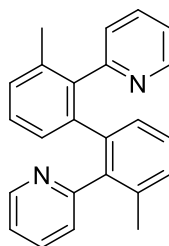


^1H NMR (500 MHz, CDCl_3) δ 9.38 (d, J = 8.0 Hz, 1H), 9.00 (dd, J = 4.4, 1.8 Hz, 1H), 8.15 (dd, J = 8.0, 1.7 Hz, 1H), 7.90 (d, J = 9.3 Hz, 1H), 7.77 (dd, J = 7.5, 1.4 Hz, 1H), 7.74 – 7.70 (m, 1H), 7.66 (d, J = 9.3 Hz, 1H), 7.50 (dd, J = 8.0, 4.4 Hz, 1H), 4.10 (q, J = 7.1 Hz, 2H), 1.80 (s, 7H), 1.02 (t, J = 7.1 Hz, 3H). **^{13}C NMR** (126 MHz, CDCl_3) δ 178.85, 148.81, 146.83, 141.08, 135.81, 132.46, 131.42, 126.65, 125.53, 125.22, 125.07, 124.07, 123.96, 121.96, 61.15, 46.58, 27.88, 14.05. **HR-MS** (ESI) m/z : calculated for $\text{C}_{19}\text{H}_{19}\text{NO}_2$ $[\text{M}+\text{H}]^+$ 294.1494, found: 294.1517. ν_{max} (neat) / cm^{-1} : 2979, 1718, 1592, 1428



2-(2-methylphenyl)pyridine (1 mmol, 169 mg), ethyl 2-bromoisobutyrate (3 mmol, 0.44 mL), $[\text{RuCl}_2(\text{p-cymene})]_2$ (5 mol%, 30 mg), and KOAc (2 mmol, 196 mg) were reacted together in 1,4-Dioxane (4 mL) according to general procedure A to afford product **12** as a white solid (50 mg 29%).

2,2'-(3,3'-dimethylbiphenyl-2,2'-diyl)dipyridine (12)

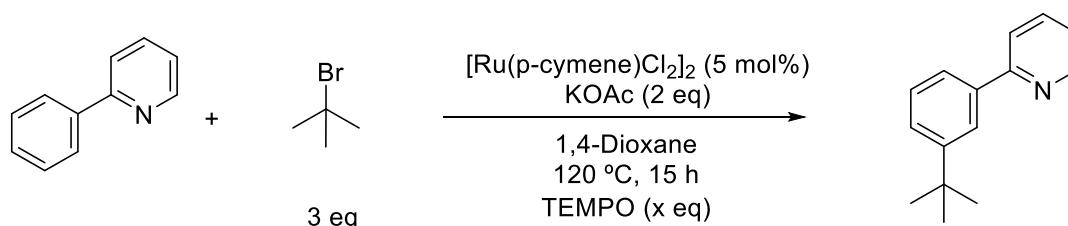


¹H NMR (500 MHz, CDCl₃) δ 8.57 (d, *J* = 4.2 Hz, 2H), 7.55 (t, *J* = 7.1 Hz, 2H), 7.36 – 7.30 (m, *J* = 6.2 Hz, 2H), 7.10 – 7.06 (m, 2H), 7.04 (d, *J* = 7.5 Hz, 2H), 6.93 (t, *J* = 7.6 Hz, 2H), 6.77 (d, *J* = 7.6 Hz, 2H), 2.10 (s, 6H). **¹³C NMR** (126 MHz, CDCl₃) δ 159.38, 148.63, 140.35, 139.62, 136.03, 135.83, 128.89, 128.75, 126.83, 125.87, 121.40, 20.64. **HR-MS** (ESI) *m/z*: calculated for C₂₄H₂₀N₂ [M+Na]⁺ 359.1524, found: 359.1517

Data conforms to literature.⁶

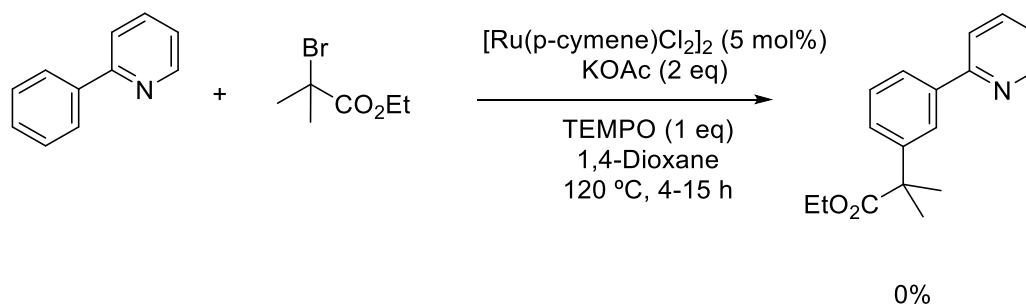
Reactions with TEMPO

Reactions were carried out as per general procedure A.



TEMPO stoichiometry	Conversion (%)
0	71
0.1	41
1	0
3	0

Reaction with ethyl 2-bromoisobutrate carried out as per general procedure A. No trapped TEMPO adducts could be observed or isolated.



References

1. S. Goggins, E. Rosevere, C. Bellini, J. C. Allen, B. J. Marsh, M. F. Mahon, and C. G. Frost, *Org. Biomol. Chem.*, 2014, **12**, 47–52.
2. J. Yang, S. Liu, J. F. Zheng, and J. Zhou, *European J. Org. Chem.*, 2012, 6248–6259.
3. X. Chen, C. E. Goodhue, and J. Q. Yu, *J. Am. Chem. Soc.*, 2006, **128**, 12634–12635.
4. C. Liu, Q. Ni, P. Hu, and J. Qiu, *Org. Biomol. Chem.*, 2011, **9**, 1054–1060.
5. B. Li, T. Roisnel, C. Darcel, and P. H. Dixneuf, *Dalt. Trans.*, 2012, **41**, 10934.
6. X. Guo, G. Deng, and C.-J. Li, *Adv. Synth. Catal.*, 2009, **351**, 2071–2074.

6.2 Supporting information and data for: Mechanistic insight into ruthenium catalysed *meta*-sulfonation of 2-phenylpyridine

General Considerations

All chemicals used were reagent grade and used as supplied unless otherwise specified. HPLC grade acetonitrile (CH₃CN), and diethyl ether were dried using a solvent purification system (PS-400-7®). ¹H and ¹³C NMR spectra were recorded on Bruker, AV 300, AV 400 or AV 500 spectrometers in CD₃CN as solvent. Chemical shifts (δ) were referenced internally to residual protic solvent signal for CD₃CN (1.94 ppm ¹H (q), 1.39 ppm ¹³C (sep)). 2D correlation spectra (gCOSY, gHSQC and gHMBC) were recorded to fully characterise the non-reported ruthenium complexes. Multiplicities are presented as: singlet (s), broad singlet (br s), doublet (d), apparent doublet (app d), doublet of doublets (dd), doublet of doublet of doublets (ddd), triplet (t), triplet of doublets (td), doublet doublet doublet of doublets (dddd), triplet of triplets (tt), quartet (q), quintet (quint.), and multiplet (m). Coupling constants (J) were expressed in Hertz (Hz).

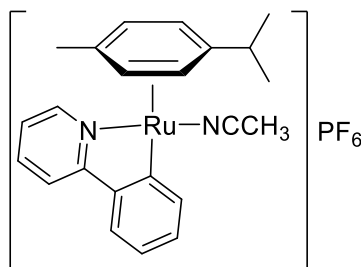
ESI MS were run on an Agilent® 1200 Series LC/MSD. Elemental analysis (C, H, N, S) was run in London Metropolitan University. Analytical thin layer chromatography (TLC) was performed on Merck® silica gel 60 F254 glass or aluminium plates. Organic Compounds were visualized by UV (254 nm) irradiation. Flash column chromatography was carried out using forced flow or by gravity of the indicated solvent on Fluka® silica gel 60 (230-400 mesh) or on Acros® neutral aluminium oxide (50-200 μm, 60 Å).

All complexes were synthesised using standard Schlenck techniques under nitrogen atmosphere. The precursor catalyst [RuCl₂(*p*-cymene)]₂ was purchased from Strem Chemicals and used without further purification. [RuCl(PhPy)(*p*-cymene)],¹ D⁵-2-phenylpyridine² and D³-2-phenylpyridine³ were prepared according literature methods.

CCDC 1479685 contains the supplementary crystallographic data for this paper. These data can be obtained free of charge from The Cambridge Crystallographic Data Centre via www.ccdc.cam.ac.uk/data_request/cif.

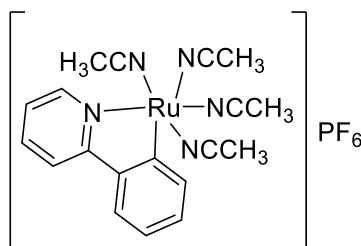
1. Synthesis of Ru Complexes

1.1. Preparation of [Ru(PhPy)(*p*-cymene)(CH₃CN)]PF₆ (**4**)



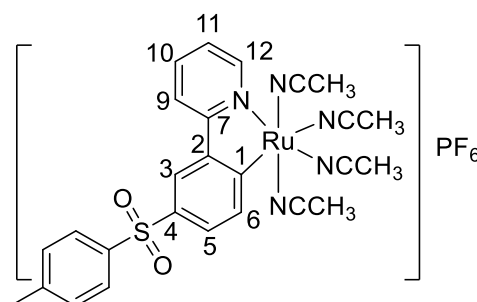
Dixneuf and Jutand method¹ was used for the synthesis of **4** with modifications. **3** (0.5 g, 1.2 mmol) was dissolved in CH₃CN (12 mL) and AgPF₆ (0.44 g, 1.7 mmol) was added. The reaction mixture was stirred for 30 min at room temperature. An aliquot from the reaction mixture was taken and diluted into CD₃CN and analysed by ¹H NMR showing the complete consumption of the starting material. The reaction mixture was filtered over oven-dried neutral alumina and eluted with anhydrous CH₃CN under nitrogen. The solvent was removed under vacuum and the solution poured into petroleum ether. After filtration and drying, **4** was obtained as green solid (0.66 g, 98%). Spectroscopic data was in good agreement with those previously reported.¹

1.2. Preparation of [Ru(PhPy)(CH₃CN)₄](PF₆) (**5**)



Dixneuf and Jutand method¹ was used for the synthesis of **5** with modifications. **4** (0.5 g, 0.87 mmol) was dissolved in CH₃CN (5.4 mL). The reaction mixture was stirred for 2 days at 70 °C. An aliquot from the reaction mixture was taken and diluted into CD₃CN and analysed by ¹H NMR showing the complete consumption of the starting material. The reaction mixture was purified by flash chromatography over oven-dried neutral alumina and eluted with anhydrous CH₃CN under nitrogen. The solution was concentrated under vacuum and the solution poured into petroleum ether. After filtration and drying, **5** was obtained as yellow-green solid (0.37 g, 75%). Spectroscopic data was in good agreement with those previously reported.¹

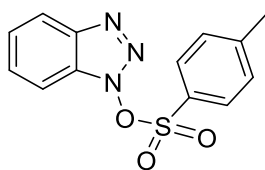
1.3. Preparation of [Ru(TsPhPy)(CH₃CN)₄](PF₆) (**7**)



A dried Schlenk tube under argon was charged with molecular sieves 4 Å, complex **5** (0.1 g, 0.18 mmol) and dry CH₃CN (1.8 mL). Then, *p*-toluenesulfonyl chloride (TsCl) (67 mg, 0.35 mmol) and oven-dried K₂CO₃ (61 mg, 0.44 mmol) were added. After stirring the reaction mixture for 15 h at 120 °C, the reaction crude was purified through oven-dried neutral alumina (Al₂O₃) and eluted with CH₃CN. The solution was concentrated under reduced pressure and precipitated with diethyl ether. After filtration and drying, complex **7** was obtained as green solid (66 mg, 52%). Crystals of **7** were grown by vapour diffusion using CH₃CN–Et₂O.

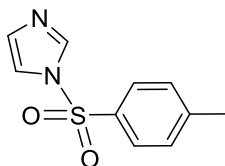
¹H NMR (500 MHz, CD₃CN) δ 8.92 (d, *J* = 5.5 Hz, 1H, H12), 8.22 (d, *J* = 8.0 Hz, 1H, H6), 8.14 (d, *J* = 1.8 Hz, 1H, H3), 8.04 (d, *J* = 8.1 Hz, 1H, H9), 7.88 (d, *J* = 8.3 Hz, 2H, Ts), 7.81 (td, *J* = 8.0, 1.5 Hz, 1H, H10), 7.49 (dd, *J* = 8.0, 1.9 Hz, 1H, H5), 7.37 (d, *J* = 8.2 Hz, 2H, Ts), 7.25 (t, *J* = 6.5 Hz, 1H, H11), 2.50 (s, 3H, CH₃CN), 2.38 (s, 3H, Ts), 2.14 (s, 16H, CH₃CN), 1.97 (s, 5H, CH₃CN), 1.96 (s, 3H, CH₃CN). **¹³C NMR** (126 MHz, CD₃CN) δ 201.76 (C1), 167.73 (C7), 153.96 (C12), 149.45 (C2), 145.40 (Ts), 141.64 (Ts), 140.55 (C6), 137.92 (C10), 135.27 (C4), 131.35 (Ts), 128.44 (Ts), 125.52 (C5), 123.74 (C11), 121.56 (C3), 120.02 (C9), 118.69 (s), 21.89 (Ts), 4.75 (CH₃CN), 4.50 (CH₃CN). **HRMS-ESI** Calcd for C₂₄H₂₃N₄O₂RuS: 533.0585 [M-CH₃CN]⁺. Found 533.0573. **Elemental Analysis.** Calcd for C₂₆H₂₆F₆N₅O₂PRuS: C, 43.46; H, 3.65; N, 9.75; Found: C, 43.35; H, 3.75; N, 9.67.

1.4. Preparation of 1H-benzo[d][1,2,3]triazol-1-yl 4-methylbenzenesulfonate (**8**)



Synthesis of **8** was carried out using the reported method.⁴ To a solution of 1-hydroxybenzotriazole hydrate (0.99 g, 7.4 mmol) in dry dichloromethane (30 mL), imidazole (0.51 g, 7.6 mmol) was added. The mixture was cooled to 0 °C under N₂ and a solution of TsCl (recrystallized) (1.43 g, 7.5 mmol) in dichloromethane (4 mL) was added dropwise over a 10 min period. The reaction mixture was warmed to rt and stirred for a further 3 h. The reaction mixture was diluted with dichloromethane (30 mL) and filtered in a sintered funnel over MgSO₄ under N₂. The solvent was removed *in vacuo* and the resulting colourless residue was recrystallized from dry dichloromethane/hexane. The product was filtered to recover the pure final compound as a white crystalline solid (1.46 g, 69%). ¹H NMR (300 MHz, CDCl₃) δ 8.02 – 7.99 (m, 1H, Ar), 7.81 – 7.75 (m, 2H, Ar), 7.65 (dt, *J* = 8.3, 1.0 Hz, 1H, Ar), 7.62 – 7.55 (m, 1H, Ar), 7.47 – 7.38 (m, 3H, Ar), 2.50 (s, 3H, CH₃). ¹³C NMR (75 MHz, CDCl₃) δ 141.6 (q), 139.8 (q), 134.6 (q), 131.2, 129.8, 129.2 (2 x ArCH), 128.9 (q), 125.9 (2 x ArCH), 114.6, 112.5, 21.4 (CH₃). HRMS-ESI calculated for C₁₃H₁₁N₃O₃SNa: 312.0419 [M+Na]⁺. Found: 312.0399.

1.5. Preparation of 1-tosyl-1H-imidazole (**9**)



Synthesis of **9** was carried out with some modifications of the reported method.⁵ A solution of imidazole (1.38 g, 20.3 mmol) in dry dichloromethane (10 mL) was stirred at 0 °C for 1.5 h under N₂. In a separate flask, a solution of TsCl (recrystallised) (1.74 g, 9.1 mmol) in dry dichloromethane (10 mL) was stirred at rt for 1.5 h under N₂. The *p*-toluenesulfonyl solution was added dropwise to the imidazole solution for 30 min at 0 °C. The reaction mixture was allowed to reach rt and stirred for a further 17 h. The resulting mixture was filtered through a pad of silica and washed with hexane (20 mL) followed by a mixture of EtOAc:hexane (1:1) (300 mL). The filtrate was concentrate *in vacuo* and the oil residue was dissolved in the minimum amount of EtOAc (1.5 mL) and crashed out with hexane (125 mL) to afford the pure compound as a white solid (1.39 g, 68%). ¹H NMR (300 MHz, CDCl₃) δ 8.01 (s, 1H, NCHN), 7.85 – 7.79 (m, 2H, Ar), 7.35 (d, *J* = 8.1 Hz, 1H, Ar), 7.29 (t, *J* = 1.4 Hz, 1H, SO₂NCH), 7.08 (s, 1H, Ar), 2.44 (s, 3H, CH₃). ¹³C NMR (75 MHz, CDCl₃) δ 146.5 (q), 136.8, 135.1 (q), 131.6, 130.6, 127.5, 128.9 (q), 125.9,

114.6, 112.5, 21.4 (CH₃). **HRMS-ESI** calculated for C₁₀H₁₁N₂O₂S: 223.0541 [M+H]⁺. Found: 223.0535.

2. Study of the Ru(II) complexes involved in the *meta*-sulfonation reaction

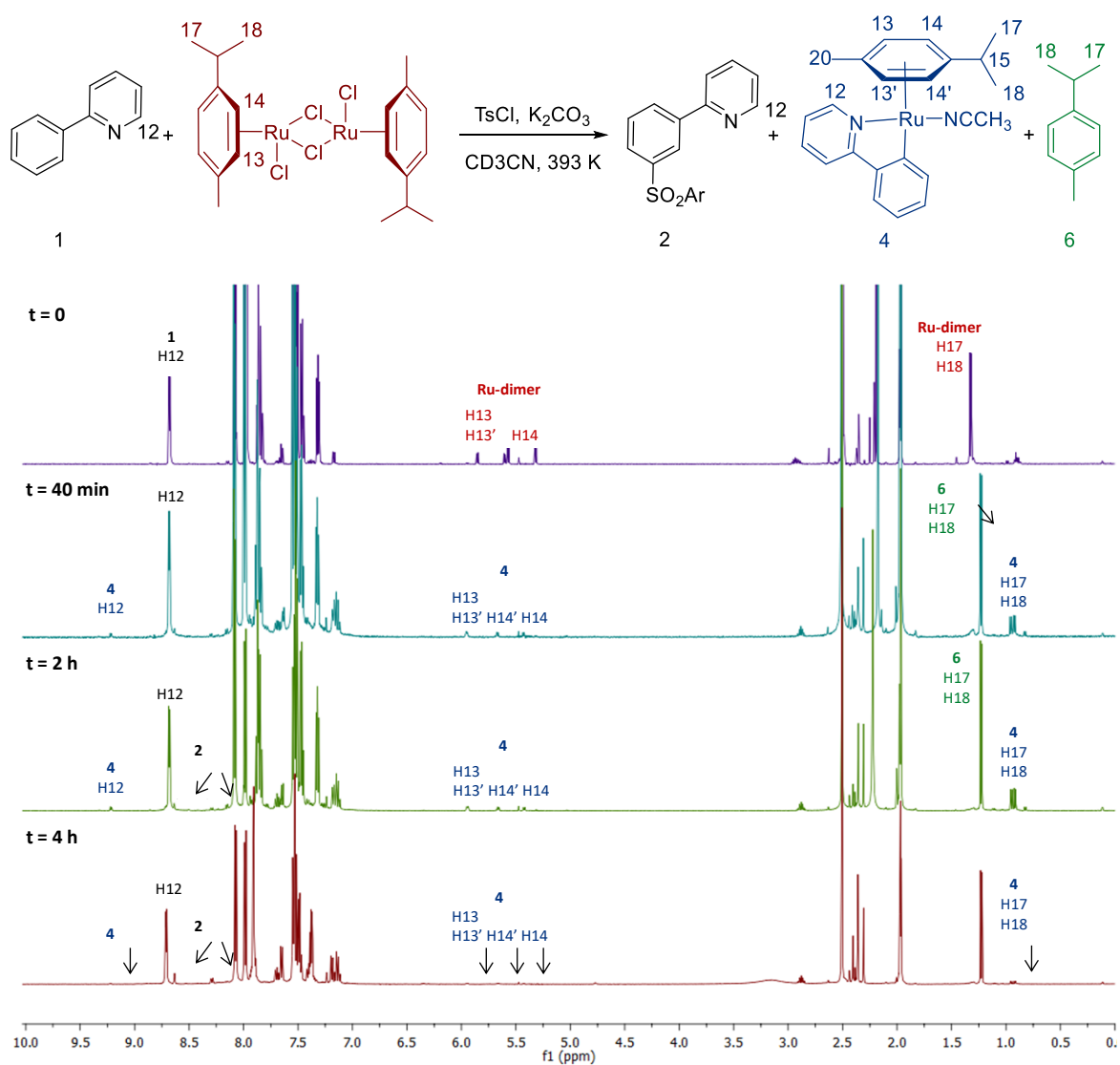
2.1. Catalytic reactions

To a nitrogen-purged ampule, [RuCl₂(*p*-cymene)]₂ (21 mg, 5 mol%), [RuCl(PhPy)(*p*-cymene)] (30 mg, 10 mol%) or [Ru(PhPy)(*p*-cymene)(CH₃CN)]PF₆ (40 mg, 10 mol%) was dissolved in dry CH₃CN (4 mL). Then, phenylpyridine (0.1 mL, 0.70 mmol), K₂CO₃ (0.193 g, 1.4 mmol) and TsCl (0.4 g, 2.1 mmol) were added and the reaction mixture was heated at 120 °C in an oil bath for 15 h. The reaction crude was filtered over celite using EtOAc as eluent and the resulting mixture was purified by flash chromatography (from 20% EtOAc:hexane to 40% EtOAc) affording **2** as yellowish solid (0.11 g, 50%).

2.2. Study of the catalyst behaviour during the *meta*-sulfonation of 2-phenylpyridine

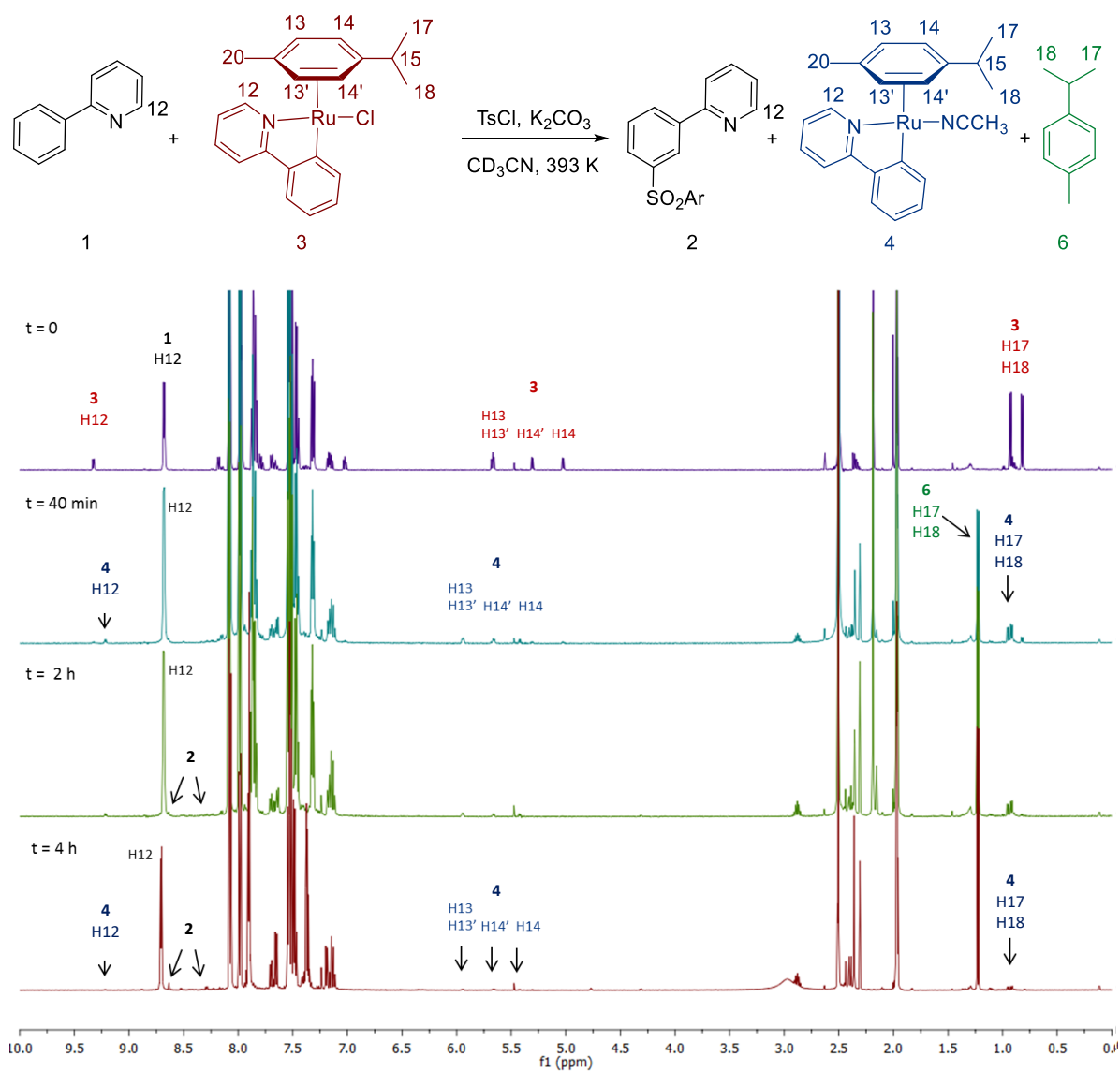
Following the reaction conditions detailed above, the reaction using [RuCl₂(*p*-cymene)]₂, [RuCl(PhPy)(*p*-cymene)] and [Ru(PhPy)(*p*-cymene)(CH₃CN)]PF₆ were prepared in CD₃CN and they were followed by ¹H-NMR taking samples at different times.

Figure S1. ^1H NMR *meta*-sulfonation of phenylpyridine using $[\text{RuCl}_2(p\text{-cymene})]_2$



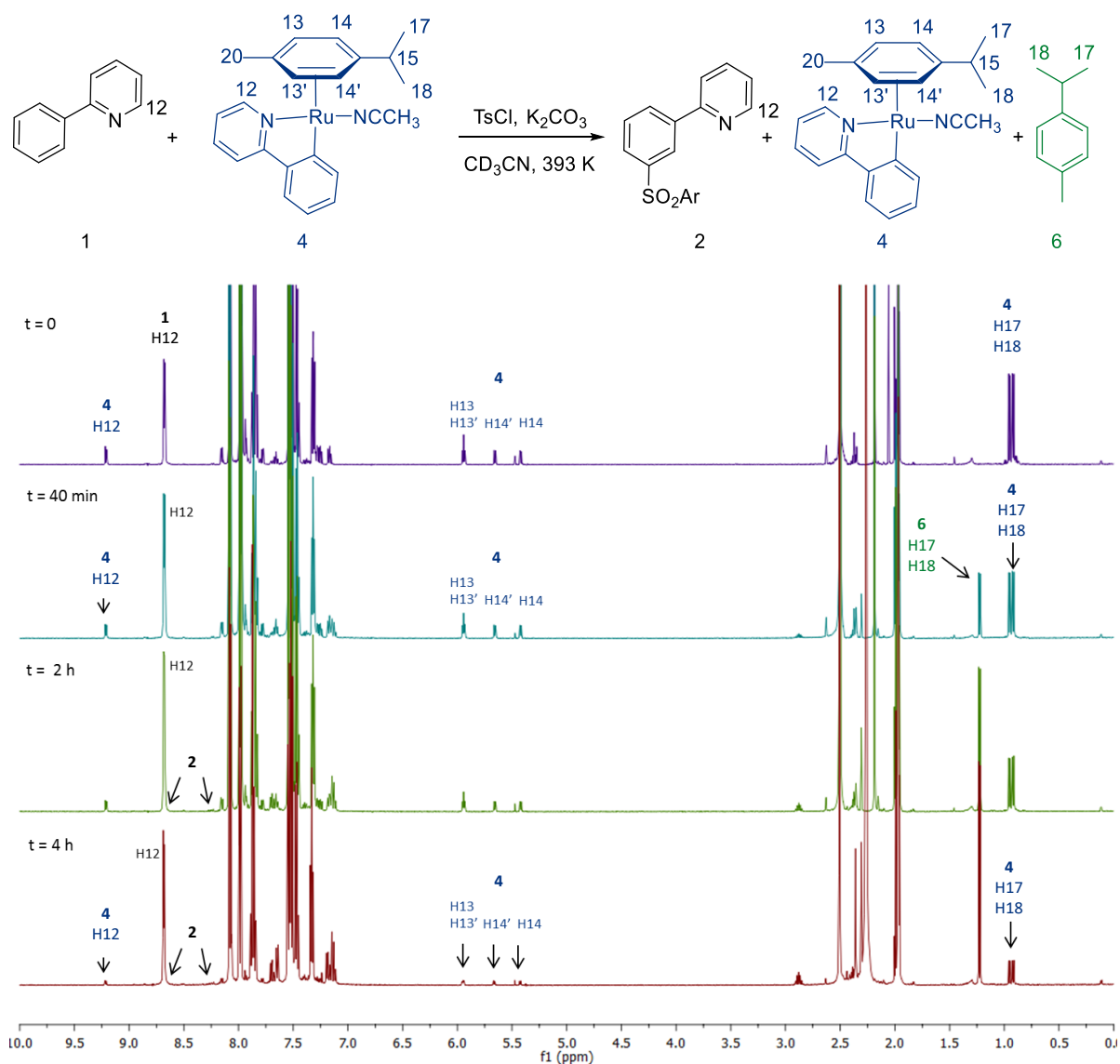
^1H NMR (500 MHz, CD_3CN) recorded at 298K

Figure S2. ^1H NMR *meta*-sulfonation of phenylpyridine using $[\text{RuCl}(\text{PhPy})(p\text{-cymene})]$



^1H NMR (500 MHz, CD_3CN) recorded at 298K

Figure S3. ^1H NMR *meta*-sulfonation of phenylpyridine using $[\text{Ru}(\text{PhPy})(p\text{-cymene})(\text{CH}_3\text{CN})]\text{PF}_6$

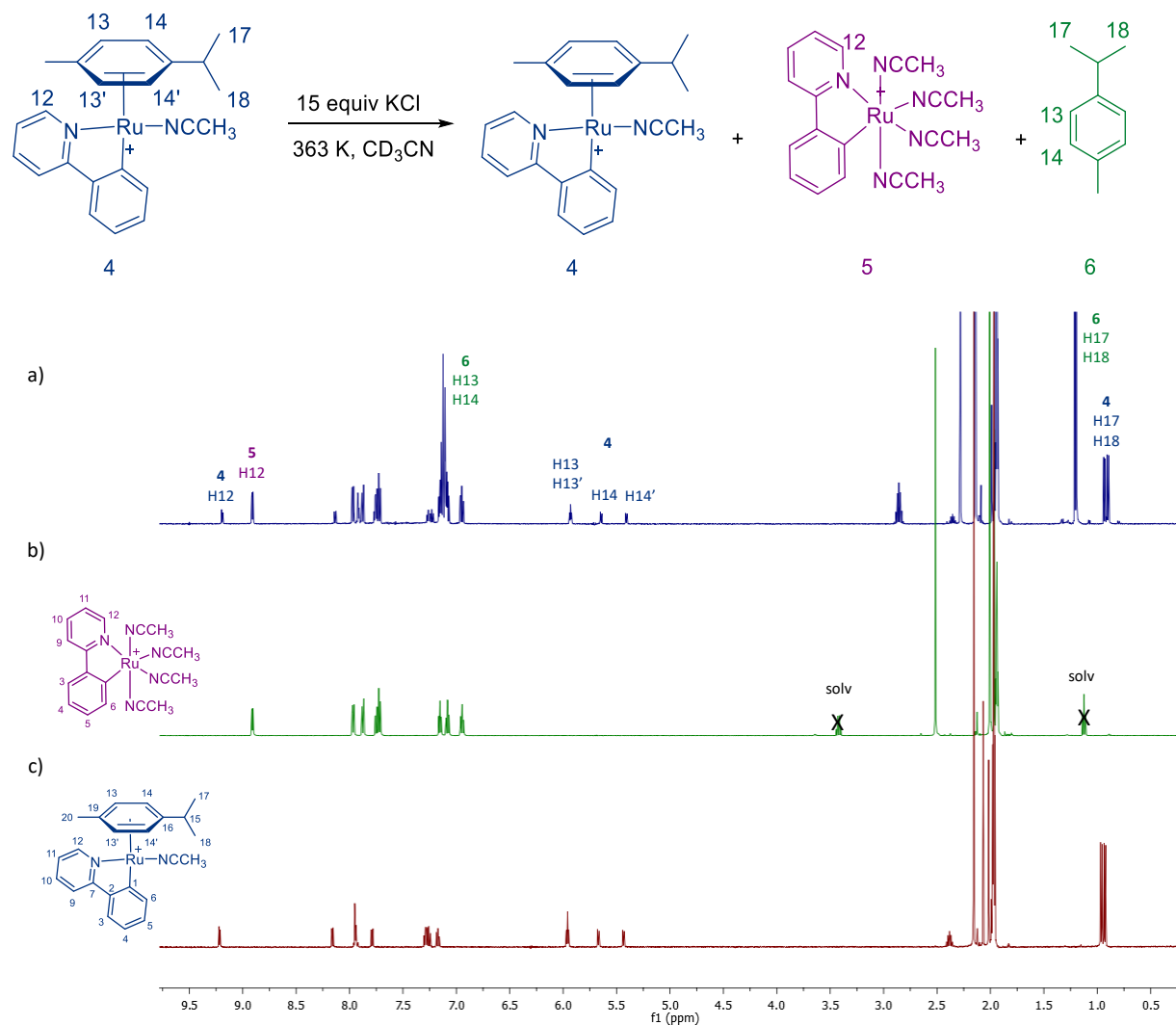


^1H NMR (500 MHz, CD_3CN) recorded at 298 K

2.4. Reaction of [Ru(PhPy)(*p*-cymene)(CH₃CN)]PF₆ with KCl

In a flame-dried NMR tube with a young cap, [Ru(PhPy)(*p*-cymene)(CH₃CN)]PF₆ (10 mg, 0.017 mmol) was dissolved in CD₃CN (0.5 mL) and KCl (20 mg, 0.27 mmol) was added. The NMR sample was heated for 15 h at 363 K.

Figure S4. Reaction of [RuPhPy(*p*-cymene)]PF₆ with KCl



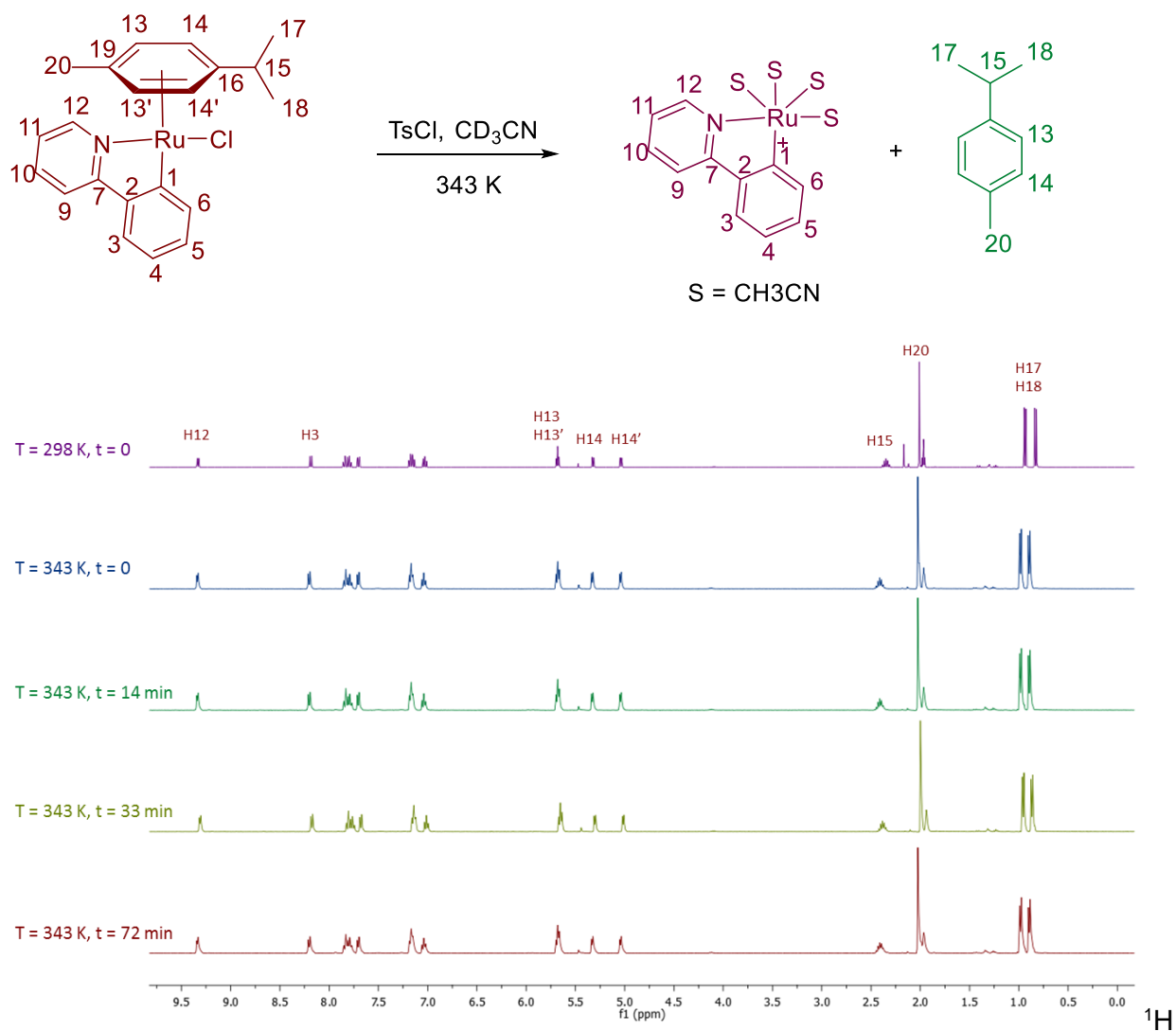
¹H NMR (500 MHz, CD₃CN) recorded at 298 K a) ¹H-NMR of the reaction mixture after heating **4** at 363 K; b) ¹H-NMR of **5** for comparison; c) ¹H-NMR of **4** for comparison.

2.5. Study of the stability of [RuCl(PhPy)(*p*-cymene)] in the presence of TsCl

In a flame-dried NMR tube with a young cap, [RuCl(PhPy)(*p*-cymene)] (34 mg, 0.08 mmol) was dissolved in CD₃CN. The sample was placed in the NMR spectrometer which was previously heated at 343 K. ¹H-NMR were recorded over time at this temperature. After 1 h TsCl (23 mg, 0.12 mmol) was added and heated at the same temperature in the NMR spectrometer recording several ¹H spectra overtime.

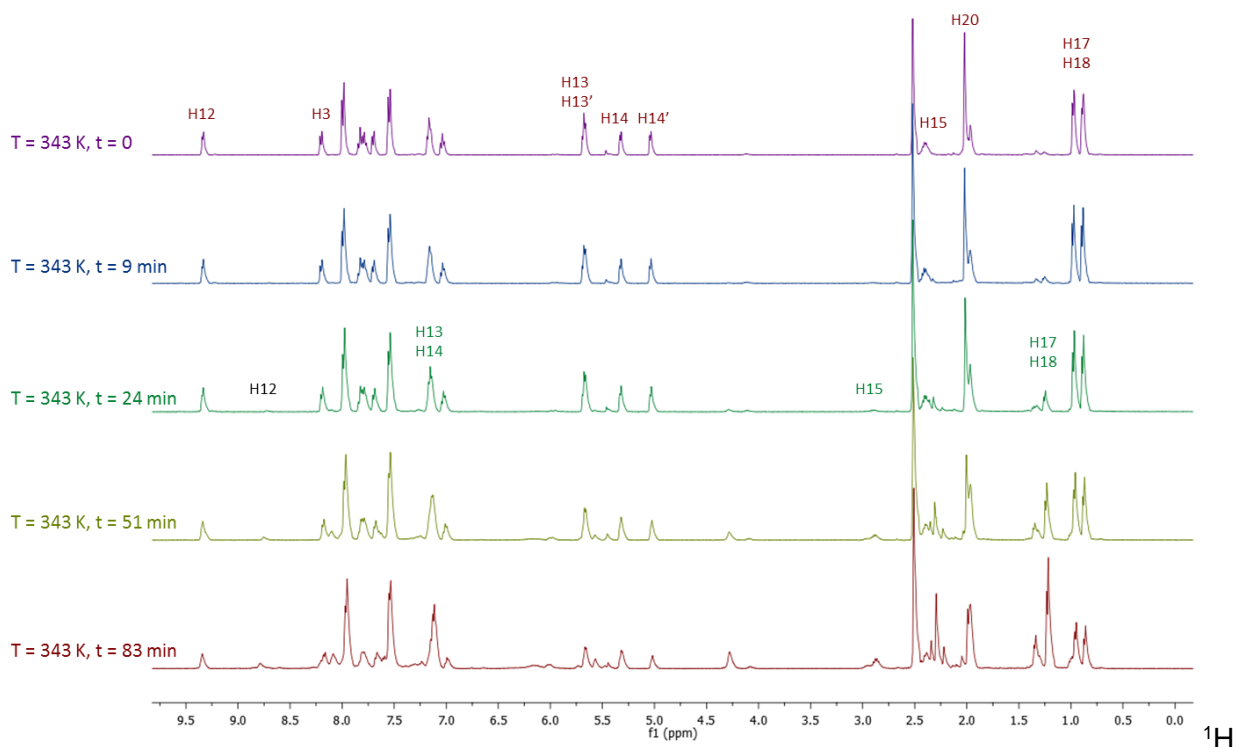
Figure S5. Stability of $[\text{RuCl}(\text{PhPy})(p\text{-cymene})]$ in the presence of TsCl

a) $[\text{RuCl}(\text{PhPy})(p\text{-cymene})]$ in CD_3CN heated at 343 K



NMR (400 MHz, CD_3CN) recorded at 298K and 343 K

b) $[\text{RuCl}(\text{PhPy})(p\text{-cymene})]$ in CD_3CN heated at 343 K in the presence of TsCl

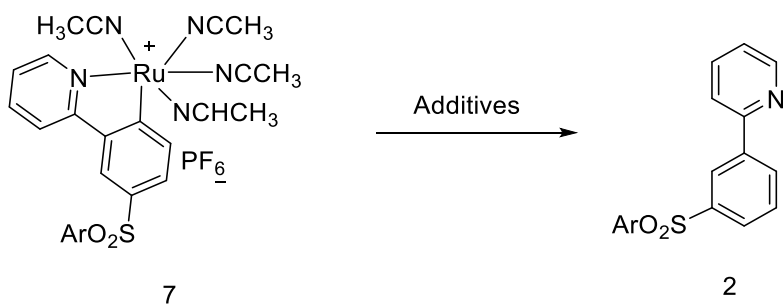


NMR (400 MHz, CD_3CN) recorded at 343 K

3. Study of the protodemetalation step

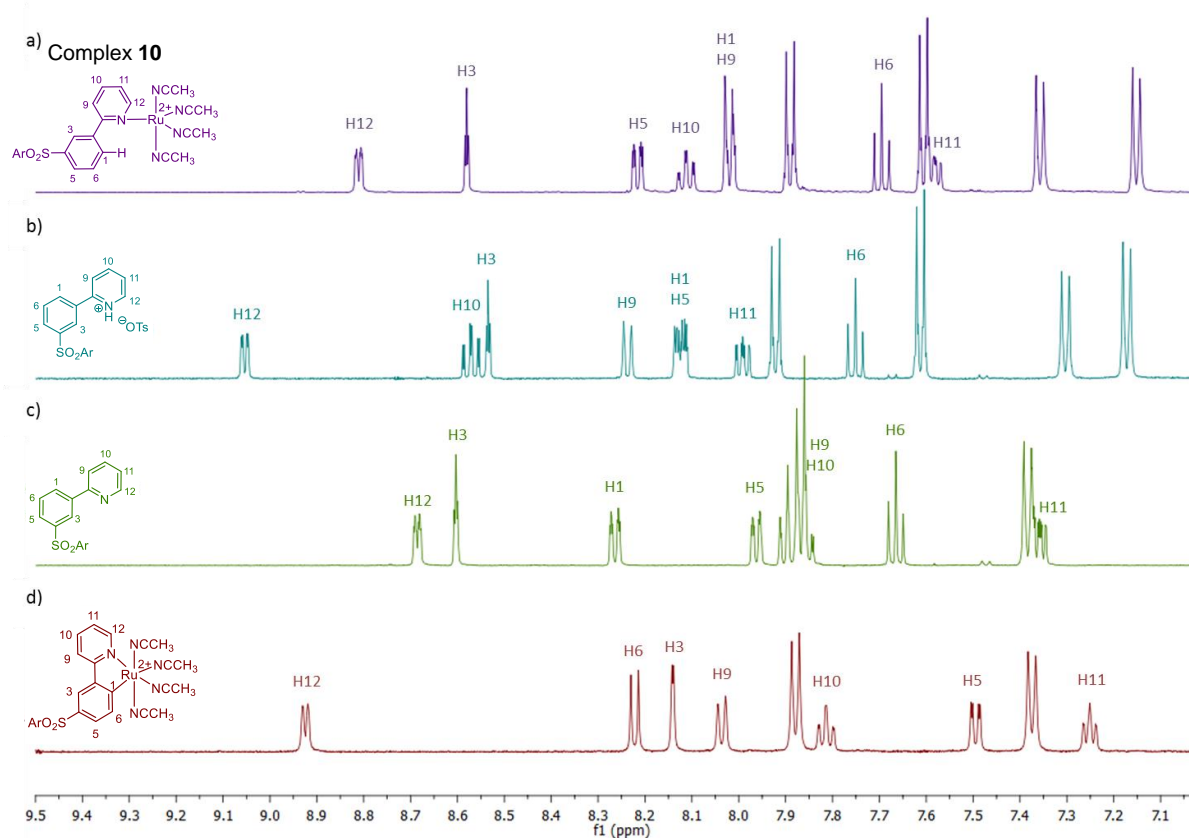
3.1. Protodemetalation of **7**

In a flame dried NMR tube with a young cap $[\text{Ru}(\text{TsPhPy})(\text{CH}_3\text{CN})_4]\text{PF}_6$ (7 mg, 0.01 mmol) was dissolved in CD_3CN (0.5 mL) and KHCO_3 (9.7 mg, 0.1 mmol), MesCO_2H (1.6 mg, 0.01 mmol) and K_2CO_3 (2.7 mg, 0.02 mmol), MesCO_2H (2.4 mg, 0.015 mmol), MesCO_2H (16 mg, 0.1 mmol), *p*-toluenesulfonic acid (*p*-TSA) (18 mg, 0.094 mmol) or a mixture of PhPy (1.4 mL, 0.01 mmol) and K_2CO_3 (2.7 mg, 0.02 mmol) were added depending on the experiment. The sample was heated for 15 h at 373 K in an oil bath.

Table S1. Protodemetalation conditions of **7**

Entry	Proton source	2 (%)
1	10 equiv KHCO ₃	--
2	1 equiv MesCO ₂ H	--
	2 equiv K ₂ CO ₃	
3	1.5 equiv MesCO ₂ H	--
4	10 equiv MesCO ₂ H	--
5	1 equiv PhPy	--
	2 equiv K ₂ CO ₃	
6	1.5 equiv <i>p</i> -TSA	Complex 10
7	4.5 equiv TsCl	23%
	2 equiv K ₂ CO ₃	
8	10 equiv PhPy	26%
	2 equiv K ₂ CO ₃	

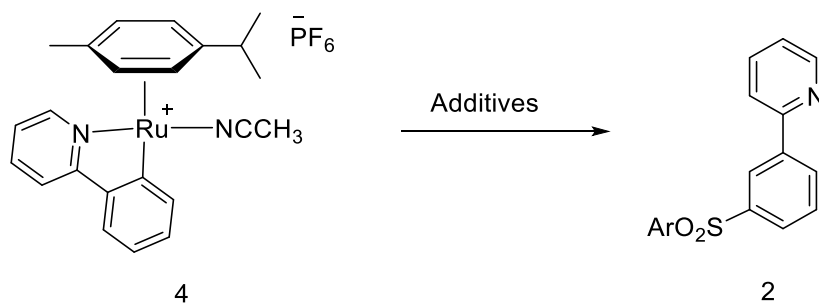
Figure S6. Formation of complex **10**



a) ^1H -NMR for the compound obtained by treatment of **7** with *p*-TSA and assigned to complex **10**; b) ^1H -NMR of the tosylated phenylpyridine salt in CD_3CN by its treatment with 1.5 equivalents of *p*-TSA; c) ^1H -NMR of **2** for comparison; d) ^1H -NMR of **7** for comparison.

3.2. Protodemetalation of **4**

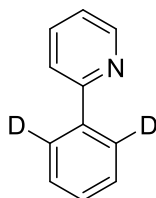
In a flame dried NMR tube with a young cap $[\text{Ru}(\text{PhPy})(p\text{-cymene})(\text{CH}_3\text{CN})]\text{PF}_6$ (7 mg, 0.01 mmol) was dissolved in CD_3CN (0.5 mL) and K_2CO_3 (8 mg, 0.06 mmol), KHCO_3 (12 mg, 0.12 mmol) or a mixture of PhPy (2.2 μL , 0.015 mmol) and K_2CO_3 (8 mg, 0.06 mmol) and PhPy (5.7 μL , 0.04 mmol) and K_2CO_3 (8 mg, 0.06 mmol) were added depending on the experiment. The sample was heated for 15 h at 393 K in an oil bath (Table S1).

Table S2. Protodemetalation conditions for **4**

Entry	Proton source	2 (%)
1	1.5 equiv TsCl	14
	5 equiv K ₂ CO ₃	
2	1.5 equiv TsCl	11
	10 equiv KHCO ₃	
3	1.5 equiv TsCl	33
	5 equiv K ₂ CO ₃	
	1.5 equiv PhPy	
4	1.5 equiv TsCl	46
	5 equiv K ₂ CO ₃	
	3.5 equiv PhPy	

4. Experiments with isotopically labelled compounds

4.1. Synthesis of 2-(2,6-dideuterophenyl)pyridine

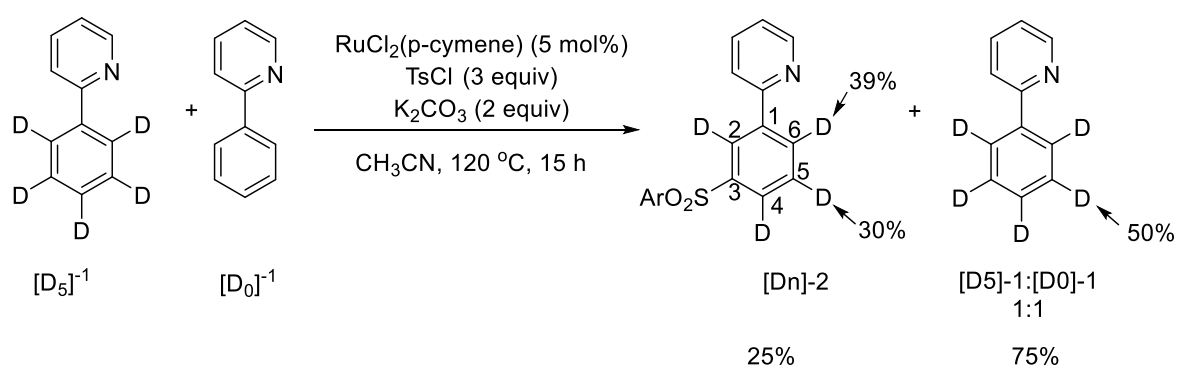


A suspension of [RuCl₂(*p*-cymene)]₂ (76.5 mg, 0.124 mmol), AcOD (0.1 mL, 1.74 mmol), K₂CO₃ (1.38 g, 10 mmol) and **1** (0.71 mL, 4.97 mmol) in degassed D₂O (20 mL) was stirred under N₂ for 20 h at 100 °C. EtOAc (50 mL) and H₂O (50 mL) were added to the reaction mixture at ambient temperature. The separated aqueous phase was extracted with EtOAc (2 × 50 mL). The combined organic layers were washed with brine (50 mL), dried over MgSO₄ and concentrated in vacuo. The remaining residue was purified by column chromatography on silica gel (hexane:EtOAc 5:1) and Kugelrohr-distillation to yield [**D**₂]-**1** (56 mg, 72%) as a colourless oil.

4.2. General procedure for the competitive experiments

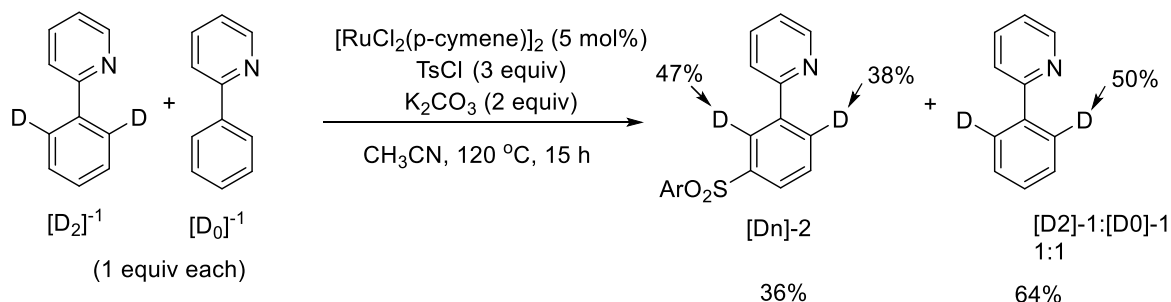
To a nitrogen-purged ampule, $[\text{RuCl}_2(p\text{-cymene})]_2$ (11 mg, 5 mol%) was dissolved in dry CD_3CN (4 mL). Then, phenylpyridine (50 μL , 0.35 mmol), $[\text{D}_5]\text{-1}$ (56 mg, 0.35 mmol), $[\text{D}_2]\text{-1}$ (51 mg, 0.35 mmol) or $[\text{D}_3]\text{-1}$ (55 mg, 0.35 mmol) along with K_2CO_3 (97 mg, 0.7 mmol) and TsCl (0.2 g, 1 mmol) were added. The reaction mixture was heated at 120 $^\circ\text{C}$ in an oil bath. The reaction mixture was filtered through a pad of celite and the crude was purified by flash chromatography on silica gel (from 20% EtOAc:hexane to 40% EtOAc).

4.2.1. Intramolecular competition experiment between 2-(2,3,4,5,6-pentadeuterophenyl)pyridine and phenylpyridine



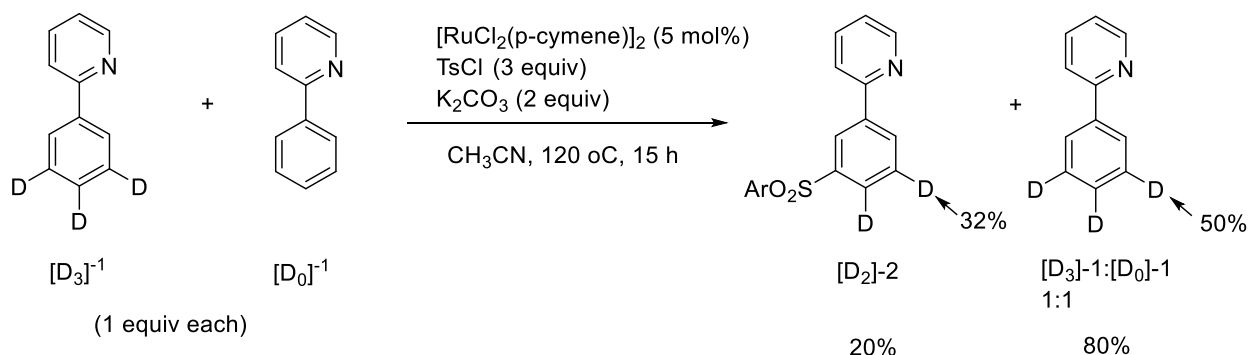
Following the general procedure described above, a mixture of $[\text{D}_n]\text{-2}$ (^1H NMR ratio H2/H6:D2/D6 1.6:1 and H5:D5 2.3:1, 54 mg, 25%) and a mixture of the re-isolated $[\text{D}_0]\text{-1}$ and $[\text{D}_5]\text{-1}$ (^1H NMR ratio 1:1, 83 mg, 75%) was obtained.

4.2.2. Intramolecular competition experiment between 2-(2,6-dideuterophenyl)pyridine and phenylpyridine



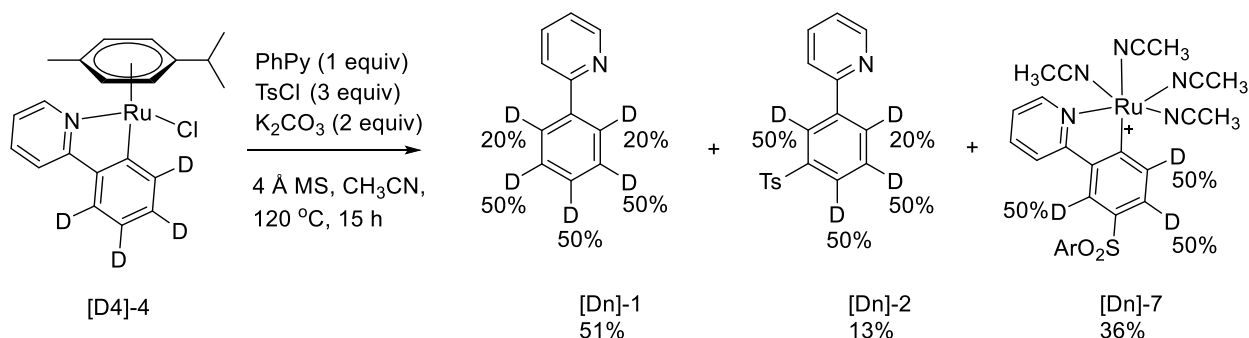
Following the general procedure described above, a mixture of $[\text{D}_n]\text{-2}$ (^1H NMR ratio H6:D6 1.6:1 and H2/D2 1.1:1, 78 mg, 36%) and a mixture of the re-isolated $[\text{D}_0]\text{-1}$ and $[\text{D}_2]\text{-1}$ (^1H NMR ratio 1:1, 67 mg, 64%) was obtained.

4.2.3. Intramolecular competition experiment between 2-(3,4,5-trideuterophenyl)pyridine and phenylpyridine



Following the general procedure described above, a mixture of $[D_n]-2$ (1H NMR ratio H5:D5 2.1:1, 43 mg, 20%) and a mixture of the re-isolated $[D_0]-1$ and $[D_5]-1$ (1H NMR ratio 1:1, 87 mg, 80%) was obtained.

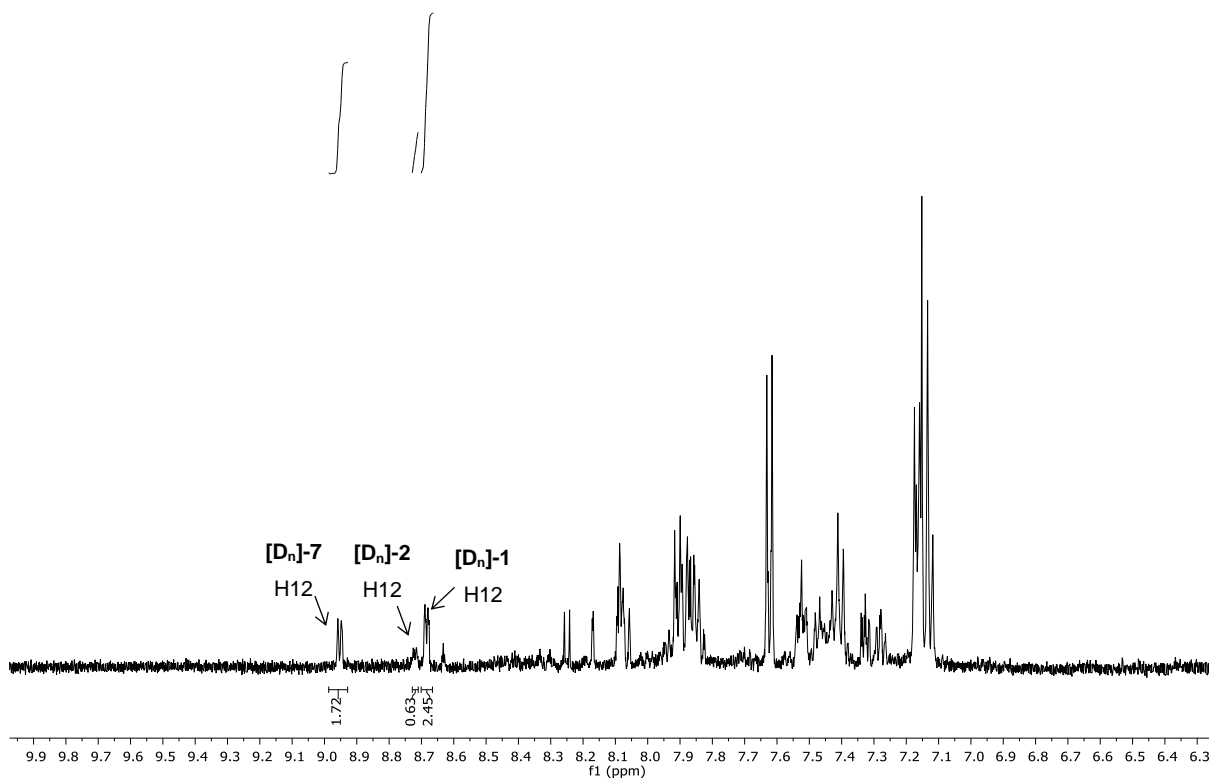
4.2. Single turnover experiment



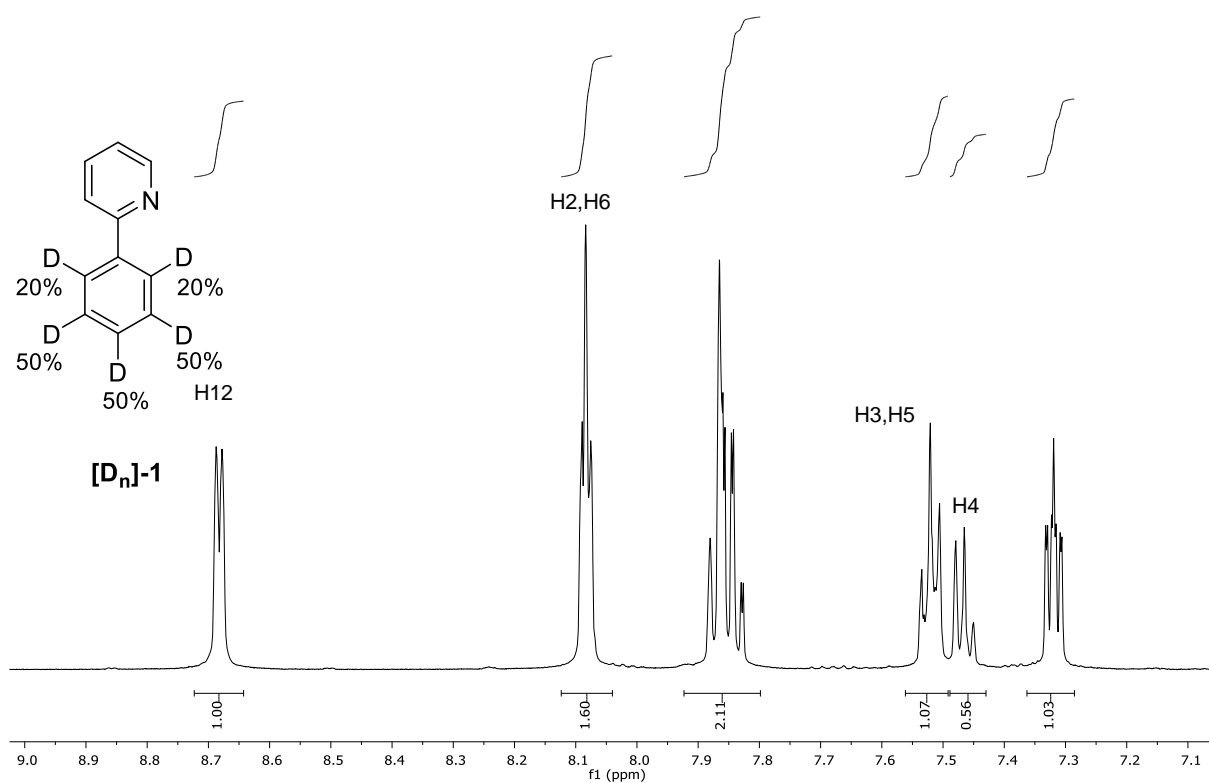
2-Phenyl pyridine was purified by distillation and dried using 4 Å molecular sieves before use. Tosyl chloride was purified by recrystallisation and thoroughly dried before use.

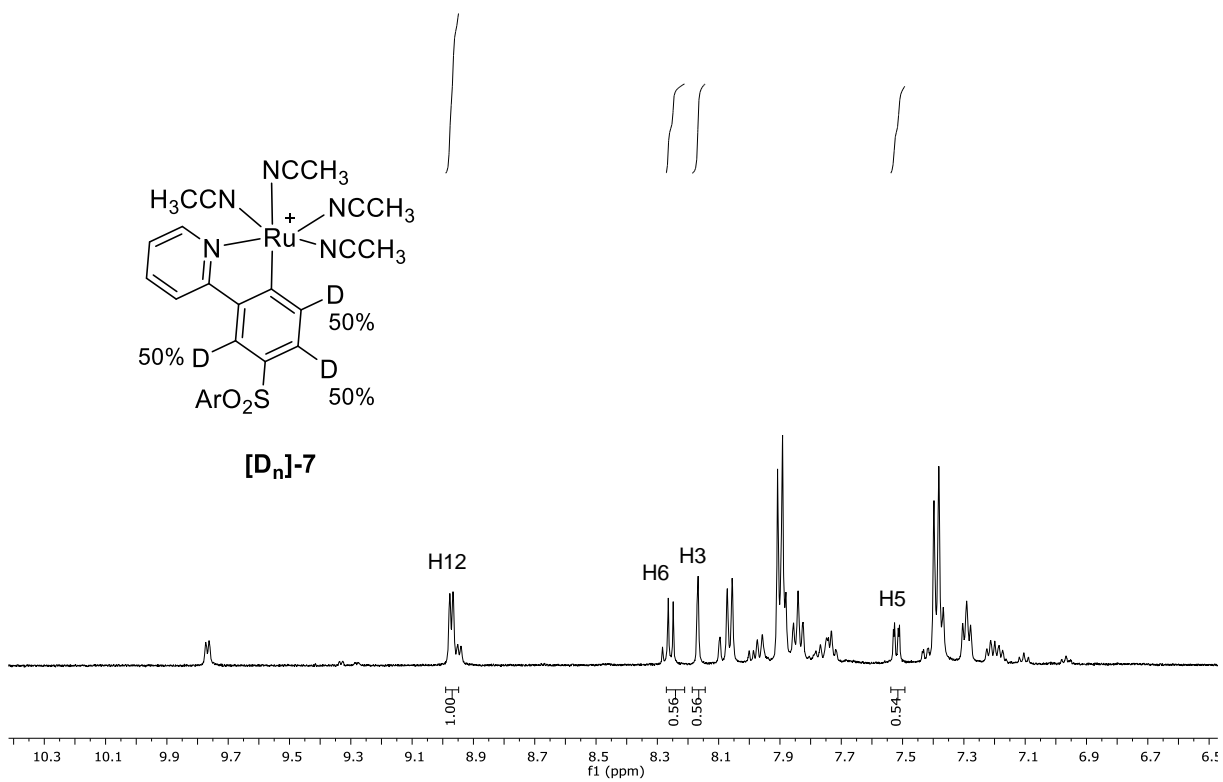
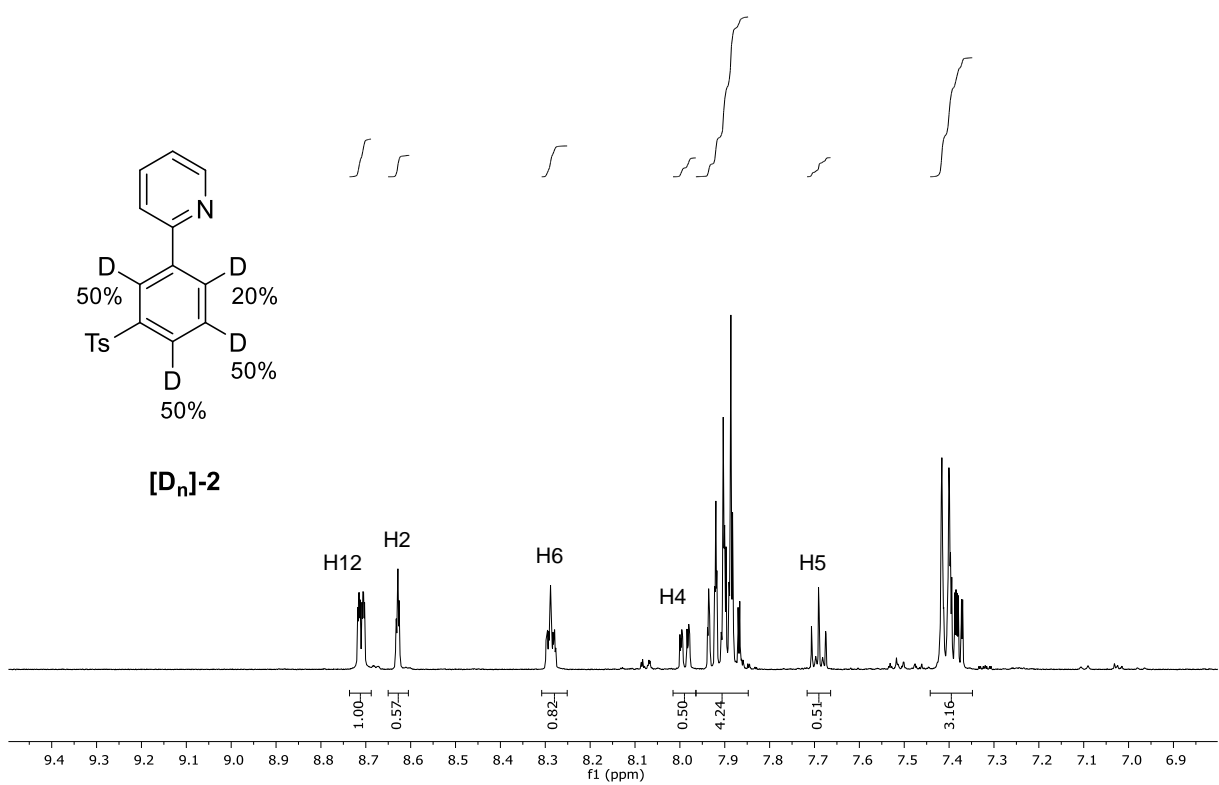
To a flame dried ampule purged with argon, K_2CO_3 (69 mg, 0.5 mmol) and activated molecular sieves 4 Å (100 mg) were added. Ruthenium complex $[D_4]-5$ (107 mg, 0.15 mmol), 2-phenyl pyridine (35 μ L, 0.25 mmol), tosyl chloride (143 mg, 0.75 mmol) and dry CH_3CN (2.5 mL) were then added and the reaction mixture was heated at 120 °C for 15 h. Analysis of the crude reaction mixture by 1H -NMR was used to calculate reaction composition with respect to total pyridine content. The reaction mixture was purified through oven-dried neutral alumina (Al_2O_3) and eluted with CH_3CN to separate the Ru complex $[D_n]-7$ and a mixture of $[D_n]-1$ and $[D_n]-2$. The fraction corresponding to the mixture of $[D_n]-1$ and $[D_n]-2$ was re-purified by flash chromatography over silica. Deuterium incorporation was calculated by 1H -NMR.

Ratios of [D_n]-1, [D_n]-2 and [D_n]-7



Deuterium Incorporation





- 1) (a) J.-P. Djukic, A. Berger, M. Duquenne, M. Pfeffer, A. de Cian and N. Kyritsakas-Gruber, *Organometallics*, 2004, **23**, 5757; (b) Y. Boutadla, O. Al-Duaij, D. L. Davies, G. A. Griffith and K. Singh, *Organometallics*, 2009, **28**, 433; (c) E. Ferrer-Flegeau, C. Bruneau, P. H. Dixneuf and A. Jutand, *J. Am. Chem. Soc.*, 2011, **133**, 10161.
- 2) (a) S. I. Kozhushkov, D. S. Yufit and L. Ackermann, *Org. Lett.*, 2008, **10**, 3409; (b) V. Bonnet, F. Mongin, F. Trécourt, G. Quéguiner and P. Knochel, *Tetrahedron*, 2002, **58**, 4429.
- 3) N. Hofmann and L. Ackermann, *J. Am. Chem. Soc.*, 2013, **135**, 5877.
- 4) L. A. Carpino, J. Xia, C. Zhang and A. El-Faham, *J. Org. Chem.*, 2004, **69**, 62.
- 5) D. R. Hicks and B. Fraser-Reid, *Synthesis*, 1974, 203.

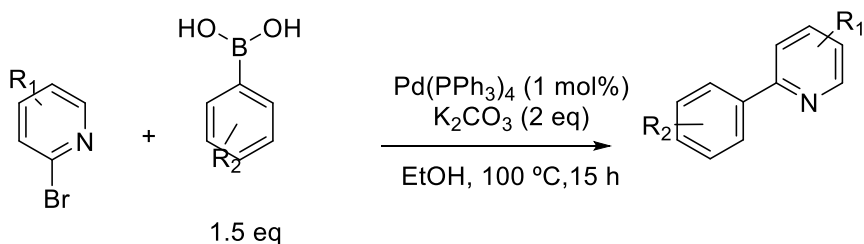
6.3 Supporting information and data for: α -halo carbonyls enable *meta* primary, secondary and tertiary C-H alkylations

General Considerations:

^1H , ^{13}C and ^{19}F nuclear magnetic resonance (NMR) spectra were recorded on an Agilent Technologies spectrometer (^1H NMR at 500 MHz, ^{13}C NMR at 126 MHz, and ^{19}F NMR at 470 MHz). Chemical shifts for protons are reported downfield from tetramethylsilane and are referenced to residual protium in the solvent (^1H NMR: CHCl_3 at 7.26 ppm). Chemical shifts for carbons are reported in parts per million downfield from tetramethylsilane and are referenced to the carbon resonances of the solvent peak (^{13}C NMR: CDCl_3 at 77.0 ppm). Chemical shifts for fluorine resonances are reported in parts per million referenced to CFCl_3 . NMR data are represented as follows: chemical shift (integration, multiplicity [s = singlet, bs = broad singlet, d = double, dd = doublet of doublet, t = triplet, q = quartet, hept = heptet, m = multiplet], coupling constants (Hz)). IR spectra were recorded on a Perkin-Elmer 1600 FT IR spectrophotometer, with absorbencies quoted as ν in cm^{-1} . High resolution mass spectrometry was performed on a Bruker Daltonik μTOF electrospray time-of-flight (ESI-TOF) mass spectrometer. HPLC analysis was conducted on an Agilent 1260 infinity quaternary LC instrument equipped with a Zorbax Eclipse XDB-C18 4.6 x 250 mm 5 μm analytical column. Analytical thin layer chromatography (TLC) were performed using aluminium-backed plates coated with Alugram[®] SIL G/UV₂₅₄ purchased from Macherey-Nagel and visualised by UV light (254 nm) and/or KMnO_4 staining. Silica gel column chromatography was carried out using 60 Å, 200-400 mesh particle size silica gel purchased from Sigma-Aldrich. All reactions were carried out under an atmosphere of argon, in oven-dried glassware unless otherwise stated. Anhydrous solvents were used in all experiments and stored under an atmosphere of argon prior to use. Reagents were purchased from commercial sources and used without further purification unless their synthesis is provided in the following sections.

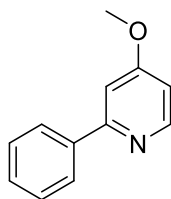
Synthesis of 2-Aryl Pyridine Derivatives

General Procedure



To an oven dried, argon purged flask equipped with magnetic stirrer and condenser was added $\text{Pd(PPh}_3)_4$ (1 mol%), K_2CO_3 (2 eq) and ethanol (1 M). A solution of the boronic acid (1.5 eq) in EtOH (1 M) was then added to the reaction vessel followed by the addition of the 2-bromopyridine reagent (1 eq). The reaction mixture was then heated to $100\text{ }^\circ\text{C}$ and refluxed for 15 hours. After cooling to room temperature, aqueous NaOH (1 M) was added and extracted three times with EtOAc. The organic extracts were then combined, washed with brine, dried with MgSO_4 and then concentrated under reduced pressure. The crude product was then purified by silica gel column chromatography (Hexane / EtOAc).

4-methoxy-2-phenylpyridine (1b)

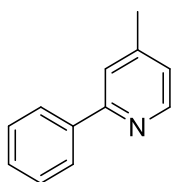


2-bromo,4-methoxy pyridine (5.3 mmol, 1g), phenyl boronic acid (7 mmol, 854 mg), Pd(PPh₃)₄ (0.053 mmol, 65 mg), K₂CO₃ (10 mmol, 1.38 g) were reacted together in EtOH (5 mL) according to the general procedure to afford the title compound as a white solid (684 mg, 70%).

¹H NMR (500 MHz, CDCl₃) δ 8.52 (d, *J* = 5.7 Hz, 1H), 8.05 – 7.92 (m, 2H), 7.50 – 7.38 (m, 3H), 7.24 (d, *J* = 2.4 Hz, 1H), 6.78 (dd, *J* = 5.7, 2.4 Hz, 1H), 3.91 (s, *J* = 0.8 Hz, 3H). **¹³C NMR** (126 MHz, CDCl₃) δ 166.42, 159.20, 150.84, 139.38, 129.01, 128.67, 126.97, 108.11, 106.88, 55.17.

Data conforms to literature.¹

4-methyl-2-phenylpyridine (1c)

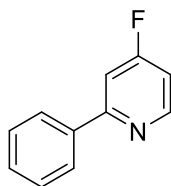


2-bromo,4-methyl pyridine (6.8 mmol, 1.16g), phenyl boronic acid (8 mmol, 1 g), Pd(PPh₃)₄ (0.068 mmol, 79 mg), K₂CO₃ (14 mmol, 1.9 g) were reacted together in EtOH (20 mL) according to the general procedure to afford the title compound as a colourless oil (1.08 g, 94%).

¹H NMR (500 MHz, CDCl₃) δ 8.58 (d, *J* = 5.0 Hz, 1H), 8.04 – 7.98 (m, 2H), 7.56 (d, *J* = 0.7 Hz, 1H), 7.52 – 7.46 (m, 2H), 7.45 – 7.39 (m, 1H), 7.07 (dd, *J* = 5.0, 0.8 Hz, 1H), 2.42 (s, 3H). **¹³C NMR** (101 MHz, CDCl₃) δ 157.40, 149.43, 147.76, 139.55, 128.83, 128.70, 126.96, 123.15, 121.56, 21.22.

Data conforms to literature.²

4-fluoro-2-phenylpyridine (1d)

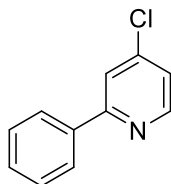


2-chloro,4-fluoropyridine (35 mmol, 4.6 g), phenyl boronic acid (42 mmol, 5.08 g), Pd(PPh₃)₄ (0.35 mmol, 404 mg), and K₂CO₃ (70 mmol, 9.66 g) were reacted together in EtOH (100 mL) according to the general procedure to afford the title compound as a yellow / white crystalline solid (5.4 g, 90%).

¹H NMR (500 MHz, CDCl₃) δ 8.65 (dd, *J* = 8.8, 5.6 Hz, 1H), 7.98 (dd, *J* = 8.2, 1.3 Hz, 2H), 7.54 – 7.33 (m, 4H), 6.96 (ddd, *J* = 8.1, 5.5, 2.4 Hz, 1H). **¹³C NMR** (126 MHz, CDCl₃) δ 169.37 (d, *J* = 261.1 Hz), 160.65 (d, *J* = 6.9 Hz), 151.93 (d, *J* = 7.2 Hz), 138.29 (d, *J* = 3.3 Hz), 129.60 (s), 128.83 (s), 126.93 (s), 109.91 (d, *J* = 16.4 Hz), 108.10 (d, *J* = 17.3 Hz). **¹⁹F NMR** (470 MHz, CDCl₃) δ -102.60 (ddd, *J* = 10.4, 8.6 Hz).

Data conforms to literature ³

4-chloro-2-phenylpyridine (1e)

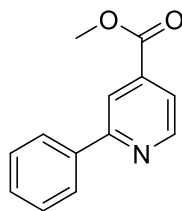


2-bromo,4-chloro pyridine (5.2 mmol, 1g), phenyl boronic acid (7 mmol, 854 mg), Pd(PPh₃)₄ (0.052 mmol, 60 mg), K₂CO₃ (10.4 mmol, 1.44 g) were reacted together in EtOH (10 mL) according to the general procedure to afford the title compound as a white solid (929 mg, 94%).

¹H NMR (500 MHz, CDCl₃) δ 8.59 (d, *J* = 5.3 Hz, 1H), 8.03 – 7.91 (m, 2H), 7.74 (d, *J* = 1.8 Hz, 1H), 7.54 – 7.39 (m, 3H), 7.26 – 7.23 (m, 1H). **¹³C NMR** (126 MHz, CDCl₃) δ 159.01, 150.48, 144.73, 138.13, 129.59, 128.85, 126.99, 126.97, 122.27, 120.85.

Data conforms to literature ¹

methyl 2-phenylisonicotinate (1f)

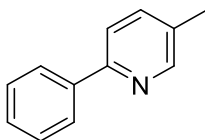


methyl 2-bromoisonicotinate (7 mmol, 1.5g), phenyl boronic acid (8.5 mmol, 1 g), Pd(PPh₃)₄ (0.07 mmol, 81 mg), K₂CO₃ (28 mmol, 3.8 g) were reacted together in Toluene (20 mL), THF (10 mL) and H₂O (20 mL) according to the general procedure to afford the title compound as a colourless oil (988 mg, 65%).

¹H NMR (500 MHz, CDCl₃) δ 8.83 (dd, *J* = 5.0, 0.9 Hz, 1H), 8.30 (dd, *J* = 1.4, 1.0 Hz, 1H), 8.10 – 8.01 (m, *J* = 4.2, 3.5, 1.9 Hz, 2H), 7.77 (dd, *J* = 5.0, 1.5 Hz, 1H), 7.54 – 7.41 (m, 3H), 3.98 (d, *J* = 1.5 Hz, 3H). **¹³C NMR** (126 MHz, CDCl₃) δ 165.76, 158.45, 150.42, 138.49, 138.15, 129.45, 128.84, 126.97, 121.10, 119.70, 52.71.

Data conforms to literature ¹

5-methyl-2-phenylpyridine (1g)

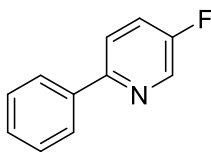


¹H NMR (500 MHz, CDCl₃) δ 8.53 (d, *J* = 0.7 Hz, 1H), 7.98 (d, *J* = 8.3 Hz, 2-bromo,5-methyl pyridine (15 mmol, 2.6g), phenyl boronic acid (22.5 mmol, 2.7 g), Pd(PPh₃)₄ (0.15 mmol, 173 mg), K₂CO₃ (30 mmol, 4.2 g) were reacted together in EtOH (30 mL) according to the general procedure to afford the title compound as a colourless oil (2.28 g, 90%).

¹H NMR (500 MHz, CDCl₃) δ 8.57 (s, 1H), 7.97 – 7.90 (m, 2H), 7.63 (d, *J* = 8.1 Hz, 1H), 7.56 (dd, *J* = 8.0, 1.7 Hz, 1H), 7.47 (t, *J* = 7.5 Hz, 2H), 7.42 – 7.35 (m, 1H), 2.38 (s, 3H). **¹³C NMR** (126 MHz, CDCl₃) δ 154.80, 150.04, 139.39, 137.30, 131.58, 128.68, 128.58, 126.68, 120.03, 18.15.

Data conforms to literature.⁴

5-fluoro-2-phenylpyridine (1h)

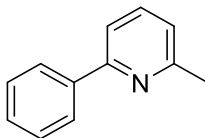


2-bromo,5-fluoropyridine (35 mmol, 6.2 g), phenyl boronic acid (42 mmol, 5.08 g), Pd(PPh₃)₄ (0.35 mmol, 404 mg), and K₂CO₃ (70 mmol, 9.66 g) were reacted together in EtOH (100 mL) according to the general procedure to afford the title compound as a yellow / white crystalline solid (5.5 g, 91%).

¹H NMR (500 MHz, CDCl₃) δ 8.55 (d, *J* = 2.9 Hz, 1H), 7.97 – 7.90 (m, 2H), 7.72 (ddd, *J* = 8.8, 4.3, 0.6 Hz, 1H), 7.50 – 7.44 (m, 3H), 7.44 – 7.39 (m, 1H). **¹³C NMR** (126 MHz, CDCl₃) δ 158.81 (d, *J* = 256.3 Hz), 153.77 (d, *J* = 3.8 Hz), 138.42, 137.73 (d, *J* = 23.5 Hz), 128.86, 128.78, 126.75, 123.48 (d, *J* = 18.5 Hz), 121.28 (d, *J* = 4.2 Hz). **¹⁹F NMR** (470 MHz, CDCl₃) δ -129.88 (m).

Data conforms to literature.⁵

6-methyl-2-phenylpyridine (1i)

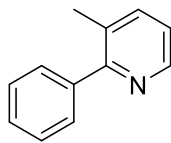


2-bromo,6-methyl pyridine (6.8 mmol, 1.16g), phenyl boronic acid (8 mmol, 1 g), Pd(PPh₃)₄ (0.068 mmol, 79 mg), K₂CO₃ (14 mmol, 1.9 g) were reacted together in EtOH (20 mL) according to the general procedure to afford the title compound as a colourless oil (1.14 g, 99%).

¹H NMR (400 MHz, CDCl₃) δ 8.10 – 7.99 (m, 2H), 7.64 (t, *J* = 7.7 Hz, 1H), 7.58 – 7.48 (m, 3H), 7.46 (dt, *J* = 9.6, 4.3 Hz, 1H), 7.12 (d, *J* = 7.6 Hz, 1H), 2.69 (s, 3H). **¹³C NMR** (101 MHz, CDCl₃) δ 158.39, 157.00, 139.84, 136.92, 128.74, 127.20, 127.07, 121.65, 117.65, 24.80.

Data conforms to literature.⁴

3-methyl-2-phenylpyridine(1j)

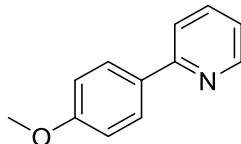


2-bromo,3-methyl pyridine (6.8 mmol, 1.16g), phenyl boronic acid (8 mmol, 1 g), Pd(PPh₃)₄ (0.068 mmol, 79 mg), K₂CO₃ (14 mmol, 1.9 g) were reacted together in EtOH (20 mL) according to the general procedure to afford the title compound as a colourless oil (1.1 g, 96%).

¹H NMR (400 MHz, CDCl₃) δ 8.55 (dd, *J* = 4.7, 1.1 Hz, 1H), 7.59 (dd, *J* = 7.4, 1.1 Hz, 1H), 7.57 – 7.52 (m, 2H), 7.50 – 7.43 (m, 3H), 7.18 (dd, *J* = 7.7, 4.8 Hz, 1H), 2.37 (s, 3H). **¹³C NMR** (101 MHz, CDCl₃) δ 158.73, 147.00, 140.68, 138.46, 130.79, 128.95, 128.14, 127.90, 122.06, 20.06.

Data conforms to literature.⁴

2-(4-methoxyphenyl)pyridine (1k)

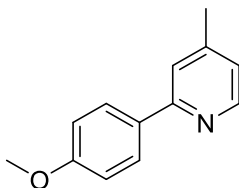


2-bromopyridine (25 mmol, 2.4 mL), 4-methoxyphenyl boronic acid (33 mmol, 5.0 g), Pd(PPh₃)₄ (0.25 mmol, 289 mg), K₂CO₃ (50 mmol, 6.90 g) were reacted together in EtOH (25 mL) according to the general procedure to afford the title compound as a white solid (4.4 g, 95%).

¹H NMR (500 MHz, CDCl₃) δ 8.65 (ddd, *J* = 4.8, 1.7, 1.0 Hz, 1H), 7.96 (d, *J* = 8.9 Hz, 2H), 7.76 – 7.64 (m, 2H), 7.17 (ddd, *J* = 7.2, 4.8, 1.3 Hz, 1H), 7.00 (d, *J* = 8.9 Hz, 2H), 3.87 (s, 3H). **¹³C NMR** (126 MHz, CDCl₃) δ 160.43, 157.08, 149.47, 136.67, 131.92, 128.15, 121.38, 119.79, 114.11, 55.34.

Data conforms to literature.⁶

2-(4-methoxyphenyl)-4-methylpyridine (1l)

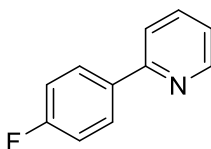


2-bromo,4-methylpyridine (15 mmol, 1.66 mL), 4-methoxyphenyl boronic acid (22.5 mmol, 3.42 g), Pd(PPh₃)₄ (0.15 mmol, 173 mg), K₂CO₃ (30 mmol, 4.14 g) were reacted together in Ethanol (25 mL) according to the general procedure to afford the title compound as a colourless oil (2.71 g, 91%).

¹H NMR (500 MHz, CDCl₃) δ 8.51 (d, *J* = 5.0 Hz, 1H), 7.98 – 7.90 (m, 2H), 7.49 (d, *J* = 0.4 Hz, 1H), 7.05 – 6.92 (m, 3H), 3.87 (s, 3H), 2.40 (s, 3H). **¹³C NMR** (126 MHz, CDCl₃) δ 160.33, 156.99, 149.26, 147.57, 132.12, 128.14, 122.46, 120.73, 114.03, 55.31, 21.21.

Data conforms to literature.⁷

2-(4-fluorophenyl)pyridine (1n)

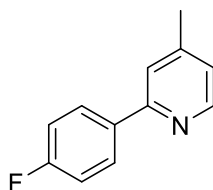


2-bromopyridine (20 mmol, 1.9 mL), 4-fluorophenyl boronic acid (30 mmol, 4.20 g), Pd(PPh₃)₄ (0.2 mmol, 231 mg), and K₂CO₃ (40 mmol, 5.52 g) were reacted together in EtOH (20 mL) according to the general procedure to afford the title compound as a yellow / white crystalline solid (3.20 g, 92%).

¹H NMR (500 MHz, CDCl₃) δ 8.68 (ddd, *J* = 4.8, 1.6, 0.9 Hz, 1H), 7.98 (dd, *J* = 8.9, 5.4 Hz, 2H), 7.77 – 7.72 (m, 1H), 7.68 (dt, *J* = 8.0, 1.0 Hz, 1H), 7.22 (ddd, *J* = 7.4, 4.8, 1.1 Hz, 1H), 7.16 (t, *J* = 8.7 Hz, 2H). **¹³C NMR** (126 MHz, CDCl₃) δ 163.51 (d, ¹*J*_{C-F} = 248.4 Hz), 135.51 (d, ⁴*J*_{C-F} = 3.1 Hz), 128.68 (d, ³*J*_{C-F} = 8.4 Hz), 115.63 (d, ²*J*_{C-F} = 21.6 Hz). **¹⁹F NMR** (470 MHz, CDCl₃) δ -113.14 – -113.24 (m).

Data conforms to literature.⁶

2-(4-fluorophenyl)-4-methylpyridine (1o)

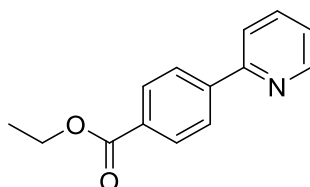


2-bromo,4-methylpyridine (15 mmol, 1.66 mL), 4-fluorophenyl boronic acid (22.5 mmol, 3.15 g), Pd(PPh₃)₄ (0.15 mmol, 173 mg), K₂CO₃ (30 mmol, 4.14 g) were reacted together in EtOH (25 mL) according to the general procedure to afford the title compound as a colourless oil (2.24 g, 80%).

¹H NMR (500 MHz, CDCl₃) δ 8.52 (d, *J* = 5.0 Hz, 1H), 8.01 – 7.88 (m, 2H), 7.50 (s, *J* = 0.6 Hz, 1H), 7.18 – 7.09 (m, 2H), 7.05 (ddd, *J* = 5.1, 1.4, 0.7 Hz, 1H), 2.41 (s, 3H). **¹³C NMR** (126 MHz, CDCl₃) δ 164.41, 162.44, 156.36, 149.40, 147.84, 135.67, 128.72, 128.65, 123.06, 121.21, 115.63, 115.46, 21.21. **¹⁹F NMR** (470 MHz, CDCl₃) δ -113.42 (m).

Data conforms to literature.⁸

ethyl 4-(pyridin-2-yl)benzoate (1p)

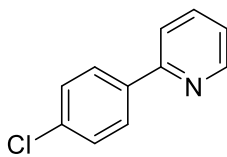


2-bromopyridine (13 mmol, 1.2 mL), 4-(methoxycarbonyl)phenyl boronic acid (20 mmol, 3.04 g), Pd(PPh₃)₄ (0.13 mmol, 150 mg), and K₂CO₃ (26 mmol, 3.58 g) were reacted together in EtOH (13 mL) according to the general procedure to afford the title compound as a white solid (2.42 g, 82%).

¹H NMR (500 MHz, CDCl₃) δ 8.73 (d, *J* = 4.6 Hz, 1H), 8.15 (d, *J* = 8.2 Hz, 2H), 8.07 (d, *J* = 8.3 Hz, 2H), 7.87 – 7.71 (m, 2H), 7.29 (dd, *J* = 8.3, 4.8 Hz, 1H), 4.41 (q, *J* = 7.1 Hz, 2H), 1.42 (t, *J* = 7.1 Hz, 3H). **¹³C NMR** (126 MHz, CDCl₃) δ 166.56, 156.38, 149.93, 143.42, 137.15, 130.90, 130.16, 126.95, 123.00, 121.19, 77.16, 61.22, 14.50.

Data conforms to literature.⁶

2-(4-chlorophenyl)pyridine (1q)

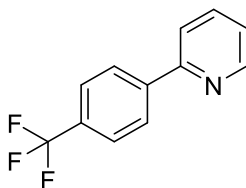


2-bromopyridine (13 mmol, 1.2 mL), 4-chlorophenyl boronic acid (20 mmol, 3.04 g), Pd(PPh₃)₄ (0.13 mmol, 150 mg), and K₂CO₃ (26 mmol, 3.58 g) were reacted together in EtOH (13 mL) according to the general procedure to afford the title compound as a pale yellow crystalline solid (1.20 g, 89%).

¹H NMR (500 MHz, CDCl₃) δ 8.69 (dd, J = 4.8, 0.8 Hz, 1H), 7.95 (d, J = 8.4 Hz, 2H), 7.81 – 7.74 (m, 1H), 7.71 (dd, J = 7.9, 0.9 Hz, 1H), 7.45 (d, J = 8.5 Hz, 2H), 7.29 – 7.24 (m, 1H). **¹³C NMR** (126 MHz, CDCl₃) δ 155.97, 149.35, 137.31, 137.26, 135.30, 128.97, 128.23, 122.45, 120.49.

Data conforms to literature.⁶

2-(4-trifluoromethylphenyl)pyridine (1r)

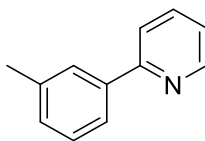


2-bromopyridine (10 mmol, 0.92 mL), 4-(trifluoromethyl)phenyl boronic acid (15 mmol, 2.85 g), Pd(PPh₃)₄ (0.10 mmol, 115 mg), and K₂CO₃ (20 mmol, 2.76 g) were reacted together in EtOH (10 mL) according to the general procedure to afford the title compound as an off white solid (1.38 g, 62%).

¹H NMR (500 MHz, CDCl₃) δ 8.73 (d, J = 4.7 Hz, 1H), 8.11 (d, J = 8.2 Hz, 2H), 7.84 – 7.69 (m, 4H), 7.33 – 7.27 (m, 1H). **¹³C NMR** (126 MHz, CDCl₃) δ 155.98 (s), 150.03 (s), 142.77 (s), 137.13 (s), 130.91 (q, ²J_{C-F} = 32.5 Hz), 127.31 (s), 125.81 (q, ³J_{C-F} = 3.8 Hz), 124.32 (q, ¹J_{C-F} = 272.0 Hz), 123.09 (s), 121.00 (s). **¹⁹F NMR** (470 MHz, CDCl₃) δ -62.61 (s).

Data conforms to literature.⁶

2-(3-methylphenyl)pyridine (1s)

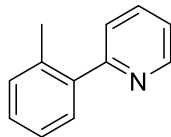


2-bromopyridine (5 mmol, 0.46 mL), 3-methylphenylboronic acid (7 mmol, 1.0 g), $\text{Pd}(\text{PPh}_3)_4$ (0.05 mmol, 58 mg), and K_2CO_3 (10 mmol, 1.38 g) were reacted together in EtOH (7.5 mL) according to the general procedure to afford the title compound as a yellow oil (772 mg, 91%).

^1H NMR (500 MHz, CDCl_3) δ 8.73 (d, J = 4.7 Hz, 1H), 7.87 (s, 1H), 7.84 – 7.73 (m, 3H), 7.39 (dd, J = 7.6 Hz, 1H), 7.29 – 7.24 (m, 2H), 2.46 (s, 3H). **^{13}C NMR** (126 MHz, CDCl_3) δ 157.40, 149.18, 138.81, 138.50, 137.16, 129.94, 128.69, 127.72, 124.09, 122.11, 120.86, 21.51.

Data conforms to literature.⁶

2-(2-methylphenyl)pyridine (1t)

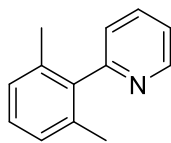


2-bromopyridine (20 mmol, 1.84 mL), 2-methylphenylboronic acid (30 mmol, 4.08 g), $\text{Pd}(\text{PPh}_3)_4$ (0.2 mmol, 231 mg), and K_2CO_3 (40 mmol, 5.52 g) were reacted together in EtOH (30 mL) according to the general procedure to afford the title compound as a yellow oil (2.96 g, 88%).

^1H NMR (500 MHz, CDCl_3) δ 8.71 (d, J = 3.9 Hz, 1H), 7.85 – 7.69 (m, 1H), 7.42 (dd, J = 13.6, 4.5 Hz, 2H), 7.33 – 7.25 (m, 4H), 2.29 (s, 3H). **^{13}C NMR** (126 MHz, CDCl_3) δ 159.67, 148.75, 139.86, 136.60, 135.77, 130.77, 129.64, 128.46, 125.91, 124.30, 121.76, 20.27.

Data conforms to literature.⁶

2-(2,6-dimethylphenyl)pyridine (1u)

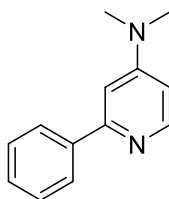


2-bromopyridine (13 mmol, 1.2 mL), 2,6-dimethylphenylboronic acid (20 mmol, 3.0 g), Pd(PPh₃)₄ (0.13 mmol, 150 mg), and K₂CO₃ (26 mmol, 3.59 g) were reacted together in EtOH (15 mL) according to the general procedure to afford the title compound as a red oil (1.96 g, 82%).

¹H NMR (500 MHz, CDCl₃) δ 8.74 (d, *J* = 4.5 Hz, 1H), 7.82 (dd, *J* = 7.6 Hz, 1H), 7.34 – 7.30 (m, 1H), 7.28 (d, *J* = 8.2 Hz, 1H), 7.21 (t, *J* = 7.6 Hz, 1H), 7.12 (d, *J* = 7.6 Hz, 2H). **¹³C NMR** (126 MHz, CDCl₃) δ 159.56, 149.17, 139.76, 137.09, 135.93, 128.25, 127.72, 124.93, 122.02, 77.16, 20.33.

Data conforms to literature.⁶

4-dimethylamino-2-phenylpyridine (1v)

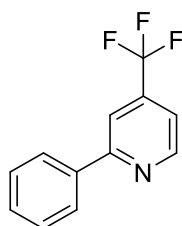


2-bromo,4-dimethylaminoopyridine (13.8 mmol, 2.7 g), phenyl boronic acid (20.7 mmol, 2.5 g), Pd(PPh₃)₄ (0.14 mmol, 160 mg), and K₂CO₃ (28 mmol, 3.8 g) were reacted together in EtOH (25 mL) according to the general procedure to afford the title compound as a white crystalline solid (2.40 g, 86%).

¹H NMR (400 MHz, CDCl₃) δ 8.25 (d, *J* = 5.9 Hz, 1H), 7.86 (dd, *J* = 8.3, 1.3 Hz, 2H), 7.41 – 7.23 (m, 3H), 6.82 (d, *J* = 2.5 Hz, 1H), 6.40 (dd, *J* = 5.9, 2.6 Hz, 1H), 2.97 (s, 6H). **¹³C NMR** (101 MHz, CDCl₃) δ 158.01, 155.07, 149.73, 140.77, 128.50, 127.05, 105.45, 103.65, 39.25. **MP** 84-85 °C

Data conforms to literature.⁹

4-trifluoromethyl-2-phenylpyridine (1w)

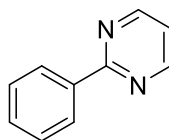


2-bromo,4-trifluoromethyl pyridine (12 mmol, 2.74g), phenyl boronic acid (18 mmol, 2.2 g), Pd(PPh₃)₄ (0.12 mmol, 140 mg), K₂CO₃ (24 mmol, 1.44 g) were reacted together in EtOH (30 mL) according to the general procedure to afford the title compound as a colourless oil (2.54 g, 95%).

¹H NMR (500 MHz, CDCl₃) δ 8.87 (d, *J* = 5.0 Hz, 1H), 8.08 – 8.00 (m, 2H), 7.93 (s, *J* = 0.7 Hz, 1H), 7.61 – 7.40 (m, 4H). **¹³C NMR** (126 MHz, CDCl₃) δ 158.79, 150.61, 138.97 (q, *J* = 33.8 Hz), 138.03, 129.82, 128.95, 127.01, 122.94 (q, *J* = 273.1 Hz), 117.49 (q, *J* = 3.5 Hz), 116.00 (q, *J* = 3.6 Hz). **¹⁹F NMR** (470 MHz, CDCl₃) δ -64.85 (m).

Data conforms to literature.¹⁰

2-phenylpyrimidine (5a)

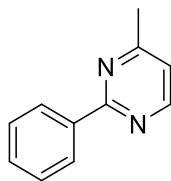


2-chloropyrimidine (50 mmol, 5.7g), phenyl boronic acid (60 mmol, 7.26 g), Pd(PPh₃)₄ (0.5 mmol, 578 mg), K₂CO₃ (100 mmol, 13.8 g) were reacted together in EtOH (100 mL) according to the general procedure to afford the title compound as a white crystalline solid (7.02 g, 90%).

¹H NMR (400 MHz, CDCl₃) δ 8.78 (d, *J* = 4.9 Hz, 1H), 8.53 – 8.42 (m, 2H), 7.58 – 7.45 (m, 3H), 7.13 (t, *J* = 4.8 Hz, 1H). **¹³C NMR** (101 MHz, CDCl₃) δ 164.73, 157.22, 137.63, 130.80, 128.62, 128.19, 119.08. **MP** 37-39 °C

Data conforms to literature.¹¹

4-methyl-2-phenylpyrimidine (5b)

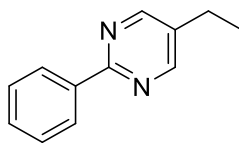


2-chloro,4-methylpyrimidine (30 mmol, 3.84g), phenyl boronic acid (36 mmol, 4.35 g), Pd(PPh₃)₄ (0.3 mmol, 346 mg), K₂CO₃ (60 mmol, 8.3 g) were reacted together in EtOH (100 mL) according to the general procedure to afford the title compound as a colourless oil (5.4 g, 92%).

¹H NMR (400 MHz, CDCl₃) δ 8.67 (d, *J* = 5.0 Hz, 1H), 8.51 – 8.43 (m, 2H), 7.55 – 7.46 (m, 3H), 7.07 (d, *J* = 5.1 Hz, 1H), 2.61 (s, 3H). **¹³C NMR** (101 MHz, CDCl₃) δ 167.27, 164.43, 156.81, 137.87, 130.53, 128.53, 128.18, 118.59, 24.42.

Data conforms to literature.¹²

5-ethyl-2-phenylpyrimidine (5c)

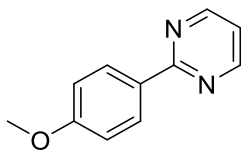


2-chloro,5-ethylpyrimidine (36 mmol, 5.11g), phenyl boronic acid (43 mmol, 5.2 g), Pd(PPh₃)₄ (0.36 mmol, 415 mg), K₂CO₃ (72 mmol, 10 g) were reacted together in EtOH (100 mL) according to the general procedure to afford the title compound as a colourless oil (5.5 g, 83%).

¹H NMR (400 MHz, CDCl₃) δ 8.62 (s, 2H), 8.53 – 8.32 (m, 2H), 7.56 – 7.40 (m, 3H), 2.61 (q, *J* = 7.6 Hz, 2H), 1.26 (t, *J* = 7.7 Hz, 3H). **¹³C NMR** (101 MHz, CDCl₃) δ 162.62, 156.62, 137.73, 134.12, 130.32, 128.54, 127.91, 23.36, 14.89.

Data conforms to literature.¹¹

2-(4-methoxyphenyl)pyrimidine (5d)



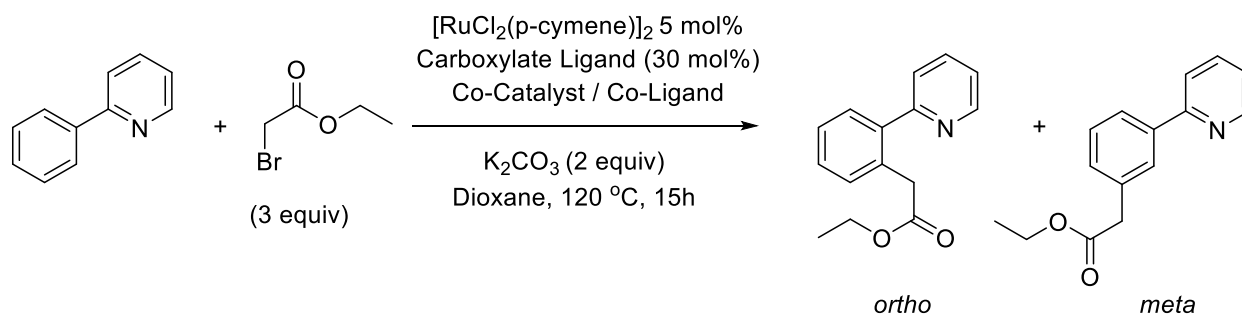
2-chloropyrimidine (50 mmol, 5.7g), 4-methoxyphenyl boronic acid (60 mmol, 9 g), Pd(PPh₃)₄ (0.5 mmol, 578 mg), K₂CO₃ (100 mmol, 13.8 g) were reacted together in EtOH (100 mL) according to the general procedure to afford the title compound as a white crystalline solid (7.44 g, 80%).

¹H NMR (500 MHz, CDCl₃) δ 8.73 (d, *J* = 4.8 Hz, 2H), 8.40 (d, *J* = 9.0 Hz, 2H), 7.09 (t, *J* = 4.8 Hz, 1H), 7.02 – 6.96 (m, 2H), 3.86 (s, 3H). **¹³C NMR** (126 MHz, CDCl₃) δ 164.60, 162.02, 157.23, 130.32, 129.88, 118.43, 114.04, 77.16, 55.45, 11.37. **MP** 52-56 °C

Data conforms to literature.¹¹

Synthesis of *meta*-Substituted Products

Reaction Optimization

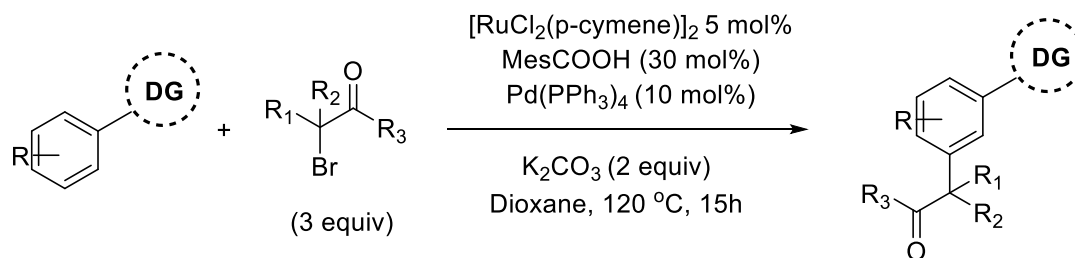


To an oven dried, argon purged carousel tube equipped with magnetic stirrer was added $[\text{RuCl}_2(\text{p-cymene})]_2$ (15 mg, 0.025 mmol), a carboxylate ligand (0.015 mmol), K_2CO_3 (1 mmol, 138 mg), a co-catalyst / co-ligand the substrate molecule (0.5 mmol), ethyl bromoacetate (0.17 mL, 1.5 mmol), and 1,4-Dioxane (2 mL). The carousel tube was then sealed and refluxed on a carousel at 120°C for 15h. After cooling to room temperature the reaction mixture was dry loaded onto silica and a mixed fraction collected by silica gel column chromatography (Hexane / EtOAc).

Ortho / *meta* ratio calculated using the corresponding benzyl peaks: *ortho* δ 3.82 ppm (s, 2H) *meta* δ 3.70 ppm (s, 2H). Major product consistent with *meta* substituted product and is fully characterised in section below. Minor isomer consistent with *ortho* substituted product.¹³ Example spectra shown below.



General procedure for synthesis of *meta* substituted compounds

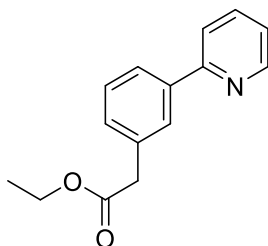


To an oven dried, argon purged carousel tube equipped with magnetic stirrer was added [RuCl₂(p-cymene)]₂ (15 mg, 0.025 mmol), 2,4,6 trimethylbenzoic acid (25 mg, 0.015 mmol), *Pd(PPh₃)₄ (57 mg, 0.05 mmol), K₂CO₃ (1 mmol, 138 mg), the substrate molecule (0.5 mmol), 1,4-Dioxane (2 mL) and the corresponding coupling partner (1.5 mmol). The carousel tube was then sealed and refluxed on a carousel at 120 °C for 15 h. After cooling to room temperature the reaction mixture was dry loaded onto silica and purified by silica gel column chromatography (Hexane / EtOAc).

*Certain reactions did not require the addition of Pd(PPh₃)₄ please refer to individual preparations.

**The following compounds are ordered as per their appearance in the main text

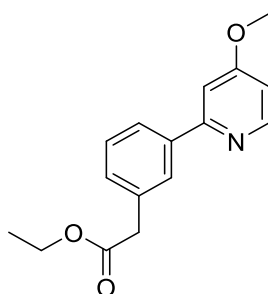
ethyl 2-(3-(pyridin-2-yl)phenyl)acetate (3aa)



2-phenylpyridine (0.5 mmol, 0.07 mL), ethyl bromoacetate (1.5 mmol, 0.17 mL), [RuCl₂(p-cymene)]₂ (5 mol%, 15 mg), Pd(PPh₃)₄ (10 mol%, 57 mg), 2,4,6-Trimethylbenzoic acid (0.15 mmol, 25 mg) and K₂CO₃ (1 mmol, 138 mg) were reacted together in 1,4-Dioxane (2 mL) according to general procedure to afford the title compound as a colourless oil (69 mg, 58%).

¹H NMR (500 MHz, CDCl₃) δ 8.68 (dt, *J* = 4.9, 1.2 Hz, 1H), 7.93 (s, 1H), 7.87 (d, *J* = 7.8 Hz, 1H), 7.75 – 7.69 (m, 2H), 7.43 (t, *J* = 7.7 Hz, 1H), 7.35 (d, *J* = 7.7 Hz, 1H), 7.21 (ddd, *J* = 5.4, 5.0, 2.8 Hz, 1H), 4.15 (q, *J* = 7.1 Hz, 2H), 3.70 (s, 2H), 1.25 (t, *J* = 7.1 Hz, 3H). **¹³C NMR** (126 MHz, CDCl₃) δ 171.56, 157.25, 149.72, 139.77, 136.80, 134.77, 129.92, 129.02, 128.00, 125.70, 122.25, 120.71, 60.96, 41.50, 14.27. **HR-MS** (ESI) *m/z*: calculated for C₁₅H₁₅NO₂ [M+Na]⁺ 264.100048, found: 264.100500 **v_{max}** (neat) / cm⁻¹: 2981, 1729 (C=O), 1584

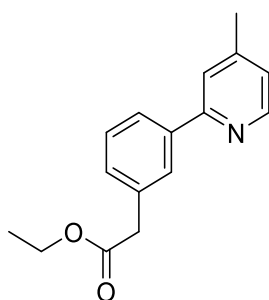
ethyl 2-(3-(4-methoxypyridin-2-yl)phenyl)acetate (3ba)



4-methoxy-2-phenylpyridine (0.5 mmol, 93 mg), ethyl bromoacetate (1.5 mmol, 0.17 mL), $[\text{RuCl}_2(\text{p-cymene})]_2$ (5 mol%, 15 mg), $\text{Pd}(\text{PPh}_3)_4$ (10 mol%, 57 mg), 2,4,6-Trimethylbenzoic acid (0.15 mmol, 25 mg) and K_2CO_3 (1 mmol, 138 mg) were reacted together in 1,4-Dioxane (2 mL) according to general procedure to afford the title compound as a colourless oil (49mg, 36%).

^1H NMR (500 MHz, CDCl_3) δ 8.51 (d, J = 5.7 Hz, 1H), 7.89 (t, J = 1.4 Hz, 1H), 7.86 – 7.81 (m, 1H), 7.42 (t, J = 7.7 Hz, 1H), 7.39 – 7.31 (m, 1H), 7.22 (d, J = 2.4 Hz, 1H), 6.77 (dd, J = 5.7, 2.4 Hz, 1H), 4.16 (q, J = 7.1 Hz, 2H), 3.90 (s, 3H), 3.70 (s, 2H), 1.25 (t, J = 7.1 Hz, 3H). **^{13}C NMR** (126 MHz, CDCl_3) δ 171.63, 166.53, 159.10, 151.00, 139.88, 134.75, 130.03, 129.01, 128.13, 125.81, 108.35, 107.07, 61.02, 55.32, 41.55, 14.32. **HR-MS** (ESI) m/z : calculated for $\text{C}_{16}\text{H}_{17}\text{NO}_3$ $[\text{M}+\text{Na}]^+$ 294.110613 found: 294.110500 ν_{max} (neat) / cm^{-1} : 2980, 1729 (C=O), 1591, 1563

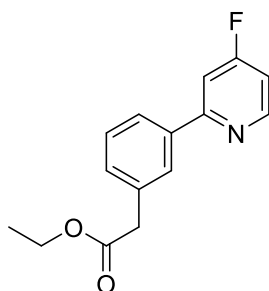
ethyl 2-(3-(4-methylpyridin-2-yl)phenyl)acetate (3ca)



4-methyl-2-phenylpyridine (0.5 mmol, 85 mg), ethyl bromoacetate (1.5 mmol, 0.17 mL), [RuCl₂(p-cymene)]₂ (5 mol%, 15 mg), Pd(PPh₃)₄ (10 mol%, 57 mg), 2,4,6-Trimethylbenzoic acid (0.15 mmol, 25 mg) and K₂CO₃ (1 mmol, 138 mg) were reacted together in 1,4-Dioxane (2 mL) according to general procedure to afford the title compound as a colourless oil (80 mg, 63%).

¹H NMR (500 MHz, CDCl₃) δ 8.53 (d, *J* = 4.9 Hz, 1H), 7.91 (t, *J* = 1.4 Hz, 1H), 7.88 – 7.84 (m, 1H), 7.57 – 7.50 (m, 1H), 7.42 (t, *J* = 7.6 Hz, 1H), 7.36 – 7.30 (m, 1H), 7.08 – 7.02 (m, 1H), 4.16 (q, *J* = 7.1 Hz, 2H), 3.70 (s, 2H), 2.40 (s, 3H), 1.25 (t, *J* = 7.1 Hz, 3H). **¹³C NMR** (126 MHz, CDCl₃) δ 171.65, 157.17, 149.48, 147.85, 139.91, 134.69, 129.80, 128.98, 128.04, 125.75, 123.31, 121.71, 60.98, 41.53, 21.31, 14.29. **HR-MS** (ESI) *m/z*: calculated for C₁₆H₁₇NO₂ [M+Na]⁺ 278.115698, found: 278.117900 *v*_{max} (neat) / cm⁻¹: 2980, 1731 (C=O), 1601

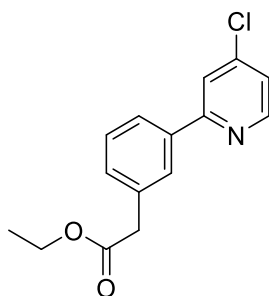
ethyl 2-(3-(4-fluoropyridin-2-yl)phenyl)acetate (3da)



4-fluoro-2-phenylpyridine (0.5 mmol, 87 mg), ethyl bromoacetate (1.5 mmol, 0.17 mL), [RuCl₂(p-cymene)]₂ (5 mol%, 15 mg), Pd(PPh₃)₄ (10 mol%, 57 mg), 2,4,6-Trimethylbenzoic acid (0.15 mmol, 25 mg) and K₂CO₃ (1 mmol, 138 mg) were reacted together in 1,4-Dioxane (2 mL) according to general procedure to afford the title compound as a colourless oil (80 mg, 62%).

¹H NMR (500 MHz, CDCl₃) δ 8.62 (dd, *J* = 8.8, 5.6 Hz, 1H), 7.92 (s, 1H), 7.85 (d, *J* = 7.7 Hz, 1H), 7.45 – 7.40 (m, 2H), 7.37 (d, *J* = 7.6 Hz, 1H), 6.95 (ddd, *J* = 6.4, 5.7, 2.2 Hz, 1H), 4.15 (q, *J* = 7.1 Hz, 2H), 3.69 (s, 2H), 1.24 (t, *J* = 7.1 Hz, 3H). **¹³C NMR** (126 MHz, CDCl₃) δ 171.44, 169.43 (d, *J* = 261.3 Hz), 160.43 (d, *J* = 6.9 Hz), 151.98 (d, *J* = 7.2 Hz), 138.64 (d, *J* = 3.5 Hz), 134.92, 130.61, 129.11, 128.03, 125.72, 110.08 (d, *J* = 16.4 Hz), 108.27 (d, *J* = 17.6 Hz), 61.00, 41.39, 14.25. **¹⁹F NMR** (470 MHz, CDCl₃) δ -102.49 – -102.61 (m). **HR-MS** (ESI) *m/z*: calculated for C₁₅H₁₄NO₂F [M+Na]⁺ 260.108682, found: 260.108000. **v_{max}** (neat) / cm⁻¹: 2981, 1730 (C=O), 1595, 1574

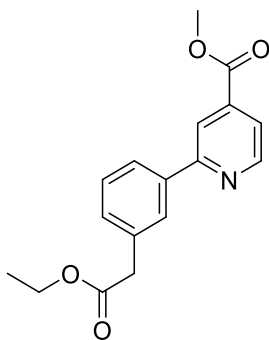
ethyl 2-(3-(4-chloropyridin-2-yl)phenyl)acetate (3ea)



4-chloro-2-phenylpyridine (0.5 mmol, 95 mg), ethyl bromoacetate (1.5 mmol, 0.17 mL), [RuCl₂(p-cymene)]₂ (5 mol%, 15 mg), Pd(PPh₃)₄ (10 mol%, 57 mg), 2,4,6-Trimethylbenzoic acid (0.15 mmol, 25 mg) and K₂CO₃ (1 mmol, 138 mg) were reacted together in 1,4-Dioxane (2 mL) according to general procedure to afford the title compound as a colourless oil (62 mg, 45%).

¹H NMR (500 MHz, CDCl₃) δ 8.57 (dd, *J* = 5.2, 0.5 Hz, 1H), 7.91 (t, *J* = 1.8 Hz, 1H), 7.88 – 7.84 (m, 1H), 7.73 (dd, *J* = 1.9, 0.6 Hz, 1H), 7.44 (t, *J* = 7.7 Hz, 1H), 7.39 – 7.35 (m, 1H), 7.24 (dd, *J* = 5.3, 1.9 Hz, 1H), 4.17 (q, *J* = 7.1 Hz, 2H), 3.70 (s, 2H), 1.26 (t, *J* = 7.1 Hz, 3H). **¹³C NMR** (126 MHz, CDCl₃) δ 171.52, 158.87, 150.61, 144.89, 138.57, 135.00, 130.66, 129.21, 128.13, 125.85, 122.51, 121.08, 61.09, 41.49, 14.32. **HR-MS** (ESI) *m/z*: calculated for C₁₅H₁₄NO₂Cl [M+Na]⁺ 276.079131, found: 276.079800. **ν_{max}** (neat) / cm⁻¹: 2981, 1730 (C=O), 1571, 1560

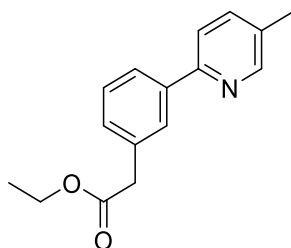
methyl 2-(3-(2-ethoxy-2-oxoethyl)phenyl)isonicotinate (3fa)



methyl 2-phenylisonicotinate (0.5 mmol, 107 mg), ethyl bromoacetate (1.5 mmol, 0.17 mL), $[\text{RuCl}_2(\text{p-cymene})]_2$ (5 mol%, 15 mg), $\text{Pd}(\text{PPh}_3)_4$ (10 mol%, 57 mg), 2,4,6-Trimethylbenzoic acid (0.15 mmol, 25 mg) and K_2CO_3 (1 mmol, 138 mg) were reacted together in 1,4-Dioxane (2 mL) according to general procedure to afford the title compound as a colourless oil (46 mg, 31%).

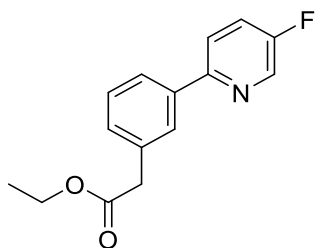
^1H NMR (500 MHz, CDCl_3) δ 8.83 (dd, $J = 5.0, 0.9$ Hz, 1H), 8.29 (dd, $J = 1.5, 0.9$ Hz, 1H), 7.99 (t, $J = 1.8$ Hz, 1H), 7.97 – 7.93 (m, 1H), 7.78 (dd, $J = 5.0, 1.5$ Hz, 1H), 7.46 (t, $J = 7.6$ Hz, 1H), 7.41 – 7.37 (m, 1H), 4.17 (q, $J = 7.1$ Hz, 2H), 4.00 (s, 3H), 3.72 (s, 2H), 1.27 (t, $J = 7.1$ Hz, 3H). **^{13}C NMR** (126 MHz, CDCl_3) δ 171.59, 165.92, 158.35, 150.58, 138.95, 138.34, 135.02, 130.56, 129.25, 128.15, 125.90, 121.38, 119.95, 61.11, 52.91, 41.56, 14.34. **HR-MS** (ESI) m/z : calculated for $\text{C}_{17}\text{H}_{17}\text{NO}_4$ $[\text{M}+\text{H}]^+$ 300.123583, found: 300.122200. ν_{max} (neat) / cm^{-1} : 2980, 1731 (C=O), 1599, 1559

ethyl 2-(3-(5-methylpyridin-2-yl)phenyl)acetate (3ga)



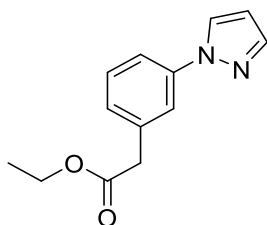
5-methyl-2-phenylpyridine (0.5 mmol, 85 mg), ethyl bromoacetate (1.5 mmol, 0.17 mL), [RuCl₂(p-cymene)]₂ (5 mol%, 15 mg), Pd(PPh₃)₄ (10 mol%, 57 mg), 2,4,6-Trimethylbenzoic acid (0.15 mmol, 25 mg) and K₂CO₃ (1 mmol, 138 mg) were reacted together in 1,4-Dioxane (2 mL) according to general procedure to afford the title compound as a colourless oil (65 mg, 51%).

¹H NMR (500 MHz, CDCl₃) δ 8.50 (s, 1H), 7.90 (s, 1H), 7.84 (d, *J* = 6.8 Hz, 1H), 7.61 (d, *J* = 8.0 Hz, 1H), 7.53 (dd, *J* = 4.4, 3.6 Hz, 1H), 7.41 (dt, *J* = 7.7, 3.6 Hz, 1H), 7.35 – 7.29 (m, 1H), 4.15 (q, *J* = 7.1 Hz, 2H), 3.69 (s, 2H), 2.35 (s, *J* = 3.1 Hz, 3H), 1.24 (t, *J* = 7.1 Hz, 3H). **¹³C NMR** (126 MHz, CDCl₃) δ 171.63, 154.60, 150.13, 139.78, 137.37, 134.70, 131.77, 129.56, 128.97, 127.78, 125.49, 120.20, 60.95, 41.52, 18.24, 14.28. **HR-MS** (ESI) *m/z*: calculated for C₁₆H₁₇NO₂ [M+H]⁺ 256.133754, found: 256.134800 **v_{max}** (neat) / cm⁻¹: 2982, 1730 (C=O), 1599, 1566

ethyl 2-(3-(5-fluoropyridin-2-yl)phenyl)acetate (3ha)

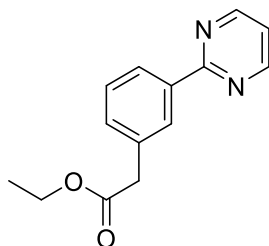
5-fluoro-2-phenylpyridine (0.5 mmol, 87 mg), ethyl bromoacetate (1.5 mmol, 0.17 mL), [RuCl₂(p-cymene)]₂ (5 mol%, 15 mg), Pd(PPh₃)₄ (10 mol%, 57 mg), 2,4,6-Trimethylbenzoic acid (0.15 mmol, 25 mg) and K₂CO₃ (1 mmol, 138 mg) were reacted together in 1,4-Dioxane (2 mL) according to general procedure to afford the title compound as a colourless oil (65 mg, 50%).

¹H NMR (500 MHz, CDCl₃) δ 8.54 (d, *J* = 2.9 Hz, 1H), 7.88 (t, *J* = 1.5 Hz, 1H), 7.84 – 7.79 (m, 1H), 7.72 (ddd, *J* = 8.8, 4.2, 0.4 Hz, 1H), 7.49 – 7.45 (m, 1H), 7.43 (t, *J* = 7.5 Hz, 1H), 4.17 (q, *J* = 7.1 Hz, 2H), 3.70 (s, 3H), 1.26 (t, *J* = 7.1 Hz, 3H). **¹³C NMR** (126 MHz, CDCl₃) δ 171.62, 159.02 (d, *J* = 256.2 Hz), 153.66 (d, *J* = 3.9 Hz), 138.87, 137.90 (d, *J* = 23.5 Hz), 134.93, 129.95, 129.17, 127.95, 125.65, 123.66 (d, *J* = 18.5 Hz), 121.57 (d, *J* = 4.3 Hz), 61.09, 41.54, 14.35. **¹⁹F NMR** (470 MHz, CDCl₃) δ -129.64 – -129.69 (m). **HR-MS** (ESI) *m/z*: calculated for C₁₅H₁₄NO₂F [M+H]⁺ 260.108682, found: 260.108500. **v_{max}** (neat) / cm⁻¹: 2981, 1733 (C=O), 1580

ethyl 2-(3-(1H-pyrazol-1-yl)phenyl)acetate (4aa)

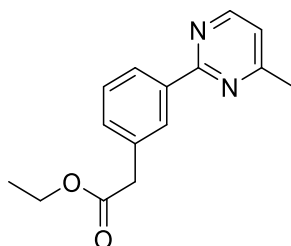
1-phenyl-1H-pyrazole (0.5 mmol, 0.67 mL), ethyl bromoacetate (1.5 mmol, 0.17 mL), [RuCl₂(p-cymene)]₂ (5 mol%, 15 mg), Pd(PPh₃)₄ (10 mol%, 57 mg), 2,4,6-Trimethylbenzoic acid (0.15 mmol, 25 mg) and K₂CO₃ (1 mmol, 138 mg) were reacted together in 1,4-Dioxane (2 mL) according to general procedure to afford the title compound as a colourless oil (60 mg, 52%).

¹H NMR (300 MHz, CDCl₃) δ 7.92 (d, *J* = 2.4 Hz, 1H), 7.71 (d, *J* = 1.5 Hz, 1H), 7.66 (t, *J* = 1.6 Hz, 1H), 7.58 (dd, *J* = 8.1, 1.2 Hz, 1H), 7.40 (t, *J* = 7.8 Hz, 1H), 7.21 (d, *J* = 7.7 Hz, 1H), 6.47 – 6.43 (m, 1H), 4.16 (q, *J* = 7.1 Hz, 2H), 3.67 (s, 2H), 1.25 (t, *J* = 7.1 Hz, 3H). **¹³C NMR** (75 MHz, CDCl₃) δ 171.26, 141.20, 140.41, 135.75, 129.67, 127.45, 126.90, 120.29, 117.90, 107.74, 61.14, 41.33, 14.28. **HR-MS** (ESI) *m/z*: calculated for C₁₃H₁₄N₂O₂ [M+Na]⁺ 253.095297, found: 253.096000. **v_{max}** (neat) / cm⁻¹: 2981, 1729 (C=O), 1609, 1594

ethyl 2-(3-(pyrimidin-2-yl)phenyl)acetate (5aa)

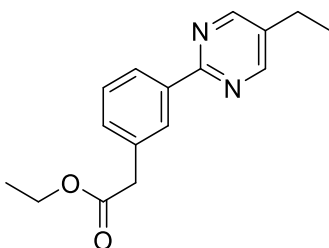
2-phenylpyrimidine (0.5 mmol, 78 mg), ethyl bromoacetate (1.5 mmol, 0.17 mL), [RuCl₂(p-cymene)]₂ (5 mol%, 15 mg), Pd(PPh₃)₄ (10 mol%, 57 mg), 2,4,6-Trimethylbenzoic acid (0.15 mmol, 25 mg) and K₂CO₃ (1 mmol, 138 mg) were reacted together in 1,4-Dioxane (2 mL) according to general procedure to afford the title compound as a colourless oil (80 mg, 66%).

¹H NMR (500 MHz, CDCl₃) δ 8.79 (d, *J* = 4.8 Hz, 2H), 8.37 (d, *J* = 0.5 Hz, 1H), 8.35 (ddd, *J* = 7.4, 1.6 Hz, 1H), 7.48 – 7.41 (m, 2H), 7.17 (t, *J* = 4.8 Hz, 1H), 4.16 (q, *J* = 7.1 Hz, 2H), 3.71 (s, 2H), 1.24 (t, *J* = 7.1 Hz, 3H). **¹³C NMR** (126 MHz, CDCl₃) δ 171.57, 164.61, 157.32, 137.95, 134.69, 131.79, 129.21, 128.95, 127.02, 119.26, 60.99, 41.46, 14.29. **HR-MS** (ESI) *m/z*: calculated for C₁₄H₁₄N₂O₂ [M+H]⁺ 243.113353, found: 243.112100 **v_{max}** (neat) / cm⁻¹: 2981, 1730 (C=O), 1568, 1556

ethyl 2-(3-(4-methylpyrimidin-2-yl)phenyl)acetate (5ba)

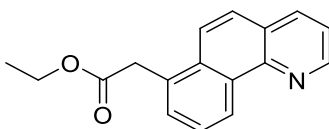
4-methyl-2-phenylpyrimidine (0.5 mmol, 85 mg), ethyl bromoacetate (1.5 mmol, 0.17 mL), [RuCl₂(p-cymene)]₂ (5 mol%, 15 mg), Pd(PPh₃)₄ (10 mol%, 57 mg), 2,4,6-Trimethylbenzoic acid (0.15 mmol, 25 mg) and K₂CO₃ (1 mmol, 138 mg) were reacted together in 1,4-Dioxane (2 mL) according to general procedure to afford the title compound as a colourless oil (95 mg, 74%).

¹H NMR (500 MHz, CDCl₃) δ 8.62 (d, *J* = 5.1 Hz, 1H), 8.37 – 8.36 (m, 1H), 8.34 (ddd, *J* = 7.4, 1.6 Hz, 1H), 7.47 – 7.39 (m, 2H), 7.02 (d, *J* = 5.2 Hz, 1H), 4.15 (q, *J* = 7.1 Hz, 2H), 3.71 (s, 2H), 2.56 (s, 3H), 1.24 (t, *J* = 7.1 Hz, 3H). **¹³C NMR** (126 MHz, CDCl₃) δ 171.59, 167.32, 164.18, 156.84, 138.21, 134.53, 131.50, 129.18, 128.83, 127.02, 118.74, 60.94, 41.47, 24.46, 14.27. **HR-MS** (ESI) *m/z*: calculated for C₁₅H₁₆N₂O₂ [M+Na]⁺ 279.110947, found: 279.110100. **v_{max}** (neat) / cm⁻¹: 2981, 1731 (C=O), 1573, 1554

ethyl 2-(3-(5-ethylpyrimidin-2-yl)phenyl)acetate (5ca)

5-ethyl-2-phenylpyrimidine (0.5 mmol, 92 mg), ethyl bromoacetate (1.5 mmol, 0.17 mL), [RuCl₂(p-cymene)]₂ (5 mol%, 15 mg), Pd(PPh₃)₄ (10 mol%, 57 mg), 2,4,6-Trimethylbenzoic acid (0.15 mmol, 25 mg) and K₂CO₃ (1 mmol, 138 mg) were reacted together in 1,4-Dioxane (2 mL) according to general procedure to afford the title compound as a colourless oil (80 mg, 59%).

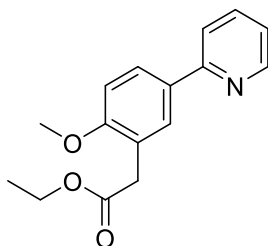
¹H NMR (500 MHz, CDCl₃) δ 8.62 (d, *J* = 3.5 Hz, 2H), 8.34 – 8.32 (m, *J* = 1.5 Hz, 1H), 8.31 (ddd, *J* = 7.6, 1.5 Hz, 1H), 7.44 (t, *J* = 7.6 Hz, 1H), 7.39 (ddd, *J* = 7.6, 1.5 Hz, 1H), 4.15 (q, *J* = 7.1 Hz, 2H), 3.70 (s, 2H), 2.65 (q, *J* = 7.6 Hz, 2H), 1.28 (t, *J* = 7.6 Hz, 3H), 1.24 (t, *J* = 7.1 Hz, 3H). **¹³C NMR** (126 MHz, CDCl₃) δ 171.56, 162.49, 156.71, 138.02, 134.60, 134.33, 131.31, 128.92, 128.87, 126.71, 60.93, 41.46, 23.49, 15.03, 14.27. **HR-MS** (ESI) *m/z*: calculated for C₁₆H₁₈N₂O₂ [M+Na]⁺ 293.126598, found: 293.127600. **v_{max}** (neat) / cm⁻¹: 2971, 1731 (C=O), 1586, 1544

ethyl 2-(benzo[h]quinolin-7-yl)acetate (6aa)

benzo[h]quinoline (0.5 mmol, 90 mg), ethyl bromoacetate (1.5 mmol, 0.17 mL), [RuCl₂(p-cymene)]₂ (5 mol%, 15 mg), Pd(PPh₃)₄ (10 mol%, 57 mg), 2,4,6-Trimethylbenzoic acid (0.15 mmol, 25 mg) and K₂CO₃ (1 mmol, 138 mg) were reacted together in 1,4-Dioxane (2 mL) according to general procedure to afford the title compound as a white solid (60 mg, 45%). Recrystallization using dichloromethane and 60:40 petroleum ether afforded crystals suitable for X-Ray analysis.

¹H NMR (500 MHz, CDCl₃) δ 9.33 (d, *J* = 8.2 Hz, 1H), 9.01 (dd, *J* = 4.4, 1.8 Hz, 1H), 8.17 (dd, *J* = 8.0, 1.8 Hz, 1H), 8.02 (d, *J* = 9.1 Hz, 1H), 7.74 (d, *J* = 9.2 Hz, 1H), 7.70 (dd, *J* = 8.2, 7.2 Hz, 1H), 7.63 (dd, *J* = 7.1, 1.2 Hz, 1H), 7.52 (dd, *J* = 8.0, 4.4 Hz, 1H), 4.16 (q, *J* = 7.1 Hz, 2H), 4.13 (s, 2H), 1.22 (t, *J* = 7.1 Hz, 3H). **¹³C NMR** (126 MHz, CDCl₃) δ 171.59, 149.11, 146.83, 135.83, 132.34, 132.20, 130.87, 130.54, 126.82, 126.01, 125.83, 124.34, 123.60, 122.01, 77.16, 61.16, 39.64, 14.29. **HR-MS** (ESI) *m/z*: calculated for C₁₇H₁₅NO₂ [M+H]⁺ 266.118104, found: 266.117500. **v_{max}** (neat) / cm⁻¹: 2985, 1725 (C=O), 1590. **MP**: (from CH₂Cl₂) 95-96 °C

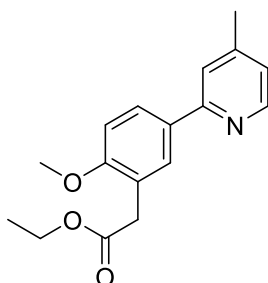
ethyl 2-(2-methoxy-5-(pyridin-2-yl)phenyl)acetate (3ka)



2-(4-methoxyphenyl)pyridine (0.5 mmol, 93 mg), ethyl bromoacetate (1.5 mmol, 0.17 mL), $[\text{RuCl}_2(\text{p-cymene})]_2$ (5 mol%, 15 mg), $\text{Pd}(\text{PPh}_3)_4$ (10 mol%, 57 mg), 2,4,6-Trimethylbenzoic acid (0.15 mmol, 25 mg) and K_2CO_3 (1 mmol, 138 mg) were reacted together in 1,4-Dioxane (2 mL) according to general procedure to afford the title compound as a colourless oil (56 mg, 41%).

^1H NMR (500 MHz, CDCl_3) δ 8.64 (ddd, $J = 4.8, 1.8, 1.1$ Hz, 1H), 7.90 (dd, $J = 8.5, 2.4$ Hz, 1H), 7.87 (d, $J = 2.3$ Hz, 1H), 7.72 – 7.66 (m, 2H), 7.16 (ddd, $J = 7.1, 4.8, 1.5$ Hz, 1H), 6.96 (d, $J = 8.5$ Hz, 1H), 4.17 (q, $J = 7.1$ Hz, 2H), 3.87 (s, 3H), 3.70 (s, 2H), 1.25 (t, $J = 7.1$ Hz, 3H). **^{13}C NMR** (126 MHz, CDCl_3) δ 171.82, 158.64, 157.15, 149.63, 136.74, 131.92, 129.76, 127.25, 123.72, 121.54, 119.99, 110.71, 60.75, 55.75, 36.39, 14.38. **HR-MS** (ESI) m/z : calculated for $\text{C}_{16}\text{H}_{17}\text{NO}_3$ $[\text{M}+\text{Na}]^+$ 294.110613, found: 294.112700. ν_{max} (neat) / cm^{-1} : 2978, 1732 (C=O), 1610, 1564

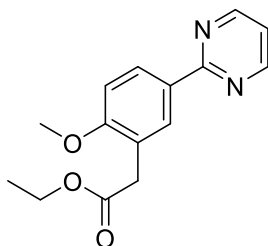
ethyl 2-(2-methoxy-5-(4-methylpyridin-2-yl)phenyl)acetate (3la)



2-(4-methoxyphenyl)-4-methylpyridine (0.5 mmol, 100 mg), ethyl bromoacetate (1.5 mmol, 0.17 mL), $[\text{RuCl}_2(\text{p-cymene})]_2$ (5 mol%, 15 mg), $\text{Pd}(\text{PPh}_3)_4$ (10 mol%, 57 mg), 2,4,6-Trimethylbenzoic acid (0.15 mmol, 25 mg) and K_2CO_3 (1 mmol, 138 mg) were reacted together in 1,4-Dioxane (2 mL) according to general procedure to afford the title compound as a colourless oil (70 mg, 49%).

^1H NMR (500 MHz, CDCl_3) δ 8.49 (d, $J = 5.0$ Hz, 1H), 7.89 (dd, $J = 8.5, 2.3$ Hz, 1H), 7.85 (d, $J = 2.3$ Hz, 1H), 7.52 – 7.46 (m, 1H), 6.99 (dd, $J = 5.0, 0.8$ Hz, 1H), 6.95 (d, $J = 8.6$ Hz, 1H), 4.16 (q, $J = 7.1$ Hz, 2H), 3.87 (s, 3H), 3.69 (s, 2H), 2.39 (s, 3H), 1.25 (t, $J = 7.1$ Hz, 3H). **^{13}C NMR** (126 MHz, CDCl_3) δ 171.85, 158.52, 157.01, 149.37, 147.69, 132.01, 129.76, 127.24, 123.61, 122.61, 120.92, 110.66, 60.74, 55.74, 36.38, 21.35, 14.37. **HR-MS** (ESI) m/z : calculated for $\text{C}_{17}\text{H}_{19}\text{NO}_3$ $[\text{M}+\text{H}]^+$ 308.126263, found: 308.125900. ν_{max} (neat) / cm^{-1} : 2978, 1733 (C=O), 1604, 1559

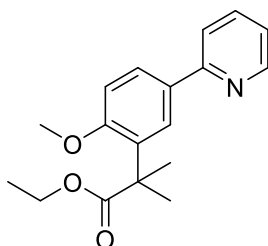
ethyl 2-(2-methoxy-5-(pyrimidin-2-yl)phenyl)acetate (5da)



2-(4-methoxyphenyl)pyrimidine (0.5 mmol, 93 mg), ethyl bromoacetate (1.5 mmol, 0.17 mL), $[\text{RuCl}_2(\text{p-cymene})]_2$ (5 mol%, 15 mg), $\text{Pd}(\text{PPh}_3)_4$ (10 mol%, 57 mg), 2,4,6-Trimethylbenzoic acid (0.15 mmol, 25 mg) and K_2CO_3 (1 mmol, 138 mg) were reacted together in 1,4-Dioxane (2 mL) according to general procedure to afford the title compound as a colourless oil (75 mg, 55%).

^1H NMR (500 MHz, CDCl_3) δ 8.73 (d, J = 4.8 Hz, 2H), 8.37 (dd, J = 8.6, 2.3 Hz, 1H), 8.29 (d, J = 2.2 Hz, 1H), 7.09 (t, J = 4.8 Hz, 1H), 6.96 (d, J = 8.6 Hz, 1H), 4.16 (q, J = 7.1 Hz, 2H), 3.88 (s, 3H), 3.70 (s, 2H), 1.24 (t, J = 7.1 Hz, 3H). **^{13}C NMR** (126 MHz, CDCl_3) δ 171.67, 164.45, 160.04, 157.17, 131.08, 130.02, 128.99, 123.53, 118.43, 110.40, 60.68, 55.70, 36.34, 14.31. **HR-MS** (ESI) m/z : calculated for $\text{C}_{15}\text{H}_{16}\text{N}_2\text{O}_3$ $[\text{M}+\text{H}]^+$ 273.123917, found: 273.122300. ν_{max} (neat) / cm^{-1} : 2978, 1730 (C=O), 1608, 1591

ethyl 2-(2-methoxy-5-(pyridin-2-yl)phenyl)-2-methylpropanoate (3kb)

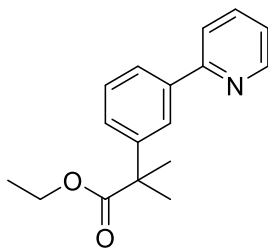


2-(4-methoxyphenyl)pyridine (0.5 mmol, 93 mg), ethyl 2-bromo-2-methylpropanoate (1.5 mmol, 0.22 mL), $[\text{RuCl}_2(\text{p-cymene})]_2$ (5 mol%, 15 mg), 2,4,6-Trimethylbenzoic acid (0.15 mmol, 25 mg) and K_2CO_3 (1 mmol, 138 mg) were reacted together in 1,4-Dioxane (2 mL) according to general procedure to afford the title compound as a colourless oil (120 mg, 80%).

^1H NMR (500 MHz, CDCl_3) δ 8.66 (ddd, J = 4.9, 1.6, 1.0 Hz, 1H), 7.99 (d, J = 2.2 Hz, 1H), 7.85 (dd, J = 8.5, 2.3 Hz, 1H), 7.74 – 7.70 (m, 1H), 7.68 (ddd, J = 8.0, 1.2 Hz, 1H), 7.17 (ddd, J = 7.0, 4.9, 1.4 Hz, 1H), 6.93 (d, J = 8.5 Hz, 1H), 4.11 (q, J = 7.1 Hz, 2H), 3.81 (s, 3H), 1.59 (s, 6H), 1.15 (t, J = 7.1 Hz, 3H). **^{13}C NMR** (126 MHz, CDCl_3) δ 177.86, 157.76, 157.57, 149.62, 136.69, 134.63, 131.97, 126.57, 124.61, 121.46, 120.08, 110.92, 60.40, 55.34, 44.55, 25.75, 14.30.

Data conforms to literature.⁶

ethyl 2-methyl-2-(3-(pyridin-2-yl)phenyl)propanoate(3ab)

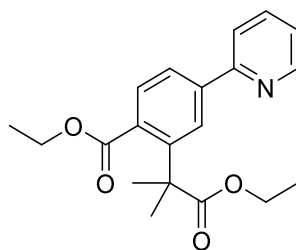


2-Phenylpyridine (0.5 mmol, 0.07 mL), ethyl 2-bromo-2-methylpropanoate (1.5 mmol, 0.22 mL), [RuCl₂(p-cymene)]₂ (5 mol%, 15 mg), 2,4,6-Trimethylbenzoic acid (0.15 mmol, 25 mg) and K₂CO₃ (1 mmol, 138 mg) were reacted together in 1,4-Dioxane (2 mL) according to general procedure to afford the title compound as a colourless oil (95 mg, 71%).

¹H NMR (500 MHz, CDCl₃) δ 8.69 (ddd, *J* = 4.9, 1.7, 1.0 Hz, 1H), 7.99 (dd, *J* = 1.9 Hz, 1H), 7.86 – 7.83 (m, 1H), 7.77 – 7.74 (m, 1H), 7.71 (ddd, *J* = 8.0, 1.1 Hz, 1H), 7.43 (dd, *J* = 7.7 Hz, 1H), 7.40 – 7.37 (m, 1H), 7.23 (ddd, *J* = 7.3, 4.9, 1.3 Hz, 1H), 4.13 (q, *J* = 7.1 Hz, 2H), 1.64 (s, 6H), 1.18 (t, *J* = 7.1 Hz, 3H). **¹³C NMR** (126 MHz, CDCl₃) δ 176.80, 157.50, 149.54, 145.50, 139.34, 137.05, 128.87, 126.72, 125.45, 124.36, 122.27, 120.92, 60.96, 46.73, 26.70, 14.18. **HR-MS** (ESI) *m/z*: calculated for C₁₇H₁₉NO₂ [M+H]⁺ 270.149404, found: 270.150600. **v_{max}** (neat) / cm⁻¹: 2978, 1723 (C=O), 1585, 1566

Data conforms to literature.⁶

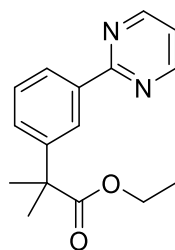
ethyl 2-(1-ethoxy-2-methyl-1-oxopropan-2-yl)-4-(pyridin-2-yl)benzoate (3pb)



ethyl 4-(pyridin-2-yl)benzoate (0.5 mmol, 114 mg), ethyl 2-bromo-2-methylpropanoate (1.5 mmol, 0.22 mL), [RuCl₂(p-cymene)]₂ (5 mol%, 15 mg), 2,4,6-Trimethylbenzoic acid (0.15 mmol, 25 mg) and K₂CO₃ (1 mmol, 138 mg) were reacted together in 1,4-Dioxane (2 mL) according to general procedure to afford the title compound as a colourless oil (39 mg, 23%).

¹H NMR (500 MHz, CDCl₃) δ 8.74 – 8.72 (m, 1H), 8.22 (d, *J* = 1.7 Hz, 1H), 7.98 (d, *J* = 8.1 Hz, 1H), 7.87 (dd, *J* = 8.1, 1.7 Hz, 1H), 7.81 – 7.74 (m, 2H), 7.30 – 7.26 (m, 1H), 4.31 (q, *J* = 7.1 Hz, 2H), 4.11 (q, *J* = 7.1 Hz, 2H), 1.72 (s, 6H), 1.38 (t, *J* = 7.2 Hz, 3H), 1.17 (t, *J* = 7.1 Hz, 3H). **¹³C NMR** (126 MHz, CDCl₃) δ 177.01, 168.20, 156.65, 149.98, 146.04, 142.42, 136.96, 131.63, 130.52, 125.62, 124.81, 122.84, 121.13, 61.25, 60.65, 47.24, 28.07, 14.29, 14.13. **HR-MS** (ESI) *m/z*. calculated for C₂₀H₂₃NO₄ [M+H]⁺ 342.170533, found: 342.170800. **v_{max}** (neat) / cm⁻¹: 2980, 1720 (C=O), 1608, 1587

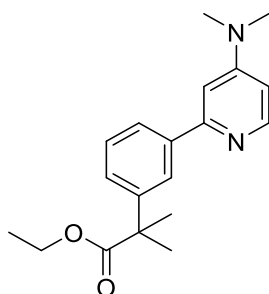
ethyl 2-methyl-2-(3-(pyrimidin-2-yl)phenyl)propanoate (5ab)



2-phenylpyrimidine (0.5 mmol, 78 mg), ethyl 2-bromo-2-methylpropanoate (1.5 mmol, 0.22 mL), $[\text{RuCl}_2(\text{p-cymene})]_2$ (5 mol%, 15 mg), 2,4,6-Trimethylbenzoic acid (0.15 mmol, 25 mg) and K_2CO_3 (1 mmol, 138 mg) were reacted together in 1,4-Dioxane (2 mL) according to general procedure to afford the title compound as a colourless oil (80 mg, 59%).

^1H NMR (500 MHz, CDCl_3) δ 8.80 (d, $J = 4.8$ Hz, 2H), 8.51 – 8.46 (m, 1H), 8.32 (ddd, $J = 6.3, 2.4, 1.7$ Hz, 1H), 7.49 – 7.40 (m, 2H), 7.18 (t, $J = 4.8$ Hz, 1H), 4.14 (q, $J = 7.1$ Hz, 2H), 1.66 (s, 6H), 1.18 (t, $J = 7.1$ Hz, 3H). **^{13}C NMR** (126 MHz, CDCl_3) δ 176.83, 164.86, 157.34, 145.45, 137.78, 128.74, 128.54, 126.65, 125.50, 119.21, 60.97, 46.79, 26.74, 14.19. **HR-MS** (ESI) m/z : calculated for $\text{C}_{16}\text{H}_{18}\text{N}_2\text{O}_2$ $[\text{M}+\text{H}]^+$ 271.144653, found: 271.144100. ν_{max} (neat) / cm^{-1} : 2977, 1724 (C=O), 1568, 1554

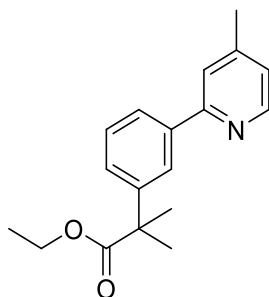
ethyl 2-(3-(4-(dimethylamino)pyridin-2-yl)phenyl)-2-methylpropanoate (3vb)



N,N-dimethyl-2-phenylpyridin-4-amine (0.5 mmol, 99 mg), ethyl 2-bromo-2-methylpropanoate (1.5 mmol, 0.22 mL), [RuCl₂(p-cymene)]₂ (5 mol%, 15 mg), 2,4,6-Trimethylbenzoic acid (0.15 mmol, 25 mg) and K₂CO₃ (1 mmol, 138 mg) were reacted together in 1,4-Dioxane (2 mL) according to general procedure to afford the title compound as a colourless oil (87 mg, 56%).

¹H NMR (500 MHz, CDCl₃) δ 8.32 (d, *J* = 6.0 Hz, 1H), 7.91 (dd, *J* = 1.8 Hz, 1H), 7.75 (ddd, *J* = 7.4, 1.5 Hz, 1H), 7.39 (dd, *J* = 7.6 Hz, 1H), 7.36 – 7.33 (m, 1H), 6.85 (d, *J* = 2.5 Hz, 1H), 6.47 (dd, *J* = 6.0, 2.6 Hz, 1H), 4.12 (q, *J* = 7.1 Hz, 2H), 3.04 (s, 6H), 1.63 (s, 6H), 1.18 (t, *J* = 7.1 Hz, 3H). **¹³C NMR** (126 MHz, CDCl₃) δ 176.91, 158.19, 155.14, 149.64, 145.18, 140.90, 128.54, 126.16, 125.55, 124.46, 105.53, 103.93, 60.87, 46.72, 39.33, 26.71, 14.17. **HR-MS** (ESI) *m/z*: calculated for C₁₉H₂₄N₂O₂ [M+H]⁺ 313.1994, found: 313.2012. **ν_{max}** (neat) / cm⁻¹: 2977, 1723 (C=O), 1594, 1541

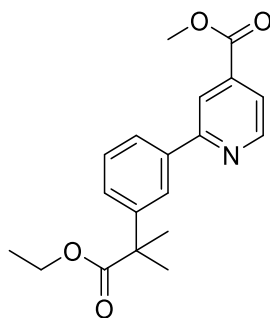
ethyl 2-methyl-2-(3-(4-methylpyridin-2-yl)phenyl)propanoate (3cb)



4-methyl-2-phenylpyridine (0.5 mmol, 85 mg), ethyl 2-bromo-2-methylpropanoate (1.5 mmol, 0.22 mL), [RuCl₂(p-cymene)]₂ (5 mol%, 15 mg), 2,4,6-Trimethylbenzoic acid (0.15 mmol, 25 mg) and K₂CO₃ (1 mmol, 138 mg) were reacted together in 1,4-Dioxane (2 mL) according to general procedure to afford the title compound as a colourless oil (106 mg, 56%).

¹H NMR (500 MHz, CDCl₃) δ 8.54 (d, *J* = 5.0 Hz, 1H), 7.96 (s, 1H), 7.83 (d, *J* = 7.4 Hz, 1H), 7.51 (s, 1H), 7.44 – 7.35 (m, 2H), 7.05 (d, *J* = 4.9 Hz, 1H), 4.13 (q, *J* = 7.1 Hz, 2H), 2.41 (s, 3H), 1.64 (s, 6H), 1.18 (t, *J* = 7.1 Hz, 3H). **¹³C NMR** (126 MHz, CDCl₃) δ 176.85, 157.58, 149.53, 147.79, 145.36, 139.78, 128.76, 126.44, 125.45, 124.34, 123.24, 121.76, 60.93, 46.73, 26.71, 21.33, 14.17. **HR-MS** (ESI) *m/z*: calculated for C₁₈H₂₁NO₂ [M+Na]⁺ 306.146999, found: 306.146900. **ν_{max}** (neat) / cm⁻¹: 2977, 1723 (C=O), 1599, 1559

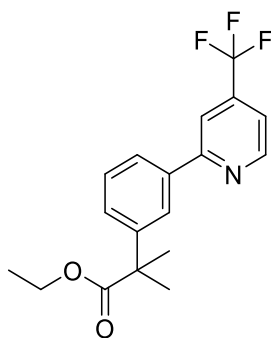
methyl 2-(3-(1-ethoxy-2-methyl-1-oxopropan-2-yl)phenyl)isonicotinate (3fb)



4-methyl-2-phenylpyridine (0.5 mmol, 107 mg), ethyl 2-bromo-2-methylpropanoate (1.5 mmol, 0.22 mL), [RuCl₂(p-cymene)]₂ (5 mol%, 15 mg), 2,4,6-Trimethylbenzoic acid (0.15 mmol, 25 mg) and K₂CO₃ (1 mmol, 138 mg) were reacted together in 1,4-Dioxane (2 mL) according to general procedure to afford the title compound as a colourless oil (90 mg, 55%).

¹H NMR (500 MHz, CDCl₃) δ 8.79 (d, *J* = 5.0 Hz, 1H), 8.23 (s, 1H), 8.04 (s, *J* = 1.8 Hz, 1H), 7.87 (ddd, *J* = 6.9, 1.9 Hz, 1H), 7.72 (dd, *J* = 5.0, 1.4 Hz, 1H), 7.44 – 7.36 (m, 2H), 4.12 (q, *J* = 7.1 Hz, 2H), 3.94 (s, 3H), 1.63 (s, 6H), 1.16 (t, *J* = 7.1 Hz, 3H). **¹³C NMR** (126 MHz, CDCl₃) δ 176.56, 165.72, 158.47, 150.43, 145.57, 138.63, 138.14, 128.85, 127.03, 125.38, 124.32, 121.13, 119.74, 77.16, 60.87, 52.70, 46.65, 26.61, 14.07. **HR-MS** (ESI) *m/z*: calculated for C₁₉H₂₁NO₄ [M+H]⁺ 328.154883, found: 328.154800. **v_{max}** (neat) / cm⁻¹: 2978, 1726 (C=O), 1597, 1558

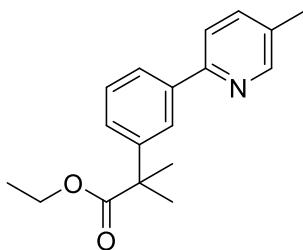
ethyl 2-methyl-2-(3-(4-(trifluoromethyl)pyridin-2-yl)phenyl)propanoate (3wb)



2-phenyl-4-(trifluoromethyl)pyridine (0.5 mmol, 112 mg), ethyl 2-bromo-2-methylpropanoate (1.5 mmol, 0.22 mL), [RuCl₂(p-cymene)]₂ (5 mol%, 15 mg), 2,4,6-Trimethylbenzoic acid (0.15 mmol, 25 mg) and K₂CO₃ (1 mmol, 138 mg) were reacted together in 1,4-Dioxane (2 mL) according to general procedure to afford the title compound as a colourless oil (67 mg, 40%).

¹H NMR (500 MHz, CDCl₃) δ 8.86 (d, *J* = 5.0 Hz, 1H), 8.06 – 8.04 (m, 1H), 7.90 – 7.89 (m, 1H), 7.87 (ddd, *J* = 5.6, 3.5, 1.8 Hz, 1H), 7.49 – 7.42 (m, 3H), 4.15 (q, *J* = 7.1 Hz, 2H), 1.66 (s, 6H), 1.19 (t, *J* = 7.1 Hz, 3H). **¹³C NMR** (126 MHz, CDCl₃) δ 176.63, 158.97, 150.75, 145.87, 139.20 (q, *J* = 33.9 Hz) 138.29, 129.06, 127.52, 125.50, 124.53, 123.07 (q, *J* = 273.3 Hz), 117.63 (q, *J* = 3.4 Hz), 116.21 (q, *J* = 3.7 Hz), 61.02, 46.76, 26.69, 14.16. **¹⁹F NMR** (470 MHz, CDCl₃) δ -64.84 (s). **HR-MS** (ESI) *m/z*: calculated for C₁₈H₁₈NO₂F₃ [M+H]⁺ 338.136788, found: 338.136897. **ν_{max}** (neat) / cm⁻¹: 2978, 1726 (C=O), 1603, 1568

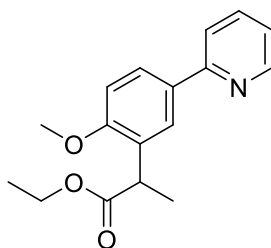
ethyl 2-methyl-2-(3-(5-methylpyridin-2-yl)phenyl)propanoate (3gb)



5-methyl-2-phenylpyridine (0.5 mmol, 85 mg), ethyl 2-bromo-2-methylpropanoate (1.5 mmol, 0.22 mL), [RuCl₂(p-cymene)]₂ (5 mol%, 15 mg), 2,4,6-Trimethylbenzoic acid (0.15 mmol, 25 mg) and K₂CO₃ (1 mmol, 138 mg) were reacted together in 1,4-Dioxane (2 mL) according to general procedure to afford the title compound as a colourless oil (76 mg, 54%).

¹H NMR (500 MHz, CDCl₃) δ 8.52 (dd, *J* = 1.4, 0.7 Hz, 1H), 7.96 (dd, *J* = 1.8 Hz, 1H), 7.84 – 7.79 (m, 1H), 7.60 (d, *J* = 7.9 Hz, 1H), 7.57 – 7.52 (m, 1H), 7.41 (dd, *J* = 7.7 Hz, 1H), 7.36 (ddd, *J* = 7.8, 1.8, 1.3 Hz, 1H), 4.13 (q, *J* = 7.1 Hz, 3H), 2.37 (s, 3H), 1.64 (s, 6H), 1.18 (t, *J* = 7.1 Hz, 3H). **¹³C NMR** (126 MHz, CDCl₃) δ 176.89, 155.04, 150.22, 145.42, 139.69, 137.37, 131.72, 128.80, 126.26, 125.22, 124.13, 120.30, 60.96, 46.77, 26.74, 18.30, 14.21. **HR-MS** (ESI) *m/z*: calculated for C₁₈H₂₁NO₂ [M+Na]⁺ 306.146999, found: 306.146000. **v_{max}** (neat) / cm⁻¹: 2977, 1725 (C=O), 1600, 1566

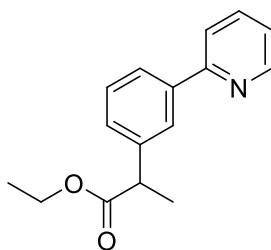
ethyl 2-(2-methoxy-5-(pyridin-2-yl)phenyl)propanoate (3kc)



2-(4-methoxyphenyl)pyridine (0.5 mmol, 93 mg), ethyl 2-bromopropanoate (1.5 mmol, 0.22 mL), [RuCl₂(p-cymene)]₂ (5 mol%, 15 mg), 2,4,6-Trimethylbenzoic acid (0.15 mmol, 25 mg) and K₂CO₃ (1 mmol, 138 mg) were reacted together in 1,4-Dioxane (2 mL) according to general procedure to afford the title compound as a colourless oil (83 mg, 58%).

¹H NMR (500 MHz, CDCl₃) δ 8.63 (d, *J* = 4.3 Hz, 1H), 7.89 (dd, *J* = 8.4, 2.3 Hz, 1H), 7.88 (d, *J* = 2.2 Hz, 1H), 7.71 – 7.67 (m, 1H), 7.65 (d, *J* = 7.9 Hz, 1H), 7.15 (ddd, *J* = 7.0, 4.9, 1.3 Hz, 1H), 6.94 (d, *J* = 8.4 Hz, 1H), 4.13 (q, *J* = 7.1 Hz, 2H), 4.04 (q, *J* = 7.2 Hz, 1H), 3.84 (s, 3H), 1.51 (d, *J* = 7.2 Hz, 3H), 1.18 (t, *J* = 7.1 Hz, 3H). **¹³C NMR** (126 MHz, CDCl₃) δ 175.01, 157.88, 157.13, 149.42, 136.95, 130.13, 127.07, 126.93, 121.56, 120.13, 110.91, 60.64, 55.71, 40.04, 17.36, 14.35. **HR-MS** (ESI) *m/z*: calculated for C₁₇H₁₉NO₃ [M+Na]⁺ 308.126263, found: 308.128100. **v_{max}** (neat) / cm⁻¹: 2978, 1727 (C=O), 1607, 1586

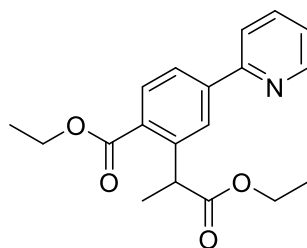
ethyl 2-(3-(pyridin-2-yl)phenyl)propanoate (3ac)



2-Phenylpyridine (0.5 mmol, 0.07 mL), ethyl 2-bromopropanoate (1.5 mmol, 0.22 mL), [RuCl₂(p-cymene)]₂ (5 mol%, 15 mg), 2,4,6-Trimethylbenzoic acid (0.15 mmol, 25 mg) and K₂CO₃ (1 mmol, 138 mg) were reacted together in 1,4-Dioxane (2 mL) according to general procedure to afford the title compound as a colourless oil (70 mg, 55%).

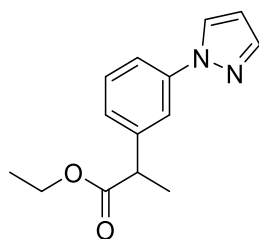
¹H NMR (500 MHz, CDCl₃) δ 8.67 (dd, *J* = 4.6, 1.2 Hz, 1H), 7.93 (s, 1H), 7.85 (dd, *J* = 7.6, 1.4 Hz, 1H), 7.75 – 7.68 (m, 2H), 7.41 (dd, *J* = 7.6 Hz, 1H), 7.36 (dd, *J* = 7.6, 1.1 Hz, 1H), 7.22 – 7.17 (m, 1H), 4.18 – 4.03 (m, 3H), 3.79 (q, *J* = 7.1 Hz, 1H), 1.54 (dd, *J* = 7.2, 1.0 Hz, 3H), 1.18 (td, *J* = 7.1, 1.1 Hz, 3H). **¹³C NMR** (126 MHz, CDCl₃) δ 174.51, 157.29, 149.68, 141.29, 139.76, 136.76, 129.05, 128.00, 126.35, 125.72, 122.20, 120.69, 60.80, 45.69, 18.77, 14.17. **HR-MS** (ESI) *m/z*: calculated for C₁₆H₁₇NO₂ [M+Na]⁺ 278.115698, found: 278.116500. **v_{max}** (neat) / cm⁻¹: 2980, 1727 (C=O), 1584, 1566

ethyl 2-(1-ethoxy-1-oxopropan-2-yl)-4-(pyridin-2-yl)benzoate (3pc)



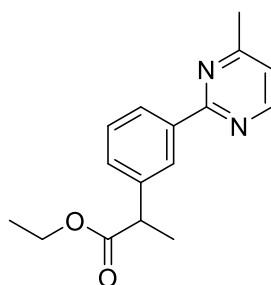
ethyl 4-(pyridin-2-yl)benzoate (0.5 mmol, 114 mg), ethyl 2-bromopropanoate (1.5 mmol, 0.22 mL), $[\text{RuCl}_2(\text{p-cymene})]_2$ (5 mol%, 15 mg), $\text{Pd}(\text{PPh}_3)_4$ (10 mol%, 57 mg), 2,4,6-Trimethylbenzoic acid (0.15 mmol, 25 mg) and K_2CO_3 (1 mmol, 138 mg) were reacted together in 1,4-Dioxane (2 mL) according to general procedure to afford the title compound as a colourless oil (72 mg, 44%).

^1H NMR (500 MHz, CDCl_3) δ 8.73 – 8.70 (m, 1H), 8.02 (dd, J = 4.9, 3.1 Hz, 2H), 7.94 (dd, J = 8.2, 1.8 Hz, 1H), 7.80 – 7.73 (m, 2H), 7.29 – 7.25 (m, 1H), 4.69 (q, J = 7.2 Hz, 1H), 4.38 (qd, J = 7.1, 0.6 Hz, 2H), 4.21 – 4.05 (m, 2H), 1.62 (d, J = 7.2 Hz, 3H), 1.41 (t, J = 7.2 Hz, 3H), 1.19 (t, J = 7.1 Hz, 3H). **^{13}C NMR** (126 MHz, CDCl_3) δ 174.64, 167.46, 156.26, 150.00, 142.87, 142.65, 136.97, 131.40, 130.05, 127.25, 125.27, 122.95, 121.13, 61.28, 60.86, 42.55, 18.49, 14.40, 14.27. **HR-MS** (ESI) m/z : calculated for $\text{C}_{19}\text{H}_{21}\text{NO}_4$ $[\text{M}+\text{H}]^+$ 328.154883, found: 328.156100. ν_{max} (neat) / cm^{-1} : 2981, 1716 (C=O), 1609, 1587

ethyl 2-(3-(1H-pyrazol-1-yl)phenyl)propanoate (4ac)

1-phenyl-1H-pyrazole (0.5 mmol, 0.67 mL), ethyl 2-bromopropanoate (1.5 mmol, 0.22 mL), [RuCl₂(p-cymene)]₂ (5 mol%, 15 mg), 2,4,6-Trimethylbenzoic acid (0.15 mmol, 25 mg) and K₂CO₃ (1 mmol, 138 mg) were reacted together in 1,4-Dioxane (2 mL) according to general procedure to afford the title compound as a colourless oil (55 mg, 45%).

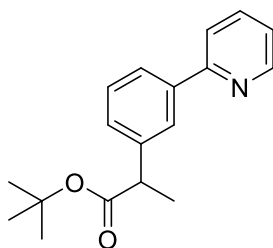
¹H NMR (500 MHz, CDCl₃) δ 7.92 (dd, *J* = 2.5, 0.5 Hz, 1H), 7.71 (d, *J* = 1.4 Hz, 1H), 7.67 (t, *J* = 1.9 Hz, 1H), 7.57 (ddd, *J* = 8.1, 2.2, 1.0 Hz, 1H), 7.39 (t, *J* = 7.9 Hz, 1H), 7.25 – 7.21 (m, 1H), 6.46 (dd, *J* = 2.4, 1.8 Hz, 1H), 4.18 – 4.07 (m, 2H), 3.77 (q, *J* = 7.2 Hz, 1H), 1.54 (d, *J* = 7.2 Hz, 3H), 1.21 (t, *J* = 7.1 Hz, 3H). **¹³C NMR** (126 MHz, CDCl₃) δ 174.22, 142.39, 141.20, 140.52, 129.73, 126.94, 125.65, 118.74, 118.01, 107.72, 77.16, 61.02, 45.66, 18.70, 14.25. **HR-MS** (ESI) *m/z*: calculated for C₁₄H₁₆N₂O₂ [M+H]⁺ 245.129003, found: 245.126900. **v_{max}** (neat) / cm⁻¹: 2980, 1727 (C=O), 1608, 1593

ethyl 2-(3-(4-methylpyrimidin-2-yl)phenyl)propanoate (5bc)

4-methyl-2-phenylpyrimidine (0.5 mmol, 85 mg), ethyl 2-bromopropanoate (1.5 mmol, 0.22 mL), [RuCl₂(p-cymene)]₂ (5 mol%, 15 mg), 2,4,6-Trimethylbenzoic acid (0.15 mmol, 25 mg) and K₂CO₃ (1 mmol, 138 mg) were reacted together in 1,4-Dioxane (2 mL) according to general procedure to afford the title compound as a colourless oil (50 mg, 37%).

¹H NMR (500 MHz, CDCl₃) δ 8.62 (d, *J* = 5.0 Hz, 1H), 8.38 (s, 1H), 8.34 – 8.30 (m, 1H), 7.43 (dd, *J* = 3.8, 1.5 Hz, 2H), 7.02 (d, *J* = 5.1 Hz, 1H), 4.21 – 4.00 (m, 2H), 3.82 (q, *J* = 7.2 Hz, 1H), 2.57 (s, 4H), 1.55 (d, *J* = 7.2 Hz, 4H), 1.19 (t, *J* = 7.1 Hz, 3H). **¹³C NMR** (126 MHz, CDCl₃) δ 174.58, 167.33, 164.27, 156.85, 141.13, 138.25, 129.58, 128.89, 127.65, 127.07, 118.73, 77.16, 60.82, 45.73, 24.48, 18.78, 14.21. **HR-MS** (ESI) *m/z*: calculated for C₁₆H₁₈N₂O₂ [M+H]⁺ 271.144653, found: 271.142900. **v_{max}** (neat) / cm⁻¹: 2980, 1728 (C=O), 1572, 1555

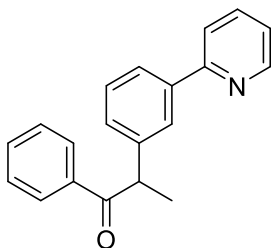
tert-butyl 2-(3-(pyridin-2-yl)phenyl)propanoate (3ad)



2-Phenylpyridine (0.5 mmol, 0.07 mL), tert-butyl 2-bromopropanoate (1.5 mmol, 0.28 mL), [RuCl₂(p-cymene)]₂ (5 mol%, 15 mg), 2,4,6-Trimethylbenzoic acid (0.15 mmol, 25 mg) and K₂CO₃ (1 mmol, 138 mg) were reacted together in 1,4-Dioxane (2 mL) according to general procedure to afford the title compound as a colourless oil (58 mg, 41%).

¹H NMR (500 MHz, CDCl₃) δ 8.67 (ddd, *J* = 4.7, 1.3 Hz, 1H), 7.92 (dd, *J* = 1.8 Hz, 1H), 7.86 (ddd, *J* = 7.6, 1.4 Hz, 1H), 7.73 – 7.68 (m, 2H), 7.41 (dd, *J* = 7.6 Hz, 1H), 7.38 – 7.34 (m, 1H), 7.21 – 7.17 (m, 1H), 3.71 (q, *J* = 7.2 Hz, 1H), 1.50 (d, *J* = 7.2 Hz, 3H), 1.39 (s, 9H). **¹³C NMR** (126 MHz, CDCl₃) δ 173.88, 157.50, 149.75, 141.84, 139.69, 136.80, 129.00, 128.01, 126.39, 125.58, 122.20, 120.72, 80.64, 46.70, 28.07, 18.84. **HR-MS** (ESI) *m/z*: calculated for C₁₈H₂₁NO₂ [M+H]⁺ 284.165054, found: 284.161700. **ν_{max}** (neat) / cm⁻¹: 2977, 1723 (C=O), 1584, 1566

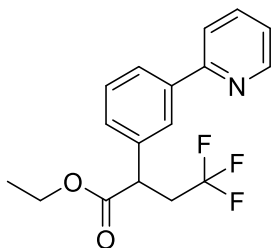
1-phenyl-2-(3-(pyridin-2-yl)phenyl)propan-1-one (3ae)



2-Phenylpyridine (0.5 mmol, 0.07 mL), 2-bromo-1-phenylpropan-1-one (1.5 mmol, 0.23 mL), $[\text{RuCl}_2(\text{p-cymene})]_2$ (5 mol%, 15 mg), 2,4,6-Trimethylbenzoic acid (0.15 mmol, 25 mg) and K_2CO_3 (1 mmol, 138 mg) were reacted together in 1,4-Dioxane (2 mL) according to general procedure to afford the title compound as a colourless oil (59 mg, 41%).

^1H NMR (500 MHz, CDCl_3) δ 8.71 (ddd, $J = 4.8, 1.8, 1.0$ Hz, 1H), 8.00 – 7.99 (m, 1H), 7.98 – 7.96 (m, 2H), 7.81 (ddd, $J = 7.7, 1.7, 1.2$ Hz, 1H), 7.74 (ddd, $J = 7.8, 7.4, 1.8$ Hz, 1H), 7.69 (ddd, $J = 8.0, 1.1$ Hz, 1H), 7.48 – 7.44 (m, 1H), 7.42 – 7.35 (m, 3H), 7.34 – 7.32 (m, 1H), 7.23 (ddd, $J = 7.3, 4.8, 1.3$ Hz, 1H), 4.80 (q, $J = 6.9$ Hz, 1H), 1.59 (d, $J = 6.9$ Hz, 3H). **^{13}C NMR** (126 MHz, CDCl_3) δ 200.42, 157.25, 149.69, 142.19, 140.13, 136.97, 136.56, 133.04, 132.94, 130.11, 129.51, 128.92, 128.63, 128.41, 128.38, 126.66, 125.69, 122.39, 120.95, 77.16, 48.09, 19.76. **HR-MS** (ESI) m/z : calculated for $\text{C}_{20}\text{H}_{17}\text{NO}$ $[\text{M}+\text{H}]^+$ 288.138839, found: 288.141000. ν_{max} (neat) / cm^{-1} : 2974, 1678 (C=O), 1582, 1566

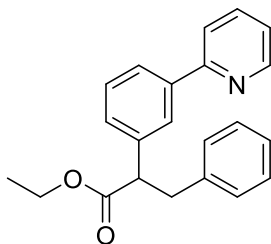
ethyl 4,4,4-trifluoro-2-(3-(pyridin-2-yl)phenyl)butanoate (3ai)



2-Phenylpyridine (0.5 mmol, 0.07 mL), ethyl 2-bromo-4,4,4-trifluorobutanoate (1.5 mmol, 332 mg), $[\text{RuCl}_2(\text{p-cymene})]_2$ (5 mol%, 15 mg), 2,4,6-Trimethylbenzoic acid (0.15 mmol, 25 mg) and K_2CO_3 (1 mmol, 138 mg) were reacted together in 1,4-Dioxane (2 mL) according to general procedure to afford the title compound as a colourless oil (65 mg, 40%).

^1H NMR (500 MHz, CDCl_3) δ 8.70 (dd, $J = 4.8, 0.7$ Hz, 1H), 7.96 (s, 1H), 7.91 (d, $J = 7.7$ Hz, 1H), 7.78 – 7.73 (m, 1H), 7.72 (d, $J = 7.8$ Hz, 1H), 7.46 (dd, $J = 7.8$ Hz, 1H), 7.37 (d, $J = 7.7$ Hz, 1H), 7.25 – 7.22 (m, 1H), 4.25 – 4.16 (m, 1H), 4.14 – 4.06 (m, 1H), 3.99 (dd, $J = 9.2, 4.7$ Hz, 1H), 3.26 – 3.09 (m, 1H), 2.61 – 2.46 (m, 1H), 1.21 (t, $J = 7.1$ Hz, 3H). **^{13}C NMR** (126 MHz, CDCl_3) δ 172.00, 156.91, 149.88, 140.35, 137.87, 136.94, 129.53, 128.08, 126.65, 126.47, 126.16 (q, $J = 277.2$ Hz), 122.54, 120.79, 61.72, 45.60 (q, $J = 2.8$ Hz), 37.57 (q, $J = 28.8$ Hz), 14.10. **^{19}F NMR** (470 MHz, CDCl_3) δ -65.35 (t, $J = 10.4$ Hz). **HR-MS** (ESI) m/z : calculated for $\text{C}_{20}\text{H}_{17}\text{NO}$ $[\text{M}+\text{Na}]^+$ 346.103083, found: 346.104300. ν_{max} (neat) / cm^{-1} : 2986, 1732 (C=O), 1585, 1567

ethyl 3-phenyl-2-(3-(pyridin-2-yl)phenyl)propanoate (3aj)

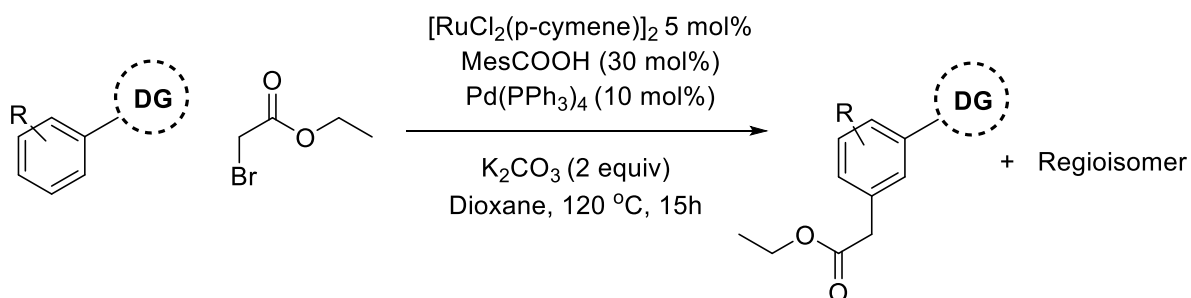


2-Phenylpyridine (0.5 mmol, 0.07 mL), ethyl 2-bromo-3-phenylpropanoate (1.5 mmol, 384 mg), $[\text{RuCl}_2(\text{p-cymene})]_2$ (5 mol%, 15 mg), 2,4,6-Trimethylbenzoic acid (0.15 mmol, 25 mg) and K_2CO_3 (1 mmol, 138 mg) were reacted together in 1,4-Dioxane (2 mL) according to general procedure to afford the title compound as a colourless oil (74 mg, 45%).

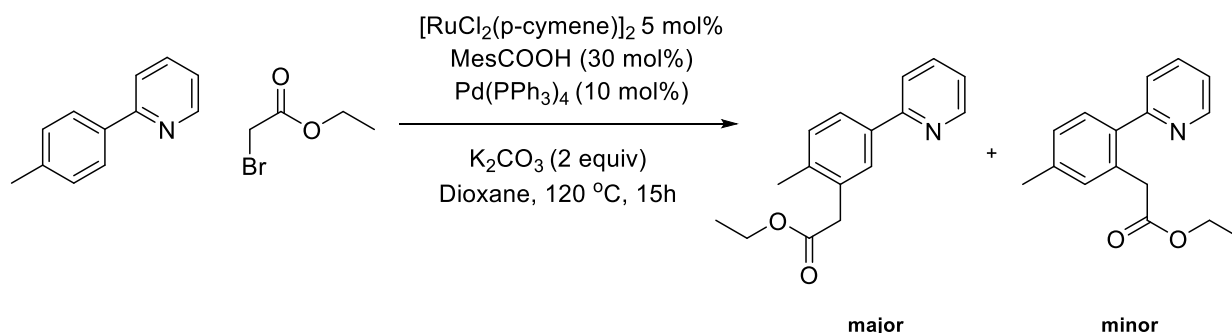
^1H NMR (500 MHz, CDCl_3) δ 8.70 (ddd, $J = 4.8, 1.8, 1.0$ Hz, 1H), 7.96 (dd, $J = 1.6$ Hz, 1H), 7.90 (ddd, $J = 7.2, 1.8$ Hz, 1H), 7.77 – 7.72 (m, 1H), 7.70 (ddd, $J = 8.0, 1.1$ Hz, 1H), 7.46 – 7.38 (m, 2H), 7.27 – 7.21 (m, 3H), 7.20 – 7.15 (m, 3H), 4.14 – 4.00 (m, 2H), 3.96 (dd, $J = 9.3, 6.3$ Hz, 1H), 3.47 (dd, $J = 13.7, 9.3$ Hz, 1H), 3.09 (dd, $J = 13.7, 6.3$ Hz, 1H), 1.12 (t, $J = 7.1$ Hz, 3H). **^{13}C NMR** (126 MHz, CDCl_3) δ 173.41, 157.35, 149.80, 139.89, 139.49, 139.19, 136.85, 129.16, 129.13, 128.57, 128.45, 126.80, 126.50, 126.09, 122.31, 120.81, 77.16, 60.92, 53.91, 40.14, 14.18. **HR-MS** (ESI) m/z : calculated for $\text{C}_{22}\text{H}_{21}\text{NO}_2$ $[\text{M}+\text{Na}]^+$ 354.146999, found: 354.147500. ν_{max} (neat) / cm^{-1} : 2981, 1726 (C=O), 1603, 1584

Determination of regioisomeric by-products

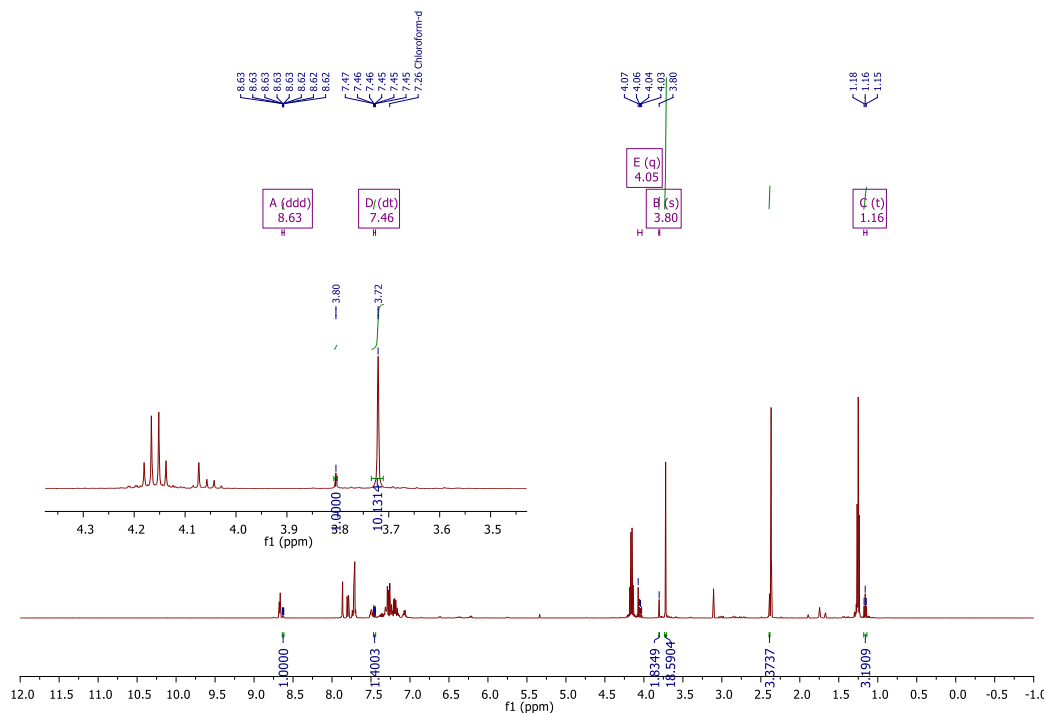
Compounds 3ka-3ua contained significant amount of regioisomeric by-products. These reactions were conducted as per the general procedure and a mixed fraction was collected by column chromatography. The ratio between the major and minor isomer was determined by suitable signals in the ^1H or ^{19}F NMR spectra where available. The minor product was identified by literature reference where possible and when unavailable the regioselectivity is not stated. The major product in most cases could be further purified and are characterised below.



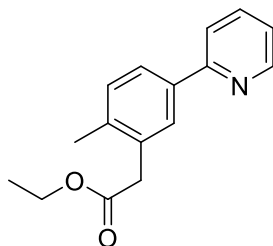
Reaction with 2-(p-tolyl)pyridine



2-(p-tolyl)pyridine (0.5 mmol, 85 mg), ethyl bromoacetate (1.5 mmol, 0.17 mL), $[\text{RuCl}_2(\text{p-cymene})]_2$ (5 mol%, 15 mg), $\text{Pd}(\text{PPh}_3)_4$ (10 mol%, 57 mg), 2,4,6-Trimethylbenzoic acid (0.15 mmol, 25 mg) and K_2CO_3 (1 mmol, 138 mg) were reacted together in 1,4-Dioxane (2 mL) according to general procedure to afford a mixed fraction of title compound and a regioisomeric by-product (40 mg, 31%) major:minor 10:1 (determined from ^1H spectra below). The major isomer was purified further by column chromatography and is characterised below. The minor isomer is consistent with the ortho substituted product.¹³

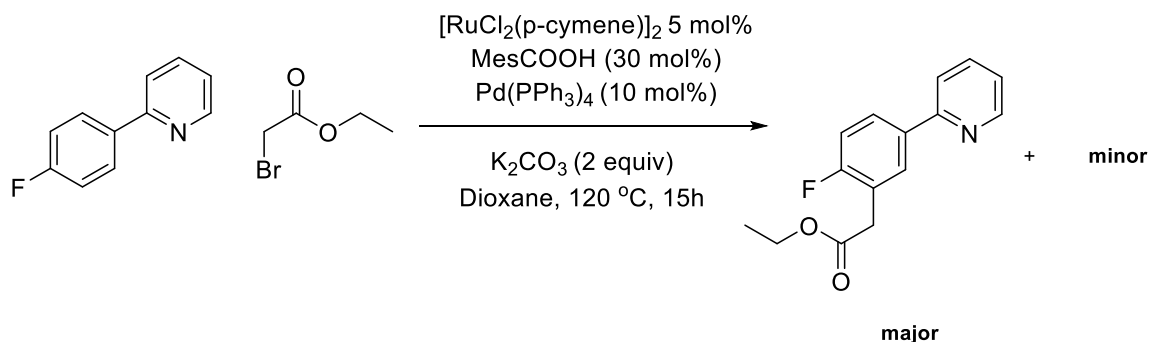


ethyl 2-(2-methyl-5-(pyridin-2-yl)phenyl)acetate (3ma)

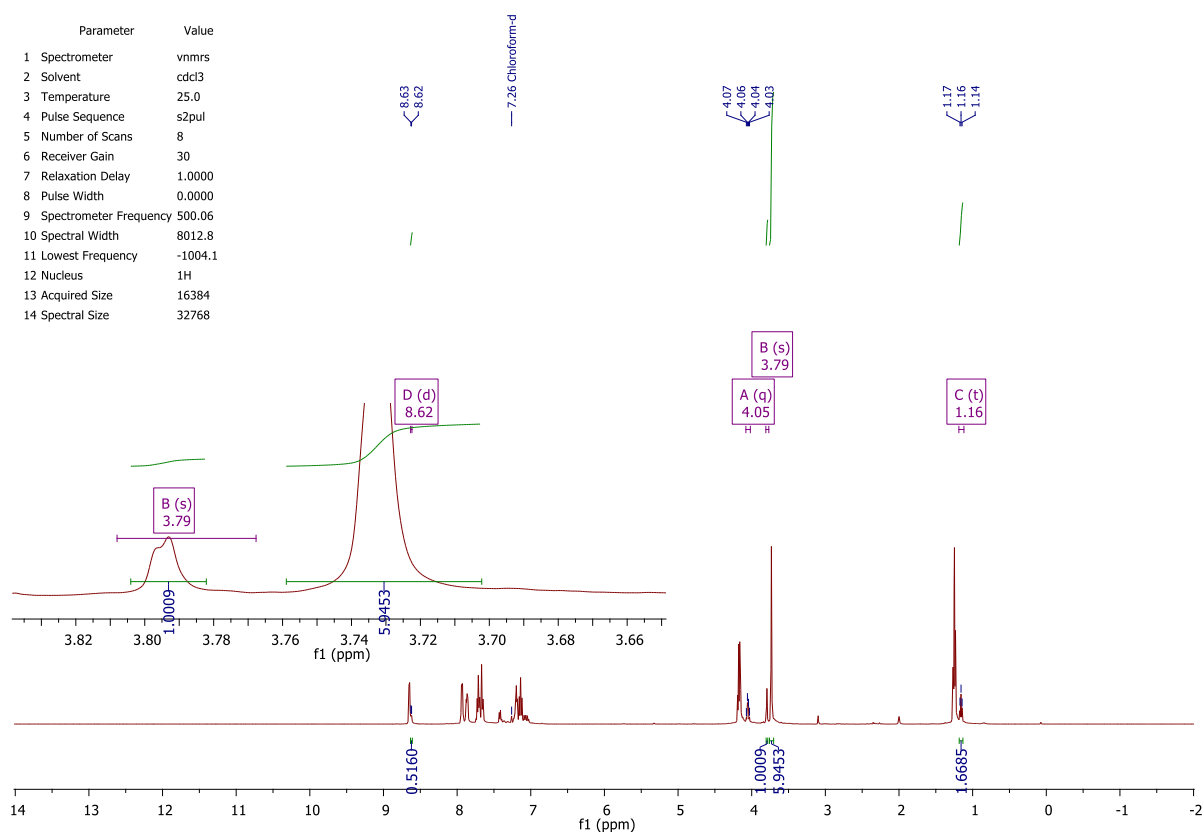


^1H NMR (500 MHz, CDCl_3) δ 8.70 – 8.65 (m, 1H), 7.86 (d, J = 1.9 Hz, 1H), 7.80 (dd, J = 7.9, 2.0 Hz, 1H), 7.76 – 7.67 (m, 2H), 7.28 (d, J = 7.9 Hz, 1H), 7.23 – 7.17 (m, 1H), 4.16 (q, J = 7.1 Hz, 2H), 3.72 (s, 2H), 2.37 (s, 3H), 1.25 (t, J = 7.1 Hz, 3H). **^{13}C NMR** (126 MHz, CDCl_3) δ 171.51, 157.34, 149.73, 138.13, 137.46, 136.80, 133.53, 130.94, 128.93, 125.89, 122.03, 120.47, 60.99, 39.62, 19.61, 14.36. **HR-MS** (ESI) m/z calculated for $\text{C}_{16}\text{H}_{17}\text{NO}_2$ $[\text{M}+\text{Na}]^+$ 278.115698, found: 278.115000. **ν_{max}** (neat) / cm^{-1} : 2978, 1731 (C=O), 1588

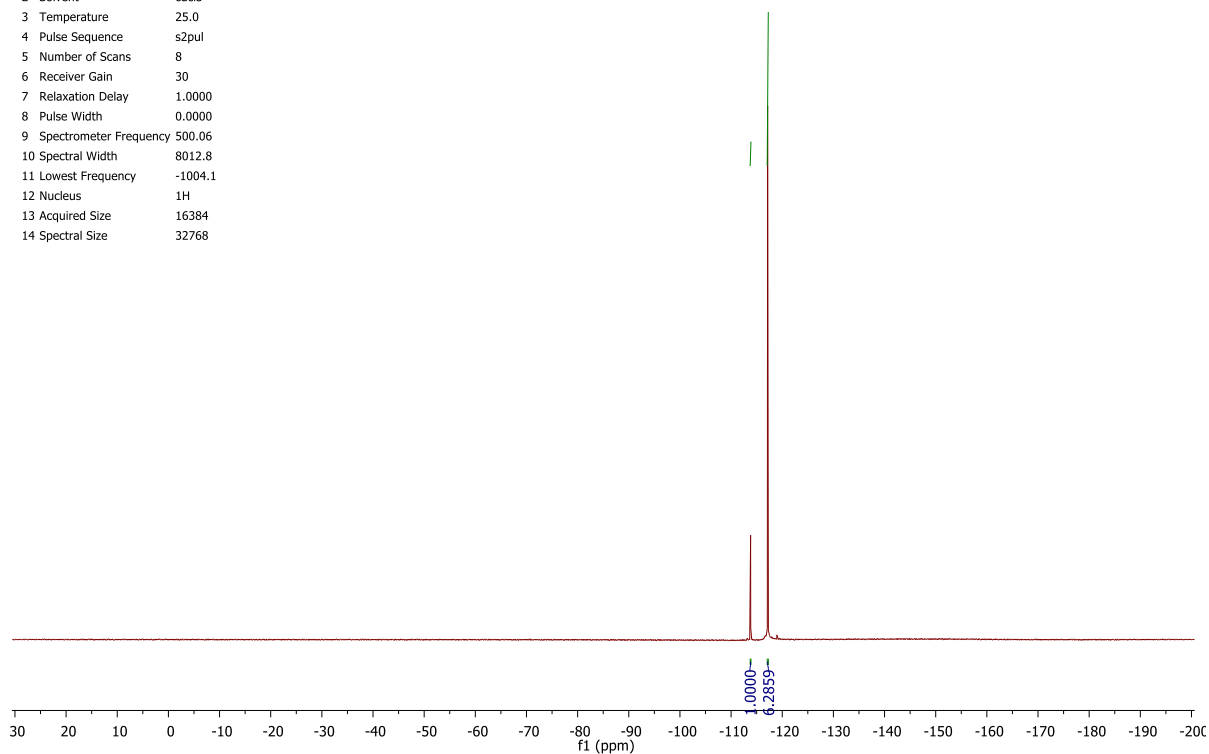
Reaction with 2-(4-fluorophenyl)pyridine



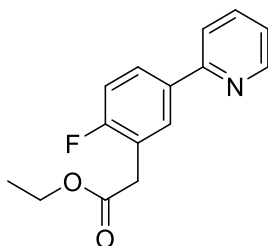
2-(4-fluorophenyl)pyridine (0.5 mmol, 87 mg), ethyl bromoacetate (1.5 mmol, 0.17 mL), [RuCl₂(p-cymene)]₂ (5 mol%, 15 mg), Pd(PPh₃)₄ (10 mol%, 57 mg), 2,4,6-Trimethylbenzoic acid (0.15 mmol, 25 mg) and K₂CO₃ (1 mmol, 138 mg) were reacted together in 1,4-Dioxane (2 mL) according to general procedure to afford a mixed fraction of title compound and a regioisomeric by-product (75 mg, 58%) major:minor 6:1 (determined from ¹H and ¹⁹F spectra shown below). The major isomer was purified further by column chromatography and is characterised below.



Parameter	Value
1 Spectrometer	nmrs
2 Solvent	cdcl3
3 Temperature	25.0
4 Pulse Sequence	s2pul
5 Number of Scans	8
6 Receiver Gain	30
7 Relaxation Delay	1.0000
8 Pulse Width	0.0000
9 Spectrometer Frequency	500.06
10 Spectral Width	8012.8
11 Lowest Frequency	-1004.1
12 Nucleus	1H
13 Acquired Size	16384
14 Spectral Size	32768

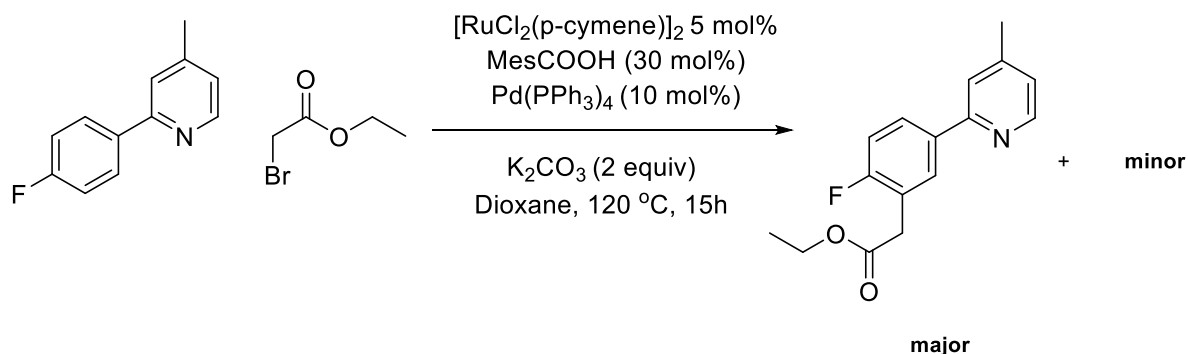


ethyl 2-(2-fluoro-5-(pyridin-2-yl)phenyl)acetate (3na)

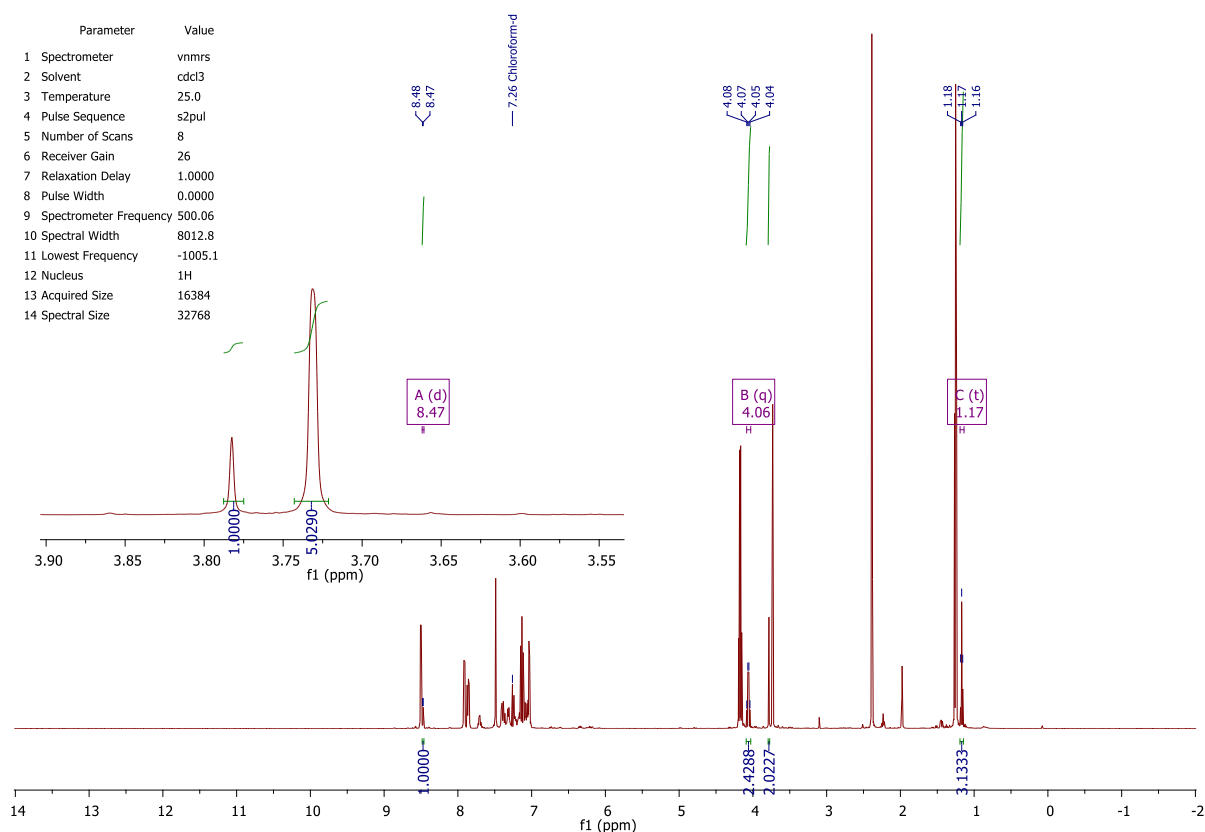


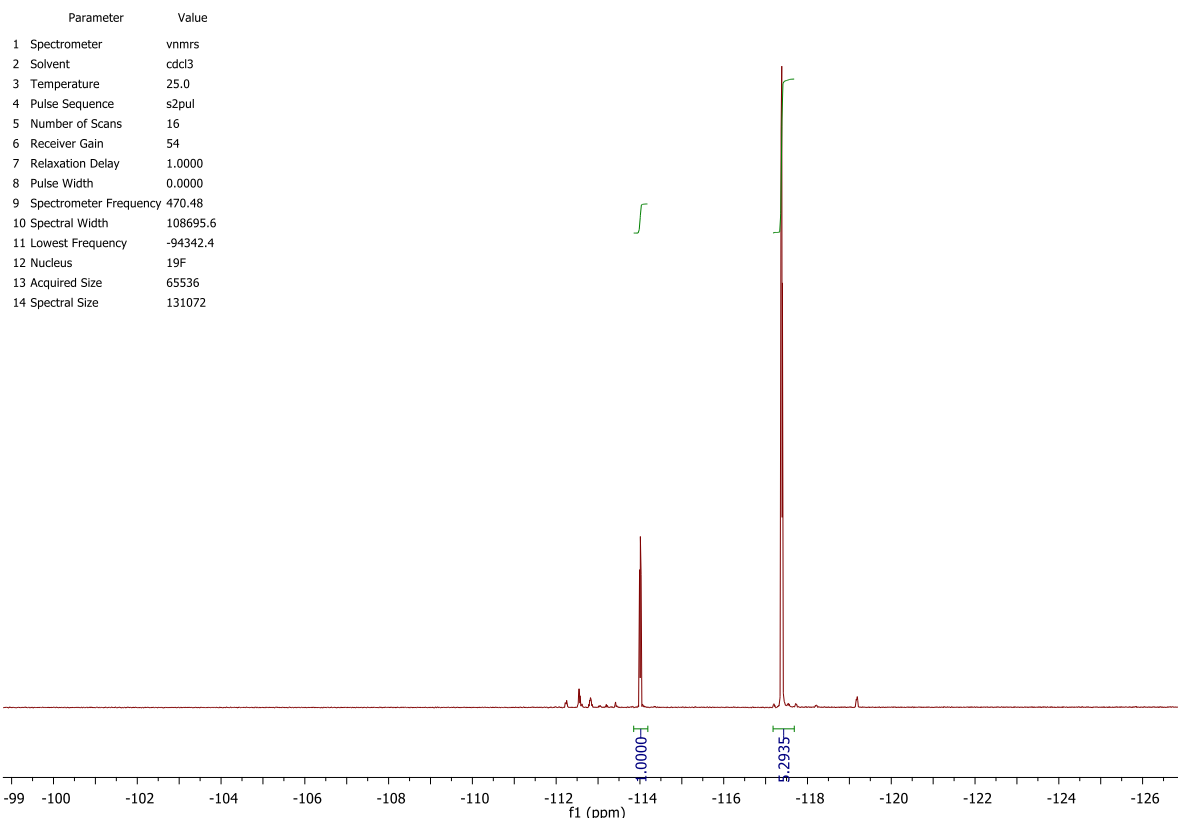
¹H NMR (500 MHz, CDCl₃) δ 8.67 (ddd, *J* = 4.8, 1.8, 1.0 Hz, 1H), 7.94 (dd, *J* = 7.2, 2.3 Hz, 1H), 7.88 (ddd, *J* = 8.5, 5.0, 2.4 Hz, 1H), 7.76 – 7.71 (m, 1H), 7.68 (ddd, *J* = 8.0, 1.1 Hz, 1H), 7.22 (ddd, *J* = 7.4, 4.8, 1.2 Hz, 1H), 7.18 – 7.13 (m, 1H), 4.18 (q, *J* = 7.1 Hz, 2H), 3.74 (d, *J* = 0.8 Hz, 2H), 1.26 (t, *J* = 7.1 Hz, 3H). **¹³C NMR** (126 MHz, CDCl₃) δ 170.70, 161.97 (d, *J* = 249.4 Hz), 156.43, 149.79, 136.95, 135.72 (d, *J* = 3.4 Hz), 130.42 (d, *J* = 4.5 Hz), 127.76 (d, *J* = 8.6 Hz), 122.23, 122.05 (d, *J* = 16.4 Hz), 120.44, 115.83 (d, *J* = 22.4 Hz), 61.24, 34.95 (d, *J* = 2.7 Hz), 14.31. **¹⁹F NMR** (470 MHz, CDCl₃) δ -116.97 – -117.30 (m). **HR-MS** (ESI) *m/z* calculated for C₁₅H₁₄NO₂F [M+Na]⁺ 282.090627, found: 282.090800. **ν_{max}** (neat) / cm⁻¹: 2984, 1734 (C=O), 1589, 1567

Reaction with 2-(4-fluorophenyl)pyridine

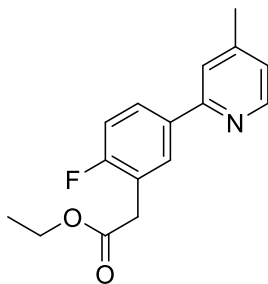


2-(4-fluorophenyl)-4-methylpyridine (0.5 mmol, 94 mg), ethyl bromoacetate (1.5 mmol, 0.17 mL), $[\text{RuCl}_2(\text{p-cymene})]_2$ (5 mol%, 15 mg), $\text{Pd}(\text{PPh}_3)_4$ (10 mol%, 57 mg), 2,4,6-Trimethylbenzoic acid (0.15 mmol, 25 mg) and K_2CO_3 (1 mmol, 138 mg) were reacted together in 1,4-Dioxane (2 mL) according to general procedure to afford a mixed fraction of title compound and a regioisomeric by-product (90 mg, 66%) major:minor 5:1 (determined from ^1H and ^{19}F spectra shown below). The major isomer was purified further by column chromatography and is characterised below.



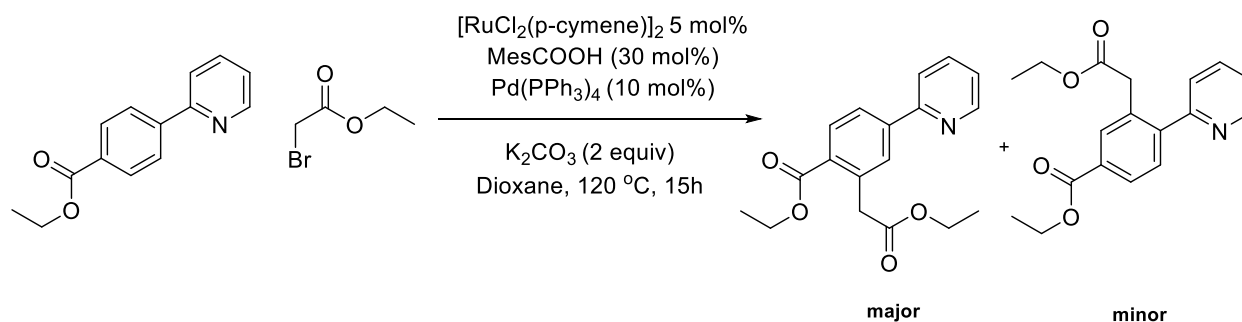


ethyl 2-(2-fluoro-5-(4-methylpyridin-2-yl)phenyl)acetate (30a)

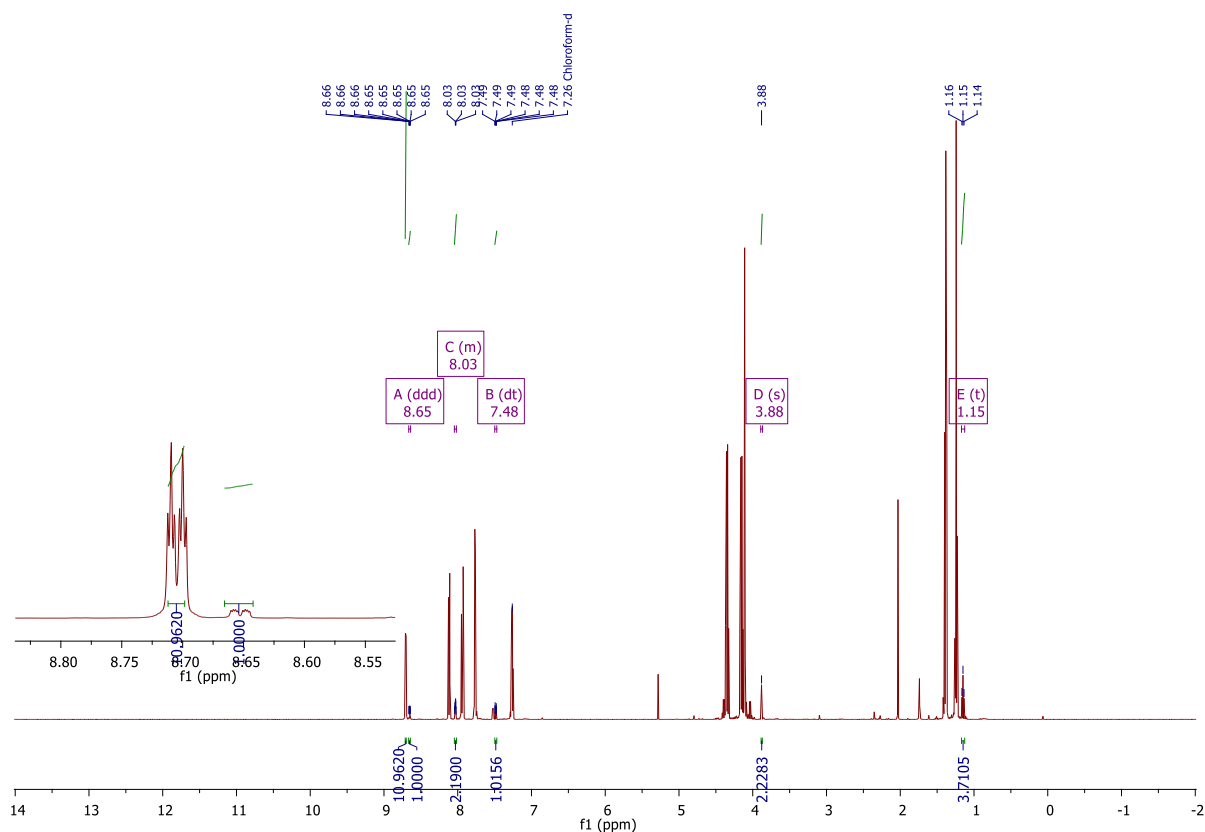


¹H NMR (500 MHz, CDCl₃) δ 8.51 (d, *J* = 5.0 Hz, 1H), 7.92 (dd, *J* = 7.2, 2.3 Hz, 1H), 7.87 (ddd, *J* = 7.9, 5.0, 2.4 Hz, 1H), 7.50 (s, 1H), 7.14 (t, *J* = 9.0 Hz, 1H), 7.05 (dd, *J* = 5.0, 0.6 Hz, 1H), 4.18 (q, *J* = 7.1 Hz, 2H), 3.74 (s, 2H), 2.40 (s, 3H), 1.26 (t, *J* = 7.1 Hz, 3H). **¹³C NMR** (126 MHz, CDCl₃) δ 170.72, 161.89 (d, *J* = 248.9 Hz), 156.26, 149.44, 148.08, 130.42 (d, *J* = 4.5 Hz), 127.78 (d, *J* = 8.5 Hz), 121.95 (d, *J* = 16.5 Hz), 118.11 (d, *J* = 22.0 Hz), 115.76 (d, *J* = 22.4 Hz), 61.21, 34.93 (d, *J* = 2.6 Hz), 21.36, 14.30. **¹⁹F NMR** (470 MHz, CDCl₃) δ -115.47 – -119.82 (m). **HR-MS** (ESI) *m/z*: calculated for C₁₆H₁₆NO₂ F [M+Na]⁺ 296.106277, found: 296.106700. **v_{max}** (neat) / cm⁻¹: 2986, 1735 (C=O), 1604, 1562

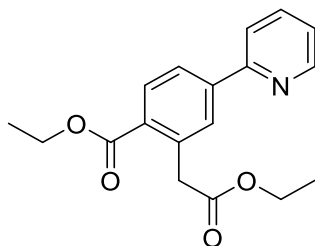
Reaction with 2-(4-fluorophenyl)pyridine



ethyl 4-(pyridin-2-yl)benzoate (0.5 mmol, 114 mg), ethyl bromoacetate (1.5 mmol, 0.17 mL), $[\text{RuCl}_2(\text{p-cymene})]_2$ (5 mol%, 15 mg), $\text{Pd}(\text{PPh}_3)_4$ (10 mol%, 57 mg), 2,4,6-Trimethylbenzoic acid (0.15 mmol, 25 mg) and K_2CO_3 (1 mmol, 138 mg) were reacted together in 1,4-Dioxane (2 mL) according to general procedure to afford a mixed fraction of title compound and a regioisomeric by-product (91 mg, 58%) major:minor 10:1 (determined from ^1H spectra below). The major isomer was purified further by column chromatography and is characterised below. The minor isomer is consistent with the ortho substituted product.¹³

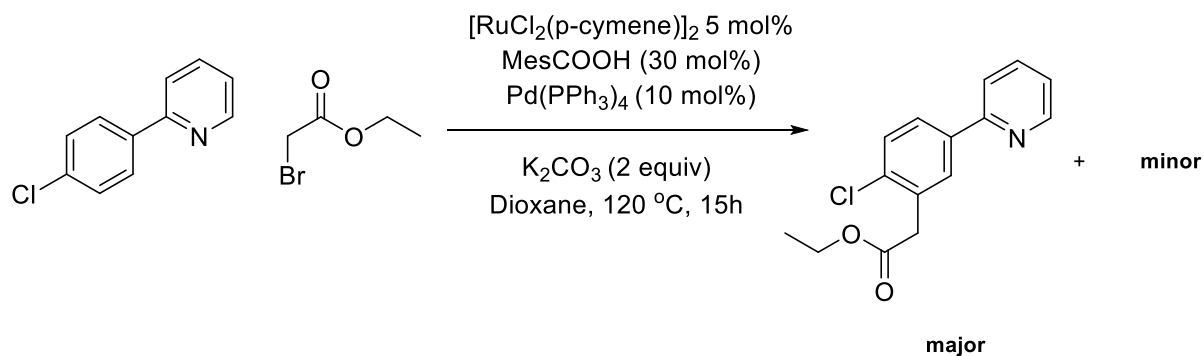


ethyl 2-(2-ethoxy-2-oxoethyl)-4-(pyridin-2-yl)benzoate (3pa)

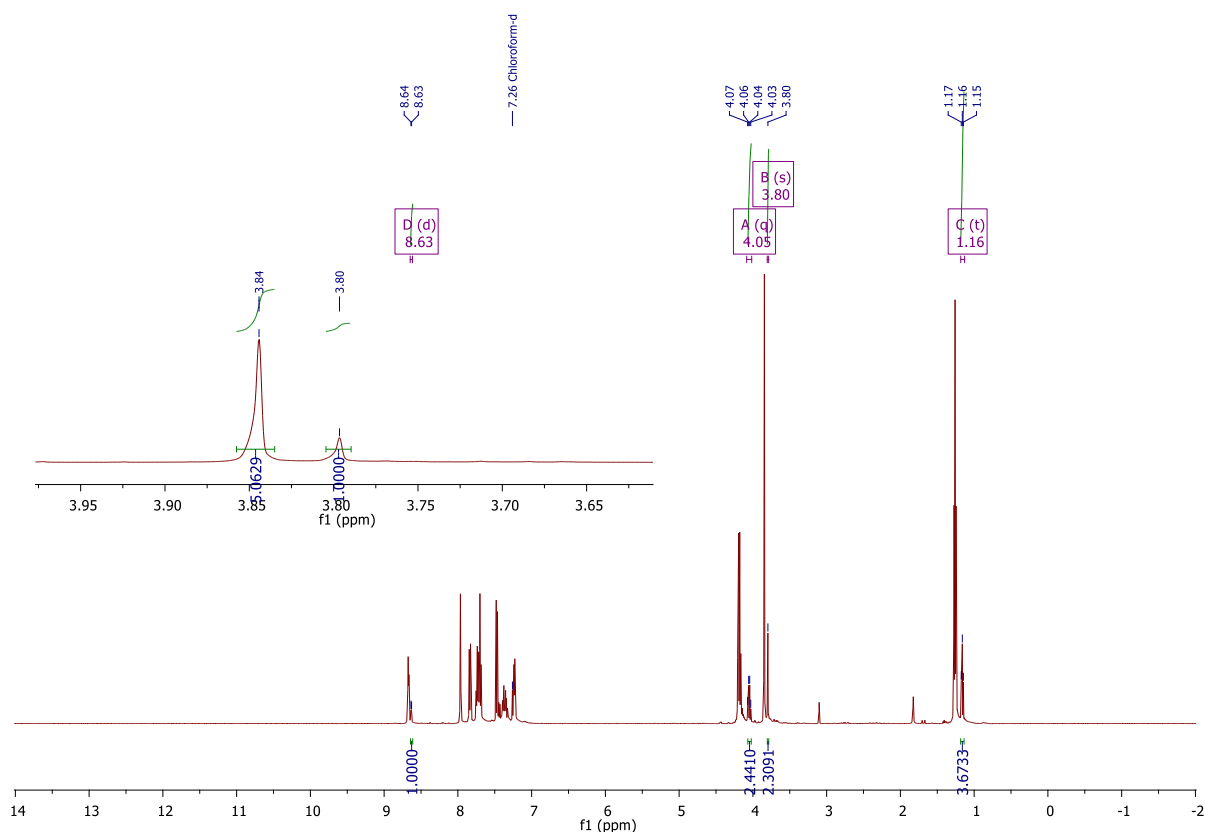


¹H NMR (500 MHz, CDCl₃) δ 8.71 (ddd, *J* = 4.8, 1.4 Hz, 1H), 8.12 (d, *J* = 8.1 Hz, 1H), 7.95 (dd, *J* = 8.1, 1.9 Hz, 1H), 7.93 – 7.92 (m, 1H), 7.78 – 7.76 (m, 2H), 7.27 (ddd, *J* = 4.0, 3.5 Hz, 1H), 4.35 (q, *J* = 7.1 Hz, 2H), 4.16 (q, *J* = 7.1 Hz, 2H), 4.11 (s, 2H), 1.39 (t, *J* = 7.2 Hz, 3H), 1.25 (t, *J* = 7.1 Hz, 3H). **¹³C NMR** (126 MHz, CDCl₃) δ 171.51, 167.06, 156.05, 149.95, 142.79, 136.99, 136.61, 131.65, 130.84, 130.45, 125.65, 122.98, 121.11, 61.15, 60.86, 41.08, 14.36, 14.32. **HR-MS** (ESI) *m/z*: calculated for C₁₈H₁₉NO₄ [M+H]⁺ 314.139233, found: 314.141000. **ν_{max}** (neat) / cm⁻¹: 2982, 1732 (C=O), 1712 (C=O), 1610, 1587

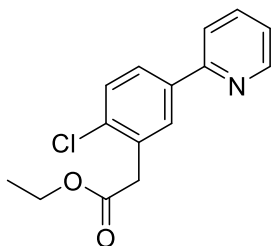
Reaction with 2-(4-chlorophenyl)pyridine



2-(4-chlorophenyl)pyridine (0.5 mmol, 95 mg), ethyl bromoacetate (1.5 mmol, 0.17 mL), $[\text{RuCl}_2(\text{p-cymene})]_2$ (5 mol%, 15 mg), $\text{Pd}(\text{PPh}_3)_4$ (10 mol%, 57 mg), 2,4,6-Trimethylbenzoic acid (0.15 mmol, 25 mg) and K_2CO_3 (1 mmol, 138 mg) were reacted together in 1,4-Dioxane (2 mL) according to general procedure to afford a mixed fraction of title compound and a regioisomeric by-product (76 mg, 55%) major:minor 5:1 (determined from ^1H spectra shown below). The major isomer was purified further by column chromatography and is characterised below.

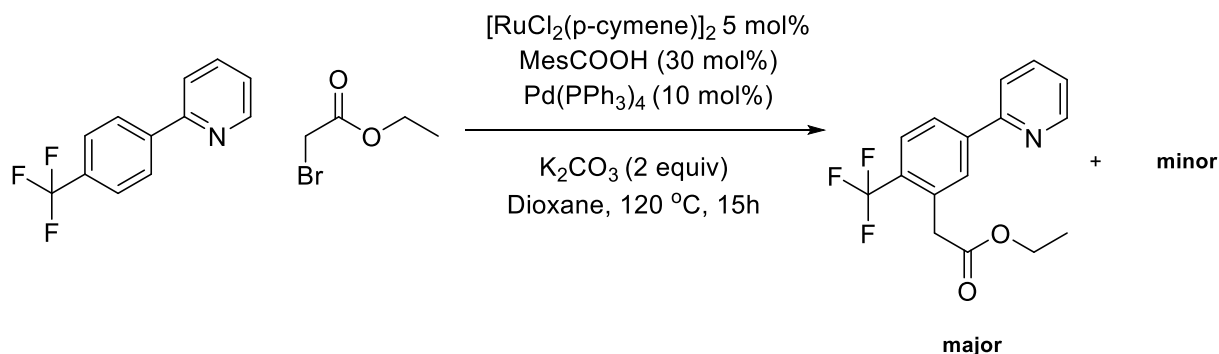


ethyl 2-(2-chloro-5-(pyridin-2-yl)phenyl)acetate (3qa)

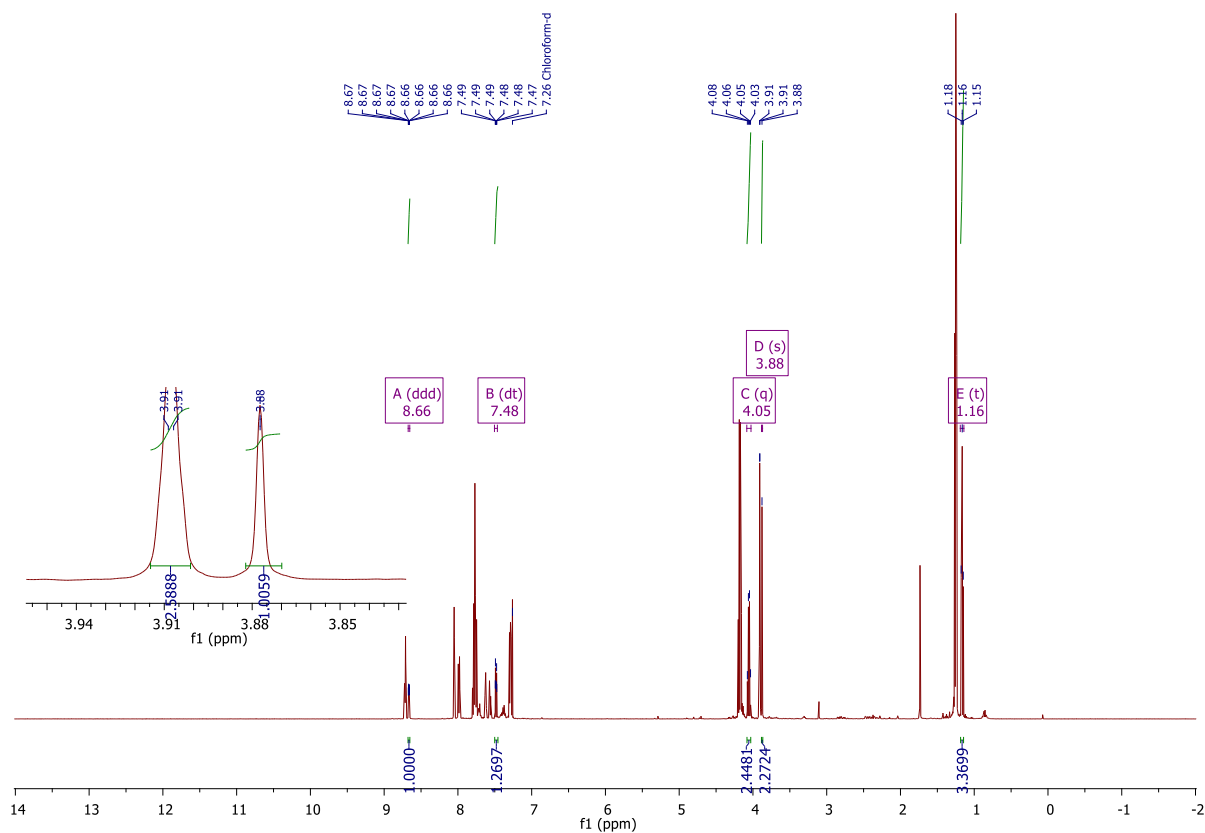


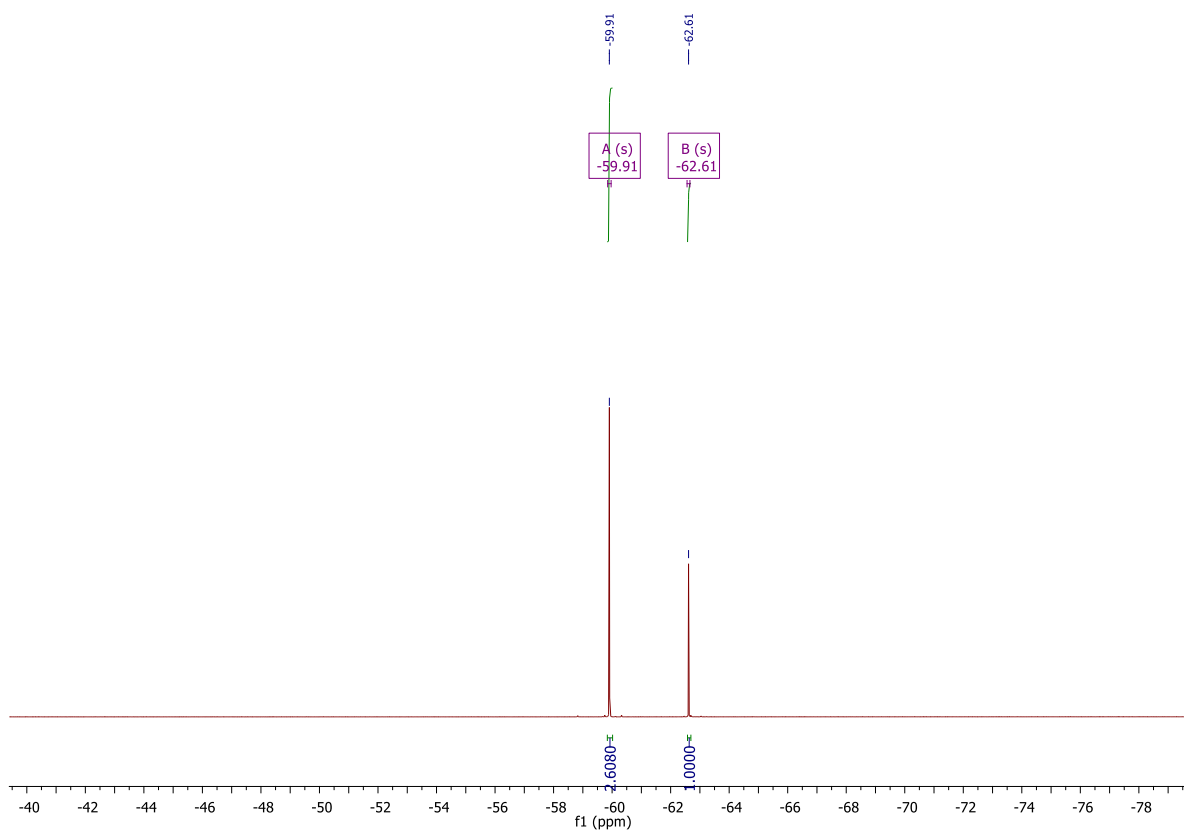
¹H NMR (500 MHz, CDCl₃) δ 8.68 (ddd, *J* = 4.8, 1.8, 1.0 Hz, 1H), 7.96 (d, *J* = 2.2 Hz, 1H), 7.84 (dd, *J* = 8.3, 2.2 Hz, 1H), 7.77 – 7.73 (m, 1H), 7.71 (ddd, *J* = 8.0, 1.2 Hz, 1H), 7.48 (d, *J* = 8.3 Hz, 1H), 7.24 (ddd, *J* = 7.3, 4.8, 1.3 Hz, 1H), 4.19 (q, *J* = 7.1 Hz, 2H), 3.85 (s, 2H), 1.27 (t, *J* = 7.1 Hz, 3H). **¹³C NMR** (126 MHz, CDCl₃) δ 170.59, 156.18, 149.86, 138.31, 136.98, 135.61, 133.07, 130.13, 129.93, 127.09, 122.55, 120.55, 61.21, 39.53, 14.32. **HR-MS** (ESI) *m/z*: calculated for C₁₅H₁₄NO₂ Cl [M+H]⁺ 276.079131, found: 276.079900. **ν_{max}** (neat) / cm⁻¹: 2980, 1734 (C=O), 1588

Reaction with 2-(4-(trifluoromethyl)phenyl)pyridine

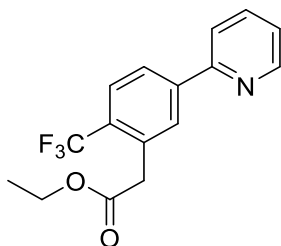


2-(4-(trifluoromethyl)phenyl)pyridine (0.5 mmol, 112 mg), ethyl bromoacetate (1.5 mmol, 0.17 mL), $[\text{RuCl}_2(\text{p-cymene})]_2$ (5 mol%, 15 mg), $\text{Pd}(\text{PPh}_3)_4$ (10 mol%, 57 mg), 2,4,6-Trimethylbenzoic acid (0.15 mmol, 25 mg) and K_2CO_3 (1 mmol, 138 mg) were reacted together in 1,4-Dioxane (2 mL) according to general procedure to afford a mixed fraction of title compound and a regioisomeric by-product (85 mg, 55%) major:minor 2.5:1 (determined from ^1H and ^{19}F spectra shown below). The major isomer was purified further by column chromatography and is characterised below.





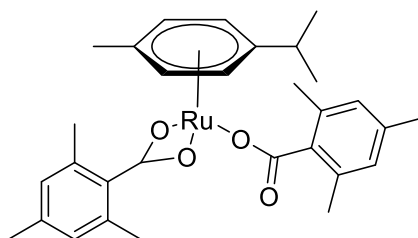
ethyl 2-(5-(pyridin-2-yl)-2-(trifluoromethyl)phenyl)acetate (3ra)



^1H NMR (500 MHz, CDCl_3) δ 8.72 (ddd, $J = 4.8, 1.7, 1.1$ Hz, 1H), 8.05 (s, 1H), 7.99 (dd, $J = 8.2, 0.8$ Hz, 1H), 7.82 – 7.73 (m, 3H), 7.30 (ddd, $J = 6.7, 4.8, 2.0$ Hz, 1H), 4.18 (q, $J = 7.1$ Hz, 2H), 3.91 (d, $J = 0.9$ Hz, 2H), 1.25 (t, $J = 7.1$ Hz, 3H). **^{19}F NMR** (470 MHz, CDCl_3) δ -59.91 (s). **HR-MS** (ESI) m/z : calculated for $\text{C}_{18}\text{H}_{18}\text{NO}_2\text{F}_3$ $[\text{M}+\text{H}]^+$ 310.1055, found: 310.1097. **ν_{max}** (neat) / cm^{-1} : 2987, 1736 (C=O), 1588, 1566

Mechanistic Studies

Synthesis of complex A

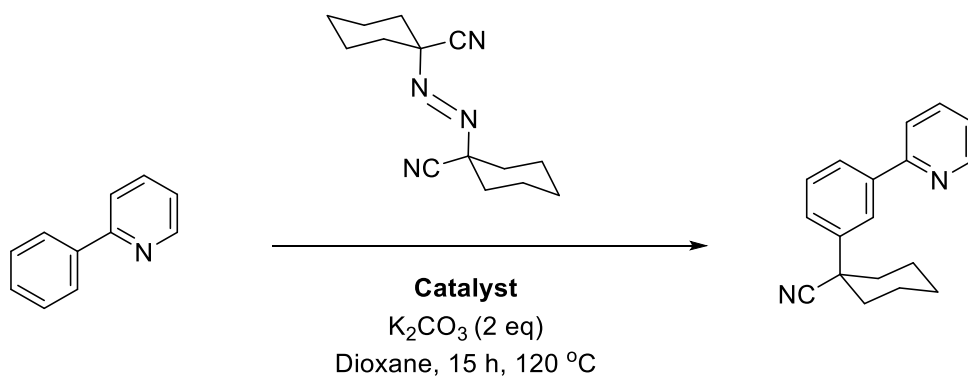


To an oven-dried, argon-purged Schlenk tube was added $[\text{Ru}(p\text{-cymene})\text{Cl}_2]_2$ (612 mg, 1 mmol), MesCOOK (889 mg, 4.4 mmol) and DCM (50 mL). The vessel was then sealed and the reaction mixture was stirred at room temperature for 16 h. The reaction mixture was then filtered through a sinter funnel and eluted with DCM. The solvent was removed under vacuum to yield complex as a yellow solid (1.1 g, 95 % yield).

$^1\text{H NMR}$ (500 MHz, CDCl_3) δ 6.68 (s, 4H), 6.00 (d, J = 5.0 Hz, 2H), 5.79 (d, J = 5.2 Hz, 2H), 2.96 (dt, J = 13.8, 6.9 Hz, 1H), 2.35 (s, 3H), 2.18 (s, 6H), 2.16 (s, 12H), 1.42 (d, J = 6.9 Hz, 6H).

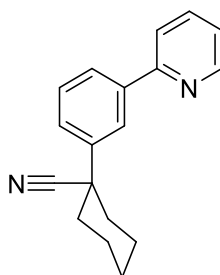
$^{13}\text{C NMR}$ (126 MHz, CDCl_3) δ 183.10, 137.43, 135.28, 134.56, 128.73, 127.91, 98.11, 79.01, 78.20, 31.68, 22.74, 21.15, 19.96, 19.00.

Reactions with ABCN



2-Phenylpyridine (0.5 mmol, 0.07 mL), 1,1'-Azobis(cyclohexanecarbonitrile) (1 mmol, 244 mg), K_2CO_3 (1 mmol, 138 mg) and a catalyst were reacted together in 1,4-Dioxane (2 mL) in the amounts specified in a carousel tube. The carousel tube was then sealed and refluxed on a carousel at 120 °C for 15h. After cooling to room temperature the reaction mixture was dry loaded onto silica and purified by silica gel column chromatography (Hexane / EtOAc).

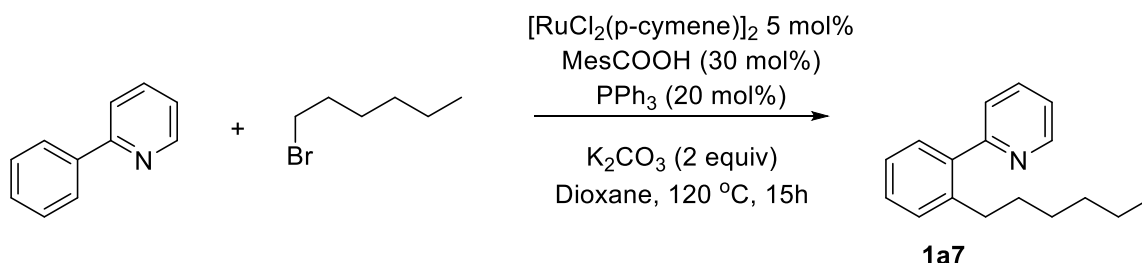
1-(3-(pyridin-2-yl)phenyl)cyclohexane-1-carbonitrile (1an)



2-Phenylpyridine (0.5 mmol, 0.07 mL), 1,1'-Azobis(cyclohexanecarbonitrile) (1 mmol, 244 mg), Complex A (0.25mmol 141 mg), and K_2CO_3 (1 mmol, 138 mg) were reacted together in 1,4-Dioxane (2 mL) according to general procedure to afford the title compound as a colourless oil (34 mg, 26%).

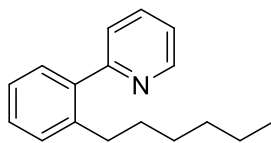
1H NMR (500 MHz, $CDCl_3$) δ 8.70 (d, J = 4.7 Hz, 1H), 8.14 (s, 1H), 7.90 (d, J = 7.6 Hz, 1H), 7.80 – 7.72 (m, 2H), 7.57 (d, J = 7.9 Hz, 1H), 7.50 (dd, J = 7.8 Hz, 1H), 7.28 – 7.23 (m, 1H), 2.26 – 2.17 (m, 2H), 1.94 – 1.81 (m, 8H). **^{13}C NMR** (126 MHz, $CDCl_3$) δ 157.09, 149.90, 142.23, 140.28, 136.98, 129.43, 126.51, 126.47, 124.30, 122.86, 122.55, 120.89, 77.16, 44.68, 37.54, 25.12, 23.77. **HR-MS** (ESI) m/z : calculated for $C_{18}H_{18}N_2$ $[M+H]^+$ 263.154824, found: 263.156900. ν_{max} (neat) / cm^{-1} : 2934, 2229 (CN), 1584, 1566

Reactions with primary alkyl halide n-Hex-Br



2-Phenylpyridine (0.5 mmol, 0.07 mL), 1-bromohexane (210 μ L, 1.5 mmol) $[Ru(p\text{-cymene})Cl_2]_2$ (15.0 mg, 0.025 mmol) 2,4,6-Trimethylbenzoic acid (0.15 mmol, 25 mg) and K_2CO_3 (1 mmol, 138 mg) were reacted together in 1,4-Dioxane (2 mL) according to general procedure. After cooling to room temperature the reaction mixture was dry loaded onto silica and purified by silica gel column chromatography (Hexane / EtOAc) to yield **1a7** as a colourless oil (56 mg, 46%).

2-(2-hexylphenyl)pyridine (1a7)



¹H NMR: (500 MHz, CDCl₃) δ 8.69 (d, *J* = 4.2 Hz, 1H), 7.75 (t, *J* = 7.6 Hz, 1H), 7.41 – 7.23 (m, 6H), 2.73 – 2.66 (m, 2H), 1.49 – 1.40 (m, 2H), 1.26 – 1.09 (m, 6H), 0.82 (t, *J* = 6.9 Hz, 2H). **¹³C NMR:** (126 MHz, CDCl₃) δ 160.32, 149.11, 140.77, 140.32, 136.03, 129.71, 129.69, 128.24, 125.70, 124.08, 121.57, 32.92, 31.48, 31.23, 29.10, 22.48, 14.05.

Data conforms to literature.²²

Computational Details / Methodology

DFT calculations were run with Gaussian 09 (Revision D.01).¹⁴ Ru centers were described with the Stuttgart RECPs and associated basis sets,¹⁵ and 6-31G** basis sets were used for all other atoms.^{16,17} Initial BP86^{18,19} optimizations were performed using the 'grid = ultrafine' option, with all stationary points being fully characterized via analytical frequency calculations as minima (all positive eigenvalues). All energies were recomputed with a larger basis set featuring cc-pVTZ on Ru and 6-311++G** on all other atoms. Corrections for the effect of 1,4-dioxane ($\epsilon = 2.2099$) solvent were run using the polarizable continuum model and BS1.²⁰ Single-point dispersion corrections to the BP86 results employed Grimme's D3 parameter set with Becke-Johnson damping as implemented in Gaussian.²¹ Natural Bond Orbital (NBO) analysis calculations were also computed with Gaussian 09.

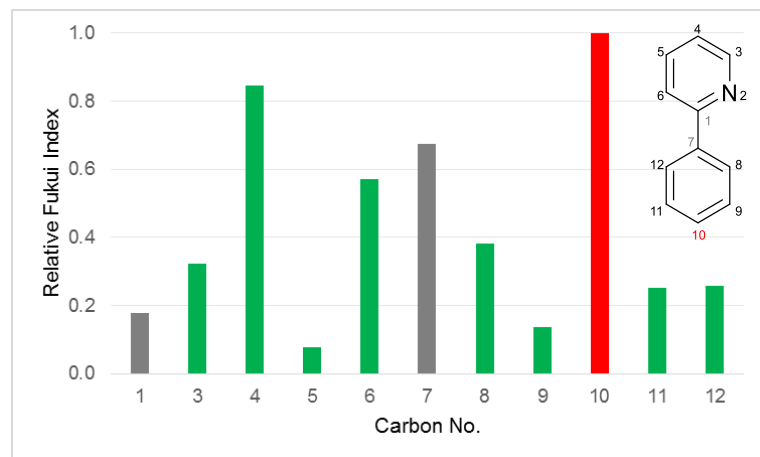
Relative Fukui Index

Relative nucleophilicity Fukui numbers were calculated by optimising the neutral molecule, and then performing NBO computations (nbo=npa, natural population analysis) on the neutral and cationic radical. For each atomic nucleophilicity Fukui number (f_A^-) the NBO charge of the cationic calculation ($P_A(N - 1)$) is subtracted from the neutral NBO charge value ($P_A(N)$) (see Eq. 1), before the values are scaled relative to the largest positive value of the molecule, which is normalised and equal to 1.00. This determines the nucleophilicity of atom A in molecule M (of N electrons), where P stands for the population of atom A in molecule M .

$$f_A^- = P_A(N) - P_A(N - 1) \quad (\text{Eq. 1})$$

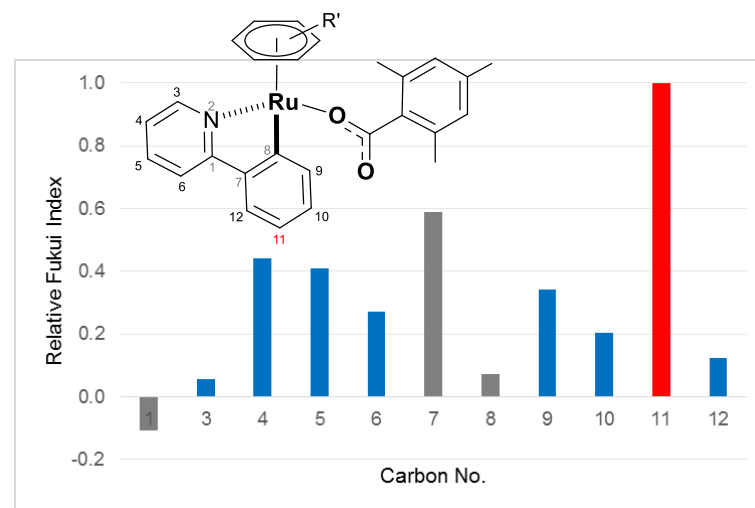
N.B. N is the number of electrons of the original molecule / ion. The equilibrium geometry of the original molecule is used for the cationic radical calculation. We also note that using the total atomic charge values gives positive Fukui values, whilst using the local atomic charge values gives the inverse of the Fukui value, i.e. $-f_A^-$.

1a



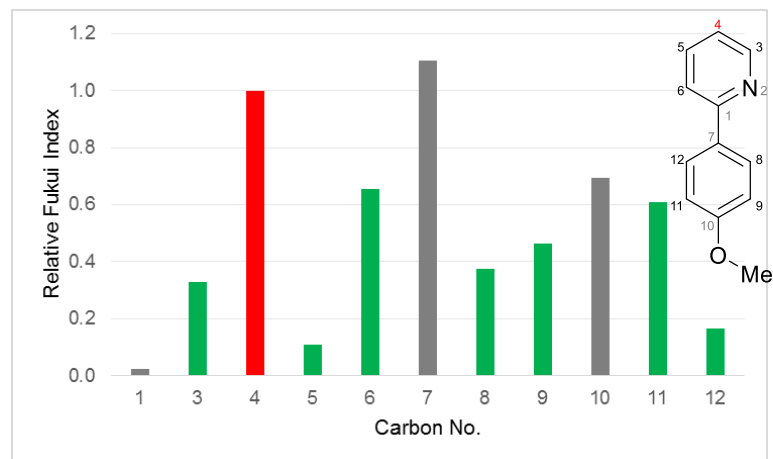
Atom	Neutral Total Charge	Cationic Total Charge	f_A^-	Relative Fukui Index
C1	5.7782	5.8032	0.0249	0.179
C3	5.9417	5.9865	0.0448	0.322
C4	6.1694	6.2869	0.1175	0.844
C5	6.2030	6.2137	0.0107	0.077
C6	6.1815	6.2608	0.0793	0.570
C7	5.9844	6.0783	0.0939	0.675
C8	6.1544	6.2077	0.0533	0.383
C9	6.2241	6.2432	0.0191	0.137
C10	6.0996	6.2387	0.1391	1.000
C11	6.2092	6.2445	0.0352	0.253
C12	6.1885	6.2244	0.0359	0.258

Aa



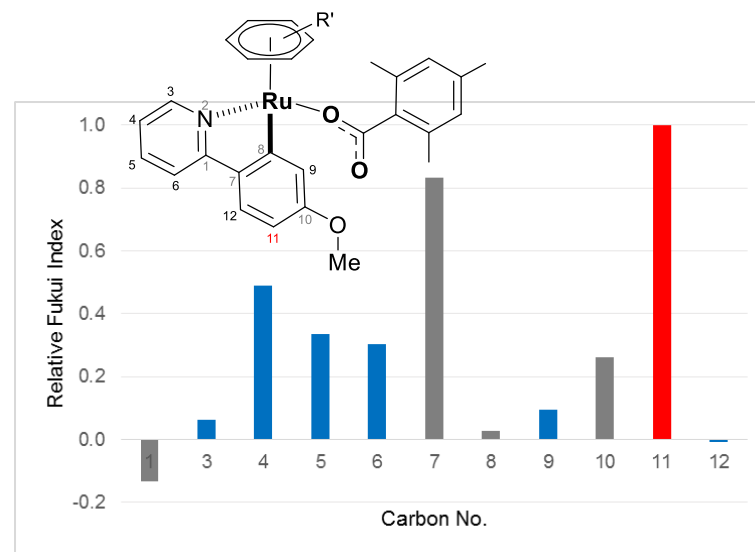
Atom	Neutral Total Charge	Cationic Total Charge	f_A^-	Relative Fukui Index
C1	5.7730	5.7674	-0.0056	-0.109
C3	5.9637	5.9667	0.0030	0.058
C4	6.2629	6.2857	0.0228	0.441
C5	6.1906	6.2117	0.0212	0.410
C6	6.2343	6.2483	0.0141	0.272
C7	6.0865	6.1169	0.0304	0.588
C8	5.9875	5.9913	0.0038	0.073
C9	6.2431	6.2608	0.0177	0.343
C10	6.2141	6.2246	0.0106	0.205
C11	6.2115	6.2632	0.0517	1.000
C12	6.2089	6.2152	0.0063	0.122

1k



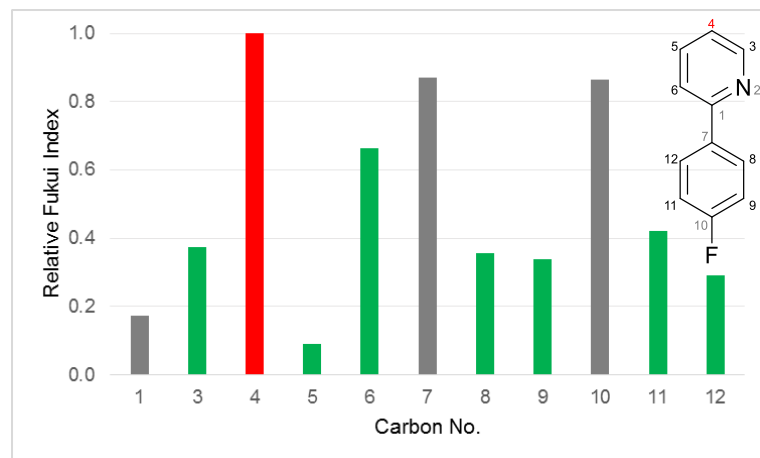
Atom	Neutral Total Charge	Cationic Total Charge	f_A^-	Relative Fukui Index
C1	5.7995	5.8020	0.0025	0.025
C3	5.9540	5.9865	0.0325	0.329
C4	6.1937	6.2924	0.0987	1.000
C5	6.2036	6.2143	0.0107	0.108
C6	6.1990	6.2636	0.0647	0.655
C7	5.9953	6.1043	0.1090	1.104
C8	6.1533	6.1904	0.0371	0.376
C9	6.2831	6.3289	0.0458	0.464
C10	5.6168	5.6853	0.0685	0.694
C11	6.2227	6.2826	0.0599	0.607
C12	6.1970	6.2132	0.0162	0.164

Ak



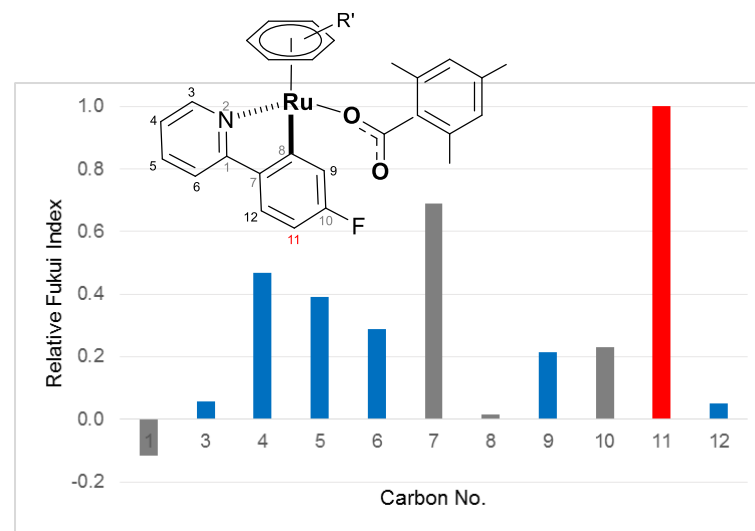
Atom	Neutral Total Charge	Cationic Total Charge	f_A^-	Relative Fukui Index
C1	5.7762	5.7685	-0.0076	-0.134
C3	5.9629	5.9665	0.0036	0.063
C4	6.2631	6.2910	0.0279	0.489
C5	6.1933	6.2124	0.0191	0.335
C6	6.2348	6.2521	0.0173	0.304
C7	6.0864	6.1339	0.0474	0.831
C8	5.9848	5.9863	0.0015	0.026
C9	6.2985	6.3038	0.0053	0.093
C10	5.6558	5.6706	0.0149	0.260
C11	6.2873	6.3444	0.0570	1.000
C12	6.1981	6.1977	-0.0004	-0.008

1n



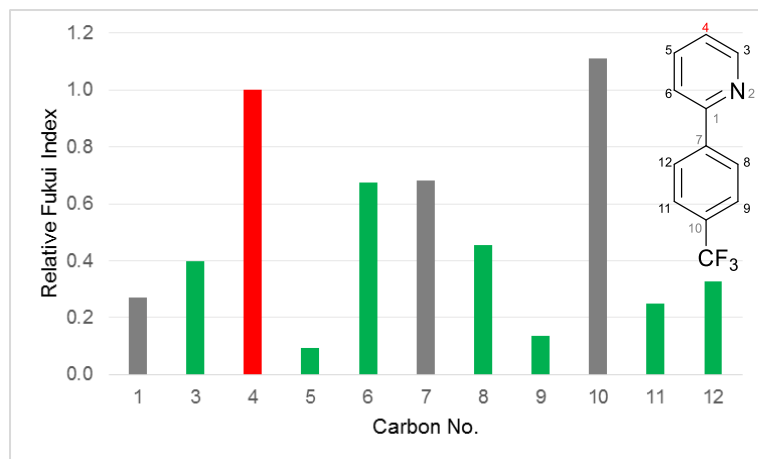
Atom	Neutral Total Charge	Cationic Total Charge	f_A^-	Relative Fukui Index
C1	5.7837	5.8035	0.0198	0.173
C3	5.9425	5.9855	0.0429	0.375
C4	6.1730	6.2875	0.1145	1.000
C5	6.2026	6.2129	0.0103	0.090
C6	6.1858	6.2618	0.0760	0.664
C7	5.9936	6.0934	0.0997	0.871
C8	6.1555	6.1964	0.0409	0.358
C9	6.2746	6.3133	0.0387	0.338
C10	5.4850	5.5838	0.0988	0.863
C11	6.2666	6.3149	0.0483	0.422
C12	6.1792	6.2126	0.0335	0.292

An



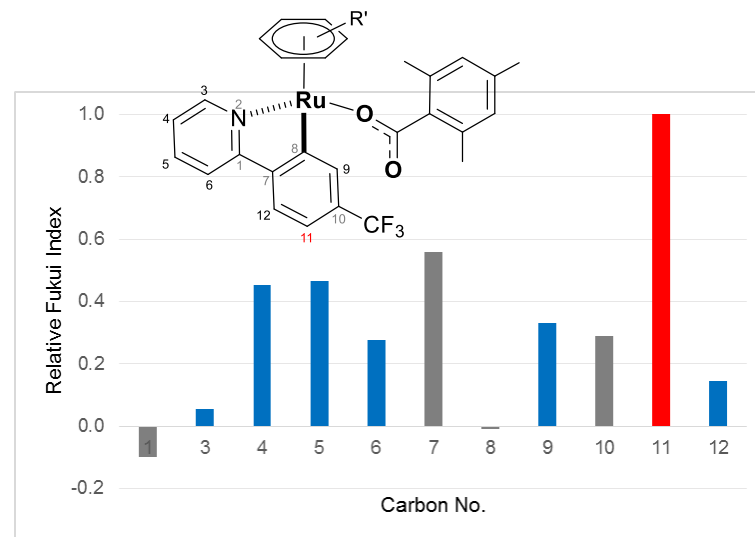
Atom	Neutral Total Charge	Cationic Total Charge	f_A^-	Relative Fukui Index
C1	5.7740	5.7679	-0.0061	-0.117
C3	5.9632	5.9662	0.0030	0.058
C4	6.2629	6.2871	0.0243	0.467
C5	6.1906	6.2109	0.0203	0.391
C6	6.2350	6.2500	0.0150	0.288
C7	6.0931	6.1290	0.0359	0.690
C8	5.9835	5.9843	0.0008	0.015
C9	6.3215	6.3326	0.0111	0.214
C10	5.5590	5.5710	0.0119	0.230
C11	6.2798	6.3318	0.0520	1.000
C12	6.2021	6.2048	0.0027	0.052

1r



Atom	Neutral Total Charge	Cationic Total Charge	f_A^-	Relative Fukui Index
C1	5.7761	5.8076	0.0315	0.272
C3	5.9386	5.9846	0.0460	0.397
C4	6.1658	6.2815	0.1157	1.000
C5	6.2012	6.2119	0.0107	0.092
C6	6.1791	6.2574	0.0783	0.676
C7	5.9854	6.0644	0.0791	0.683
C8	6.1497	6.2024	0.0527	0.456
C9	6.2018	6.2178	0.0159	0.138
C10	6.0397	6.1683	0.1286	1.111
C11	6.1901	6.2191	0.0290	0.251
C12	6.1811	6.2188	0.0377	0.326

Ar



Atom	Neutral Total Charge	Cationic Total Charge	f_A^-	Relative Fukui Index
C1	5.7745	5.7699	-0.0046	-0.101
C3	5.9632	5.9657	0.0025	0.055
C4	6.2607	6.2811	0.0205	0.452
C5	6.1895	6.2106	0.0211	0.467
C6	6.2327	6.2452	0.0125	0.276
C7	6.0800	6.1053	0.0253	0.559
C8	5.9903	5.9898	-0.0004	-0.009
C9	6.2180	6.2330	0.0150	0.331
C10	6.1433	6.1565	0.0132	0.291
C11	6.1959	6.2412	0.0453	1.000
C12	6.2041	6.2106	0.0065	0.144

Cartesian Coordinates and Computed Energies (in Hartrees)

Substrates (1x)

1a (X = H) SCF (BP86) Energy = -479.337880828 Enthalpy 0K = -479.173092 Enthalpy 298K = -479.163055 Free Energy 298K = -479.208178 Lowest Frequency = 40.4788 cm ⁻¹ Second Frequency = 91.3214 cm ⁻¹ C -2.82035 -1.22021 -0.17267 C -1.42052 -1.18871 -0.16232 C -0.72639 0.03150 0.00415 C -1.47865 1.21540 0.17687 C -2.88013 1.18211 0.16868 C -3.55762 -0.03489 -0.01029 H -3.34010 -2.17463 -0.30931 H -0.83155 -2.10242 -0.28030 H -0.97109 2.17066 0.34550 H -3.44471 2.10971 0.31090 H -4.65241 -0.05969 -0.01750 C 0.76442 0.03286 -0.00013 C 1.51734 1.21497 -0.19225 C 2.91522 1.14948 -0.17420 H 1.01709 2.17021 -0.37488 C 2.71056 -1.21703 0.18185 C 3.53611 -0.09242 0.02285 H 3.51132 2.05634 -0.32171 H 3.15301 -2.21220 0.32554 H 4.62554 -0.19184 0.04418 N 1.36757 -1.17207 0.17462	1k (X = OMe) SCF (BP86) Energy = -593.863940782 Enthalpy 0K = -593.667613 Enthalpy 298K = -593.654912 Free Energy 298K = -593.706377 Lowest Frequency = 29.8744 cm ⁻¹ Second Frequency = 57.4225 cm ⁻¹ C 2.01418 -0.98160 0.09028 C 0.61450 -1.02948 0.09002 C -0.16895 0.14003 -0.01269 C 0.51046 1.37743 -0.13072 C 1.90359 1.44261 -0.13441 C 2.66962 0.26201 -0.02003 H 2.58242 -1.91111 0.17780 H 0.09410 -1.98798 0.16942 H -0.05230 2.30950 -0.24307 H 2.42732 2.39798 -0.23289 C -1.65226 0.03615 -0.00037 C -2.49219 1.16593 0.15249 C -3.88098 0.99759 0.14465 H -2.06637 2.16339 0.29298 C -3.50574 -1.35749 -0.12953 C -4.41188 -0.29247 -0.00391 H -4.54066 1.86419 0.26135 H -3.87438 -2.38700 -0.23689 H -5.49117 -0.47166 -0.01523 N -2.16995 -1.21480 -0.13193 O 4.02982 0.43422 -0.03098 C 4.84221 -0.73707 0.07178 H 5.88307 -0.38375 0.04111 H 4.66671 -1.27405 1.02343 H 4.66688 -1.43130 -0.772037
1n (X = F) SCF (BP86) Energy = -578.572206709 Enthalpy 0K = -578.415442 Enthalpy 298K = -578.404536 Free Energy 298K = -578.451895 Lowest Frequency = 36.9301 cm ⁻¹ Second Frequency = 70.8050 cm ⁻¹ C 2.38679 -1.21663 0.14979 C 0.98861 -1.17753 0.14133 C 0.28935 0.04353 -0.00427 C 1.04079 1.23093 -0.15838 C 2.44141 1.20964 -0.15412 C 3.09545 -0.01759 0.00432 H 2.93311 -2.15646 0.26826 H 0.40298 -2.09482 0.24515 H 0.53542 2.18988 -0.30831 H 3.02826 2.12337 -0.28033 C -1.20029 0.03781 0.00079	1r (X = CF₃) SCF (BP86) Energy = -816.373644785 Enthalpy 0K = -816.204505 Enthalpy 298K = -816.190700 Free Energy 298K = -816.246328 Lowest Frequency = 16.2999 cm ⁻¹ Second Frequency = 40.1890 cm ⁻¹ C 1.28342 -1.19370 0.11775 C -0.11405 -1.16842 0.12296 C -0.81887 0.04814 -0.02443 C -0.07593 1.23758 -0.19770 C 1.32337 1.21670 -0.20530 C 2.00937 0.00061 -0.04341 H 1.81752 -2.14133 0.23131 H -0.69378 -2.08824 0.23579 H -0.58826 2.19135 -0.35614 H 1.88705 2.14181 -0.35372 C -2.30983 0.03721 -0.00476

C -1.96223 1.21761 0.17220	C -3.07061 1.21342 0.18653
C -3.35949 1.14099 0.15496	C -4.46827 1.13266 0.18511
H -1.47142 2.18093 0.33712	H -2.57938 2.17580 0.35527
C -3.13777 -1.22952 -0.16018	C -4.24242 -1.23508 -0.15840
C -3.97171 -0.10871 -0.02027	C -5.07719 -0.11720 0.00326
H -3.96205 2.04607 0.28607	H -5.07245 2.03394 0.33262
H -3.57229 -2.23041 -0.28680	H -4.67574 -2.23538 -0.29157
H -5.06032 -0.21634 -0.03976	H -6.16561 -0.22810 -0.00519
N -1.79519 -1.17404 -0.15404	N -2.90020 -1.17529 -0.16526
F 4.45191 -0.04523 0.01110	C 3.51753 -0.01598 0.01272
	F 4.03125 -1.18693 -0.46120
	F 3.97343 0.12619 1.29330
	F 4.06565 0.99868 -0.71627

Ruthenium complexes (Ax)

<p>[(p-cymene)Ru(OMes)(1x)]</p> <p>Aa SCF (BP86) Energy = -1501.49589663 Enthalpy 0K = -1500.950642 Enthalpy 298K = -1500.914203 Free Energy 298K = -1501.019014 Lowest Frequency = 15.0912 cm⁻¹ Second Frequency = 22.6119 cm⁻¹</p> <p>Ru 1.09279 -0.58811 -0.23800 O -0.99310 -0.33503 -0.37229 C -1.83608 -0.85993 0.49544 C 1.70311 -2.33692 -1.68337 C 2.77852 -1.43861 -1.35879 C 3.24098 -1.22200 -0.01410 C 0.92173 -2.88360 -0.63331 O -1.54666 -1.64375 1.42173 C 4.52745 -0.44065 0.23171 H 4.56150 0.36096 -0.53289 C 1.12380 2.20706 0.73101 C 1.13624 3.29468 1.63481 C 1.00271 0.85992 1.19185 C 0.99734 3.06267 3.00657 H 1.24007 4.32273 1.26818 C 0.81795 0.66161 2.57779 C 0.82095 1.74474 3.47283 H 1.00642 3.90163 3.70972 H 0.64412 -0.34955 2.95958 H 0.68044 1.56159 4.54449 N 1.08333 1.14902 -1.39298 C 1.14732 2.35084 -0.72097 C 2.43118 -1.79546 1.02688 C 1.28572 -2.59500 0.73584 H 0.63398 -2.93360 1.54239 H 2.65958 -1.56710 2.07180 H 3.30310 -0.92524 -2.17433 H 1.42460 -2.51419 -2.72621 C 5.74570 -1.36727 -0.00596</p>	<p>Ak SCF (BP86) Energy = -1616.02247516 Enthalpy 0K = -1615.445770 Enthalpy 298K = -1615.406604 Free Energy 298K = -1615.517575 Lowest Frequency = 16.0708 cm⁻¹ Second Frequency = 19.0663 cm⁻¹</p> <p>Ru -1.03514 -0.90512 -0.02131 O 1.05146 -0.71808 0.20241 C 1.87741 -0.58850 -0.81650 C -1.59432 -3.18634 0.00441 C -2.68472 -2.30692 0.33350 C -3.18059 -1.30231 -0.56770 C -0.83461 -2.93472 -1.16580 O 1.57899 -0.67199 -2.02481 C -4.48247 -0.57289 -0.25273 H -4.51308 -0.44008 0.84714 C -1.12536 1.85884 1.02853 C -1.16905 3.26879 1.02030 C -1.01196 1.12550 -0.19800 C -1.07621 3.98262 -0.17907 H -1.26297 3.82916 1.95805 C -0.87946 1.85416 -1.38866 C -0.91446 3.26754 -1.38885 H -1.11184 5.07410 -0.16530 H -0.71910 1.35059 -2.34670 N -1.00009 -0.30904 1.97965 C -1.09731 1.04367 2.23254 C -2.39008 -1.07381 -1.74792 C -1.23193 -1.85351 -2.04054 H -0.59608 -1.59406 -2.88801 H -2.64380 -0.24190 -2.41116 H -3.19353 -2.43300 1.29735 H -1.29039 -3.97555 0.69831 C -5.68226 -1.46833 -0.65021 H -6.63558 -0.98461 -0.37504 H -5.69332 -1.64345 -1.74063 H -5.64056 -2.45155 -0.15160</p>
--	--

H 6.68871 -0.80480 0.10687 H 5.75469 -2.19449 0.72572 H 5.73038 -1.81103 -1.01588 C 4.61020 0.22471 1.61672 H 3.73282 0.86055 1.81495 H 4.68226 -0.52752 2.42262 H 5.51614 0.85116 1.67876 C -0.28582 -3.73965 -0.91545 H -0.67059 -3.57640 -1.93442 H -0.01864 -4.80783 -0.81432 H -1.08125 -3.51597 -0.18874 C 1.17536 3.56172 -1.44496 H 1.22932 4.50815 -0.90041 C 1.11720 3.54964 -2.83994 H 1.13958 4.48831 -3.40234 C 1.01036 2.31627 -3.50725 H 0.93735 2.25568 -4.59619 C 0.98983 1.14602 -2.74583 H 0.89190 0.16018 -3.20725 C -3.27846 -0.43146 0.26098 C -4.30465 -1.41625 0.22431 C -3.61805 0.94256 0.13605 C -5.63702 -1.00955 0.03410 C -4.96974 1.30007 -0.02961 C -5.99545 0.34338 -0.09737 H -6.42040 -1.77769 -0.00059 H -5.22506 2.36493 -0.10613 C -4.01061 -2.89446 0.38023 H -3.37949 -3.27053 -0.44561 H -3.46117 -3.08688 1.31455 H -4.94492 -3.47956 0.37662 C -7.43627 0.75156 -0.32092 H -7.70325 0.71430 -1.39391 H -8.13441 0.08103 0.20857 H -7.62331 1.78183 0.02532 C -2.58174 2.04548 0.20195 H -1.89065 1.91305 1.05025 H -1.95807 2.05955 -0.70697 H -3.07232 3.02790 0.30567	C -4.60249 0.81825 -0.89955 H -3.73644 1.45409 -0.65683 H -4.68175 0.74706 -1.99917 H -5.51720 1.32088 -0.54195 C 0.38334 -3.75490 -1.50443 H 0.78583 -4.26908 -0.61740 H 0.12100 -4.52072 -2.25770 H 1.16274 -3.10652 -1.93214 C -1.11227 1.50864 3.56680 H -1.19381 2.58224 3.75700 C -1.00763 0.60860 4.62770 H -1.01945 0.96940 5.66106 C -0.86860 -0.76384 4.34931 H -0.75919 -1.50482 5.14530 C -0.86318 -1.17385 3.01493 H -0.74213 -2.22366 2.73598 C 3.31713 -0.33434 -0.38885 C 4.36227 -1.12187 -0.94632 C 3.63312 0.71583 0.51401 C 5.69121 -0.86328 -0.56707 C 4.98151 0.94974 0.84504 C 6.02676 0.16655 0.32920 H 6.48975 -1.48188 -0.99678 H 5.21822 1.77484 1.52936 C 4.09010 -2.23502 -1.93751 H 3.47705 -3.03688 -1.48719 H 3.52978 -1.85500 -2.80576 H 5.03352 -2.69050 -2.28079 C 7.46479 0.41016 0.73605 H 7.76320 -0.24757 1.57412 H 8.16132 0.20851 -0.09563 H 7.62074 1.45047 1.06742 C 2.57273 1.61483 1.11529 H 1.87157 1.99306 0.35329 H 1.96196 1.07041 1.85383 H 3.03997 2.47999 1.61515 O -0.78829 3.85801 -2.61950 C -0.78211 5.28570 -2.67592 H -0.65165 5.54282 -3.73707 H -1.73531 5.71476 -2.31160 H 0.05434 5.71347 -2.09127
An SCF (BP86) Energy = -1600.73161489 Enthalpy 0K = -1600.194438 Enthalpy 298K = -1600.157053 Free Energy 298K = -1600.264277 Lowest Frequency = 13.4396 cm ⁻¹ Second Frequency = 20.9685 cm ⁻¹ Ru -1.06752 0.69798 -0.24615 O 1.01889 0.46121 -0.40328 C 1.85223 0.80909 0.55826 C -1.66737 2.70179 -1.31196 C -2.74884 1.76274 -1.17482	Ar SCF (BP86) Energy = -1838.53275869 Enthalpy 0K = -1837.983312 Enthalpy 298K = -1837.942943 Free Energy 298K = -1838.058889 Lowest Frequency = 10.5599 cm ⁻¹ Second Frequency = 15.7328 cm ⁻¹ Ru -0.91919 -1.12082 -0.27695 O 1.16011 -0.92752 -0.01908 C 1.92919 -0.30218 -0.89102 C -1.32671 -3.25110 -1.17486 C -2.46067 -2.67301 -0.50624

C	-3.21436	1.28463	0.09847	C	-3.06074	-1.43079	-0.91191
C	-0.88739	3.02733	-0.17343	C	-0.63688	-2.48551	-2.15033
O	1.55325	1.41028	1.60942	O	1.56802	0.14562	-1.99721
C	-4.50669	0.47918	0.18297	C	-4.39283	-0.99613	-0.31018
H	-4.54745	-0.15020	-0.72830	H	-4.39010	-1.33773	0.74417
C	-1.11861	-2.23803	0.10990	C	-1.11696	1.00038	1.77458
C	-1.14151	-3.49016	0.76601	C	-1.24632	2.29264	2.33145
C	-1.00022	-1.01708	0.84737	C	-1.00624	0.80735	0.36300
C	-1.02139	-3.56190	2.15623	C	-1.24518	3.41586	1.50157
H	-1.24091	-4.41972	0.19404	H	-1.33510	2.42888	3.41518
C	-0.83580	-1.10708	2.24458	C	-0.95538	1.96011	-0.44733
C	-0.85476	-2.36130	2.86613	C	-1.08282	3.24455	0.11163
H	-1.03436	-4.51421	2.69195	H	-1.34241	4.42031	1.92079
H	-0.66563	-0.21751	2.85727	H	-0.78470	1.86356	-1.52312
N	-1.04860	-0.75735	-1.74193	N	-0.85227	-1.35733	1.79409
C	-1.12343	-2.07340	-1.33802	C	-1.00740	-0.22443	2.56301
C	-2.40365	1.63495	1.23404	C	-2.33916	-0.68086	-1.90402
C	-1.25502	2.47154	1.10987	C	-1.14512	-1.18019	-2.50527
H	-0.60373	2.63979	1.96849	H	-0.56890	-0.55101	-3.18503
H	-2.63597	1.20458	2.21235	H	-2.67964	0.32392	-2.17018
H	-3.27384	1.42538	-2.07715	H	-2.91988	-3.22095	0.32602
H	-1.38642	3.08233	-2.29831	H	-0.93945	-4.22647	-0.86657
C	-5.71695	1.44509	0.14088	C	-5.54701	-1.72964	-1.03781
H	-6.66463	0.87925	0.13972	H	-6.51763	-1.47751	-0.57690
H	-5.71832	2.10684	1.02505	H	-5.58894	-1.43227	-2.10052
H	-5.69844	2.08406	-0.75823	H	-5.42343	-2.82521	-0.99881
C	-4.59529	-0.45276	1.40426	C	-4.62469	0.52501	-0.31299
H	-3.72426	-1.12415	1.46681	H	-3.79585	1.06279	0.17397
H	-4.65938	0.12007	2.34666	H	-4.73518	0.91693	-1.33970
H	-5.50718	-1.07014	1.33979	H	-5.55774	0.76360	0.22482
C	0.32202	3.91985	-0.27778	C	0.62000	-2.99644	-2.80539
H	0.71025	3.95886	-1.30770	H	1.10009	-3.78457	-2.20443
H	0.05513	4.94789	0.02965	H	0.37777	-3.41840	-3.79825
H	1.11441	3.55702	0.39387	H	1.33032	-2.16860	-2.94979
C	-1.14704	-3.10466	-2.30189	C	-0.99801	-0.31776	3.96992
H	-1.20986	-4.14467	-1.97076	H	-1.12560	0.58888	4.56728
C	-1.07421	-2.79892	-3.66186	C	-0.81053	-1.55461	4.59114
H	-1.09310	-3.59813	-4.40938	H	-0.80343	-1.62988	5.68286
C	-0.95764	-1.45304	-4.05396	C	-0.61267	-2.69437	3.79208
H	-0.87350	-1.16498	-5.10496	H	-0.43795	-3.68031	4.23049
C	-0.94170	-0.46995	-3.06286	C	-0.63408	-2.54913	2.40330
H	-0.83648	0.59051	-3.30514	H	-0.46974	-3.39623	1.73285
C	3.29505	0.41851	0.26809	C	3.37513	-0.17692	-0.43205
C	4.32598	1.38767	0.41489	C	4.42575	-0.53082	-1.32425
C	3.62931	-0.91526	-0.08937	C	3.68932	0.34451	0.85190
C	5.65862	1.01106	0.17209	C	5.75905	-0.38539	-0.90275
C	4.98103	-1.24792	-0.29951	C	5.04074	0.49215	1.21779
C	6.01206	-0.30096	-0.18834	C	6.09307	0.12254	0.36478
H	6.44608	1.76800	0.28062	H	6.56199	-0.66802	-1.59568
H	5.23224	-2.28512	-0.55645	H	5.27416	0.91418	2.20380
C	4.03586	2.81773	0.82281	C	4.15848	-1.06338	-2.71734
H	3.41703	3.33608	0.06770	H	3.62480	-2.03080	-2.68538
H	3.47570	2.84714	1.77010	H	3.52383	-0.36719	-3.28679
H	4.97227	3.38883	0.93300	H	5.10445	-1.22451	-3.25984
C	7.45352	-0.67444	-0.46253	C	7.53783	0.25178	0.79854

H 7.73306 -0.45737 -1.51073	H 7.92065 -0.70061 1.21120
H 8.14839 -0.10805 0.18060	H 8.19222 0.52278 -0.04742
H 7.63182 -1.74971 -0.29426	H 7.65776 1.01819 1.58235
C 2.58632 -2.00530 -0.22528	C 2.62404 0.77980 1.83714
H 1.89316 -2.02175 0.63169	H 1.86092 1.41818 1.36273
H 1.96602 -1.85282 -1.12365	H 2.08857 -0.08867 2.25458
H 3.07016 -2.99386 -0.29644	H 3.07784 1.34502 2.66841
F -0.71098 -2.42663 4.21507	C -1.12166 4.44665 -0.80147
	F -0.75323 5.59357 -0.16011
	F -0.30453 4.29915 -1.88038
	F -2.38487 4.65731 -1.29008

References

- (1) Andersson, H.; Banchelin, T. S.-L.; Das, S.; Olsson, R.; Almqvist, F. *Chem. Commun.* **2010**, 46, 3384–3386.
- (2) Shen, Y.; Chen, J.; Liu, M.; Ding, J.; Gao, W.; Huang, X.; Wu, H. *Chem. Commun.* **2014**, 50, 4292–4295.
- (3) Guo, P.; Joo, J. M.; Rakshit, S.; Sames, D. *J. Am. Chem. Soc.* **2011**, 133, 16338–16341.
- (4) Zhang, E.; Tang, J.; Li, S.; Wu, P.; Moses, J. E.; Sharpless, K. B. *Chem. Eur. J.* **2016**, 22, 5692–5697.
- (5) Liu, C.; Yang, W. *Chem. Commun.* **2009**, 6267–6269.
- (6) Paterson, A.; St John-Campbell, S.; Mahon, M. F.; Press, N.; Frost, C. G. *Chem. Commun.* **2015**, 51, 12807–12810.
- (7) Li, Y.; Liu, W.; Kuang, C. *Chem. Commun.* **2014**, 50, 7124–7127.
- (8) Funaki, T.; Otsuka, H.; Onozawa-komatsuzaki, N.; Kasuga, K.; Sayama, K.; Sugihara, H. *J. Mater. Chem. A Mater. energy Sustain.* **2014**, 2, 15945–15951.
- (9) Norinder, J.; Matsumoto, A.; Yoshikai, N.; Nakamura, E. *J. Am. Ceram. Soc.* **2008**, 130, 5858–5859.
- (10) Wang, S.; Yu, X.-Q.; Wang, G.; Wang, J.; Zhang, J. *Chem. Commun.* **2012**, 48, 11769–11771.
- (11) Hong, X.; Wang, H.; Qian, G.; Tan, Q.; Xu, B. *J. Org. Chem.* **2014**, 79, 3228–3237.
- (12) Fandrick, D. R.; Reinhardt, D.; Desrosiers, J. N.; Sanyal, S.; Fandrick, K. R.; Ma, S.; Grinberg, N.; Lee, H.; Song, J. J.; Senanayake, C. H. *Org. Lett.* **2014**, 16, 2834–2837.
- (13) Baek, Y.; Kim, S.; Jeon, B.; Lee, P. H. *Org. Lett.* **2016**, 18, 104–107.
- (14) Frisch, M. J.; Trucks, G. W.; Schlegel, H. B.; Scuseria, G. E.; Robb, M. A.; Cheeseman, J. R.; Scalmani, G.; Barone, V.; Mennucci, B.; Petersson, G. A.; Nakatsuji, H.; Caricato, M.; Li, X.; Hratchian, H. P.; Izmaylov, A. F.; Bloino, J.; Zheng, G.; Sonnenb, D. J. Gaussian 09 (Revision D.01), 2009.

- (15) Andrae, D.; Häußermann, U.; Dolg, M.; Stoll, H.; Preuß, H. T. *Theor. Chim. Acta* **1990**, 77, 123–141.
- (16) Hariharan, P. C.; Pople, J. A. *Theor. Chim. Acta* **1973**, 28, 213–222.
- (17) Hehre, W. J.; Ditchfield, R.; Pople, J. A. *J. Chem. Phys.* **1972**, 56, 2257–2261.
- (18) Perdew, J. P. *Phys. Rev. B* **1986**, 33, 8822–8824.
- (19) Becke, A. D. *Phys. Rev. A* **1988**, 38, 3098–3100.
- (20) Tomasi, J.; Mennucci, B.; Cammi, R. *Chem. Rev.* **2005**, 105, 2999–3094.
- (21) Steffen, C.; Thomas, K.; Huniar, U.; Hellweg, A.; Rubner, O.; Schroer, A. *J. Comput. Chem.* **2010**, 31, 2967–2970.
- (22) L. Ackermann, P. Novák, R. Vicente and N. Hofmann, *Angew. Chem. Int. Ed.* 2009, 48, 6045–6048.